

https://dspace.org/

Mechanical and water absorption properties of resin transfer moulded kenaf fibre reinforced composites

Rassmann, Stefan

2011-04-21
http://hdl.handle.net/10539/9615

Downloaded from a DSpace repository. https://dspace.org/

MECHANICAL AND WATER ABSORPTION PROPERTIES OF RESIN TRANSFER MOULDED KENAF FIBRE REINFORCED COMPOSITES

Stefan Rassmann

A dissertation submitted to the Faculty of Engineering and the Built Environment, University of the Witwatersrand, Johannesburg, in fulfilment of the requirements for the degree of Master of Science in Engineering.

Johannesburg, 2010

DECLARATION

I declare that this dissertation is my own unaided work. It is being submitted for the degree of Master of Science in Engineering at the University of the Witwatersrand, Johannesburg. It has not been submitted before for any degree or examination at any other university.



_____

(Stefan Rassmann)

3rd day of October 2010

ABSTRACT

This investigation focuses on the tensile, flexural, impact and water absorption properties of kenaf fibre reinforced composites* manufactured by resin transfer moulding. Varying processing conditions and resin system are considered as alternatives to fibre treatments, thereby potentially avoiding additional cost and complexity in the manufacturing process. Tensile, flexural, impact and water absorption tests were conducted. Composites were produced with fibre volume fractions of 15 %, 22.5 % and 30 %. Fibre moisture content, mould temperature and mould pressure following injection were altered in polyester composites. Processing conditions were found to have little effect on properties except for pressurisation which increased tensile and flexural strength and decreased water absorption at low fibre volume fractions. Vinyl ester and epoxy composites were compared to those made using polyester resin. The results revealed that properties were affected in markedly different ways by the resin system and the fibre volume fraction. Polyester composites show good modulus and impact properties, epoxy composites display good strength values and vinyl ester composites exhibit good water absorption characteristics. Scanning electron microscope studies show that polyester composites fail by fibre pull-out, epoxy composites by fibre fracture and vinyl ester composites by a combination of the two. Theoretical models were applied to composites made using all three resin systems. There was good correlation with measured values of tensile linear moduli and flexural strength but poor correlation with measured values of tensile strength, tensile secant moduli and flexural secant and linear moduli. A comparison between kenaf and glass composites revealed that the specific tensile and flexural moduli are comparable at low fibre volume fractions. However, glass composites have much better specific properties than the kenaf composites at high fibre volume fractions for all three resin systems.

---

* For the purposes of this investigation, “composite” refers to a composite laminate.

PUBLISHED WORK

Aspects of this dissertation have been accepted for publication:

1. S. Rassmann, R.G. Reid and R. Paskaramoorthy. Effects of processing conditions on the mechanical and water absorption properties of resin transfer moulded kenaf fibre reinforced polyester composite laminates. Composites - Part A: Applied Science and Manufacturing, 41:1612-1619, 2010.

2. S. Rassmann, R.G. Reid and R. Paskaramoorthy. Effect of resin system on the mechanical properties and water absorption of kenaf fibre reinforced laminates. Materials and Design, reference as yet unavailable.

ACKNOWLEDGEMENTS

The author gratefully acknowledges the following:

Dr. R.G. Reid and Prof. R. Paskaramoorthy, for their help and support as project supervisors.

Mr. R. Kemp, Mr. L. Wolney and Mr. D. Anderson for supplying the kenaf fibre non-wovens used in this research.

The National Research Foundation and the Advanced Manufacturing Technology Strategy for their financial support.

In memory of my mother, who passed away shortly
before completion of this work.

CONTENTS

DECLARATION i
ABSTRACT ii
PUBLISHED WORK iii
ACKNOWLEDGEMENTS iv
CONTENTS vi
LIST OF FIGURES x
LIST OF TABLES xvi
LIST OF SYMBOLS xviii
1 INTRODUCTION 1
1.1 Background and motivation 1
1.2 Natural fibre classification and processing 4
1.3 Natural fibre structure 5
1.4 Manufacturing natural fibre reinforced composites 7
1.4.1 Introduction 7
1.4.2 A practical example using the hand lay-up technique 7
1.4.3 Resin transfer moulding and vacuum infusion 9
2 LITERATURE SURVEY 11
2.1 Natural fibres in RTM 11
2.2 Processing conditions 22
2.3 Resin system 23
3 OBJECTIVES 25
3.1 Development of objectives 25
3.2 Objectives 26
4 PRODUCTION 27
4.1 Production material 27
4.1.1 Fibres 27
4.1.2 Resins 28
4.2 Production equipment 29
4.2.1 Resin transfer moulding machine 29
4.2.2 Pressure pot 33
4.2.3 Mould 33

4.3 Production technique 35
4.3.1 Combinations of processing parameters 35
4.3.2 Heating the mould 37
4.3.3 Drying of fibres 37
4.3.4 Determination of fibre mass and volume fractions 40
4.3.5 Preparation of fibres 41
4.3.6 Production of composites 41
4.4 Production problems 42
4.4.1 Problems with the mould 42
4.4.2 Problems with vinyl ester resins 45
4.4.3 Other problems encountered during composite production 49
5 TESTING 50
5.1 Testing standards and specimens 50
5.1.1 Location of test specimens in composites 50
5.1.2 Tensile testing 50
5.1.3 Flexural testing 51
5.1.4 Impact testing 51
5.1.5 Water absorption testing 51
5.2 Testing equipment 51
5.2.1 Tensile testing equipment 51
5.2.2 Flexural testing equipment 53
5.2.3 Impact testing equipment 54
5.2.4 Water absorption testing equipment 55
5.2.5 Scanning electron microscope 57
6 OBSERVATIONS 58
6.1 Properties of the kenaf fibre mat 58
6.2 Mould filling 58
6.3 Composite quality 59
6.4 Testing 59
7 RESULTS 61
7.1 Introduction 61
7.2 Theoretical results 62
7.3 Specific properties 63
7.4 Results - processing conditions 64

7.4.1 Tensile tests 64
7.4.2 Flexural tests 65
7.4.3 Impact tests 67
7.4.4 SEM examinations 68
7.4.5 Water absorption tests 69
7.5 Results – resin system 72
7.5.1 Tensile tests 72
7.5.2 Flexural tests 73
7.5.3 Impact tests 75
7.5.4 SEM examinations 76
7.5.5 Water absorption tests 77
7.6 Results - specific properties 80
7.6.1 Specific tensile properties 80
7.6.2 Specific flexural properties 81
7.6.3 Specific impact properties 83
8 DISCUSSION 84
8.1 Processing conditions 84
8.1.1 Tensile tests 84
8.1.2 Flexural tests 85
8.1.3 Impact tests 86
8.1.4 SEM examinations 87
8.1.5 Water absorption tests 87
8.2 Resin System 89
8.2.1 Tensile tests 89
8.2.2 Flexural tests 91
8.2.3 Correlation of experimental and theoretical results for tensile and flexural tests 92
8.2.4 Impact tests 93
8.2.5 Water absorption tests 94
8.2.6 Hygroexpansion of kenaf fibre reinforced composites 96
8.3 Specific mechanical properties 99
8.3.1 Specific tensile properties 99
8.3.2 Specific flexural properties 100
8.3.3 Specific impact properties 100

8.4 Practical implications for kenaf fibre reinforced composites 101
8.5 Closing remarks 102
9 CONCLUSIONS AND RECOMMENDATIONS 103
9.1 Conclusions 103
9.2 Recommendations 105
Appendix A Overview of surface treatments 112
Appendix B Sample production log sheets 120
Appendix C Sample calculations 123
Appendix D Matlab codes and accelerometer data sheet 137
Appendix E SEM examinations 153
Appendix F Water absorption tests 159
Appendix G Hygroexpansion of kenaf fibre reinforced composites 173
Appendix H Results of mechanical testing 186
Appendix I Summary of material properties 206

LIST OF FIGURES

Figure 1.1 Cross-section of a flax stem (white arrows indicate fibre bundles) 4
Figure 1.2 Structure of a plant fibre.....6
Figure 2.1 SEM of impact failure surfaces of untreated and methacrylic anhydride treated hemp polyester composites.....14
Figure 2.2 Failure surfaces of composites manufactured by RTM and compression moulding.....20
Figure 4.1 Kenaf non-woven fibre mat.....27
Figure 4.2 Schematic of RTM machine.....32
Figure 4.3 RTM machine mixing head.....32
Figure 4.4 RTM machine front and back.....32
Figure 4.5 Mild steel mould: upper mould plate and lower mould plate with spacer .35
Figure 4.6 Mould temperature vs. time for mould in an oven at 55°C.....37
Figure 4.7 Effect of various drying methods on fibre moisture loss 39
Figure 4.8 Fibre mass increase vs. time after drying.....40
Figure 4.9 Lines on composites 43
Figure 4.10 Flow visualisation - resin injected from mould corners 43
Figure 4.11 Flow visualisation - resin injected from mould centre 44
Figure 4.12 Failed vinyl ester resin composite and vinyl ester resin gassing following injection.....45
Figure 4.13 Vinyl ester resin gassing with CSM glass and UD glass.....47
Figure 4.14 Composite production failure - resin curing during mould filling 49
Figure 4.15 Composite production failure - loss of vacuum 49
Figure 5.1 Location of test specimens in composites 50
Figure 5.2 Tensile test setup 52
Figure 5.3 Flexural test setup.....53
Figure 5.4 Impact test setup.....54
Figure 5.5 Aluminium rack for holding water absorption specimens 56
Figure 5.6 Water absorption test setup 56
Figure 5.7 Examples of coated SEM specimens.....57
Figure 7.1 Effect of processing conditions on tensile strength.....64
Figure 7.2 Effect of processing conditions on tensile secant modulus.....64

Figure 7.3 Effect of processing conditions on tensile linear modulus 65
Figure 7.4 Effect of processing conditions on flexural strength 65
Figure 7.5 Effect of processing conditions on flexural secant modulus 66
Figure 7.6 Effect of processing conditions on flexural linear modulus 66
Figure 7.7 Effect of processing conditions on impact energy 67
Figure 7.8 Effect of processing conditions on impact strength 67
Figure 7.9 SEM micrographs of impact failure surfaces of composites made using various processing conditions at 22.5 % fibre volume fraction 68
Figure 7.10 Effect of processing conditions on mass increase over four weeks of water absorption at 22.5 % fibre volume fraction 69
Figure 7.11 Effect of processing conditions on mass increase after four weeks of water absorption 69
Figure 7.12 Effect of processing conditions on thickness increase after four weeks of water absorption 70
Figure 7.13 Effect of processing conditions on length increase after four weeks of water absorption 70
Figure 7.14 Effect of processing conditions on width increase after four weeks of water absorption 71
Figure 7.15 Effect of resin system on tensile strength 72
Figure 7.16 Effect of resin system on tensile secant modulus 72
Figure 7.17 Effect of resin system on tensile linear modulus 73
Figure 7.18 Effect of resin system on flexural strength 73
Figure 7.19 Effect of resin system on flexural secant modulus 74
Figure 7.20 Effect of resin system on flexural linear modulus 74
Figure 7.21 Effect of resin system on impact energy 75
Figure 7.22 Effect of resin system on impact strength 75
Figure 7.23 SEM micrographs of impact failure surfaces of composites made using various resin systems at 22.5 % fibre volume fraction 76
Figure 7.24 Effect of resin system on mass increase over four weeks of water absorption at 22.5 % fibre volume fraction 77
Figure 7.25 Effect of resin system on mass increase after four weeks of water absorption 77
Figure 7.26 Effect of resin system on thickness increase after four weeks of water absorption 78

Figure 7.27 Effect of resin system on length increase after four weeks of water absorption....78
Figure 7.28 Effect of resin system on width increase after four weeks of water absorption....79
Figure 7.29 Comparison of specific tensile strength for kenaf fibre and glass fibre reinforced composites....80
Figure 7.30 Comparison of specific tensile secant modulus for kenaf fibre and glass fibre reinforced composites....80
Figure 7.31 Comparison of specific tensile linear modulus for kenaf fibre and glass fibre reinforced composites....81
Figure 7.32 Comparison of specific flexural strength for kenaf fibre and glass fibre reinforced composites....81
Figure 7.33 Comparison of specific flexural secant modulus for kenaf fibre and glass fibre reinforced composites....82
Figure 7.34 Comparison of specific flexural linear modulus for kenaf fibre and glass fibre reinforced composites....82
Figure 7.35 Comparison of specific impact energy for kenaf fibre and glass fibre reinforced composites....83
Figure 7.36 Comparison of specific impact strength for kenaf fibre and glass fibre reinforced composites....83
Figure 8.1 Representation of fibre orientation in water absorption specimen....89
Figure 8.2 Typical stress-strain curve for a polyester and an epoxy composite specimen....91
Figure 8.3 Voids in a vinyl ester composite and an epoxy composite....92
Figure 8.4 Theoretical and experimental coefficients of hygroexpansion for kenaf composites....97
Figure 8.5 Representation of two fibres in an uncompressed and a compressed non-woven fibre mat....98
Figure 8.6 Comparison of linear regions for kenaf fibre and glass fibre composite specimens....100
Figure C.1 Typical tensile stress-strain curve for a kenaf fibre composite specimen....129
Figure C.2 Typical flexural stress-strain curve for a kenaf fibre composite specimen....131

Figure C.3 Flow diagram describing matlab impact code 132
Figure E.1 SEM micrographs of impact failure surfaces of composites made using various processing conditions at 15 % fibre volume fraction 153
Figure E.2 SEM micrographs of impact failure surfaces of composites made using various processing conditions at 22.5 % fibre volume fraction 154
Figure E.3 SEM micrographs of impact failure surfaces of composites made using various processing conditions at 30 % fibre volume fraction 155
Figure E.4 SEM micrographs of impact failure surfaces of composites made using various resin systems at 15 % fibre volume fraction 156
Figure E.5 SEM micrographs of impact failure surfaces of composites made using various resin systems at 22.5 % fibre volume fraction 157
Figure E.6 SEM micrographs of impact failure surfaces of composites made using various resin systems at 30 % fibre volume fraction 157
Figure E.7 Fibres fractured at surface of 22.5 % fibre volume fraction composites . 158
Figure F.1 Effect of processing conditions on mass increase over four weeks of water absorption at 15 % fibre volume fraction 159
Figure F.2 Effect of processing conditions on mass increase over four weeks of water absorption at 22.5 % fibre volume fraction 159
Figure F.3 Effect of processing conditions on mass increase over four weeks of water absorption at 30 % fibre volume fraction 160
Figure F.4 Effect of processing conditions on thickness increase over four weeks of water absorption at 15 % fibre volume fraction 160
Figure F.5 Effect of processing conditions on thickness increase over four weeks of water absorption at 22.5 % fibre volume fraction 161
Figure F.6 Effect of processing conditions on thickness increase over four weeks of water absorption at 30 % fibre volume fraction 161
Figure F.7 Effect of processing conditions on length increase over four weeks of water absorption at 15 % fibre volume fraction 162
Figure F.8 Effect of processing conditions on length increase over four weeks of water absorption at 22.5 % fibre volume fraction 162
Figure F.9 Effect of processing conditions on length increase over four weeks of water absorption at 30 % fibre volume fraction 163
Figure F.10 Effect of processing conditions on width increase over four weeks of water absorption at 15 % fibre volume fraction 163

Figure F.11 Effect of processing conditions on width increase over four weeks of water absorption at 22.5 % fibre volume fraction.....164
Figure F.12 Effect of processing conditions on width increase over four weeks of water absorption at 30 % fibre volume fraction.....164
Figure F.13 Effect of resin system on mass increase over four weeks of water absorption at 0 % fibre volume fraction 165
Figure F.14 Effect of resin system on mass increase over four weeks of water absorption at 15 % fibre volume fraction 165
Figure F.15 Effect of resin system on mass increase over four weeks of water absorption at 22.5 % fibre volume fraction 166
Figure F.16 Effect of resin system on mass increase over four weeks of water absorption at 30 % fibre volume fraction 166
Figure F.17 Effect of resin system on thickness increase over four weeks of water absorption at 0 % fibre volume fraction 167
Figure F.18 Effect of resin system on thickness increase over four weeks of water absorption at 15 % fibre volume fraction 167
Figure F.19 Effect of resin system on thickness increase over four weeks of water absorption at 22.5 % fibre volume fraction 168
Figure F.20 Effect of resin system on thickness increase over four weeks of water absorption at 30 % fibre volume fraction 168
Figure F.21 Effect of resin system on length increase over four weeks of water absorption at 0 % fibre volume fraction 169
Figure F.22 Effect of resin system on length increase over four weeks of water absorption at 15 % fibre volume fraction 169
Figure F.23 Effect of resin system on length increase over four weeks of water absorption at 22.5 % fibre volume fraction 170
Figure F.24 Effect of resin system on length increase over four weeks of water absorption at 30 % fibre volume fraction 170
Figure F.25 Effect of resin system on width increase over four weeks of water absorption at 0 % fibre volume fraction 171
Figure F.26 Effect of resin system on width increase over four weeks of water absorption at 15 % fibre volume fraction 171
Figure F.27 Effect of resin system on width increase over four weeks of water absorption at 22.5 % fibre volume fraction 172

Figure F.28 Effect of resin system on width increase over four weeks of water absorption at 30 % fibre volume fraction 172
Figure G.1 Composite coefficients of hygroexpansion vs. fibre volume fraction 179
Figure G.2 Effect of varying input parameters on coefficients of hygroexpansion ... 180
Figure G.3 Theoretical and experimental least-squares fit curves of hygroexpansion coefficients 181
Figure G.4 Effect of varying β_{fL} on coefficients of hygroexpansion for a non-woven composite 182
Figure G.5 Theoretical and experimental least-squares fit curves of hygroexpansion coefficients (β_{fL} = -0.01) 183
Figure G.6 Representation of two fibres in an uncompressed and a compressed non-woven fibre mat 184

LIST OF TABLES

Table 1.1 Comparison of costs and volumes of various fibres 3
Table 1.2 Mechanical properties of some common natural fibres 7
Table 2.1 Mechanical properties of jute polyester composites manufactured by RTM 12
Table 2.2 Properties of hemp polyester composites manufactured by RTM 15
Table 2.3 Properties of flax composites manufactured by RTM 16
Table 2.4 Properties of hemp / kenaf polyester composites manufactured by RTM 19
Table 2.5 Properties of sisal polyester composites manufactured by RTM and compression moulding 21
Table 4.1 Expected fibre volume fractions for various numbers of fibre layers 27
Table 4.2 Properties of Scott Bader Crystic 196 polyester resin 28
Table 4.3 Properties of Derakane Momentum 411-350 vinyl ester resin 29
Table 4.4 Properties of SP Prime 27 epoxy resin 29
Table 4.5 Processing conditions for composites 36
Table 4.6 Results of test to determine source of gassing in vinyl ester resin 47
Table 4.7 Results of test to determine the source of gassing in Derakane vinyl ester resin containing inhibitor 48
Table 6.1 Mould filling times 58
Table C.1 Properties of kenaf fibres and resin systems 123
Table G.1 Mechanical properties and coefficients of hygroexpansion of kenaf fibres and epoxy resin 178
Table G.2 Lower and upper bounds of variables 180
Table H.1 Tensile results for 15 % fibre volume fraction polyester composites 186
Table H.2 Tensile results for 22.5 % fibre volume fraction polyester composites 187
Table H.3 Tensile results for 30 % fibre volume fraction polyester composites 188
Table H.4 Tensile results for vinyl ester composites 189
Table H.5 Tensile results for epoxy composites 190
Table H.6 Flexural results for 15 % fibre volume fraction polyester composites 191
Table H.7 Flexural results for 22.5 % fibre volume fraction polyester composites 192
Table H.8 Flexural results for 30 % fibre volume fraction polyester composites 193
Table H.9 Flexural results for vinyl ester composites 194
Table H.10 Flexural results for epoxy composites 195

Table H.11 Impact results for 15 % fibre volume fraction polyester composites 196
Table H.12 Impact results for 22.5 % fibre volume fraction polyester composites ..198
Table H.13 Impact results for 30 % fibre volume fraction polyester composites 200
Table H.14 Impact results for vinyl ester composites.....202
Table H.15 Impact results for epoxy composites.....204

LIST OF SYMBOLS

A - Area

β_{fL} - Fibre longitudinal coefficient of hygroexpansion

β_{fT} - Fibre transverse coefficient of hygroexpansion

β_m - Matrix coefficient of hygroexpansion

β_L - Longitudinal coefficient of hygroexpansion

β_T - Transverse coefficient of hygroexpansion

$\beta_{i\text{-}p}$ - In-plane coefficient of hygroexpansion of a randomly orientated fibre reinforced composite

β_{tt} - Through-thickness coefficient of hygroexpansion of a randomly orientated fibre reinforced composite

d - Deflection

E - Young's modulus

E_f - Young's modulus of fibres

E_m - Young's modulus of matrix

E_{secant} - Secant Young's modulus

E_{linear} - Linear Young's modulus

E_{tot} - Total energy

E_i - Initial energy

E_p - Propagative impact energy

E_{fL} - Fibre longitudinal Young's modulus

E_{fT} - Fibre transverse Young's modulus

ε - Strain

ε_f - Fibre strain

ε_m - Matrix strain

F - Force

G_m - Matrix shear modulus

G_T - Shear modulus of a unidirectional ply

I - Second moment of area

k_m - Matrix bulk modulus

k_{fT} - Fibre transverse bulk modulus

k_T - Transverse bulk modulus of a unidirectional ply

L - Support span

l - Specimen length

m - Mass

m_c - Mass of composite

m_f - Mass of fibres

m_m - Mass of matrix

M_f - Fibre mass fraction

M_m - Matrix mass fraction

M - Moment

η - Efficiency factor

ρ_c - Composite density

ρ_f - Fibre density

ρ_m - Matrix density

σ - Stress

t - Specimen thickness

t_c - Specimen thickness at centre

t_e - Specimen thickness at edge

v_c - Composite volume

v_f - Fibre volume

v_m - Matrix volume

V_f - Fibre volume fraction

V_m - Matrix volume fraction

Vel - Velocity

v_{fL} - Fibre longitudinal Poisson's ratio

v_{fT} - Fibre transverse Poisson's ratio

v_m - Matrix Poisson's ratio

v_{LT} - Longitudinal Poisson's ratio of a unidirectional ply

v_{TT} - Transverse Poisson's ratio of a unidirectional ply

w - Specimen width

X - Generalised value

$\% X$ - Generalised percentage value

y - Distance from neutral axis to specimen outer surface

1 INTRODUCTION

1.1 Background and motivation

Natural fibres are subdivided based on their origin from plants, animals or minerals [(1)]. Plant fibres are the most frequently utilised of these for the production of composites. Some of the most common plant fibres include flax, hemp, jute, sisal and kenaf.

As early as 1908, the first composite materials were used in the fabrication of large quantities of sheets, tubes and pipes. These were made from fibres such as flax, hemp and cotton with phenol-formaldehyde or melamine-formaldehyde resins [(1)]. Natural fibres fell out of favour with the invention of fibres such as glass and carbon and research on natural fibre reinforced composites all but ceased. Glass and carbon were not only structurally superior but in many cases became cheaper than some natural fibres [(1)].

Concerns about global warming and that fossil fuels will eventually run out has lead to renewed interest in natural fibres. This is driven further by the increasing prices of fossil fuels making glass and carbon fibres more expensive. Fossil fuels are used either directly or indirectly in the manufacture of these fibres. Reliance on fossil fuels can therefore be decreased through the use of natural fibres in composite materials.

When natural fibre reinforced plastics decompose or are combusted at the end of their life cycle, the carbon dioxide released by the fibres is the same as that absorbed during their growth [(1)]. Furthermore, natural fibres are easily combustible materials whereas man-made fibres have low energy values and high ash content when burnt [(2)].

Apart from carbon dioxide sequesterisation, biodegradability and enhanced energy recovery, according to Mohanty *et al.* [(3)] and Reddy *et al.* [(4)], the advantages of natural fibre composites include; low cost, low density, high toughness, reduced dermal and respiratory irritation and acceptable specific properties. Natural fibre reinforced composites are primarily utilised as low cost materials that have usable structural properties [(3)]. They have been used in applications such as automotive interior linings,

upholstery stuffing, egg-boxes and electronics packaging [1]. Thus, the use of natural fibres in commercial composites has been limited to the reinforcement of non-structural components.

The major drawback in using natural fibres in composites is that the fibres are hydrophilic meaning that they attract water, whilst the matrix materials are usually hydrophobic, meaning that they repel it [3]. This difference in hydrophility makes good wetting of fibres by the polymer matrix during production difficult to achieve. Poor interphase properties between fibres and matrix consequently result. This leads to composites with poor mechanical properties and high sensitivity to moisture [3]. Surface treatments, by physical and chemical means are being utilised by many researchers [1, 3, 5-9] in order to address this problem but attention to other elements such as processing conditions can potentially help. (Information regarding fibre treatments can be found in Appendix A).

Manufacturing techniques affect composites in many ways. They influence fibre wetting, void content [10] and the resulting fibre properties due to damaging effects from pressure and temperature [1, 5 & 11]. Manufacturing also affects material waste, cycle times and labour requirement [12] which is important as composite materials are most often labour-intensive to produce. Thermosetting polymers have generally been preferred in the composites industry due to their superior mechanical properties to thermoplastics [12]. There are many methods available for the manufacture of thermosetting composites including; hand lay up, compression moulding, vacuum bagging, pressure bagging, autoclaving, pultrusion, vacuum infusion and resin transfer moulding [12 - 14].

Natural fibres are in most cases cheaper to obtain than man made fibres such as glass and carbon. Table 1.1 shows the relative pricing of various natural fibres in comparison to E-glass fibre. Although these values give an indication as to the price of natural fibres, this is not entirely useful in the context of composite materials. Where fibre treatments are used, these treatments add an extra element in processing and thus more people and resources are involved in production which leads to higher costs. In some cases this can make fibres expensive enough that they are viewed as unattractive materials [1]. Furthermore, manufacturing techniques commonly utilised

for composites made using fibres such as glass and carbon may not be suitable for manufacturing composites with natural fibres. Production techniques for natural fibre reinforced composites need to be shown to be practically and economically viable and the only way is through mass production.

Table 1.1 Comparison of costs and volumes of various fibres [1]

Fibre	Price in Comparison to Glass Fibres (%)	Production (1000 tons)
Jute	18	3600
E-Glass	100	1200
Flax	130	800
Sisal	21	500
Banana	40	100
Coir	17	100

A market survey of South African companies revealed an interest in developing new markets and products ranging from apparel and household textiles to tourist textiles, as well as a variety of applications in the automotive, building, construction and furniture industries [15]. A fibre industry could have many advantages for countries such as South Africa with emerging and developing economies. This is because opportunities in the industry range from low-tech cultivation and processing to high-tech research and development and manufacture. Although South Africa does not have a history of fibre cultivation, institutes such as the Council for Scientific and Industrial Research (CSIR) are investigating elements including identifying indigenous fibre plants and are conducting feasibility studies on domestic cultivation of fibre plants already cultivated abroad. Pilot projects involving flax cultivation are already underway in the Eastern Cape [16]. Together with agave farmers in the Cape, the CSIR is also investigating uses of waste obtained from tequila production, an alcoholic beverage made from agave plants [16].

South Africa has recognised the need for a fibre-based industry consisting of elements right from the cultivation through to manufacturing and research and development. In June 2001, the CSIR organised a workshop during which time a consortium was

established comprising research and development organisations, universities and industrial companies located both locally and abroad [15]. There is currently one local company in South Africa (Sustainable Fibre Solutions) producing non-woven fibre mats which can be used for manufacturing composites. The fibre being used for production of these mats is kenaf, grown locally in Winterton.

1.2 Natural fibre classification and processing

Fibres can be obtained from stems and roots (bast), leaves, fruits or seeds of plants. The plants range from small shrubs to tall trees and varieties are grown in almost all climates from tropical to temperate regions.

Examples of bast fibres include flax, hemp, jute and kenaf. In order to extract bast fibres, a process known as retting is used. This process involves leaving harvested plants to be partially decomposed by microbial activity which separates the fibre bundles from the rest of the plant matter. These fibre bundles are then mechanically combed in order to separate the fibres from one another [17]. This process is known as decortication.

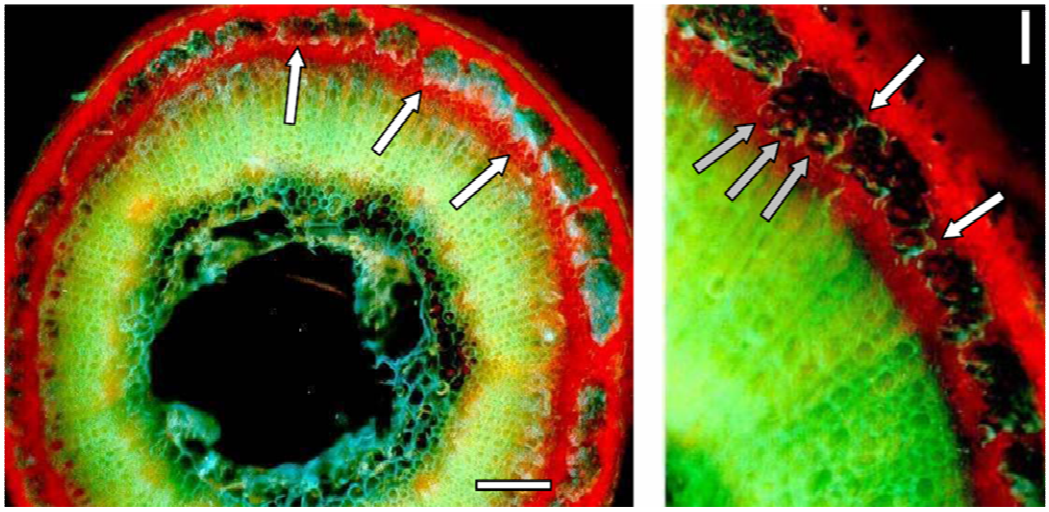

Figure 1.1 Cross-section of a flax stem (white arrows indicate fibre bundles) [17]

Leaf fibres refer to fibres obtained either from the actual leaf of a plant (for example sisal fibres) or from the sheaths connecting the leaf to the plant trunk (for example banana fibres). Fibres extracted from plant sheaths are typically obtained by decortication. Retting is sometimes also used to aid fibre extraction.

Examples of fruit and seed fibres are coir and cotton. Coir is obtained from the husk of coconuts and can be extracted either by pulling the fibres off the coconut or by retting depending on the ripeness of the fruit. Cotton comes from hairs that surround the seeds of the cotton plant and are removed by pulling the cotton bud from the plant and combing it.

1.3 Natural fibre structure

The components of natural fibres are cellulose, hemicellulose, lignin, pectin, waxes and water-soluble substances, with cellulose, hemicellulose and lignin as the basic components with regard to the mechanical properties of the fibres. The exception is cotton, as it contains no lignin [(1)].

A natural fibre is in itself a composite comprised of cellulose fibrils held together by lignin and pectin in a hemicellulose matrix [(8)]. Natural fibres can be considered natural equivalents of man made fibres such as carbon because cellulose forms a microcrystalline structure. Within this structure are regions of high order (crystalline regions) and regions of low order (amorphous regions) [(1)]. These crystalline regions are roughly aligned in the fibre direction.

Each natural fibre cell has two walls, a thin primary wall and a thick secondary wall with three layers. The middle layer of the secondary wall (S2) primarily determines the mechanical properties of a natural fibre as it constitutes around 80 % of the total thickness of the cell wall [(8)]. This layer is comprised of helically wound microfibrils made of long chains of cellulose molecules [(1)].

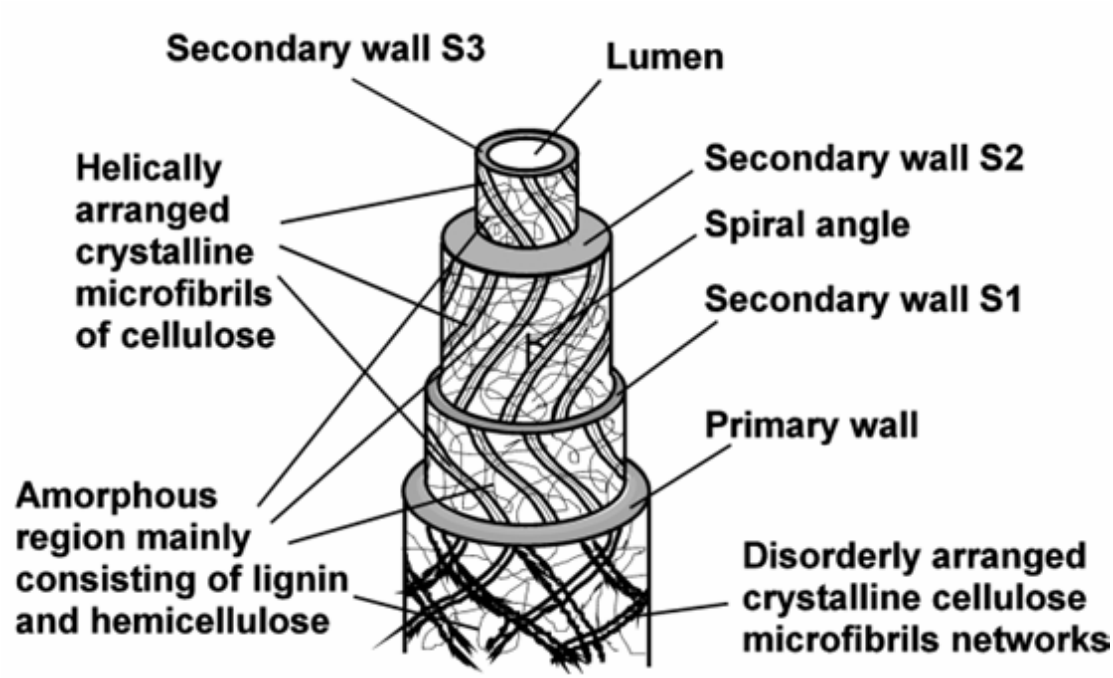

Figure 1.2 Structure of a plant fibre [8]

The mechanical properties of tensile strength and elastic modulus can be loosely correlated to the percentage of cellulose that a natural fibre comprises and the angle of the cellulose microfibrils relative to the fibre longitudinal axis respectively. Generally, higher cellulose content implies a higher tensile strength and a higher microfibril angle implies a lower elastic modulus [1]. According to Bledzki and Gassan [1], many theories have been developed in an attempt to use these two parameters to describe the mechanical properties of natural fibres but they are not greatly accurate and describe some natural fibres better than others. This is due to a number of factors. Most importantly is that the degree polymerisation differs greatly from plant to plant and the degree of polymerisation is independent of cellulose content. A higher degree of polymerisation of cellulose gives greater tensile strength. There are two types of cellulose that exist in natural fibres, type 1 and type 2. The mechanical properties of the fibre also depend on these because each type of cellulose has its own cell geometry [1]. Hemicellulose can in some cases also contribute to the strength of a natural fibre to a certain degree which is determined by the degree of polymerisation [1]. Unlike cellulose, hemicellulose differs from plant to plant and, as stated previously, forms the matrix of the micro-composite that constitutes natural fibres. Table 1.2 lists the mechanical properties of some common natural fibres.

Table 1.2 Mechanical properties of some common natural fibres

Fibre	Tensile Strength (MPa)	Tensile Modulus (GPa)	Failure Strain (%)	Specific Gravity	Reference
Flax	500-900	50-70	1.3-3.3	1.4-1.5	18
	900-1200	100	2-3	1.54	19
Hemp	310-750	30-60	2-4	1.48	18
	400-700	35	1.6-2.5	1.48	19
Jute	200-450	20-55	1.16-1.5	1.3-1.4	18
	400-700	2.5-15	1.5-2	1.45	19
Sisal	80-840	9-22	3-7	1.3-1.45	18
	500-600	9.4-16	3-7	1.45	19
Kenaf	-	-	-	1.52	18
	350-600	40	2.5-3.5	1.5	19

1.4 Manufacturing natural fibre reinforced composites

1.4.1 Introduction

In terms of mechanical properties of composites, the requirement for high performance composites (i.e. high stiffness and strength) is an optimal combination of high fibre content (fibre loading) and low porosity (void) content [11]. These two factors also have a direct bearing on moisture sensitivity. Thomas *et al.* [20], found that moisture absorption increased almost linearly with fibre loading for composites made from polyethylene and pineapple-leaf fibre and Sreekumar *et al.* [10] showed that water absorption increased with increasing void content. Reducing void content decreases the volume in which water can be stored in a composite and also decreases the number of pathways along which moisture can travel and penetrate.

1.4.2 A practical example using the hand lay-up technique

The process of hand lay-up involves the addition of resin to a chosen fibre reinforcement which is then worked in by hand using brushes and / or rollers. Composites made from glass fibre chopped strand mat using the hand lay up technique typically have a fibre mass of around 30 % of the total composite mass (this is known as the fibre mass fraction). It was found that composites made from natural

fibres using the hand lay up technique result in fibre mass fractions of around 10 % and this figure is difficult to achieve. For these mass fractions to be meaningful, they must be converted to volume fractions due to the difference in density between glass fibres and natural fibres. Consider a glass fibre reinforced composite containing 30 grams of glass fibres and 70 grams of resin:

$$M_f = \frac{m_f}{m_c} = \frac{30}{30+70} = 0.3 = 30\ \% \tag{1.1}$$

Where, M_f represents the fibre mass fraction, m_f the actual fibre mass and m_c the mass of the composite. This mass fraction can then be converted to a volume fraction as follows:

$$V_f = \frac{v_f}{v_c} = \frac{\frac{m_f}{\rho_f}}{\frac{m_f}{\rho_f}+\frac{m_m}{\rho_m}} = \frac{\frac{30}{2.6}}{\frac{30}{2.6}+\frac{70}{1.1}} = 0.153 = 15.3\ \% \tag{1.2}$$

Where, V_f represents the fibre volume fraction, v_f the fibre volume, v_c the composite volume, ρ_f the fibre density, ρ_m the matrix density and m_{m} the matrix mass. We can now reorder the above equation and substitute the value of density for natural fibres in place of that for glass fibres and determine what the equivalent mass of natural fibres is:

$$m_f = \frac{V_f \cdot \frac{m_m}{\rho_m} \cdot \rho_f}{1-V_f} = \frac{0.153.\frac{70}{1.1}.1.5}{1-0.153} = 17.243\ g \tag{1.3}$$

This can then be converted to a mass fraction by the following:

$$M_f = \frac{m_f}{m_c} = \frac{17.243}{17.243+70} = 0.198 = 19.8\ \% \tag{1.4}$$

It can be seen from this example that in order to produce composites from natural fibres having a fibre volume fraction equivalent to that produced by hand lay-up with glass fibres, a fibre mass fraction of almost 20 % is required. This figure is almost twice that which is possible to obtain using a conventional process such as hand lay-up. It is obvious that there is much need for developing manufacturing techniques for natural fibre reinforced composites.

The primary reason higher fibre fractions are hard to obtain with natural fibres is due to the lower compaction of natural fibre mats when compared to their glass counterparts. It was found that when resin was added to natural fibre mats, the level of compaction was in fact so low that resin began to flow out of the mat before adequate wetting could be obtained. Pressing fibre mats at elevated temperatures was experimented with and although it helped, it was still unable to produce high enough fibre fractions. Apart from problems associated with achieving acceptable fibre fractions, it is also difficult to determine the fibre fractions in composites produced using hand lay-up, vacuum infusion, vacuum bagging or compression moulding because the composites cannot be subjected to commonly used methods for determining fibre fractions such as burn-off tests.

1.4.3 Resin transfer moulding and vacuum infusion

Resin transfer moulding (RTM) and vacuum infusion have recently gained much popularity due to a low labour requirement, acceptable cycle times, good finish, good dimensional tolerances, good process control, reduction of material handling, low cost when compared to other processes, minimal waste, high fibre loading and low void content [(21)].

RTM utilises two rigid matching mould faces. Fibrous reinforcements are laid into the mould cavity and the mould is closed. Resin is then pumped into the mould through inlet ports under pressure. Excess resin escapes from the mould via exhaust ports once the fibres are wet out. A vacuum can be applied to the exhaust ports in addition to the pressure applied at the inlet ports to increase the resin flow rate and reduce the amount of air inside the mould that can result in voids. In the most basic form, vacuum infusion can be considered to be similar to RTM except that one of the mould

faces is replaced by a flexible skin [21]. After laying the fibrous reinforcements into the mould, it is covered by a vacuum bag which is sealed using tacky tape. A vacuum is then drawn on the exhaust ports evacuating air and drawing resin in through the inlet ports.

Vacuum infusion was experimented with before RTM in order to gain an insight into the way in which resin flows in these processes and to determine what fibre fractions are obtainable. Vacuum infusion worked with natural fibres but as in the case of hand lay up, the fibre fractions that resulted were low. Fibre mass fractions ranged from 13 % to 16 % depending on the natural fibres used (kenaf and sisal were experimented with). Looking at the example presented in the previous section, these figures are still under the 20 % required to have the same fibre fraction as hand laid-up composites made using glass fibre.

When using vacuum infusion, the fibre fraction that results is due to the pressure differential between atmospheric and vacuum pressures which compacts the fibres under the vacuum bag. The vacuum which can be drawn is most often physically limited by the resin. In the case of polyesters and vinyl esters, the styrene in these resins begins to boil if the pressure is too low (found to be around 35 - 40 kPa absolute pressure). Epoxy resins do not suffer from this problem but when the pressure differential becomes too high, other problems such as leaks caused by tacky tape flowing into the evacuated area make the process impractical. RTM avoids these problems caused by the flexible mould face and in addition, the fibres can be compressed without relying on atmospheric pressure.

RTM was chosen as the manufacturing technique to be used for this investigation. The method has many advantages such as the opportunity to alter many manufacturing parameters including pressure and temperature before during and after injection. Composite quality and cycle times can thus potentially be controlled to a greater degree. Additionally, fibre fractions obtained using RTM are some of the highest achieved by any manufacturing method in literature. Sreekumar *et al.* [10] was able to achieve fibre volume fractions of up to 50 % using RTM and non-woven fibres.

2 LITERATURE SURVEY

2.1 Natural fibres in RTM

There is not much work concerning natural fibres and RTM. The following sources represent all the works found on the subject. This section of the literature survey is presented in chronological order according to the published date and the order does not have any bearing on relevance.

O'Dell [22] is the earliest work found using RTM with natural fibres. Jute fibres were directly substituted for glass fibres in commercial RTM equipment. The aim of this work was to determine the suitability of RTM to natural fibre composites with regard to resin flow, air entrainment and surface properties. Mechanical properties and resistance to simulated weathering were also examined.

Panels of composites were produced from glass chopped strand mat (CSM), untreated jute non-woven mat and aqueous glycol treated jute non-woven mat. The resin used was a low-viscosity orthophthalic polyester into which 5 % by weight of $CaCO_3$ filler was mixed. Fibre volume fractions ranged from 10-15 %. At the beginning of injection the mould temperature was 55°C and the injection pressure was varied by an operator throughout the injection process but did not exceed 240 kPa.

It was observed that resin flowed as easily through jute as it did through glass. Fibre wet-out was the same for jute and glass with minimal visible air bubbles [22].

Tensile and flexural strength and modulus were evaluated as well as notched and unnotched impact energy (Izod) according to ASTM standards 638-90, 790-90 and D256 respectively. All of the tests were conducted in the longitudinal and transverse axes of the composites because there were more fibres oriented in the longitudinal direction [22]. Results of the tensile and flexural tests showed the jute composites to have lower tensile and flexural strength and modulus than the glass composites but values were of the same order of magnitude [22]. Impact tests revealed that the jute composites absorbed an order of magnitude less energy than the glass composites did. O'Dell [22] concluded that the glycol treatment did not improve the quality of the

composites and that jute composites had properties almost the same as those of the unreinforced resin. Table 2.1 contains a summary of the results from O'Dell [22].

Table 2.1 Mechanical properties of jute polyester composites manufactured by RTM [22]

Fibre/ Treatment	Fibre Vol. Fraction (%)	Orientation	Tensile Strength (MPa)	Tensile Modulus (GPa)	Flexural Strength (MPa)	Flexural Modulus (GPa)	Izod Impact Energy (J/m)
Jute/ Untreated	10-15	Long.	45.818	3.695	61.646	3.050	32.50 notched 38.73 unnotched
		Trans.	26.845	1.884	46.759	2.236	39.75 notched 58.85 unnotched
Jute/ Glycol	10-15	Long.	43.488	3.225	63.153	3.213	28.64 notched 32.40 unnotched
		Trans.	28.076	2.392	48.292	2.338	37.62 notched 48.96 unnotched
Glass/ Silane	10-15	Long.	114.234	7.087	161.916	6.206	376.81 notched 376.63 unnotched
		Trans.	91.358	7.063	135.459	5.070	343.46 notched 349.71 unnotched

The work of O'Dell [22] is the only work found to have utilised non-woven jute fibres for manufacturing composites using RTM. The work proved that RTM is a feasible method of manufacture for natural fibre reinforced composites. The results of the mechanical tests conducted can be used only for comparative purposes because the fibres used are jute and not kenaf. Furthermore, the data is not completely reliable because composites containing various fibre volume fractions ranging from 10-15 % were directly compared. O'Dell [22] concluded that the glycol treatment used had no effect on the composite interface and properties. Mention had been made however that a small amount of light machine oil had been applied to the fibres for ease in processing and it was not considered that this may have prevented the glycol from having the desired affect. The results reported for exposure of the composites to simulated weather conditions only include that there was no visible change in surface

appearance and do not supply any information as to the effects on mass or mechanical properties that the weathering may have had.

Sèbe *et al.* [9] produced composites made from non-woven hemp and polyester resin. Untreated fibres, methacrylic anhydride treated and pyridime treated fibres were used. Glass polyester composites were also produced for comparative purposes. Flexural and impact tests (Charpy) were conducted according to BS2782: Part 10: Method 1005: 1997 and BS2782: Part 3: Method 359: 1984. A scanning electron microscope (SEM) was used to examine failure surfaces of the untreated and treated hemp composites in order to determine modes of failure (be it fibre pull-out or fibre fracture).

Panels of composites were produced according to an industrial process for the manufacture of glass fibre reinforced car parcel shelves. Before manufacture, the fibres were equilibrated at 23°C and 50 % relative humidity. Mould temperature was 30°C at the beginning of injection and a pressure of 2 bars was used with vacuum assistance to inject resin. Samples were post cured. Untreated hemp composites were made with fibre mass fractions ranging from 0-36 %. Mass fractions were used by the authors because volume fractions were considered inaccurate due to errors introduced by the presence of voids. Treated hemp samples were produced with fibre mass fractions of 26 % only and glass samples with fibre mass fractions of 15 % only.

The flexural strength of the hemp composites only became similar to that of the glass composites at high fibre mass fractions of around 35 %. The flexural modulus of the hemp composites became similar at slightly lower mass fractions of around 28 %. According to the results, there was no change in flexural strength for either of the treated hemp composites when compared to the results for the untreated ones. Flexural modulus however was found to increase for hemp fibres subjected to the methacrylic anhydride treatment but remained the same for the pyridime treatment. The values for impact strength of the hemp fibre composites were much lower than those for the glass fibre composites. The highest value of impact strength for the hemp fibre composites was measured at the highest fibre mass fraction of 36 %. The methacrylic anhydride treated hemp fibre composites were found to have an impact strength much lower than that of the untreated hemp fibre composites. Pyridime

treated hemp fibre composites showed an impact strength that was almost exactly the same as that for the untreated ones.

Sèbe *et al.* [9] concluded that both flexural strength and modulus increased in an exponential manner with fibre content for composites made with natural fibres. Impact strength was found to decrease at low fibre content then gradually increase with further addition of fibres [9]. Methacrylic anhydride treatment lead to improved interfacial adhesion between the fibres and matrix and pyridime treatment had no effect. In methacrylic anhydride treated fibre composites, this was made evident by a change in mode of failure from fibre pull-out to fibre fracture and by increased flexural modulus and decreased impact energy. SEM micrograhs showing the change in failure mechanism can be seen in Figure 2.1. The results obtained by Sèbe *et al.* [9] for flexural strength and modulus and impact strength can be seen in Table 2.2 (results are approximate as they were estimated from graphical data).

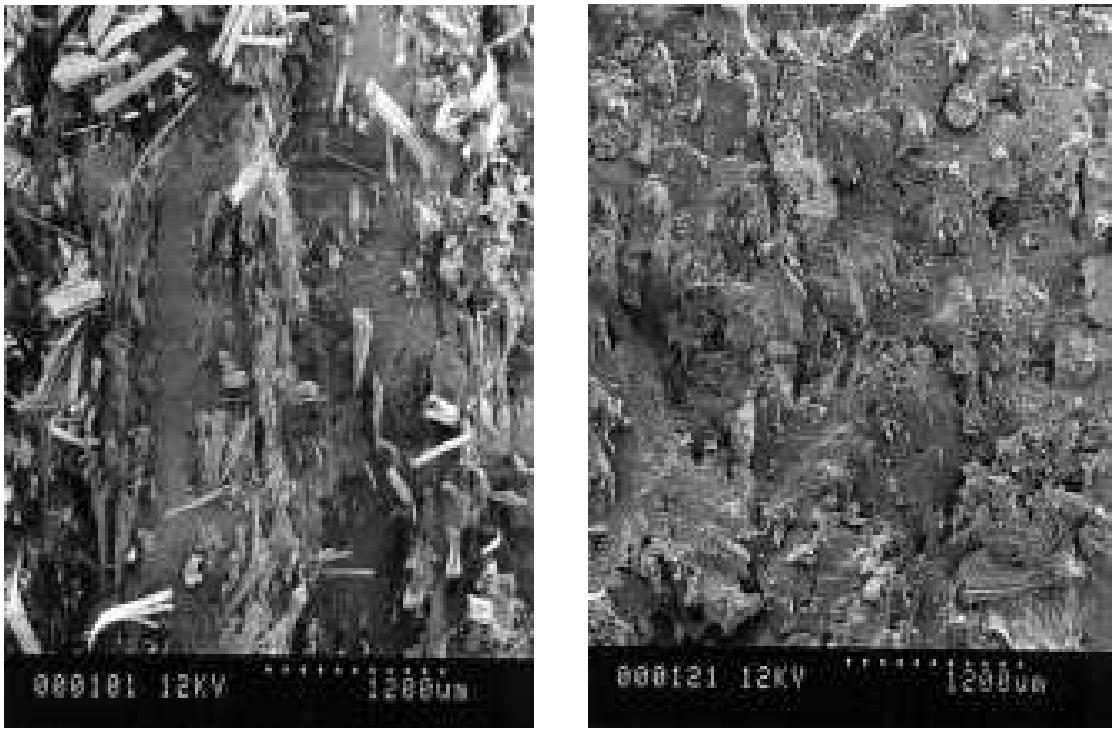

Figure 2.1 SEM of impact failure surfaces of untreated and methacrylic anhydride treated hemp polyester composites [9]

Table 2.2 Properties of hemp polyester composites manufactured by RTM [9]

Fibre/ Treatment	Fibre Mass Fraction (%)	Flexural Strength (MPa)	Flexural Modulus (GPa)	Charpy Impact Energy (Unnotched) (kJ/m^2)
Hemp/ Untreated	11	47	3.9	2.5
	17	58	4.2	7.0
	28	90	5.4	9.0
	33	96	6.0	11.0
	36	112	7.4	15.0
Hemp/ Pyridime	26	76	5.4	8.0
Hemp/ Methacrylic Anhydride	26	76	6.6	3.5

Joffe *et al.* [23] compared the tensile and tensile fracture properties of a number of natural fibre reinforced thermoset composites against glass fibre reinforced thermoplastics. These materials were compared in order to determine if natural fibre reinforced thermosetting composites could replace glass fibre reinforced thermoplastics in automotive interior parts. The aim was to choose the best resin system based on fibre-matrix compatibility, tensile strength and stiffness and fracture toughness.

Non-woven flax fibres with five thermosetting resins were investigated including three polyesters, one vinyl ester and one epoxy. For comparative purposes, glass CSM polypropylene composites were used. Natural fibre composites were produced with a 30 % fibre volume fraction and glass ones with a 20 % fibre volume fraction because these values resulted in composites with almost identical densities.

The results of the tensile tests showed that all the flax fibre composites except one of the polyesters had a higher tensile strength when compared to the glass fibre composites. In addition, all of the flax composites had a higher Young's modulus and lower strain at failure. In the fracture toughness tests, the glass composites performed best but the flax composites made with the vinyl ester and one of the polyesters were

found to have a fracture toughness within 73 % that of the glass composites. Joffe *et al.* [23] concluded that three of the resins would be suitable for manufacturing competitive natural fibre composites and include a polyester, vinyl ester and epoxy. This allows for selection of a resin system on the basis of cost and environmental impact as well as mechanical performance. The results obtained by Joffe *et al.* [23] for the tensile tests are summarised in Table 2.3.

Table 2.3 Properties of flax composites manufactured by RTM [23]

Fibre/ Matrix	Fibre Volume Fraction (%)	Tensile Strength (MPa)	Tensile Modulus (GPa)
Flax / Polyester 1	30	47.9	6.110
Flax / Polyester 2	30	71.6	8.350
Flax / Polyester 3	30	88.3	10.890
Flax / Vinyl Ester	30	79.2	10.020
Flax / Epoxy	30	91.2	9.760
Glass / PP	20	67.1	5.320

One of the most important aspects of this work is that natural fibre composites were compared against an existing product and compared on a basis that highlighted one of the motivating factors for their use i.e. acceptable specific mechanical properties. Unfortunately, only single fibre volume fractions were tested so there is not much data for comparison and it does not detail the manufacturing process.

Rouison *et al.* [24] produced a model for simulation of cure in natural fibre composites produced using RTM. This model was compared to experimental data obtained using thermocouples which were placed inside the mould prior to resin injection. In the same paper, tensile and flexural strength of the natural fibre composites and moisture absorption and rate of absorption of the fibres were determined. Tensile and flexural tests were conducted according to ASTM D638 and D790.

Flat panels were manufactured using non-woven mats comprising 67 % hemp and 33 % kenaf and polyester resin. Composites with fibre volume fractions of 10.70 %, 16.20% and 20.60 % were manufactured and tested. Composites with fibre volume fractions higher than 22 % could not be produced without risking curing of the resin before the end of the injection process [24]. The design of the aluminium mould used allowed for it to be evacuated and heated in order to dry the fibres and it also allowed for temperature control during the injection process. Resin was injected at a pressure of 172 kPa and the temperature of the mould was held constant between 15°C and 20°C during resin injection. Following resin injection, the mould temperature was increased to and maintained at 53°C for curing.

Following manufacture of the composites, it was observed that good wetting of the fibres was obtained and that few voids could be seen [24].

Both tensile and flexural strength were found to increase with increasing fibre volume fraction. For samples containing 20.6 % by volume of fibres, a tensile and flexural strength of 44.3 MPa and 71.4 MPa respectively were obtained. Comment was made that strength values could, in fact, have been improved because the degree of cure in the composites was reportedly only around 86-87 % due to the use of old initiator (catalyst). According to the authors, fibre pull-out could be observed on specimen failure surfaces indicating that fibre-matrix adhesion could be improved. SEM studies were not conducted.

In this paper, Rouison *et al.* [24] focused mainly on curing of the composites and did not investigate mechanical properties in much detail. Tensile and flexural strength were investigated while moduli were not. The results from this work do however provide much practical insight into the manufacturing of natural fibre reinforced composites by RTM in that the process and experimental setup were explained in great detail.

Another work by Rouison *et al.* [25] continued on from their previous research and built on some of the shortcomings. In the previous work, the cure model had to be corrected in order to obtain reasonable accuracy which was the result of the use of old initiator. The experiments of their previous work were repeated with new initiator and

they conducted several more mechanical tests. Tensile, flexural, Izod impact and flexural creep tests were conducted in accordance with ASTM D638, D790, D256 and D2990 respectively. This time tensile and flexural tests included modulus.

The same materials, experimental process and equipment were used as previously but composites with fibre volume fractions of up to 35 % percent were produced. This was made possible by hot pressing fibre mats at 100°C before moulding, increasing injection pressure to 308 kPa and increasing the number of inlet ports and their diameters. Curing temperatures of 50°C, 59°C and 67°C were used in this work and the samples were post-cured. Only results for the cure model were presented for all the various temperatures. The use of the new initiator resulted in their cure model producing more accurate estimates of temperatures experienced during cure than their previous tests.

The results of tensile, flexural and impact tests showed a linear increase with increasing fibre content. For composites containing a fibre volume fraction of 35 %, a tensile strength, flexural strength and impact strength of 60.2 MPa, 112.9 MPa and 14.2 kJ/m^2 respectively were obtained. Results of creep tests were for cyclic loads of 27 % and 43 % of ultimate strength as determined previously for composites containing 20.6 % fibre volume fraction. For composites loaded to 27 %, the curve of creep strain stabilised and reached a plateau while for those loaded to 43 %, the curve increased fast initially and then became linearly increasing. The results of the tensile, flexural and impact tests conducted by Rousion *et al.* [25] are summarised in Table 2.4.

Table 2.4 Properties of hemp / kenaf polyester composites manufactured by RTM [25]

Fibre	Fibre Volume Fraction (%)	Tensile Strength (MPa)	Tensile Modulus (GPa)	Flexural Strength (MPa)	Flexural Modulus (GPa)	Izod Impact Energy (kJ/m^2)
Hemp / Kenaf	20	32.9	1.421	54.0	5.02	4.8
	35	60.2	1.736	112.9	6.38	14.2
Glass	20	85.0	1.719	175.9	7.74	60.8

This paper contains more on the mechanical properties of hemp / kenaf fibre reinforced composites than the previous work by the authors. There is good data for comparison and it gives results over a reasonable cross-section of fibre volume fractions. The authors, however, state that some of the observations made can only be conclusive once further testing has been conducted as there are no samples containing between 22 % and 35 % fibre volume fraction. The results of the flexural creep tests indicate that these materials can bear moderate loads of about 30 % of the flexural breaking load without any significant deformation [25].

Sreekumar *et al.* [10] produced sisal fibre reinforced composites by RTM and compression moulding. They compared the results of tensile, flexural and water absorption tests for the two manufacturing methods and also investigated the effects of varying fibre length and fibre volume fraction. The results of these tests were then compared against theoretical models. Tensile and flexural tests were conducted in accordance with ASTM D638 and D790. In the case of water absorption tests, no testing standard was mentioned and the tests took place at 30°C, 60°C and 90°C. Sreekumar *et al.* [10] also compared the void content for RTM and compression moulded composites.

Before producing composites, the fibres were cut to the desired length (10 mm, 20 mm, 30 mm and 40 mm), washed with water, dried in air and arranged inside the mould. Resin was injected at approximately 100 kPa with vacuum assistance in composites produced by RTM. Composites produced by compression moulding were

made by first soaking the fibres in resin and then pressing at approximately 1000 kPa. Both processes took place at room temperature. Fibre volume fractions for both RTM and compression moulding ranged from around 20 % to 50 %.

Results of the tensile and flexural tests showed that a fibre length of 30 mm was optimal for producing the highest strength and modulus of composites. Composites made by RTM showed a maximum tensile strength and modulus at a fibre volume fraction of 43 % and a maximum flexural strength and modulus at a fibre volume fraction of 50 %. A similar trend was observed for composites made by compression moulding where a point was reached that increasing fibre content became detrimental to composite strength. For tensile and flexural strength and modulus, composites made by RTM performed better than those made by compression moulding. In addition, it was found that RTM composites had a lower void content and moisture uptake than those composites made by compression moulding. The authors report that SEM studies of failure surfaces indicate that composites made by RTM suffer less from fibre pull-out than those made by compression moulding. SEM micrographs comparing RTM and compression moulded composite failure surfaces can be seen in Figure 2.2. Four models for the prediction of Young's modulus were presented including parallel, series, modified rule of mixtures and Hirsch's model. The modified rule of mixtures and Hirsch's model were found to correlate well for both RTM and compression moulding. The model used for the prediction of water absorption did not correlate well with experimental data. A summary of the results of Sreekumar *et al.* [10] can be found in Table 2.5.

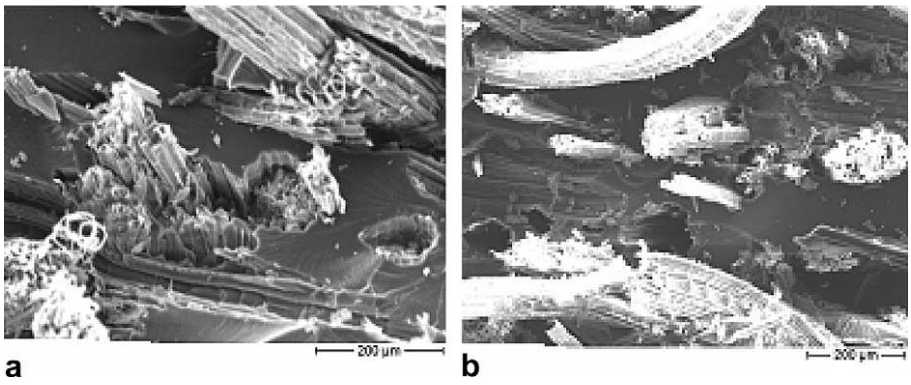

Figure 2.2 Failure surfaces of composites manufactured by (a) RTM and (b) compression moulding [10]

Sreekumar *et al.* [10] demonstrated the advantages of using RTM and directly compared results with another popular manufacturing method. Mechanical properties, water absorption and void content were all found to be superior in composites made by RTM. The authors also claim that composite failure by fibre pull-out is reduced when RTM composites are compared to their compression moulded counterparts. Examination of their SEM photographs does not conclusively support this. This is the only work found to investigate water absorption in non-woven natural fibre reinforced composites produced by RTM. The tests were not, however, conducted in accordance with any standard thereby making comparison difficult.

Table 2.5 Properties of sisal polyester composites manufactured by RTM and compression moulding [10]

Manufacturing Method	Fibre Volume Fraction (%)	Tensile Strength (MPa)	Tensile Modulus (GPa)	Flexural Strength (MPa)	Flexural Modulus (GPa)
RTM	0	41	0.968	61	2.461
	19	50	1.750	67	2.188
	27	57	1.956	76	2.934
	43	67	2.196	84	3.495
	50	61	1.856	92	3.972
Compression Moulding	0	39	0.895	57	2.432
	24	41	0.943	52	2.690
	34	52	1.400	62	3.335
	42	57	1.868	68	3.558
	48	55	1.291	58	2.585

In addition to the references already examined, there are a number of other works concerning RTM of natural fibre reinforced composites. These have been excluded from in-depth examination as they are not of significant relevance to this investigation. A brief description of each follows.

Zhang and Richardson [26] conducted an experimental investigation and flow visualisation of the RTM process for non-woven hemp fibre reinforced phenolic composites. The aim of the research was to investigate aspects of the mould filling

process including fibre-washing, edge flow, mould filling profiles and velocity profiles with various fibre mass fractions.

Oksman [2] manufactured unidirectional flax-epoxy composites by RTM. Epoxy was used due to the expected adhesion with the fibres [2]. The tensile properties of composites made using traditionally retted flax, bio-technically retted flax and glass fibre were compared. The composites made using the bio-technically retted flax were found to be superior to the traditionally retted flax composites. Although not as strong as the glass composites, the bio-technically retted flax composites had a higher tensile modulus.

Rodriguez *et al.* [7] manufactured untreated and alkali-treated fibre composites by RTM using bi-directional jute fabric and vinyl ester resin. Flexural strength and modulus and Izod impact tests were conducted. The strength and modulus of alkali-treated fibres were found to be lower than untreated fibres in fibre filament tests. The same trend was observed for the composites. Impact energy was also lower for the alkali-treated fibre composites than for those made using untreated fibres.

2.2 Processing conditions

It is common practise when manufacturing natural fibre reinforced composites that the fibres are dried or conditioned before use. This is done to remove or control moisture which can result in voids and poor fibre-matrix adhesion [18]. By removing moisture from fibres before producing composites, the mechanical properties could be increased and the need for potentially expensive surface treatments avoided. Bledzki and Gassan [1] reported a 10 % increase in tensile strength and 20 % increase in Young's modulus for jute-epoxy composites made using dried fibres but did not mention the fibre loading, fibre weave or the manufacturing method used. de Deus *et al.* [5] dried piassava fibres in an oven at 60°C for 30 minutes before producing unidirectional composites by compression moulding. An increase in flexural strength of around 30 - 40 % was reportedly achieved by drying the fibres.

Sèbe *et al.* [9] conditioned hemp fibres at 23°C and 50 % relative humidity before producing composites by RTM. Rouison *et al.* [24, 25] used RTM to produce

hemp / kenaf polyester composites and vacuum dried the fibres in the mould at 55°C for 2 hours before resin injection. Aziz *et al.* [27, 28] produced kenaf fibre reinforced composites with various polyesters and cashew nut shell liquid matrix by compression moulding and dried their fibres before fabrication in an oven at 110°C for 5 hours. In these works [9, 24, 25, 27 & 28], no composites were produced in which fibres were undried for comparison of mechanical properties.

Processing temperature can also potentially contribute to fibre-matrix interaction. It is possible that due to differing coefficients of thermal expansion between fibres and resin, the resin could either squeeze or relax around the fibres [29]. In addition, it is also possible that applying heat during production could be sufficient to drive off moisture in the fibres. Sèbe *et al.* [9], Sreekumar *et al.* [10], O'Dell [22] and Rouison *et al.* [24, 25] used mould temperatures of 30°C, 23°C, 55°C and 15-20°C respectively but did not examine the effects that the mould temperature had on the properties of the resulting composites.

In addition to fibre drying and altering processing temperature, pressurisation of composites during cure could also potentially improve fibre-matrix interaction. However, this has not been previously explored in the production of natural fibre reinforced composites.

2.3 Resin system

Surface treatments are often used to improve the properties of natural fibre reinforced composites by bridging the gap in compatibility between the hydrophilic fibres and the hydrophobic matrices. Various resin systems offer differing levels of compatibility to natural fibres and can therefore affect the properties of natural fibre reinforced composites without the need for surface treatments. There are a number of common resin systems available for the production of fibre reinforced composites and these include polyesters, vinyl esters and epoxies. All have different properties of strength, modulus, adhesion, cure shrinkage and water absorption [12 - 14].

Polyesters are the most widely used resins for fibre reinforced plastics [12, 14]. They are inexpensive, easy to use and have good mechanical properties such as impact

resistance, but, their disadvantages include poor adhesion and high cure shrinkage [12, 14]. Epoxy resins have excellent mechanical properties, low cure shrinkage, excellent adhesion and compatibility with many fibres and other materials. Epoxy resins are, however, generally expensive and can be sensitive to moisture [12 - 14]. Vinyl esters constitute a middle ground between polyester and epoxy resins and represent a compromise in cost and performance.

The effects of using different resin systems in the manufacture of non-woven flax fibre reinforced polyester composites by RTM has been investigated by Joffe *et al.* [23]. These investigators conducted tensile and fracture toughness tests on flax fibre reinforced composites made using three polyesters, a vinyl ester and an epoxy resin. These were compared to glass fibre reinforced polypropylene composites of equal density. This investigation showed that one of the three polyesters, the vinyl ester and the epoxy produced flax composites with comparable properties to those of the glass fibre reinforced polypropylene composites. SEM examinations were not conducted to determine if fibre-matrix adhesion was improved by using any of these resins.

Several investigations [9, 10, 22, 24 & 25] have used polyester resins to produce non-woven natural fibre reinforced composites by RTM. Oksman [2] used epoxy resin and unidirectional flax fibres in RTM as it was expected that this would result in good bonding. Rodriguez *et al.* [7] used vinyl ester resin and alkali-treated, bi-directional jute fibre mats to manufacture composites by RTM. However, the results of these works [2, 7, 9, 10, 22, 24 & 25] cannot be compared since they all use either different fibres or weaves.

3 OBJECTIVES

3.1 Development of objectives

It is evident from the literature review that there are a number of tests being used to characterise the properties of composites made using natural fibres. These tests include tensile, flexure, impact and water absorption. Tensile, flexural and impact tests provide data regarding the mechanical performance of composites. Water absorption tests provide data which can indicate any number of things including; sensitivity to moisture (in terms of mass and dimensional stability), fibre-wetting by the matrix, fibre-matrix adhesion and void content. Of the five authors' works examined in detail, four conducted tensile tests [10, 22, 23 & 25], four conducted flexural tests [9, 10, 22 & 25], three conducted impact tests [9, 22 & 25] and one conducted water absorption tests [10]. None of the authors conducted all four tests.

Sèbe *et al.* [9] and Sreekumar *et al.* [10] made use of electron microscopes to examine failure surfaces of either impact or tensile specimens in order to determine the mode of failure of their composites. Rouison *et al.* [24] made mention of failure mechanism but did not use an electron microscope to verify the results. Determining the mode of failure gives a good indication of fibre-matrix adhesion. In the case of poor fibre-matrix adhesion, fibre pull-out is normally the cause of composite failure and in the case of good fibre-matrix adhesion, fibre fracture is normally the cause.

The literature survey suggests that the performance of natural fibre reinforced composites can be improved by methods such as fibre drying, altering mould temperature and by utilising different resin systems. In addition to these, pressurisation of composites during cure could also potentially improve fibre-matrix interaction. If altering processing conditions or resin system proves successful, the major implication is that better performance can be obtained from composites without the need for potentially complex and expensive fibre treatments.

Work regarding the use of kenaf fibres as reinforcement in thermosetting matrices has been conducted by Aziz *et al.* [27, 28 & 30] using compression moulding and a number of works examined other non-woven natural fibre reinforced composites produced by

RTM [9, 10, 22, 23, 24 & 25]. There have been no previous works in which kenaf fibres have been used as the reinforcement in composites manufactured by RTM. Furthermore, only one work [23] has examined the effects of using various resin systems on the properties of composites manufactured by RTM. Thus, there is scope for a systematic comparison of properties of non-woven kenaf fibre reinforced composites produced by RTM using various processing conditions and a number of resin systems.

3.2 Objectives

- Determine the best method for drying of natural fibres.
- Produce kenaf fibre reinforced polyester composites by RTM and alter the mould temperature, fibre moisture content and mould pressure.
- Produce kenaf fibre and glass fibre reinforced composites using three resin systems namely polyester, vinyl ester and epoxy.
- Investigate the resulting tensile, flexural, impact and water absorption properties of composites.
- Compare the properties of the composites in an appropriate manner.
- Compare the experimental results with those of a micromechanical model where applicable.
- Conduct SEM studies into the failure mechanisms of kenaf fibre reinforced composites.

4 PRODUCTION

4.1 Production material

4.1.1 Fibres

The fibre mats used in this investigation were donated by Sustainable Fibre Solutions, South Africa. The mats are made of kenaf cultivated in South Africa and are produced by a process known as needle punching. The fibre mats were ordered with an areal density of 450 g/m^2. This value was chosen so that depending on the number of layers used, the approximate fibre volume fractions shown in Table 4.1 would result.

Table 4.1 Expected fibre volume fractions for various numbers of fibre layers

No. Layers	Fibre Volume Fraction
2 Layers	15 %
3 Layers	22.5 %
4 Layers	30 %

Using one layer of fibre mat results in fibre volume fractions too low to produce any meaningful outcomes. The highest fibre volume fraction was selected based on the literature survey and represents the maximum value other authors could practically achieve without the use of either hydraulics to close moulds or hot-pressing of fibre mats before use.

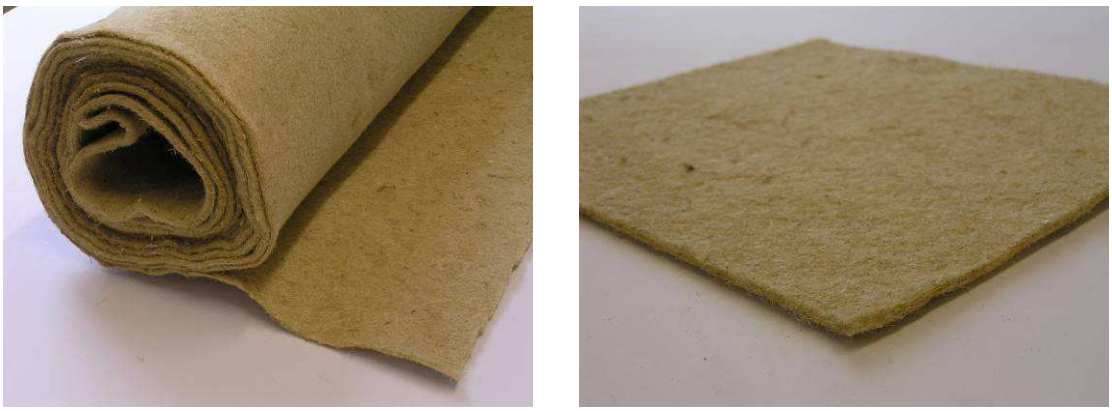

Figure 4.1 Kenaf non-woven fibre mat

4.1.2 Resins

The resins chosen included a polyester, a vinyl ester and an epoxy. All were specifically formulated for use in vacuum infusion and RTM.

Polyester Resin

The polyester resin used was “Scott Bader Crystic 1141”. It is an orthophthalic unsaturated polyester resin of low viscosity. The resin was supplied with “Crystic Accelerator E” and “Andonox KP-9” catalyst (M-200 catalyst). Scott Bader was unable to supply data regarding mechanical properties for this specific resin system but a representative in the technical department of the company provided assurance that properties for all orthophthalic polyester resins are approximately the same. A data sheet for “Scott Bader Crystic 196” was supplied by the representative.

Table 4.2 Properties of Scott Bader Crystic 196 polyester resin

Property	Unit	Value
Tensile Strength	MPa	69
Tensile Modulus	MPa	3800
Strain to Failure	%	2.3

Vinyl Ester Resin

The vinyl ester resin initially purchased was “Scott Bader DP 333” and it was supplied with “Scott Bader Accelerator VE” and “Norox MEKP 925” catalyst (M-100 catalyst). This resin system was abandoned for reasons that will be explained in section 4.4.2.

The vinyl ester resin used as a replacement was “Derakane Momentum 411-350 Epoxy Vinyl Ester Resin”. The accelerator used with this resin was Cobalt Naphthenate 1 % (the data sheet indicated the use of a 6 % concentration so quantities of accelerator were multiplied by a factor of 6 when mixing resin). The catalyst used was “Norox MEKP 925”. Although suitable for a number of production techniques,

according to the data sheet it is suitable for use in vacuum infusion and RTM. Typical properties of this resin system can be found in Table 4.3.

Table 4.3 Properties of Derakane Momentum 411-350 vinyl ester resin

Property	Unit	Value
Tensile Strength	MPa	86
Tensile Modulus	MPa	3200
Strain to Failure	%	5-6
Flexural Strength	MPa	150
Flexural Modulus	MPa	3400

Epoxy Resin

The epoxy resin used comprised of “SP Prime 27 Epoxy Resin” with “SP Prime 20 Slow Hardener”. Typical Properties of this resin system can be found in Table 4.4.

Table 4.4 Properties of SP Prime 27 epoxy resin

Property	Unit	Value
Tensile Strength	MPa	73.3
Tensile Modulus	MPa	3470
Strain to Failure	%	4.5

4.2 Production equipment

4.2.1 Resin transfer moulding machine

From experimentation conducted using vacuum infusion with polyester resin, it became evident that there were problems with resin curing too quickly and when accelerator and catalyst ratios were reduced, inadequate curing occurred. The major factor affecting cure times was that the resin had to be mixed in a large quantity in order to provide enough resin for an entire specimen (typically 600-800 grams). When quantities of this size are mixed, the exothermic reaction which the resin undergoes produces higher temperatures than if smaller quantities are mixed and this leads to

shorter cure times (curing information in data sheets is typically for 100 grams of resin). Attempts were made to separate resin into smaller quantities and to introduce it into the resin reservoir as needed. This required a lot of attention and special care. After ruining a number of specimens by not maintaining the resin level in the reservoir or not having resin mixed in time, it was decided that this method of supplying resin was impractical.

RTM typically utilises what is known as a pressure pot which is similar to using a resin reservoir in vacuum infusion. The required amount of resin is mixed, placed in the pressure pot, the pressure pot is connected to a compressed air line and resin is then injected into the mould.

It became clear that an RTM machine capable of mixing resin “in-line” would make manufacturing easier and more controllable. The main advantage of using an RTM machine of this design is that resin is mixed with catalyst just before it enters the mould so the problem of resin curing too soon is significantly reduced. Further advantages include reduced waste, easy operation, low labour requirement, lower exposure to harmful chemicals and much faster cycle times.

Given constraints on time and cost, it was decided that an RTM machine of the required design would have to be designed and built. With little knowledge about the workings of such machines, a concept was developed based on a number of photographs and an idea developed from a schematic in Zhang and Richardson [26]. The basic concept involved two cylinders with pistons, one would inject resin and another would inject catalyst and the two would be connected with an arm in order to control the ratio of resin to catalyst. The resin cylinder was to have resin on one side of the piston and air on the other, thus allowing the piston to be driven using compressed air. The resulting motion of the arm caused by the compressed air on the resin piston would also cause the catalyst piston to move. The resin and catalyst would be mixed in a static mixer.

A number of discussions were held with an experienced pneumatics engineer on how pneumatic cylinders operate in terms of the available seals (types and materials), operating pressures and a number of other parameters. A company that specialises in

custom pneumatics was contacted and two lengths of pipe were obtained to form the cylinders. One pipe was made from aluminium and had an internal diameter of 100 mm and the other from stainless steel with an internal diameter of 20 mm. These materials conformed to the requirements of chemical resistance for chemicals such as styrene (resin), peroxide (catalyst) and acetone (for cleaning). The rest of the machine was designed around these two cylinders.

Apart from the cylinders, pistons and piston rods, most of the machine was made from commercially available items such as stainless steel valves with Teflon seals, aluminium pneumatic fittings, viton and silicon o-rings and polyethylene tubing.

The RTM machine is capable of injection pressures of up to 600 kPa. It has two pressurised tanks on board allowing it to store 5 litres of resin and 5 litres of acetone for cleaning. When cleaning, injection lines can first be cleared with compressed air (air purge) and then with acetone to help reduce waste. In a single stroke, up to 1.25 litres of catalysed resin can be injected. The ratio of catalyst to resin can be varied from 1 % to 2.5 % by using a slider on the arm connecting the two cylinders.

The schematic from which the idea was obtained and pictures of the RTM machine that was built can be seen in Figure 4.2 - Figure 4.4.

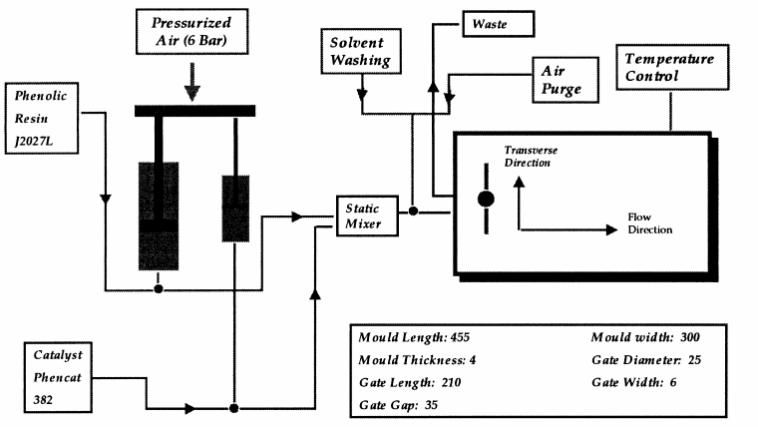

Figure 4.2 Schematic of RTM machine [26]

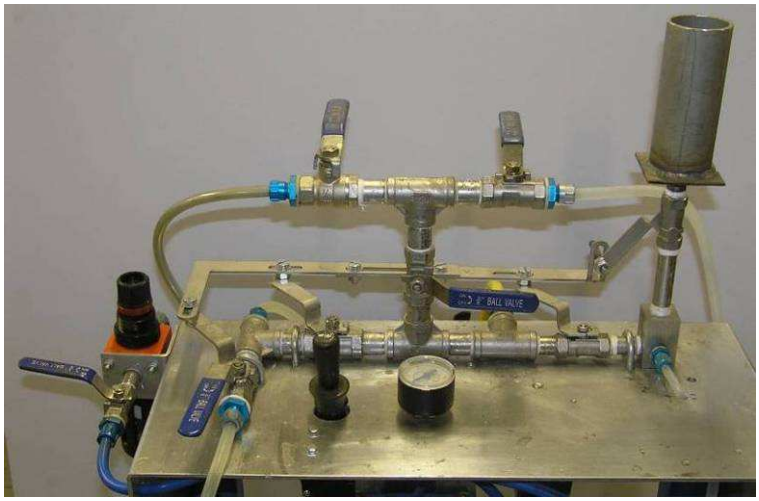

Figure 4.3 RTM machine mixing head



Figure 4.4 RTM machine front and back

4.2.2 Pressure pot

The RTM machine that was designed and built was intended to be used for polyester and vinyl ester resins which require the addition of catalyst to resin in a mass ratio of approximately 1-2.5:100. The epoxy resin used for this project requires the addition of hardener to resin in a mass ratio of approximately 28:100. Due to this ratio, the epoxy could not be used in the RTM machine and a pressure pot had to be built. Composites made using vinyl ester resin were also eventually made using the pressure pot for reasons that will be explained in section 4.4.2. As described in section 4.2.1, the use of a pressure pot is not ideal but it was unavoidable.

The pressure pot consists of a length of steel pipe with a piece of C-channel welded on one end and a piece of steel plate welded on the other (the C-channel was used to allow room for the injection line to protrude from the pressure pot). A threaded hole was made in each end of the pressure pot to allow for injection and compressed air lines to be connected.

4.2.3 Mould

The layout for the mould was based on that described by Rouison *et al.* [24, 25]. It has a rectangular mould cavity with injection ports located in the corners of one mould face and a single exhaust port located in the centre of the matching mould face.

A composite mould was initially made and showed that the port layout worked provided the fibres were correctly positioned within the cavity. The fibre mats had to be undersized inside the cavity in order to allow for resin to flow around the edge of the fibre mats freely before flowing inward and wetting out the fibres (this is known as edge-flow).

Following testing of the composite mould, a mould was made from mild steel plate. The mould consists of three components; upper and lower mould plates and a spacer into which the mould cavity and a groove for an o-ring seal were machined. The spacer was siliconed and screwed in place onto the lower mould plate. The perimeter of the upper mould plate was machined away to create a step so it could be positioned

easily by dropping partially into the mould cavity. The mould was closed using 16 M12 high tensile bolts.

The design included four inlet ports located in the four corners of the mould cavity on the lower mould surface and a single exhaust port located in the middle of the upper mould surface. By locating the inlet ports on the lower mould surface and the exhaust port on the upper mould surface, air bubbles could easily flow up and out of the mould. Injecting from the corners of the mould cavity seemed a good method as the flow front would decrease in size as it advanced and the combination of this decrease and four inlet ports would allow for fast mould filling. Problems with the composites initially produced resulted in the mould eventually being used in reverse i.e. the inlet ports were used as exhaust ports and vice versa. A more detailed explanation is provided in section 4.4.1.

The mould was designed for a pressure of up to 600 kPa. This limiting pressure is not an indication of when the mould would fail but is actually the point at which deflection in the mould would result in a noticeable change in fibre fraction. The accuracy of the fibre fraction is dependant on the accuracy with which the mass of fibres before resin injection and the mass of the resulting composite can be measured (approximately 0,1 g using the laboratory scale).

The mould was designed without built-in provision for heating in the interests of cost and simplicity. The decision was made that when the mould required heating this would be accomplished by placing it inside an oven and leaving it to reach the desired temperature. It was assumed that the thick steel used in the construction of the mould would have a high enough thermal inertia to offset any quenching effects caused by resin during filling.

All the fittings used were commercially available pneumatic fittings made either from aluminium or POM plastic. The tubing used was made from polyethylene which allowed for easy cleaning and removal of cured resin due to the self-lubricating property of polyethylene.

Composites measuring 280 mm by 260 mm by 4 mm were produced using the mould. The size of each composite was sufficient to obtain 6 specimens for tensile testing, 6 for flexural testing, 6 for impact testing and 4 for water absorption tests. These figures include one extra specimen for each test in accordance with various standards that will be detailed in section 5.1.

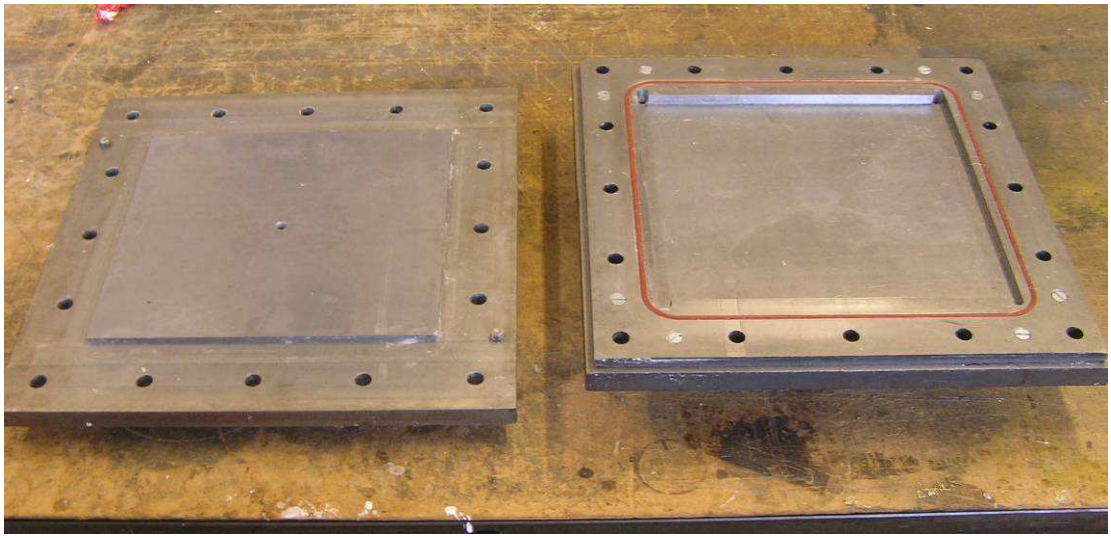

Figure 4.5 Mild steel mould: upper mould plate (left) and lower mould plate with spacer (right)

4.3 Production technique

Before production could commence, a number of issues needed to be addressed. These included: the combinations of parameters to use to produce polyester composites, how long it would take to effectively heat the mould in an oven, how best to dry fibres and how to determine the resultant fibre mass and volume fractions.

4.3.1 Combinations of processing parameters

Apart from altering fibre moisture content and mould temperature in polyester composites, it was decided that some composites would also be produced by pressurising the mould after injection in the hope of increasing fibre-matrix interaction and reducing the size of voids. The combinations that were eventually decided upon for production of polyester composites are shown in Table 4.5. The combination shown in red, “room temperature mould, fibres dried and mould pressurised”, could not be produced. Resin in the injection and exhaust tubes was

found to cure before resin inside the mould, which due to cure shrinkage resulted in compressed air entering the mould and ruining the composite inside.

The production of vinyl ester and epoxy kenaf fibre reinforced composites did not require the numerous combinations of parameters as in the case of the polyester ones. One set of parameters was decided upon and used for both resins. The fibres were dried and the mould heated as this provided reduced cycle times and according to literature should result in good quality composites. Glass equivalents were produced for comparison. Glass fibre reinforced polyester and epoxy composites were produced using a heated mould but vinyl ester ones were produced using the mould at room temperature due to difficulties in production. The problems are described in more detail in section 4.4.2. It was considered acceptable to produce these composites at room temperature because glass fibre reinforced composites were for comparative purposes only and are not the focus of this study. The parameters used for the production of vinyl ester and epoxy composites can be seen in Table 4.5.

Table 4.5 Processing conditions for composites

Fibre Volume Fraction	Resin	Room Temperature Mould	Heated Mould (50-55°C)
15, 22.5 & 30 %	Polyester	Kenaf Fibres Undried	Kenaf Fibres Undried
15, 22.5 & 30 %	Polyester	Kenaf Fibres Dried	Kenaf Fibres Dried
15, 22.5 & 30 %	Polyester	Kenaf Fibres Dried and Mould Pressurised	Kenaf Fibres Dried and Mould Pressurised
15, 22.5 & 30 %	Polyester		Glass Fibres
15, 22.5 & 30 %	Vinyl Ester		Kenaf Fibres Dried
15, 22.5 & 30 %	Vinyl Ester	Glass Fibres	
15, 22.5 & 30 %	Epoxy		Kenaf Fibres Dried
15, 22.5 & 30 %	Epoxy		Glass Fibres

4.3.2 Heating the mould

In order to find out how long it would take to heat the mould to the required temperature, an oven was pre-heated to 55°C, the mould was placed inside and measurements of the surface temperature of the mould were taken using an infrared thermometer at various time intervals. 55°C was chosen based on the values found in the literature survey. The results are shown in Figure 4.6. It was decided that the mould would need to be heated for at least 3 hours to achieve the required temperature.

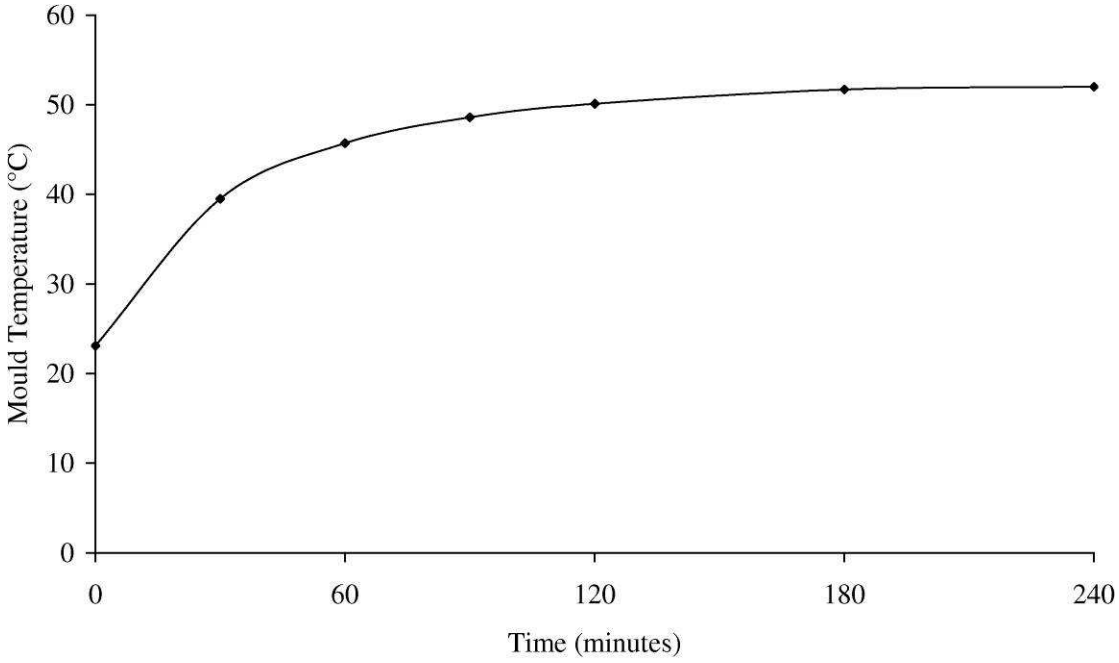

Figure 4.6 Mould temperature vs. time for mould in an oven at 55°C

4.3.3 Drying of fibres

The method of heating the mould and applying a vacuum such as that used by Rouison *et al.* [24, 25] was experimented with but the reduction in fibre moisture content was found to be low. It is well known that there are three ways in which heat can be transferred; convection, conduction and radiation. Vacuum drying eliminates convective heat transfer because there is no air through which heat can be transferred. Natural fibres are hollow in structure and are thus good insulators making conductive heat transfer between fibres poor as well. This means that vacuum drying natural fibres relies mainly on radiation for heat transfer. It was hypothesised that the cause of

the low reduction in moisture is because only fibres near the mould surface are dried as radiation is unable to penetrate to the centre of the fibre mats. To verify this, three layers of fibres were vacuum dried in the mould and the mass was recorded periodically. One layer of fibres was then vacuum dried in the mould and the fibre mass was once again recorded periodically. As expected, one layer of fibres lost a higher percentage of moisture than three layers because the radiation could penetrate proportionally deeper into the single layer of fibres. Results are shown in Figure 4.7. For comparative purposes values obtained for drying of fibres at atmospheric pressure, 83 kPa in Johannesburg, in the oven have also been included. In all cases, fibres were taken from ambient room conditions where temperatures ranged from 20-23°C and relative humidity ranged from 45-55 %. If these conditions were not met, tests would be postponed.

The investigation into the efficacy of vacuum drying prompted a further investigation regarding the drying method of Rouison *et al.* [24, 25]. The mould used by these authors was made of aluminium. According to Gray and Mueller [31] and Harrison [32], steel has a higher emissivity than aluminium. This implies that using an aluminium mould for vacuum drying should result in poorer drying of fibres than if steel is used. To investigate this, one layer of fibres was placed between two sealed aluminium plates and heated under vacuum. As expected, the fibres lost a lower mass percentage than when the steel mould was used. The results are shown in Figure 4.7. Smooth surfaces such as those required in a mould for good surface finish emit less radiation than rough or black surfaces. Rouison *et al.* [24, 25] did not provide any data to show the efficacy of their method of vacuum drying. However, the results shown in Figure 4.7 indicate that due to the low emissivity of smooth surfaces, drying of fibres under vacuum in moulds such as those used for RTM is ineffective.

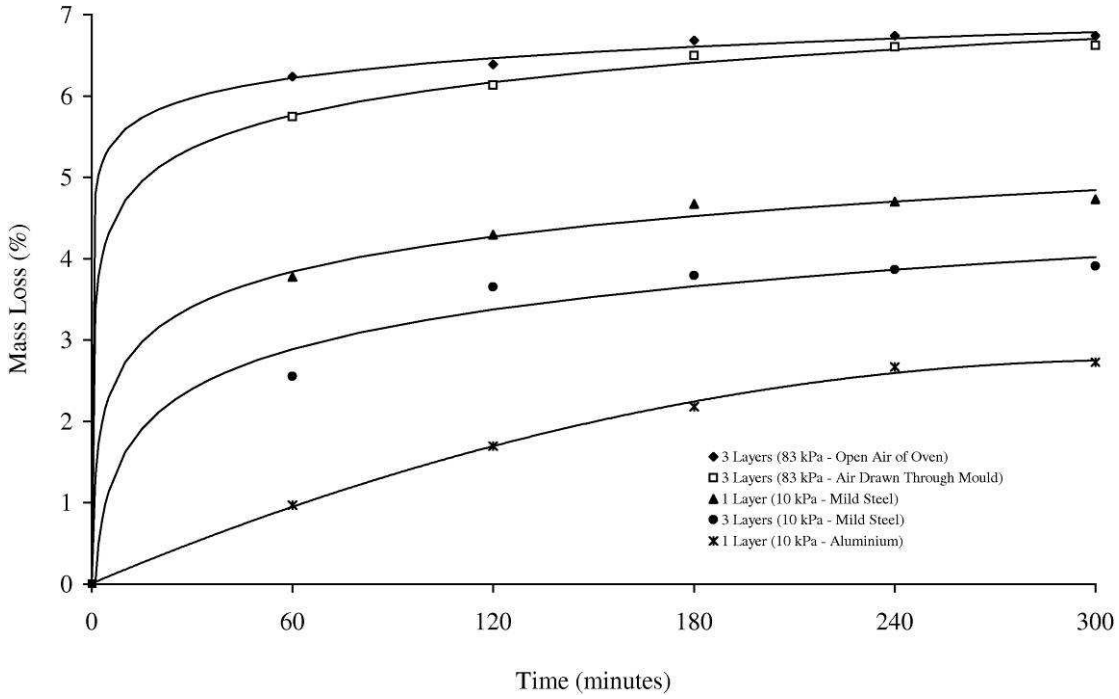

Figure 4.7 Effect of various drying methods on fibre moisture loss

It is clear that in order to adequately dry the fibres, they need to be dried in air. It was found that acceptable drying of the fibres could be achieved by loading the fibres into a preheated mould, placing the mould in the oven and drawing warm air through it. This method prevented the fibres from reabsorbing moisture while being loaded into the mould after drying. Air was drawn through the mould using a venturi connected to the inlet port. The results obtained using this method are also presented in Figure 4.7. Not all fibres could be dried in this way. Composites made using dried fibres in a room temperature mould had to be produced by drying the fibres in an oven and then placing them inside the mould quickly enough to avoid the fibres reabsorbing moisture from the atmosphere. A test was conducted and it was determined that if the fibres were removed from the oven and sealed inside the mould within two minutes, they did not absorb a significant amount of moisture. Results of this test can be seen in Figure 4.8. Fibres were dried at 55°C for five hours and then removed from the oven.

As a result of these tests, all fibres were dried for at least three hours. When fibres were dried in the oven and subsequently sealed inside the mould, this process was completed within two minutes of their removal from the oven.

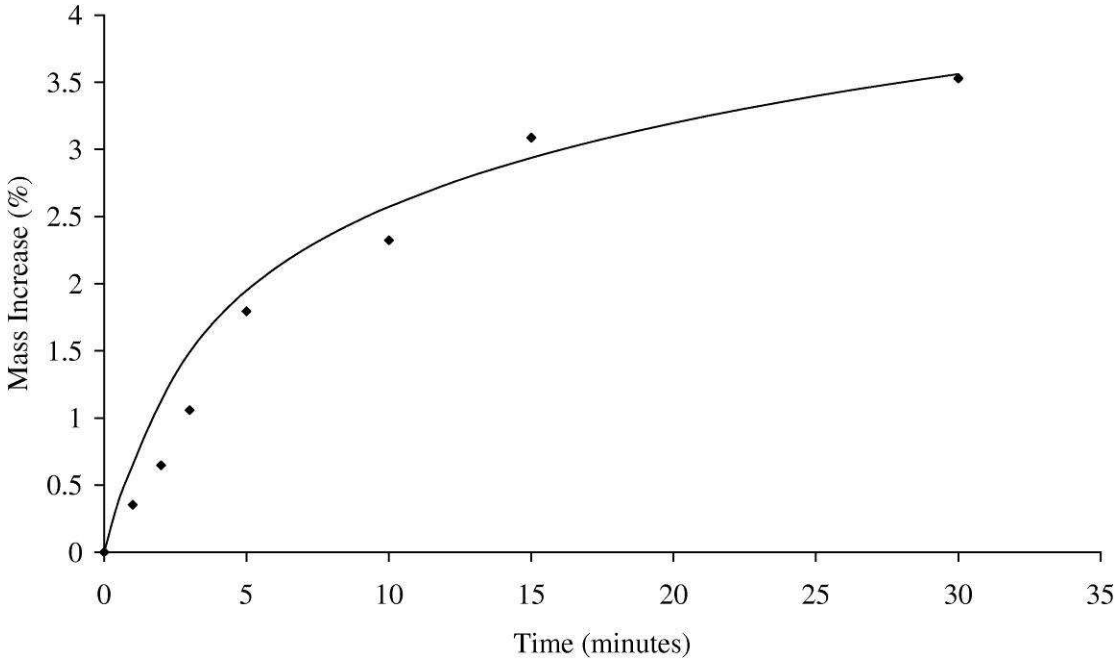

Figure 4.8 Fibre mass increase vs. time after drying

4.3.4 Determination of fibre mass and volume fractions

One of the advantages of using RTM to produce natural fibre reinforced composites is that the composite fibre fraction can be relatively easily controlled. Determination of fibre mass fraction is achieved by measuring the mass of fibres before resin injection and then measuring the mass of the composite at the end of production. From these values fibre volume fractions can then be calculated using the following equation:

$$V_f = \frac{m_f \rho_c}{m_c \rho_f} \qquad (4.1)$$

Because some fibres were to remain undried and some were to be dried without removal from the mould it was necessary to develop a technique to determine the dry mass of the fibres in each composite. The technique used was to take a small sample of fibre mat and measure the mass of both it and the mass of the fibre mats to be used in the composite. The sample could then be dried and measured in order to obtain a percentage decrease in mass due to moisture loss. Using this percentage, the dry mass of the fibres in the composite could then be determined. Sample fibre mats were dried at 105°C for 18 hours according to the method used by Madsen [(11)].

It must be emphasised that the aim of drying the fibres in this manner was to determine a value of dry fibre mass so that composites where fibres were undried or dried could be compared. Drying of fibres as described in the previous section does not result in complete removal of moisture and thus all composites contain an unavoidable content of moisture.

4.3.5 Preparation of fibres

Fibre layers were cut from a roll of fibre mat into rectangular pieces measuring 285 mm by 265 mm using a guillotine. The rectangular sections were oversized slightly to avoid the occurrence of edge-flow in the mould. The fibre layers were always cut with the sides measuring 285 mm aligned parallel to the lengthwise direction of the roll because it was assumed that it was not isotropic in the plane as found by O'Dell [22]. Sample pieces of fibre mat for determination of fibre fraction were obtained from off-cuts.

The mass of the fibre layers and the samples were measured using a scale accurate to 0.1 g. Care was taken to ensure that the mass of fibres for composites of the same fibre fraction were approximately the same in each case. Production log sheets were kept and these values of mass were recorded. An example of a log sheet for each resin can be found in Appendix B.

Depending on the composite to be produced, fibres would either be loaded into the room temperature / heated mould or placed in the oven for drying.

4.3.6 Production of composites

Resin transfer moulding with polyester resin was achieved using the RTM machine. For epoxy and vinyl ester resins, resin was mixed by hand and sucked into the pressure pot using a 40 kPa (absolute pressure) vacuum. The vacuum was maintained for 10 minutes to remove bubbles in the resins caused by mixing and in the case of vinyl ester resin also by the reaction of the resin with the catalyst. Degassing was found to be less effective for the epoxy than for the vinyl ester resin. Degassing could not be carried out for longer than 10 minutes without risking curing of resin before complete mould filling.

For polyester resin, accelerator and catalyst were mixed into the resin in a ratio of 1.5 % by mass each. For vinyl ester resin, accelerator and catalyst were mixed into the resin in a ratio of 0.3 % and 1 % by mass respectively. Hardener was mixed into epoxy resin in a ratio of 28 % by mass.

For fibre volume fractions of 15 % and 22.5 % an injection pressure of 250 kPa (gauge pressure) was used with a vacuum assist pressure of 40 kPa (absolute pressure). For the 30 % fibre volume fraction, injection pressure was increased to 350 kPa. These pressures resulted in fast cycle times and complete mould filling before cure. For glass fibre reinforced vinyl ester composites, injection pressures were 0 kPa, 100 kPa and 200 kPa for 15 %, 22.5 % and 30 % fibre volume fractions with 40 kPa vacuum pressure.

Following complete mould filling, resin was allowed to run until no air bubbles were observed in the exhaust lines. The vacuum was then released and the RTM machine or pressure pot shut-off and disconnected. The injection line connected to the mould was then plugged. In composites where the mould was pressurised after filling, a pressure of 600 kPa was applied using a compressed air line.

Composites where the mould was at room temperature during injection were left overnight to cure and then demoulded. Composites where the mould was heated were left in the mould for at least an hour before demoulding except for epoxy composites which were left overnight. All composites were post-cured according to the instructions laid out in the relevant data sheets.

4.4 Production problems

4.4.1 Problems with the mould

Trial runs using the mould revealed problems with the composites being produced. Lines were appearing on the surfaces of composites. In some cases the lines were barely visible and in other cases they were very pronounced and it appeared as if the fibres were not being wet-out along these lines. Examples of these composites can be

seen in Figure 4.9. These lines did not appear on any of the composites made using the composite mould.



Figure 4.9 Lines on composites

The lines were assumed to be related to resin flow, resin cure, moisture build-up or the accumulation of dust in the fibres along them. Flow visualisation was conducted to determine the cause of the problem by replacing one of the steel mould plates with an acrylic panel. The results can be seen in Figure 4.10.

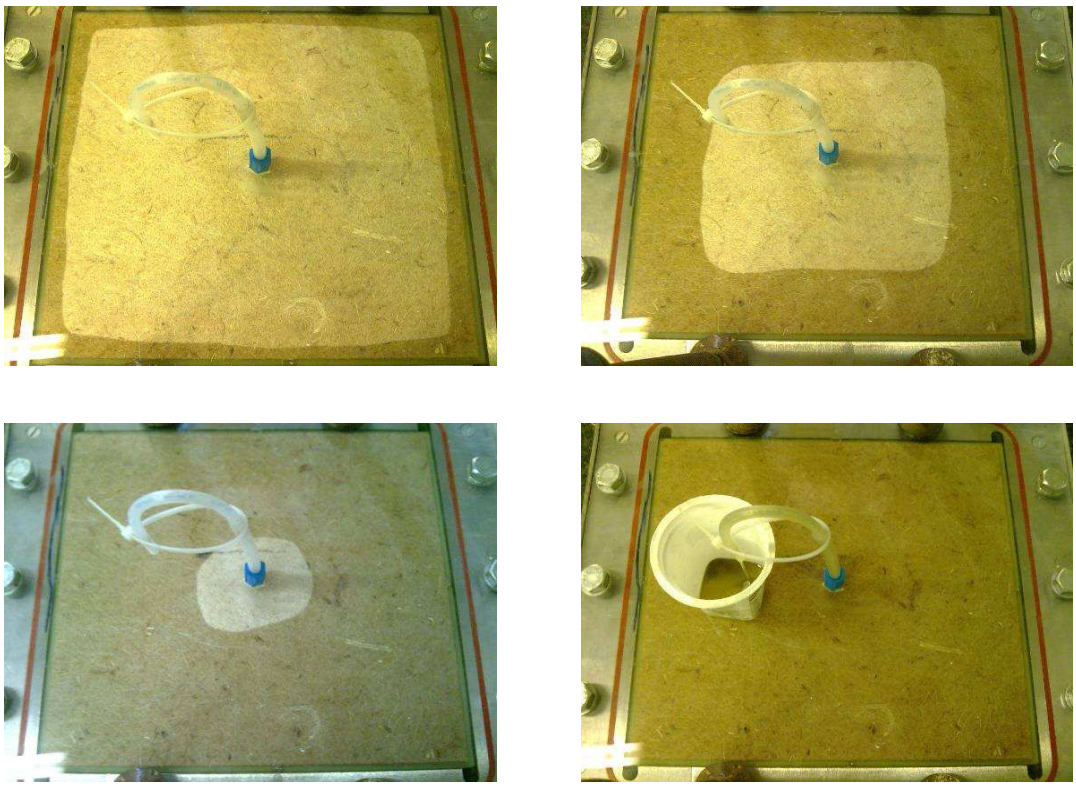

Figure 4.10 Flow visualisation - resin injected from mould corners

The exact cause of the problem cannot be determined from the pictures as the flow front appears as expected and the design of the mould is based on literature which does not mention similar problems. The lines are assumed to be “knitting lines”, a phenomenon that occurs where flow fronts meet. This is plausible considering that the lines appeared along the diagonals of the composites i.e. the lines along which the corners of the flow front moved during mould filling. In order to confirm this, the mould was filled in reverse i.e. from the centre. By filling the mould from the centre, the flow front is expected to be circular in shape and thus symmetrical along any axis. Flow visualisation was conducted again and the results can be seen in Figure 4.11.

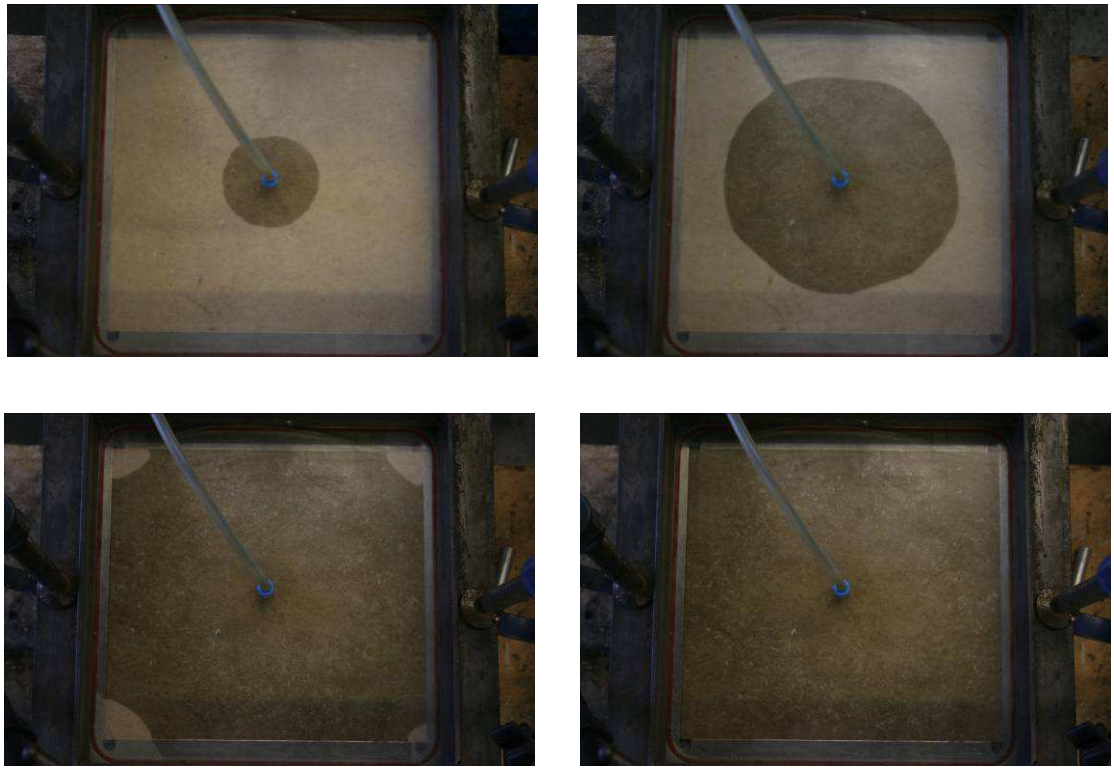

Figure 4.11 Flow visualisation - resin injected from mould centre

Filling of the mould from the centre worked and knitting lines no longer appeared on the composites. This had implications for all composites to be made in future. Mould filling would take longer than expected and most importantly, in order to use the central port for injection and the corner ports for exhausting, the mould would have to be flipped to ensure that resin flowed upward thus allowing air bubbles to escape from the mould more easily.

4.4.2 Problems with vinyl ester resins

As stated in section 4.1.2 the vinyl ester resin originally purchased was “Scott Bader DP 333” and it was supplied with “Scott Bader Accelerator VE” and “Norox MEKP 925” Catalyst (M-100 catalyst). The resin is described in the data sheet as follows:

“Low Viscosity Epoxy Vinyl Ester Resin for vacuum infusion and RTM”

Initial trials using this resin with kenaf fibres resulted in specimens where the fibres were not properly wet-out by the resin. Following completion of injection, it was also observed that resin would start to flow out of the exhaust lines after a few minutes. It appeared as if the resin was gassing.



Figure 4.12 Failed vinyl ester resin composite (left) and vinyl ester resin gassing following injection (right)

Technical staff at the supplier were contacted about the gassing problem and they included a counterpart from their U.K. division in email discussions. It was suggested that it might be the catalyst causing the gassing and that it is not a problem in open mould processes but when using a closed mould the effects are exaggerated. Although it is common for vinyl ester resins to gas upon the addition of catalyst, it had been taken for granted that this would not occur given that the resin was intended for use in closed mould processes. First a catalyst called “Trigonox 239” was recommended to overcome the gassing problem but it was not available locally. “Andonox PD-40” catalyst was then recommended as a potential replacement. Enquiries regarding obtaining some of this catalyst were unsuccessful as it had to be purchased in a minimum quantity of 25 kg which was impractical and there was in fact no guarantee

that this would solve the problem. Obtaining a small sample of this catalyst from a local company utilising it in production was also tried but unsuccessful.

Since an alternative catalyst could not be sourced, the only other means by which the gassing could be overcome was to degas the resin before injection. This meant that the pressure pot would have to be used instead of the RTM machine because the entire quantity of resin required would have to be mixed at once. This worked and kenaf fibre reinforced vinyl ester composites were successfully produced.

Following the production of the kenaf fibre reinforced vinyl ester composites, production began with the glass fibre reinforced ones. The same technique for producing the kenaf fibre composites was used but once again, the resin was gassing and this time for a different reason. Extended degassing, pressurisation during cure, reducing the amount of catalyst, altering mould temperature, washing of the fibres with catalysed resin and combinations of these were all tried but failed.

It seemed as though the sizing agent on the surface of the glass fibre chopped strand mat was reacting with the resin. When the resin came into contact with the glass fibre chopped strand mat, gassing occurred and when it came into contact with kenaf fibres, no gassing occurred. For comparison to the chopped strand mat, the resin was tested with some unidirectional glass fibres which had been successfully used with a vinyl ester resin in a different project. During this other project, no problems with gassing of resin upon contact with fibres had been experienced. Figure 4.13 shows the resin gassing with the chopped strand mat fibres and the unidirectional fibres. As can be seen, the gassing must have been caused by an interaction between the sizing on the glass fibres and the specific resin being used or one of the additives in it.



Figure 4.13 Vinyl ester resin gassing with CSM glass (left) and UD glass (right)

In order to determine if it was the resin, catalyst or accelerator that was the cause of the reaction with the sizing agent, an alternative for each was obtained from a fellow post-graduate student using a different vinyl ester resin system. These were as follows: “Derakane Momentum 411-350 Epoxy Vinyl Ester Resin”, Cobalt Naphthenate accelerator (CoNap 1 % concentration) and LA3 Catalyst (M-100 catalyst). Combinations of these were mixed in small samples and degassed and glass chopped strand mat was then added in order to see if gassing occurred. The results of this test can be found in Table 4.6 (catalyst and accelerator were added in the minimum quantities according to the data sheets available).

Table 4.6 Results of test to determine source of gassing in vinyl ester resin

Resin	Accelerator	Catalyst	Result
DP 333	Acc. VE	MEKP 925	Gas
DP 333	Acc. CoNap	Cat. LA3	Gas
DP 333	Acc. CoNap	MEKP 925	Gas
DP 333	Acc. VE	Cat. LA3	Gas
Derakane	Acc. CoNap	Cat. LA3	No Gas
Derakane	Acc. VE	MEKP 925	No Gas
Derakane	Acc. VE	Cat. LA3	No Gas
Derakane	Acc. CoNap	MEKP 925	No Gas

The results of this test indicated that the Scott Bader DP333 resin was the problem and that it should be possible to produce glass fibre composites using the Derakane resin. This meant that the kenaf fibre composites already made using the Scott Bader resin would have to be discarded and new ones produced.

Inhibitor was required with the Derakane resin because curing was occurring before mould filling was complete. Acetyl acetone inhibitor was subsequently purchased and it allowed for the mould to fill completely without problems. During production of one of the first glass composites, gassing occurred once more. It was suspected that excess inhibitor had mistakenly been added while mixing the resin. In order to verify that it was the inhibitor causing the gassing, small samples were once again mixed. The first of three samples contained 0.06 % by mass of inhibitor, the maximum indicated in the Derakane data sheet and it was left at room temperature. The second also contained 0.06 % by mass but this time the sample was heated to 55°C. (The second sample was heated to see if the reaction could be brought on by elevated temperatures). The third contained 0.12 % by mass of inhibitor and it was left at room temperature. The results of this test are presented in Table 4.7.

Table 4.7 Results of test to determine the source of gassing in Derakane vinyl ester resin containing inhibitor

Resin	Accelerator	Catalyst	Inhibitor	Temperature	Result
Derakane	Acc. CoNap	MEKP 925	0.06 %	RT	No Gas
Derakane	Acc. CoNap	MEKP 925	0.06 %	55 Celsius	No Gas
Derakane	Acc. CoNap	MEKP 925	>0.06 %	RT	Gas

As can be seen from the table, adding excess inhibitor could cause gassing of the resin. Earlier trials showed that the Scott Bader resin cured more slowly than the Derakane resin indicating it probably contained inhibitor. It is possible that the reason the Scott Bader resin gassed when it came into contact with glass fibres was that it contained an excess of inhibitor. The Scott Bader resin has since been discontinued and replaced.

Following problems with gassing in glass fibre vinyl ester composites it was decided to avoid the use of inhibitor if possible. For this reason, glass fibre reinforced vinyl ester composites were produced using the room temperature mould.

4.4.3 Other problems encountered during composite production

Throughout the course of composite production, a number of other problems were encountered and include; curing of the resin before mould filling was complete and loss of vacuum during mould filling. Examples of composites that resulted from these problems can be seen in Figure 4.14 and Figure 4.15. It is interesting to note in Figure 4.15 the presence of bands where the vacuum was lost and then reconnected.



Figure 4.14 Composite production failure - resin curing during mould filling

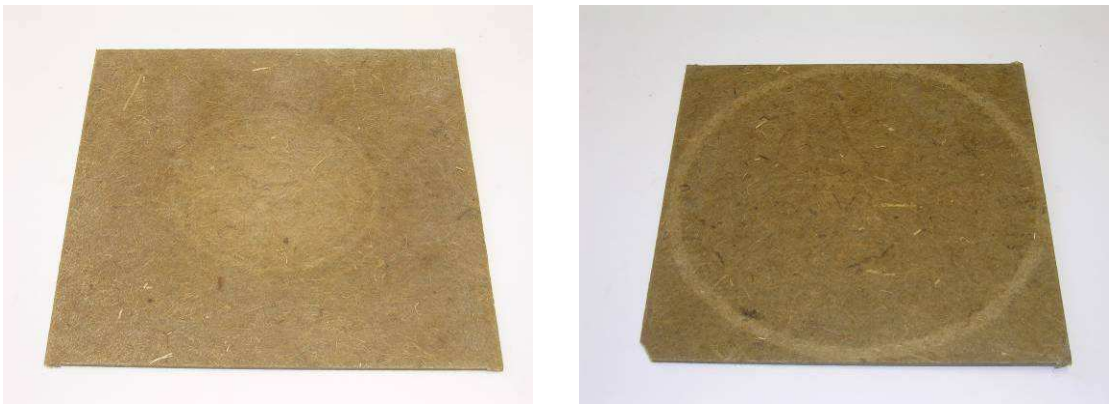

Figure 4.15 Composite production failure - loss of vacuum

5 TESTING

5.1 Testing standards and specimens

5.1.1 Location of test specimens in composites

All test specimens were aligned along the lengthwise direction of each composite. This was done because the fibre mats were potentially not isotropic in the plane as found by O'Dell [22]. The location of each test specimen can be seen in Figure 5.1.

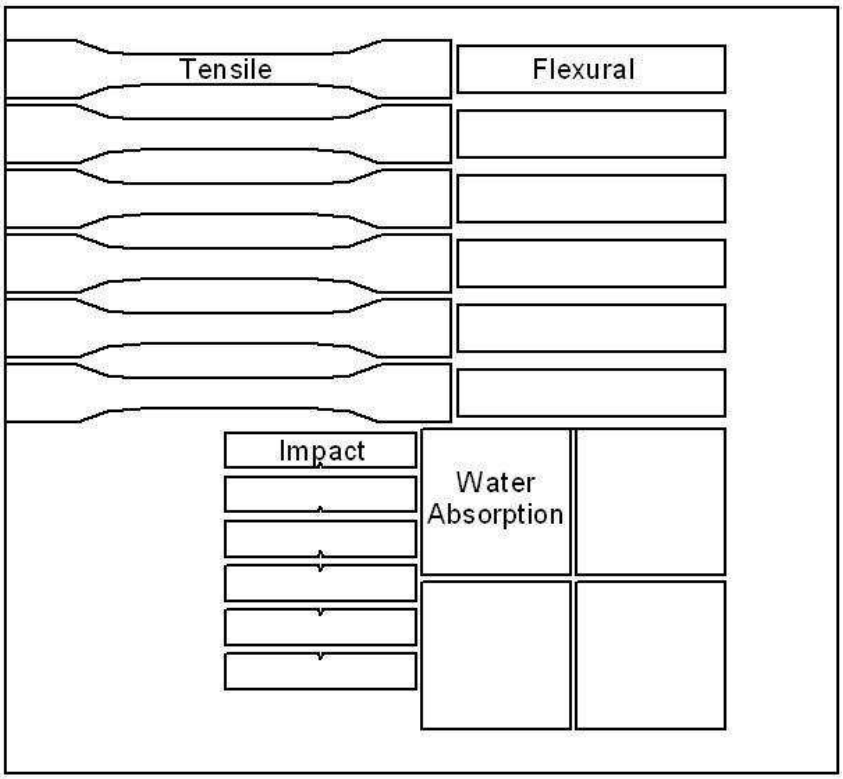

Figure 5.1 Location of test specimens in composites

5.1.2 Tensile testing

Tensile tests were conducted in accordance with ASTM D638. Test specimens were type I/II and were machined using a bench-mounted pneumatic router and a tensile specimen jig.

5.1.3 Flexural testing

Flexural tests were conducted in accordance with ASTM D790. Test specimens measured 90 mm in length, ± 16 mm in width and were machined using a bench-mounted pneumatic router and a flexural specimen jig.

5.1.4 Impact testing

Impact tests were conducted in accordance with ASTM D256 for in-plane Izod impact tests. Test specimens were first machined to size and then notched on a milling machine.

5.1.5 Water absorption testing

Water absorption tests were conducted in accordance with ISO R62 (an ASTM standard was not available). The specimens were cut on a band saw to an approximate dimension of 50 mm by 50 mm followed by which the sides were sanded on a belt sander to a more accurate size. Sanding on the belt sander also produced a uniformly smooth surface that could not be obtained using the band saw.

The standard required specimens to be immersed in water for 24 hours and measurements of mass and dimension then taken. This standard was modified so that an initial measurement was taken after 1 hour, and another after a further 23 hours. Specimens were subsequently measured at various time intervals for four weeks. When taking measurements, specimens were removed from the water, dried using paper towel and then left in air for 5 minutes to allow surface water to evaporate. The dimensions measured included length, width, thickness at the centre and thickness at a point located approximately 7.5 mm from the edge of the specimen.

5.2 Testing equipment

5.2.1 Tensile testing equipment

Tensile testing was carried out on a JJ Lloyd tensile testing machine. Specimens were mounted into rigid jaws. Depending on the specimens being tested, either a 5 kN or a 100 kN load cell was used (all kenaf fibre reinforced composites were tested using the

5 kN load cell). An external extensometer was used to measure elongation with a gauge length of 50 mm (in accordance with ASTM D638). The test setup can be seen in Figure 5.2.

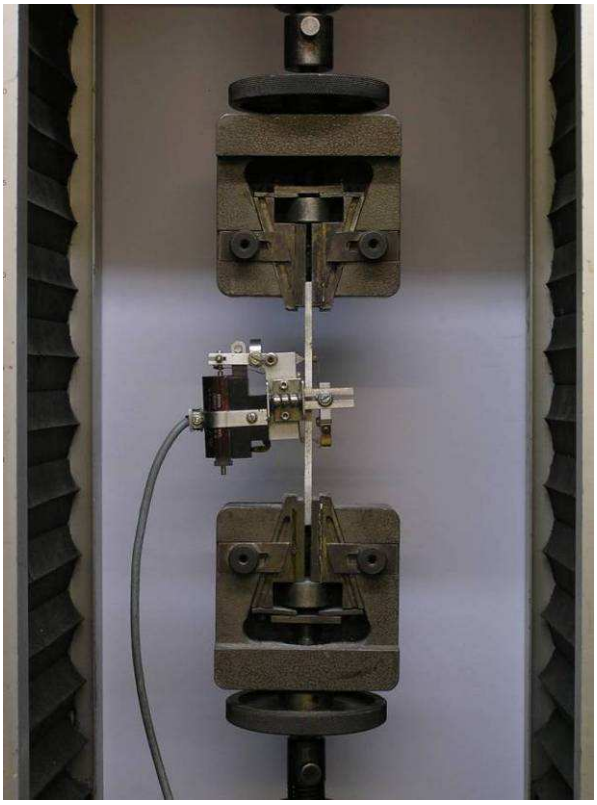

Figure 5.2 Tensile test setup

A Matlab programme was coded to process raw data. It was found that the stress-strain curves exhibited regions of both linear and non-linear behaviour and the programme produces two values of elastic modulus accordingly i.e. linear modulus and secant modulus. An example of a stress-strain curve exhibiting this behaviour can be found along with sample calculations in Appendix C. This behaviour was more pronounced in kenaf fibre composites however both linear and secant moduli were also calculated for glass fibre composites for the sake of comparison (these moduli were found to be very similar for glass fibre composites as shall be seen in section 7.6). The programme allows for processing of numerous tests specimens at a time. An output text file containing results is written by the programme which includes maximum stress, maximum strain, linear modulus, secant modulus, average values for each and the corresponding standard deviations. The code can be viewed in Appendix D.

5.2.2 Flexural testing equipment

Flexural testing was carried out on the same JJ Lloyd tensile testing machine. Specimens were tested on a three-point bending rig with a support span of 64 mm. The two end-point blocks were modified to include bearing-mounted shafts which eliminated slipping of specimens during testing. Depending on the specimens being tested, either a 0.5 kN or a 5 kN load cell was used. Deflection was measured using the internal extensometer of the testing machine.



Figure 5.3 Flexural test setup

A Matlab programme similar to that used for processing tensile data was coded and can be viewed in Appendix D.

5.2.3 Impact testing equipment

An instrumented Izod impact machine was used for impact testing. Standard impact tests allow only for the determination of total impact energy while instrumented impact tests can provide total impact energy, initial impact energy (energy absorbed before the onset of failure), propagative impact energy (energy absorbed between the onset of failure and ultimate failure) and impact strength*.

The machine used was designed by I'Ons [33], a previous postgraduate. Due to the low impact resistance of kenaf fibre reinforced composites a smaller pendulum was designed and built in accordance with ASTM standard D256 to provide better accuracy. The test setup is shown in Figure 5.4.

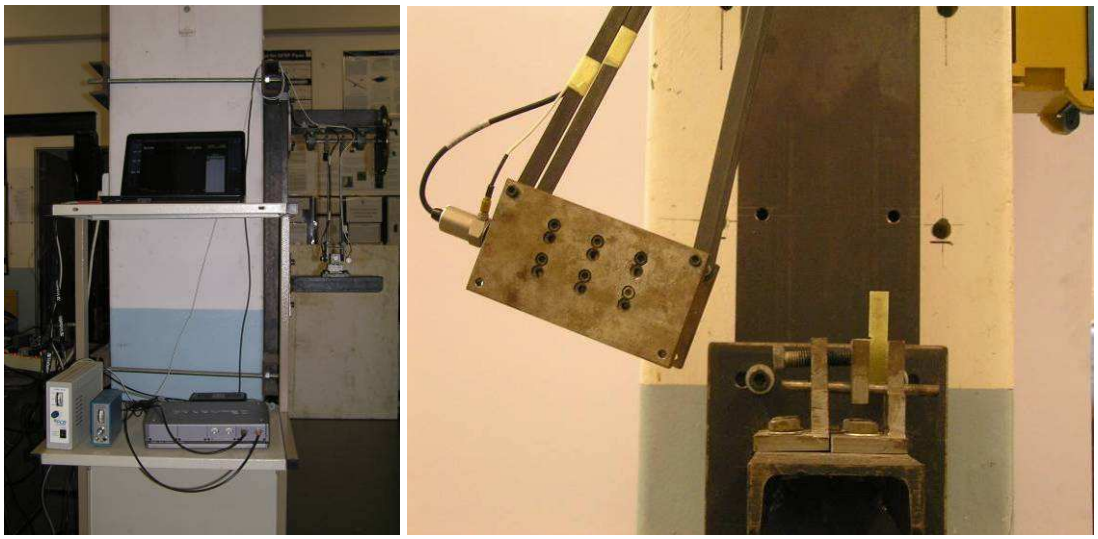

Figure 5.4 Impact test setup

A "PCB" accelerometer mounted to the back of the striking pendulum was used to measure acceleration (the data sheet for the accelerometer can be found in Appendix D). The accelerometer was connected via an amplifier to a data capturing unit which was connected to a laptop running "Graphtec Corporation" software. Using a

* The amount of energy absorbed in an impact test is conventionally referred to as impact strength. In this work, for the sake of consistency with tensile and flexural strength, impact strength refers to stress and impact energy to the amount of energy absorbed in an impact test.

conversion constant, raw data in mV could be converted into acceleration using a conversion constant of 100 mV = 9.81 m/s^2.

The raw data was filtered using a cut-off frequency of 1.5 kHz as done by I'Ons [33]. 1.5 kHz was used because it was found that a large amount of noise existed at higher frequencies. The same Matlab code written by I'Ons [33] was used to determine where noisy frequencies lay. The code analysed the data through the use of a Fast Fourier Transform. The code can be found in Appendix D.

Using the filtered accelerometer data and the pendulum mass and dimensions, force vs. time was determined. Velocity was determined by numerical integration of acceleration vs. time. A programme was coded by I'Ons [33] to perform the various integrations and produce force vs. displacement data from which he calculated the impact energy. His code was modified in a number of ways for this project. The modifications made included: updating for use on newer versions of Matlab; inclusion of code to allow for multiple specimen analysis; inclusion of code to write a text file containing test results instead of visually displaying results (the text files contained averages and standard deviations) and calculation of energy from mass and velocity instead of integrating force vs. displacement thus reducing error caused by multiple integrations of data. The Matlab code used can be found in Appendix D.

5.2.4 Water absorption testing equipment

Specimens were placed on racks made from aluminium inside plastic containers filled with distilled water. These containers were partially immersed in a tank containing tap water. The temperature in the tank was maintained at the required 23°C using a fan and a thermocouple and controller which switched a pump on and off. The fan ran permanently to produce a cooling effect on the water in the tank and when the temperature dropped below the required limit, the controller would turn on the pump and circulate water through a heating coil located outside the tank. The temperature was monitored using a thermometer and was found to be well within the limit required by the ISO standard (±0.5°C). One of the aluminium racks used and the water absorption test setup can be seen in Figure 5.5 and Figure 5.6.

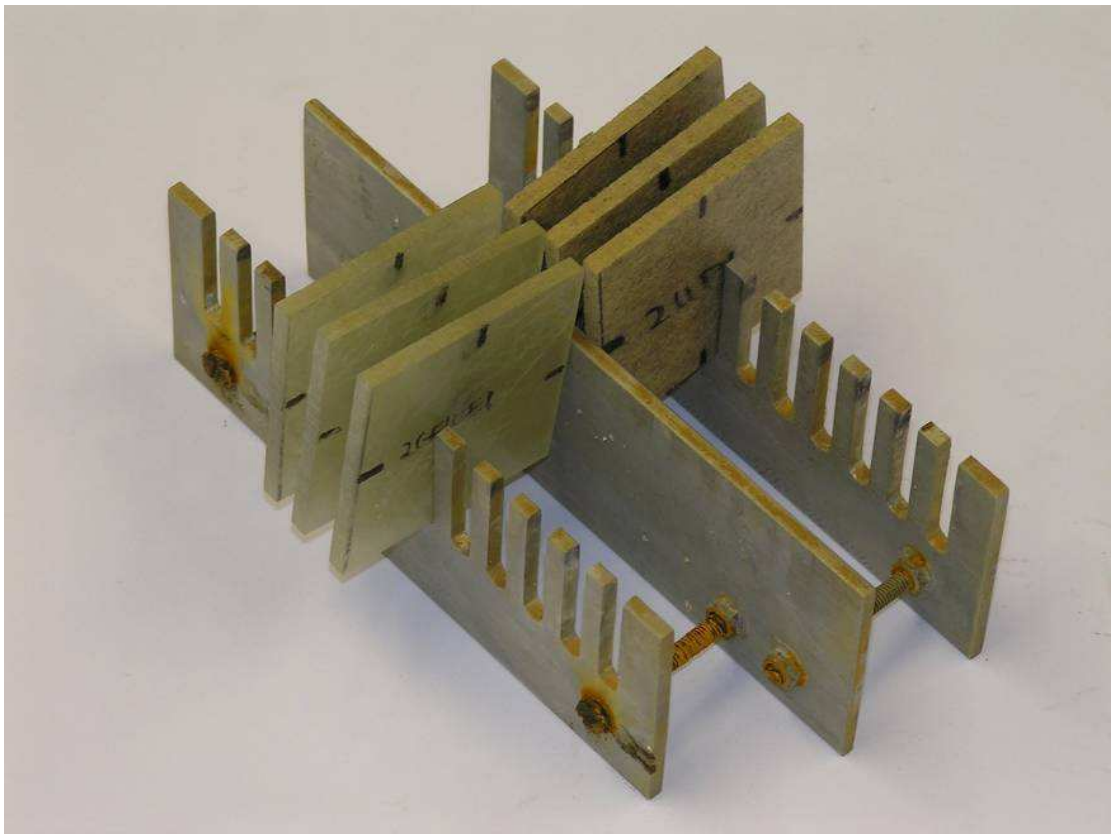

Figure 5.5 Aluminium rack for holding water absorption specimens

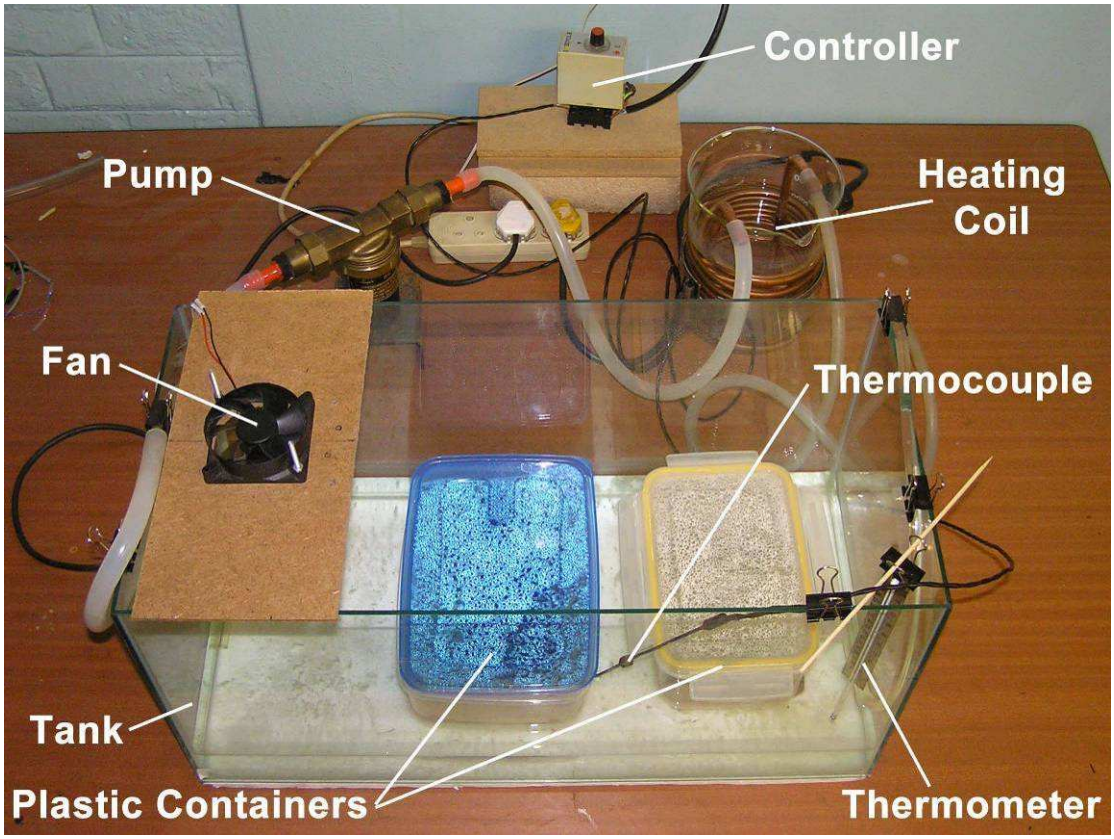

Figure 5.6 Water absorption test setup

5.2.5 Scanning electron microscope

Examination of specimen failure surfaces was conducted using a JEOL 840 scanning electron microscope. Specimens were coated with carbon and gold-palladium to increase their conductivity.



Figure 5.7 Examples of coated SEM specimens

6 OBSERVATIONS

6.1 Properties of the kenaf fibre mat

For equivalent fibre volumes, the total thickness of the kenaf fibre mats was notably thicker than that of the glass fibre mats. The thicker kenaf fibre mats were consequently more difficult to close inside the mould than the glass fibre mats. Fibre mats had to be pressed when making 30 % fibre volume fraction kenaf composites because the layers of fibres were thicker than the spacer plate of the mould. The fibre mats were pressed by placing them two at a time inside the mould and closing it. This process was time consuming but could be avoided in future by increasing the thickness of the spacer plate and size of the step in the upper mould plate.

6.2 Mould filling

Mould filling time was found to vary depending on the type of fibres and mould temperature. Table 6.1 shows the time taken for resin to appear at the exhaust ports for different fibres and mould temperatures. The results in the table are for polyester resin and values for kenaf fibre composites are averages. As can be seen, heating the mould leads to shorter filling times due to the reduction in viscosity of the resin. Glass fibre composites have much shorter filling times than kenaf fibre composites. This is probably due to the smoother, more regular surface of the glass fibres offering less resistance to resin flow than the rough kenaf fibres. In glass CSM, fibres are also better aligned in the plane of the composite which allows for resin to flow between plies more easily than in kenaf non-wovens.

Table 6.1 Mould filling times

Fibre Volume Fraction	Kenaf Fibres Room Temperature Mould	Kenaf Fibres Heated Mould	Glass Fibres Heated Mould
15 %	91 seconds	78 seconds	35 seconds
22.5 %	226 seconds	168 seconds	41 seconds
30 %	256 seconds	161 seconds	59 seconds

6.3 Composite quality

There was no difference observed in the quality of kenaf polyester composites made using either dried or undried fibres in the heated or room temperature mould. The surfaces appeared the same and composites had similar void content. Poorer surface finish was observed with increasing fibre fraction due to fibres at the surface not being properly encapsulated by the resin. This was a result of the amount of compressive force required to close the fibres inside the mould.

Epoxy composites had the best surface finish for both kenaf and glass fibres. This is probably due to the lower shrinkage of the resin when compared to polyester and vinyl ester resins. Polyester and vinyl ester kenaf composites had smoother surfaces than glass equivalents at low fibre volume fractions but not at high fibre volume fractions. Areas where polyester and vinyl ester glass composites had pulled away from the mould surfaces during curing could easily be seen. It is possible that the inherent spring-back in the kenaf fibre mats caused by their compression inside the mould allowed kenaf composites to expand and fill any areas opened up by shrinkage of the resin. This might be detrimental to the mechanical and water absorption properties of these composites if internal voids and micro cracks develop where resin resists the expansion of the fibres as suggested by Almgren *et al.* [34].

In glass fibre composites, the fibres appeared better wet out by the epoxy resin than either the polyester or vinyl ester resins. In polyester and vinyl ester glass composites, fibre bundles were visible but epoxy composites were almost transparent. Vinyl ester and epoxy glass composites appeared to have higher void content than polyester composites presumably due to these resins being mixed by hand and in the case of the vinyl ester resin due to gassing.

6.4 Testing

In tensile and impact tests, epoxy composite specimens had smoother failure surfaces than polyester and vinyl ester ones where fibres protruding from the surface could easily be seen. van den Oever *et al.* [35] observed a similar result for polypropylene (PP) and maleic anhydride polypropylene (MAPP) flax fibre composites where MAPP had bonded better to fibres than PP.

In flexural tests, epoxy composite specimens broke cleanly into two pieces while polyester and vinyl ester ones experienced failure on the tensile surface and remained in one piece. In the work of Sèbe *et al.* [9], methacrylic anhydride treated hemp fibre polyester composite specimens broke cleanly in two while untreated fibre composite specimens did not.

Based on the results of van den Oever *et al.* [35] and Sèbe *et al.* [9] these two observations imply better fibre matrix adhesion between kenaf fibres and epoxy resin than polyester or vinyl ester resin.

7 RESULTS

7.1 Introduction

The results for the different processing conditions are presented first. The effects of differing resin system are then presented and finally specific properties of kenaf fibre reinforced composites are compared to those of glass fibre reinforced composites. Where theoretical values are applicable, they have been included in results pertaining to comparison of composites made using various resin systems. Sample calculations for both experimental and theoretical results can be found in Appendix C.

Where reference is made to the mechanical properties of unreinforced resins, values were supplied by the manufacturers because specimens were found to be too brittle to be machined and tested.

Micrographs from scanning electron microscope studies are only presented for 22.5 % fibre volume fractions but are sufficient to observe results. Micrographs for 15 %, 22.5 % and 30 % and additional micrographs included for interest can be found in Appendix E.

Results for the water absorption tests are divided into mass change and dimensional change of the specimens. Dimensional changes are presented for thickness, length and width. The two measurements taken for thickness for each specimen are averaged while length and width measurements are separate as it was found that all the specimens tested experienced a larger dimensional increase in their lengthwise direction than in their widthwise direction.

Changes in mass for water absorption tests over a four week period are shown for 22.5 % fibre volume fraction composites only and have been included as examples. These are sufficient to examine trends in composite mass change. Changes in dimension for water absorption tests over a four week period have not been included in the interest of brevity. Bar graphs showing ultimate mass and dimensional change after four weeks of immersion have however been included for all fibre volume

fractions. Comprehensive results for changes in mass and dimension for 15 %, 22.5 % and 30 % fibre volume fractions can be found in Appendix F.

All results have been presented using a coding system. Each composite was coded using either three or four sets of characters. For kenaf fibre reinforced composites, the first set indicates the resin system: UP (unsaturated polyester), VE (vinyl ester) and EP (epoxy). The second set indicates whether or not fibres were dried: AD (air dried, either in the open oven or using air drawn through the mould) and ND (not dried). The third set indicates the temperature of the mould: H (heated) and NH (not heated). The fourth set is used only where applicable and indicates if the mould was pressurised following injection: P (pressurised). For glass fibre reinforced composites, the same system was used except since drying of fibres was not applied, the AD / ND characters were replaced with GE standing for glass equivalent. As an example, UP-ND-H stands for: unsaturated polyester resin, fibres not dried and heated mould.

Fibre volume fractions are presented as 15 %, 22.5 % and 30 %. These figures however represent approximate values and 14-15 %, 21-23 % and 28-30 % are more accurate. The variations in fibre volume fractions were caused by a number of factors related to the resulting composite thickness and therefore volume. The composite thickness depended to a certain degree on the number of fibre layers placed inside the mould and the type of fibres being used (kenaf or glass fibres). Placing more fibre layers inside the mould made the mould more difficult to close and potentially caused it to deflect slightly in the middle. In addition, the silicon used to seal the middle and lower mould parts together had to be replaced occasionally and this caused a variation in the depth of the mould cavity.

7.2 Theoretical results

Theoretical results for tensile and flexural strengths and elastic moduli were calculated using the rule of mixtures. According to Sreekumar *et al.* [10], Madsen [11] and Kavelin [18], the rule of mixtures although simple provides good estimates of mechanical properties of natural fibre reinforced composites. Furthermore, Sreekumar *et al.* [10] showed that many alternatives to the rule of mixtures give poor

estimates. Therefore, it was decided that it would be applied in this work in order to avoid more complex models that may provide worse or no better results.

7.3 Specific properties

Specific properties of composites were calculated by taking the relevant property and dividing the value by the density of the composite. Composite density was determined using the following equation:

$$\rho_c = \frac{m_c}{\left(\frac{m_c - m_f}{\rho_m}\right) + \left(\frac{m_f}{\rho_f}\right)} \tag{7.1}$$

7.4 Results - processing conditions

7.4.1 Tensile tests

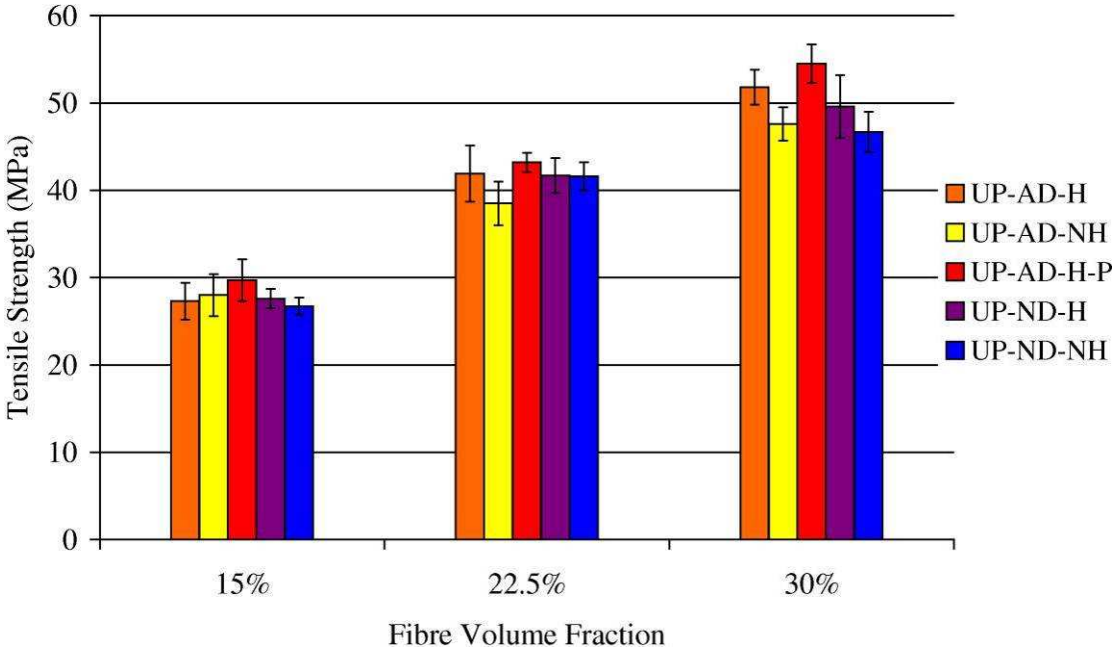

Figure 7.1 Effect of processing conditions on tensile strength

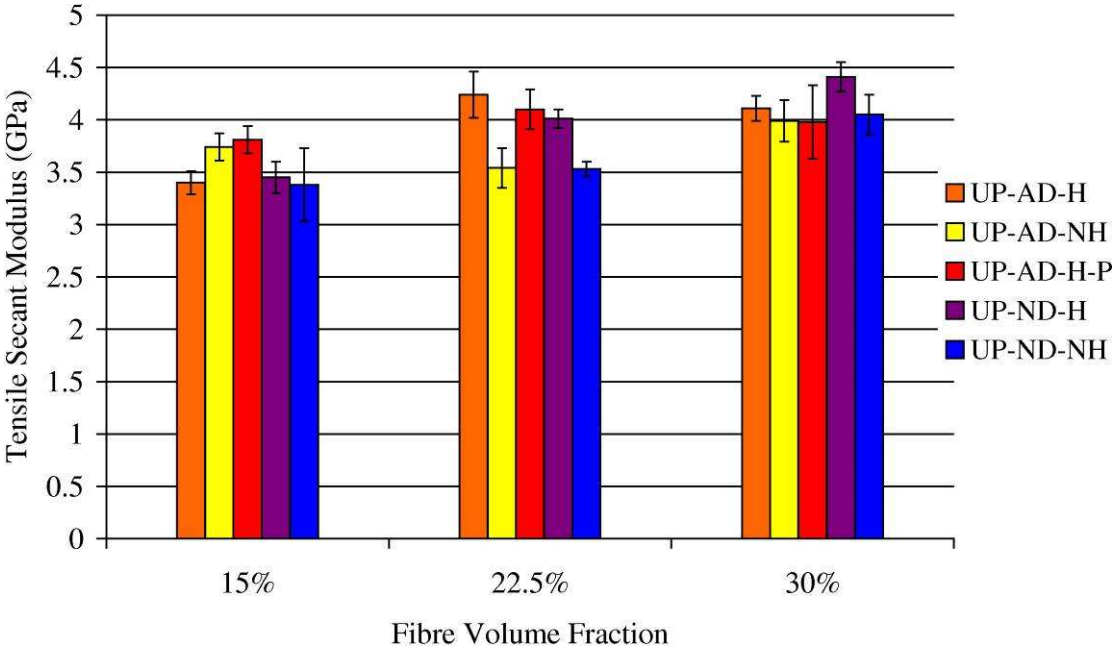

Figure 7.2 Effect of processing conditions on tensile secant modulus

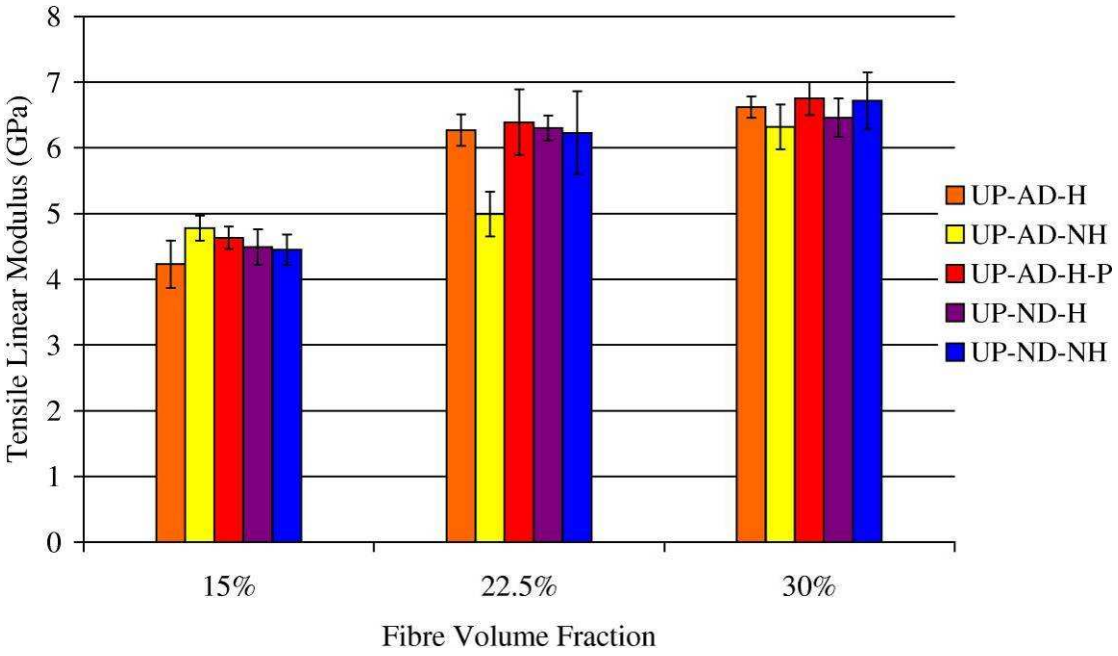

Figure 7.3 Effect of processing conditions on tensile linear modulus

7.4.2 Flexural tests

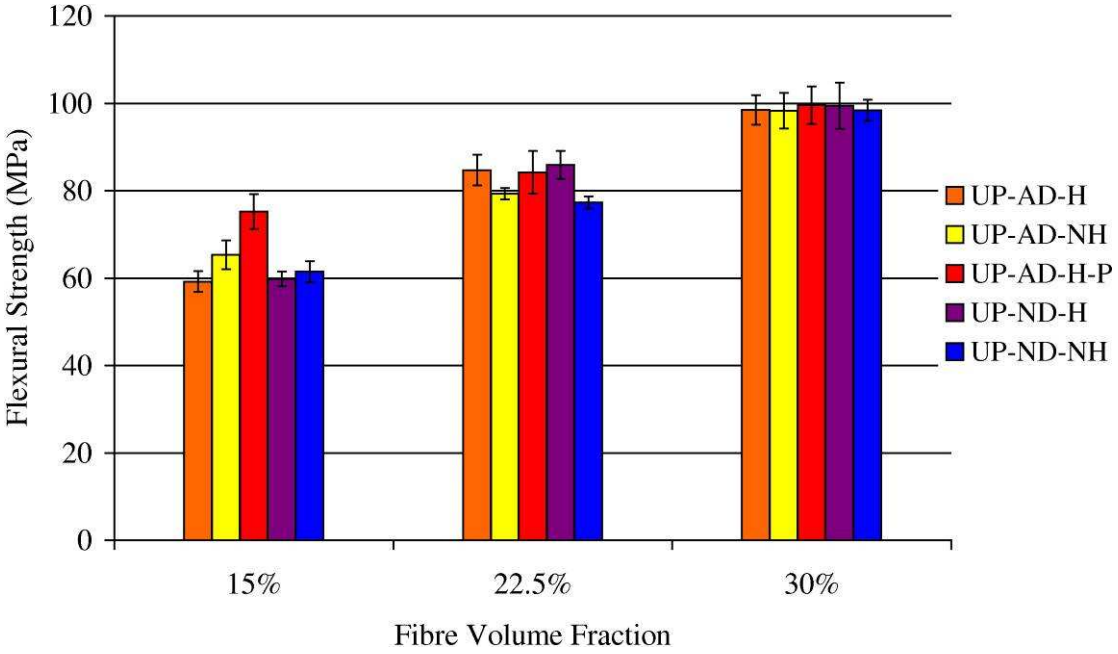

Figure 7.4 Effect of processing conditions on flexural strength

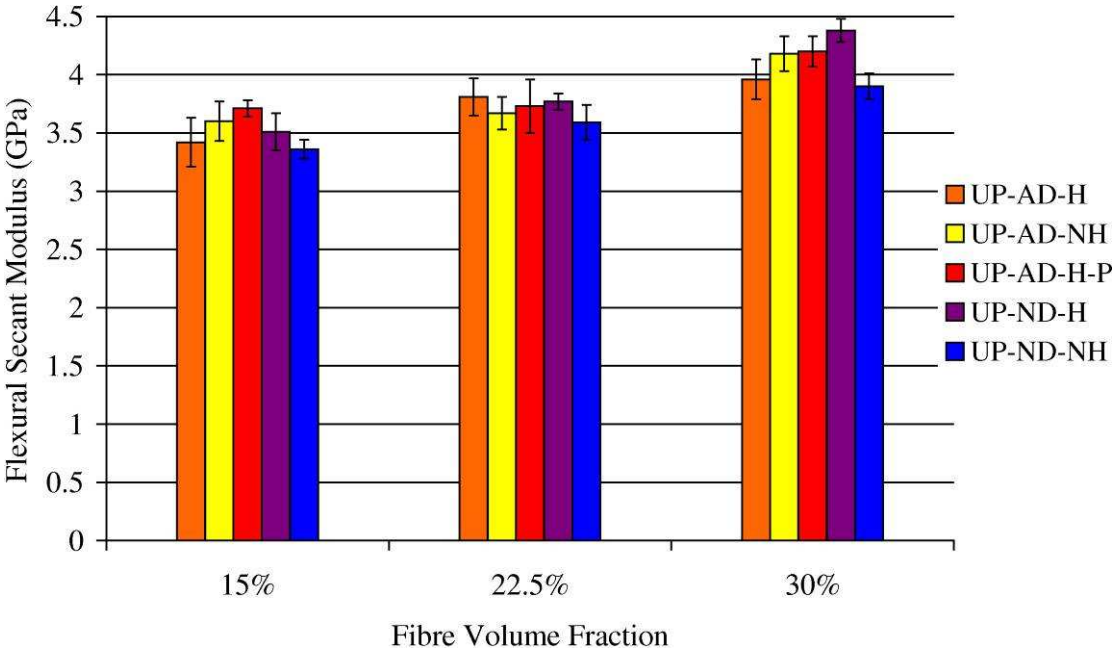

Figure 7.5 Effect of processing conditions on flexural secant modulus

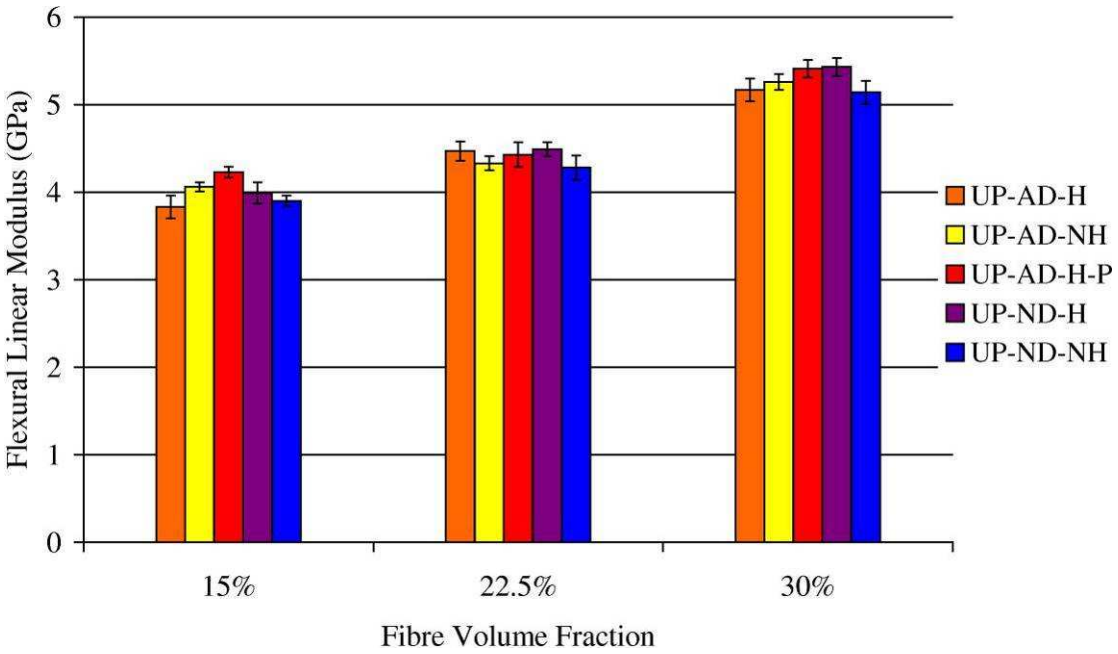

Figure 7.6 Effect of processing conditions on flexural linear modulus

7.4.3 Impact tests

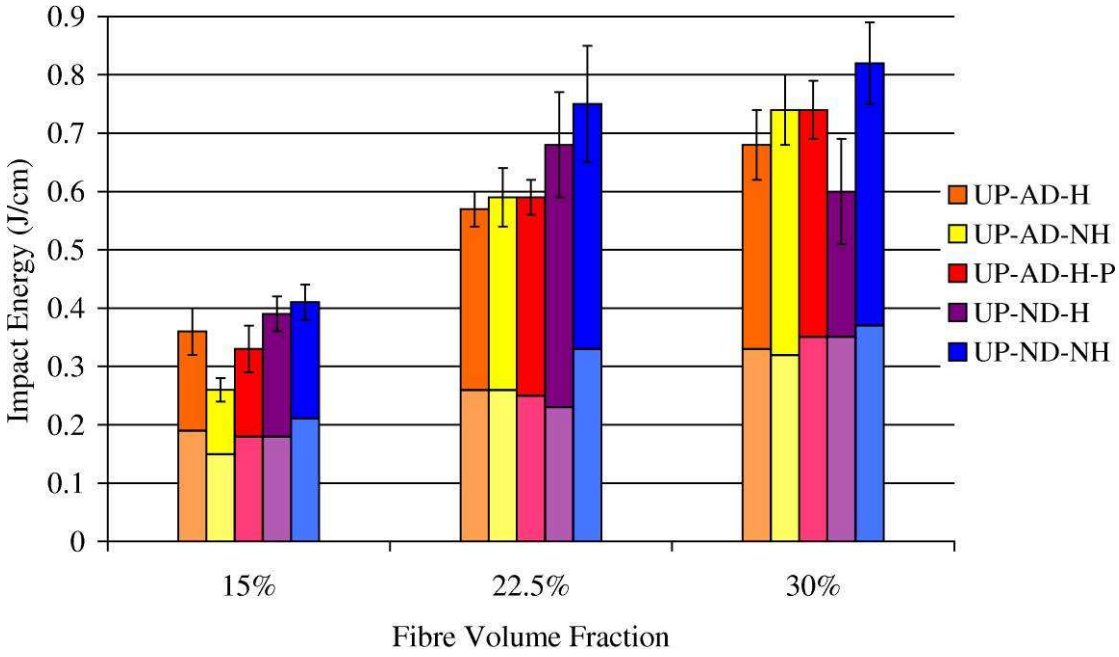

Figure 7.7 Effect of processing conditions on impact energy

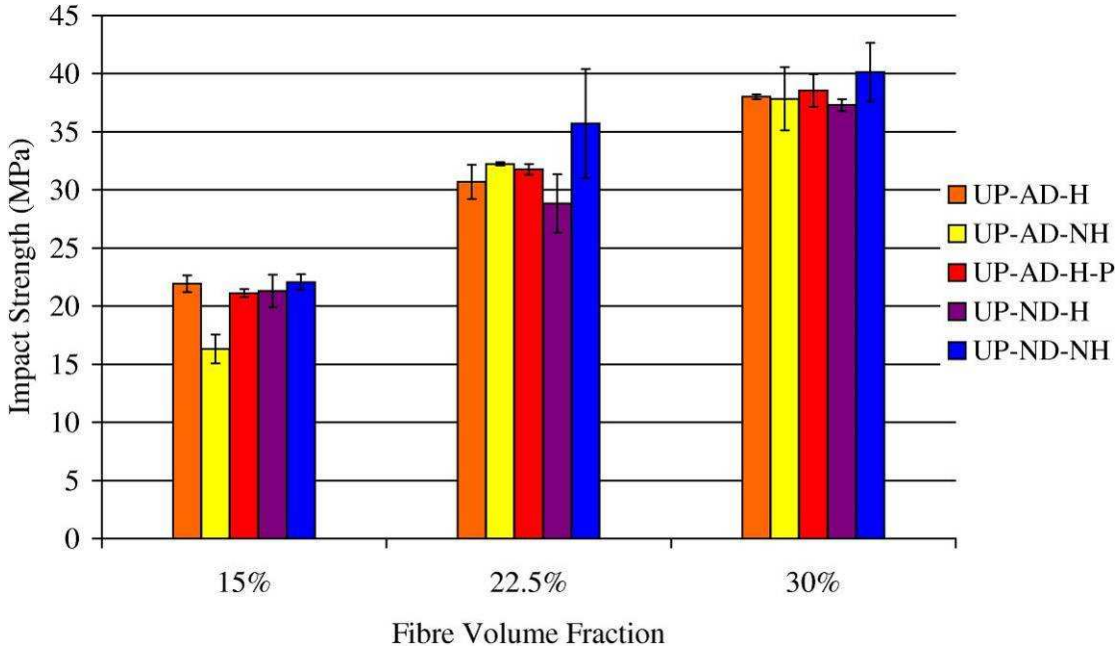

Figure 7.8 Effect of processing conditions on impact strength

7.4.4 SEM examinations

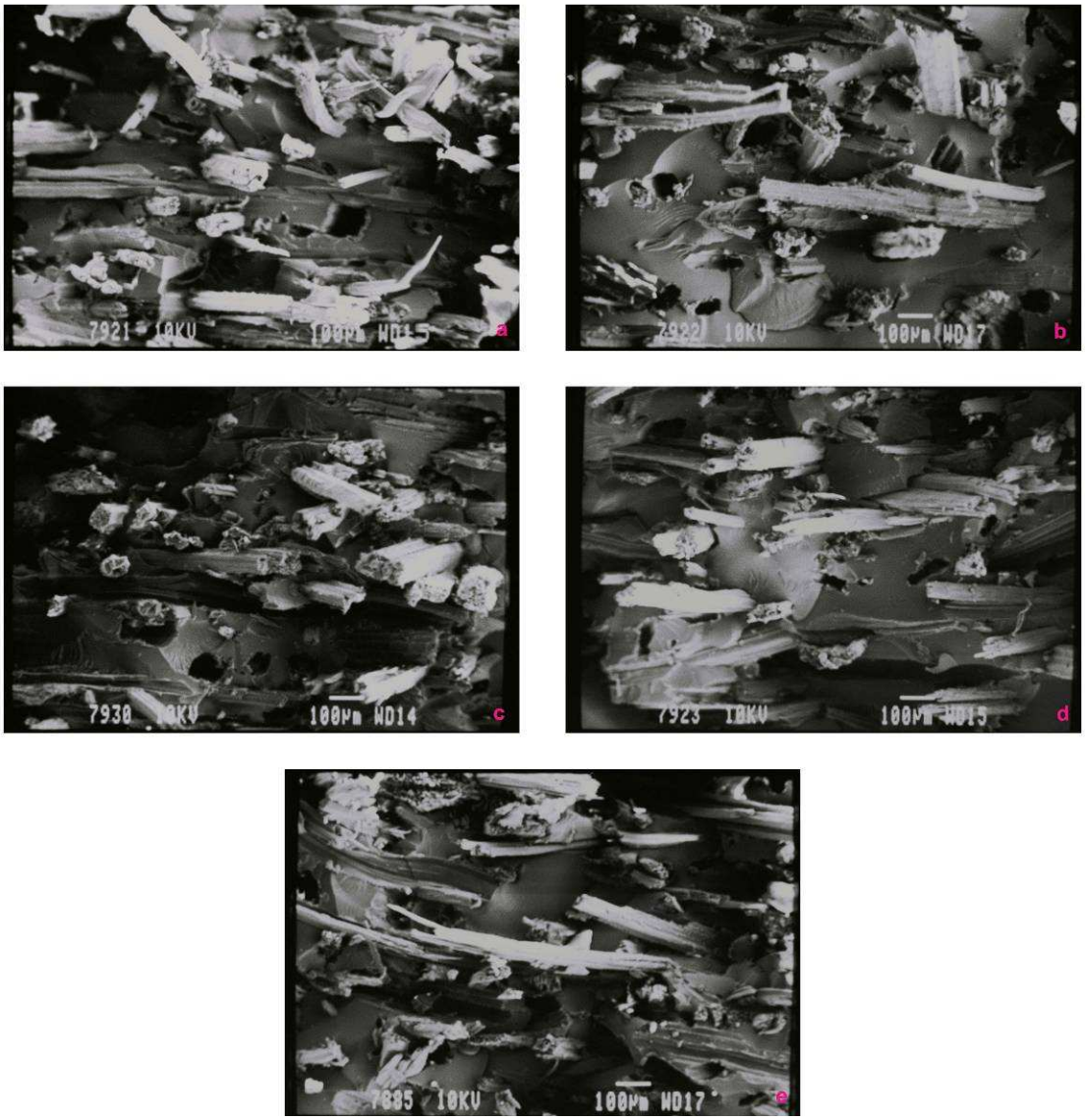

Figure 7.9 SEM micrographs of impact failure surfaces of composites made using various processing conditions at 22.5 % fibre volume fraction

In Figure 7.9 the letters correspond to the following composites:

a: UP-AD-H

b: UP-AD-NH

c: UP-AD-H-P

d: UP-ND-H

e: UP-ND-NH

7.4.5 Water absorption tests

Mass change

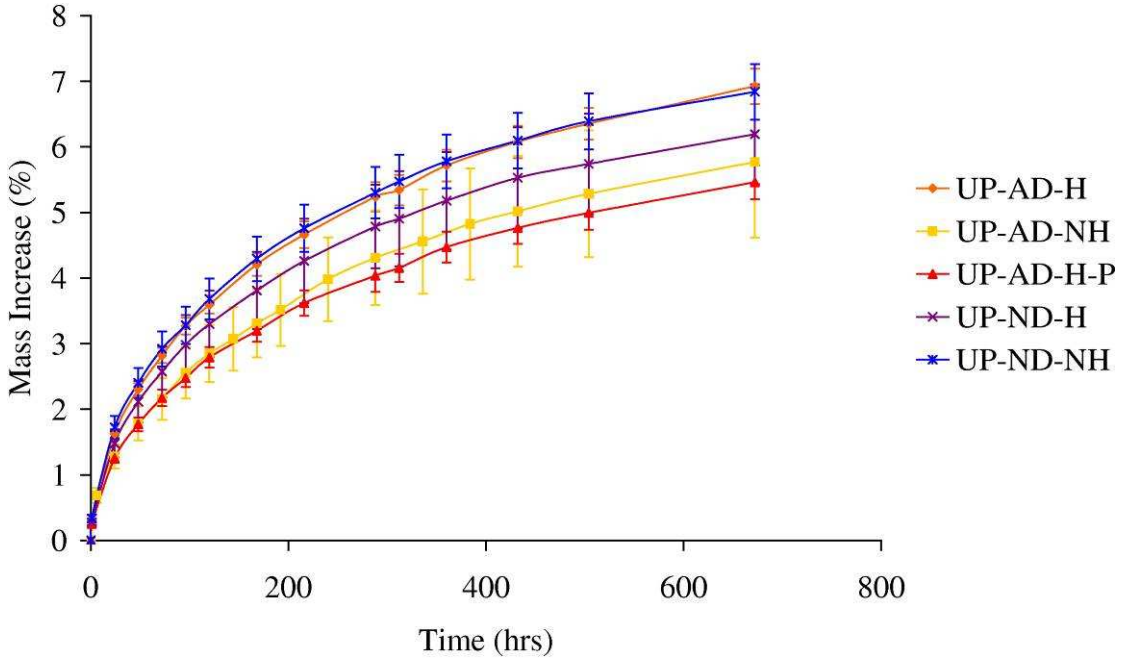

Figure 7.10 Effect of processing conditions on mass increase over four weeks of water absorption at 22.5 % fibre volume fraction

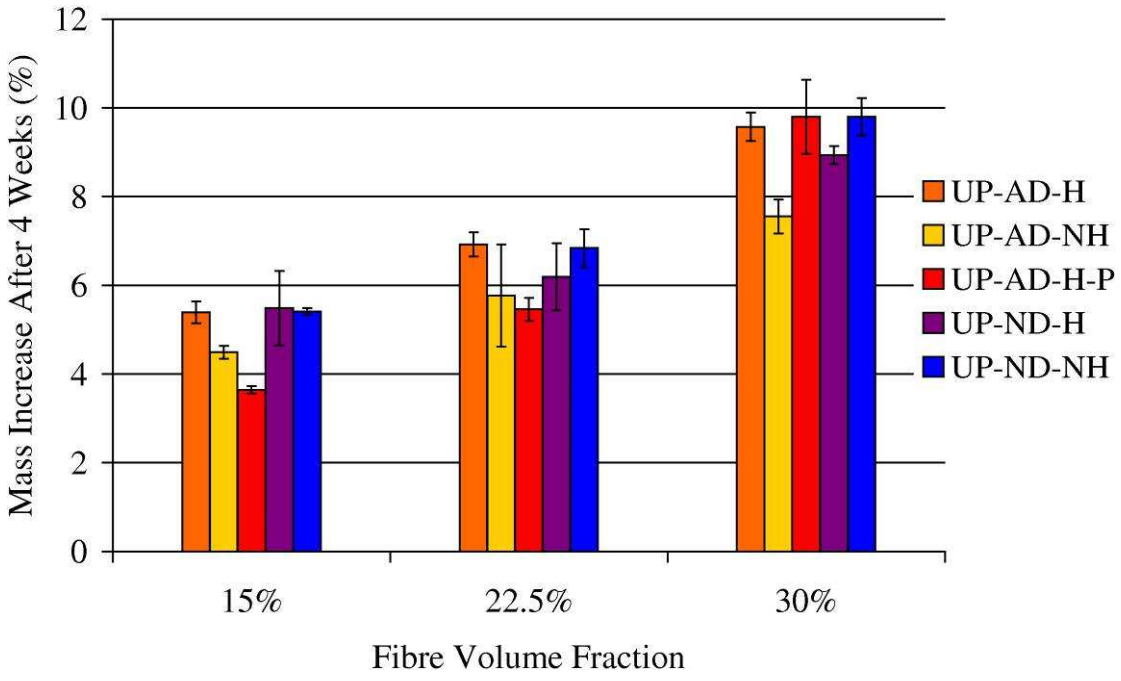

Figure 7.11 Effect of processing conditions on mass increase after four weeks of water absorption

Thickness change

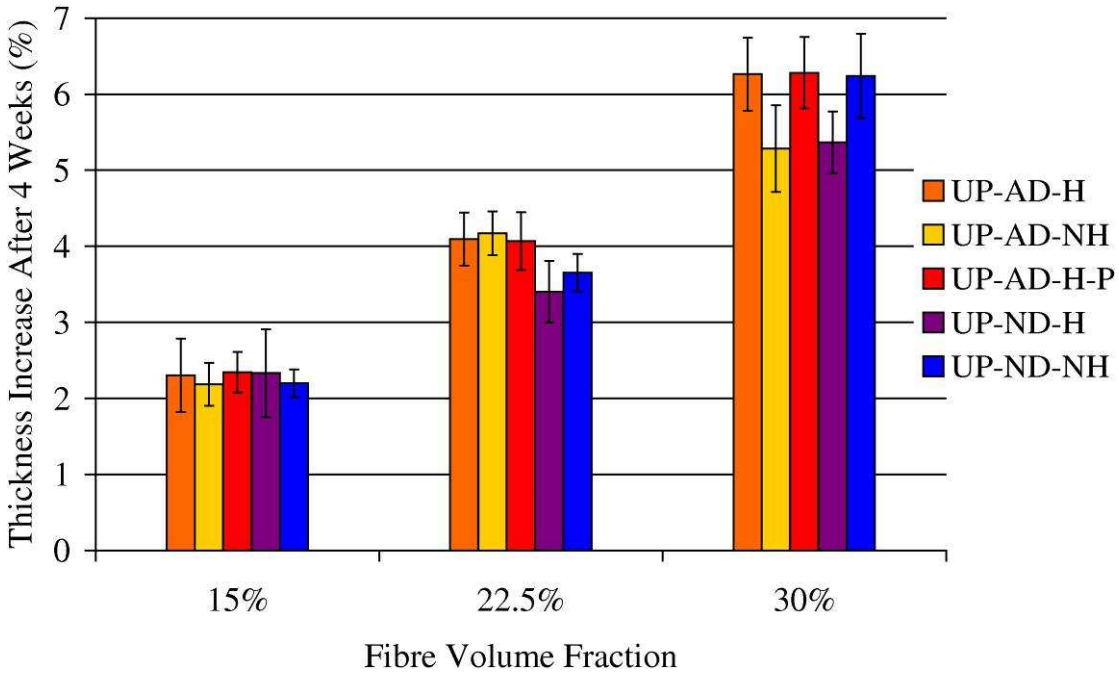

Figure 7.12 Effect of processing conditions on thickness increase after four weeks of water absorption

Length change

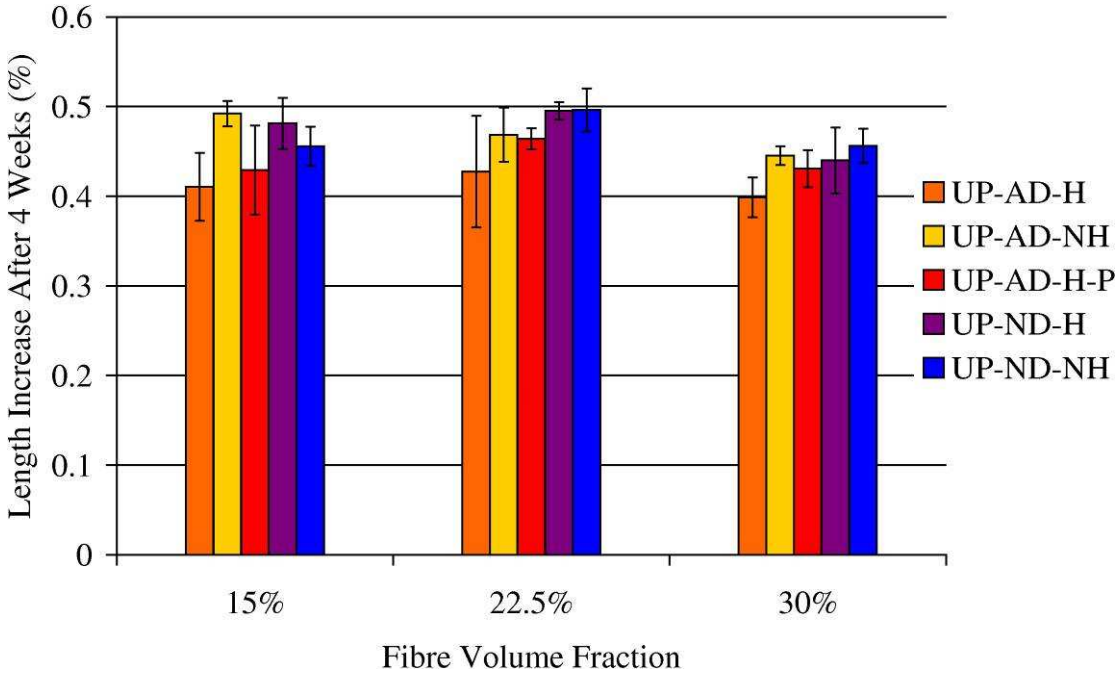

Figure 7.13 Effect of processing conditions on length increase after four weeks of water absorption

Width change

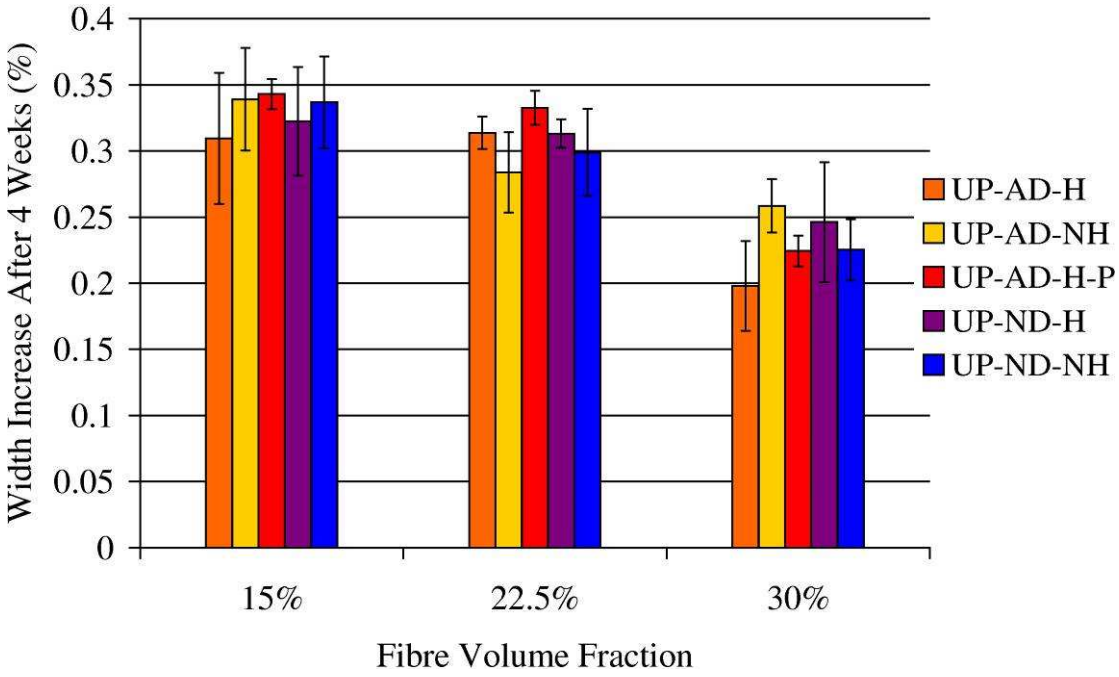

Figure 7.14 Effect of processing conditions on width increase after four weeks of water absorption

7.5 Results – resin system

7.5.1 Tensile tests

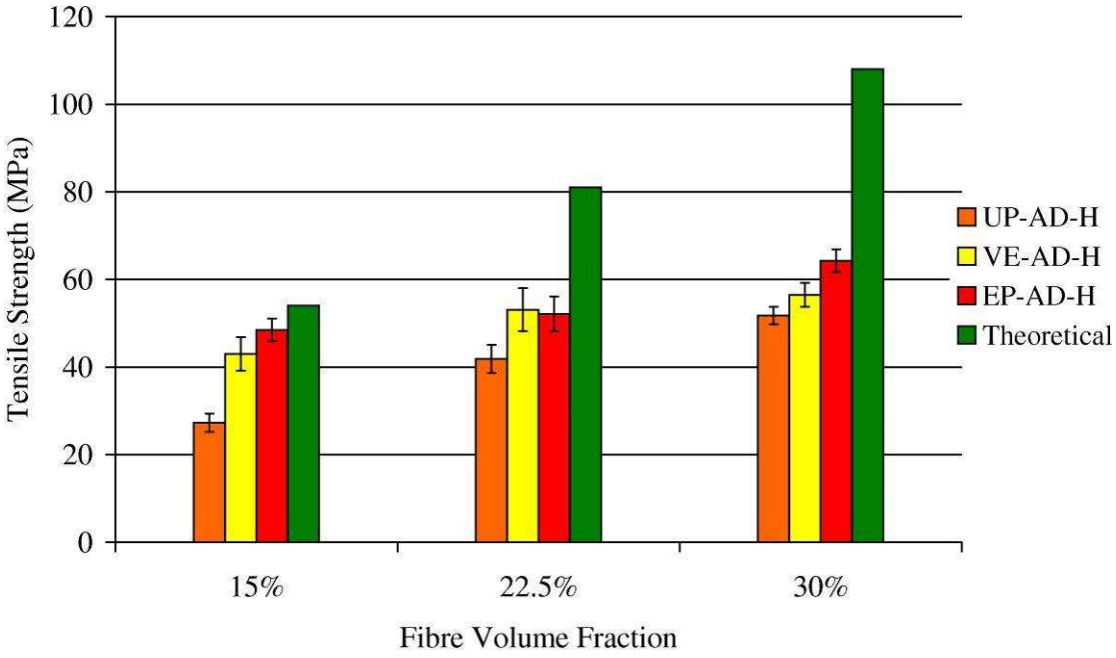

Figure 7.15 Effect of resin system on tensile strength

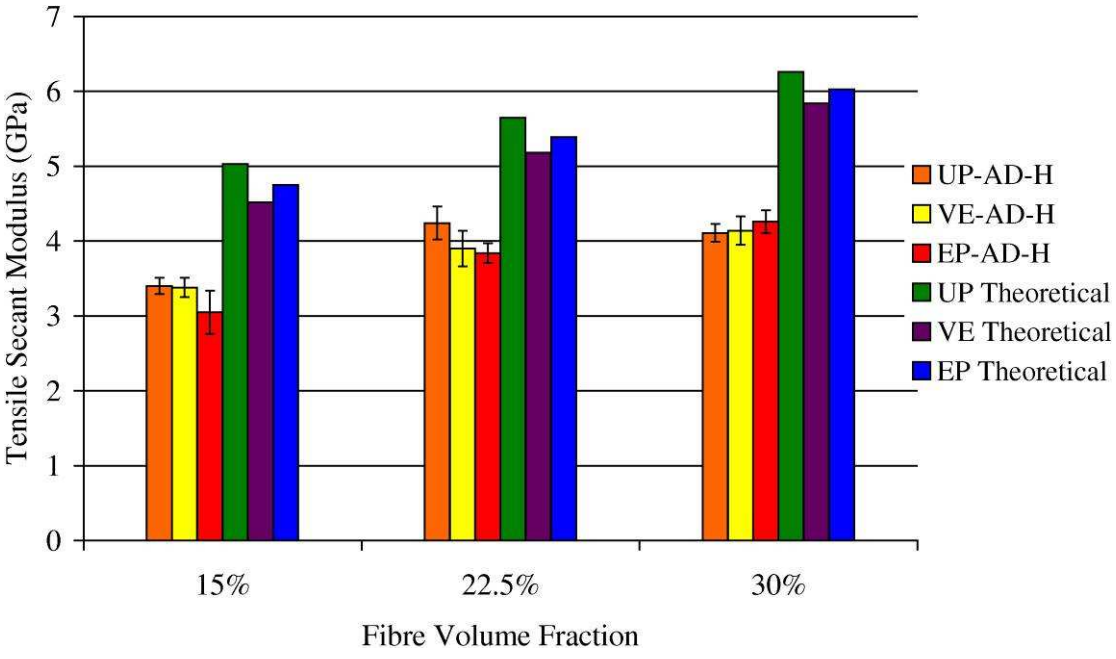

Figure 7.16 Effect of resin system on tensile secant modulus

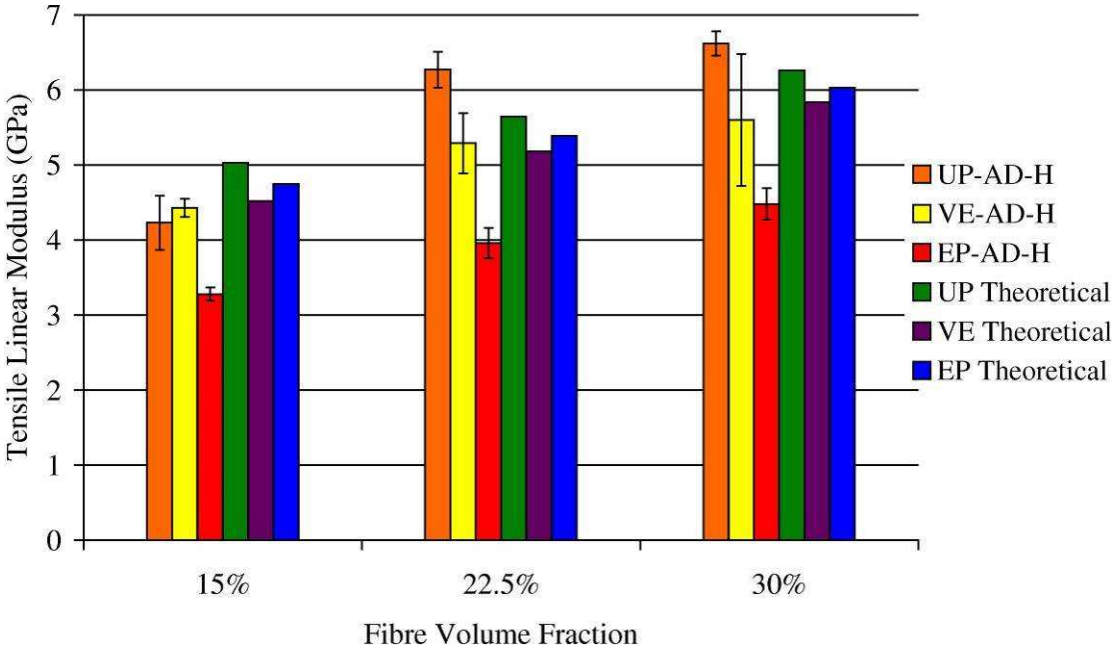

Figure 7.17 Effect of resin system on tensile linear modulus

7.5.2 Flexural tests

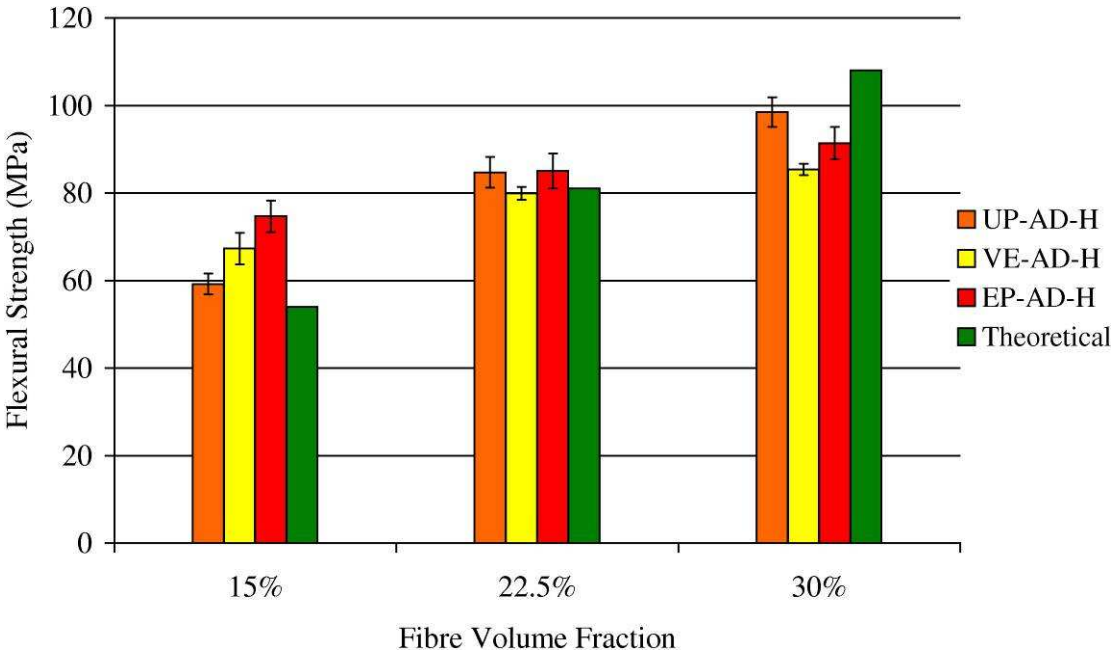

Figure 7.18 Effect of resin system on flexural strength

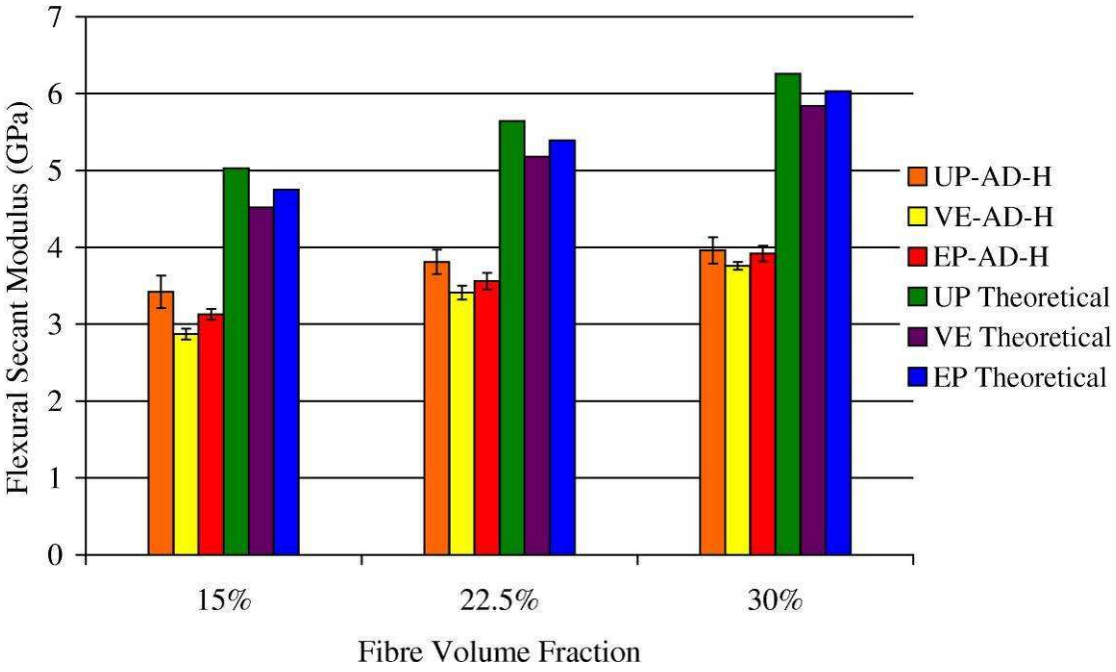

Figure 7.19 Effect of resin system on flexural secant modulus

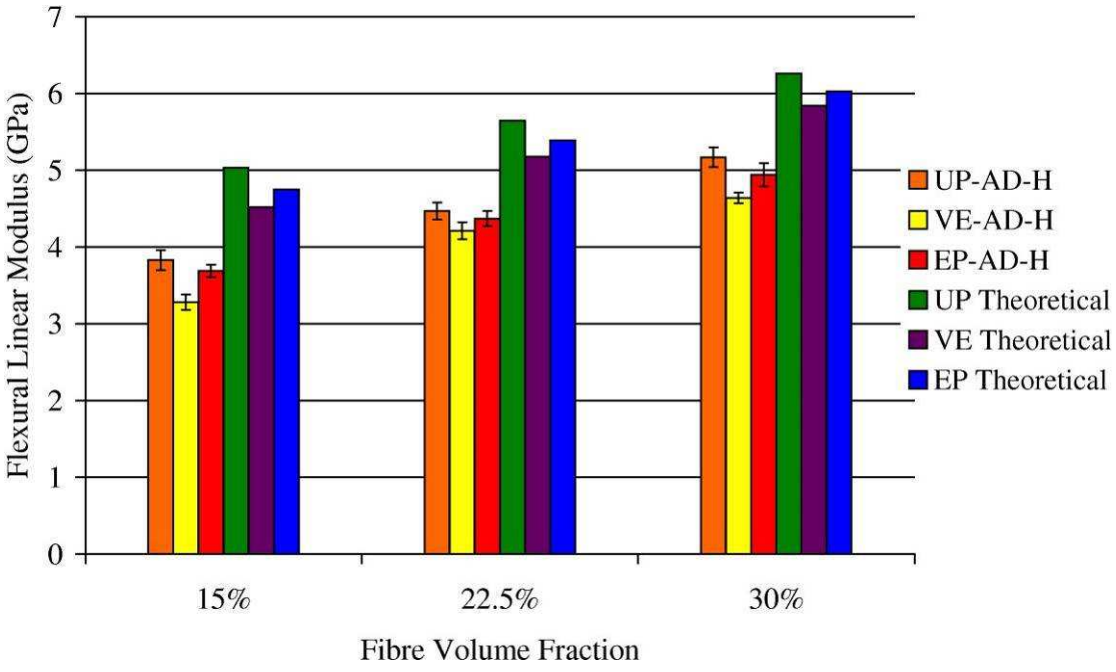

Figure 7.20 Effect of resin system on flexural linear modulus

7.5.3 Impact tests

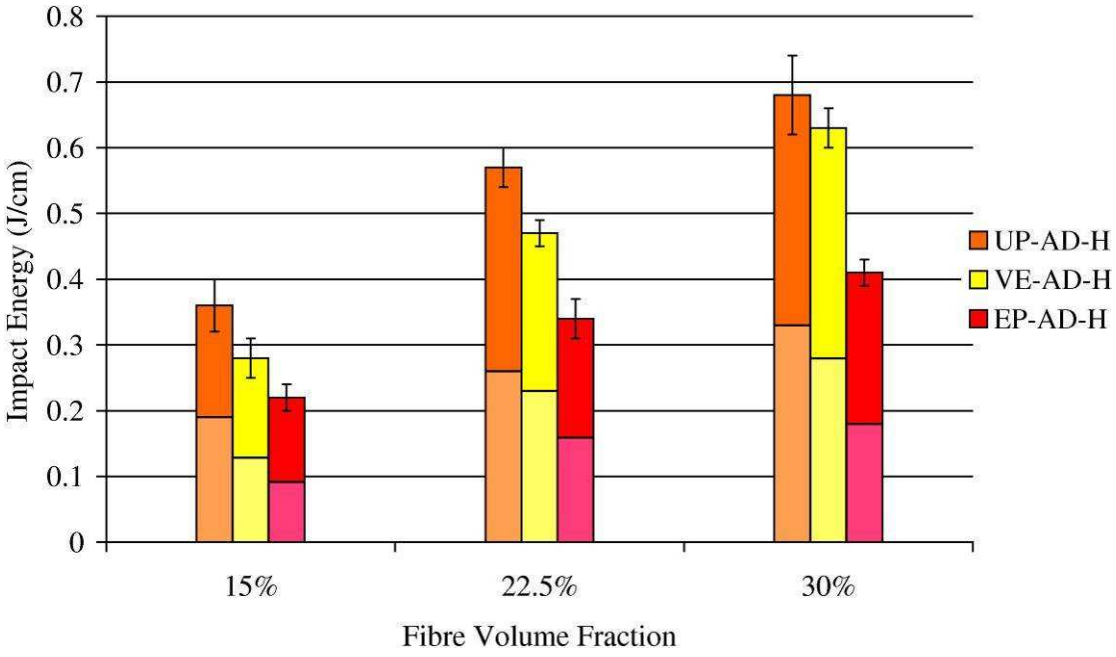

Figure 7.21 Effect of resin system on impact energy

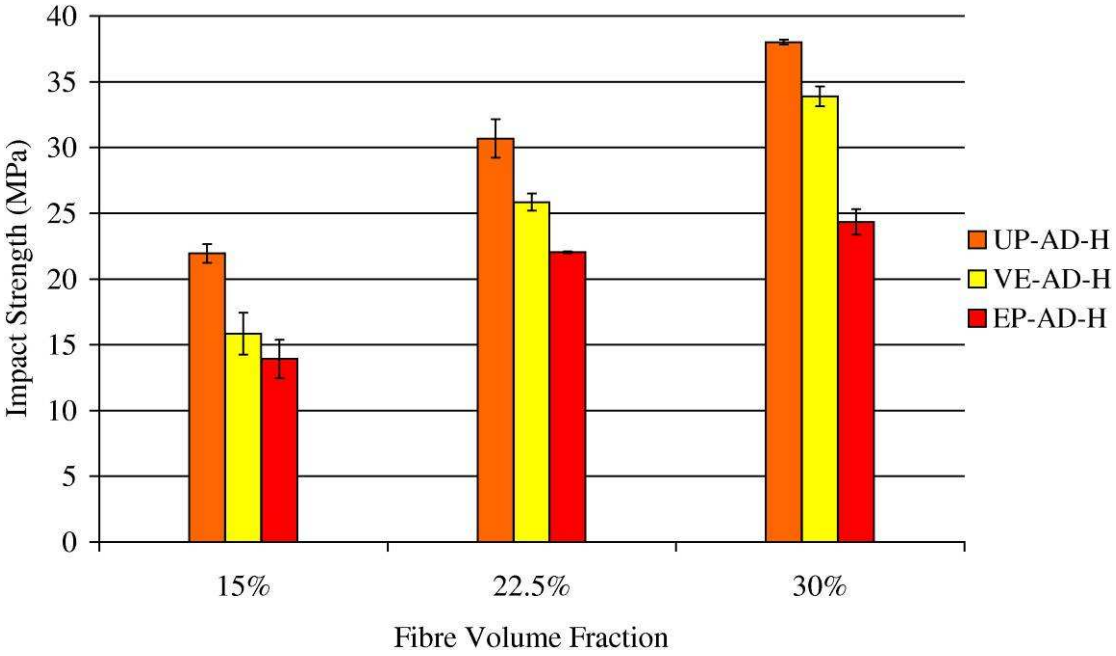

Figure 7.22 Effect of resin system on impact strength

7.5.4 SEM examinations

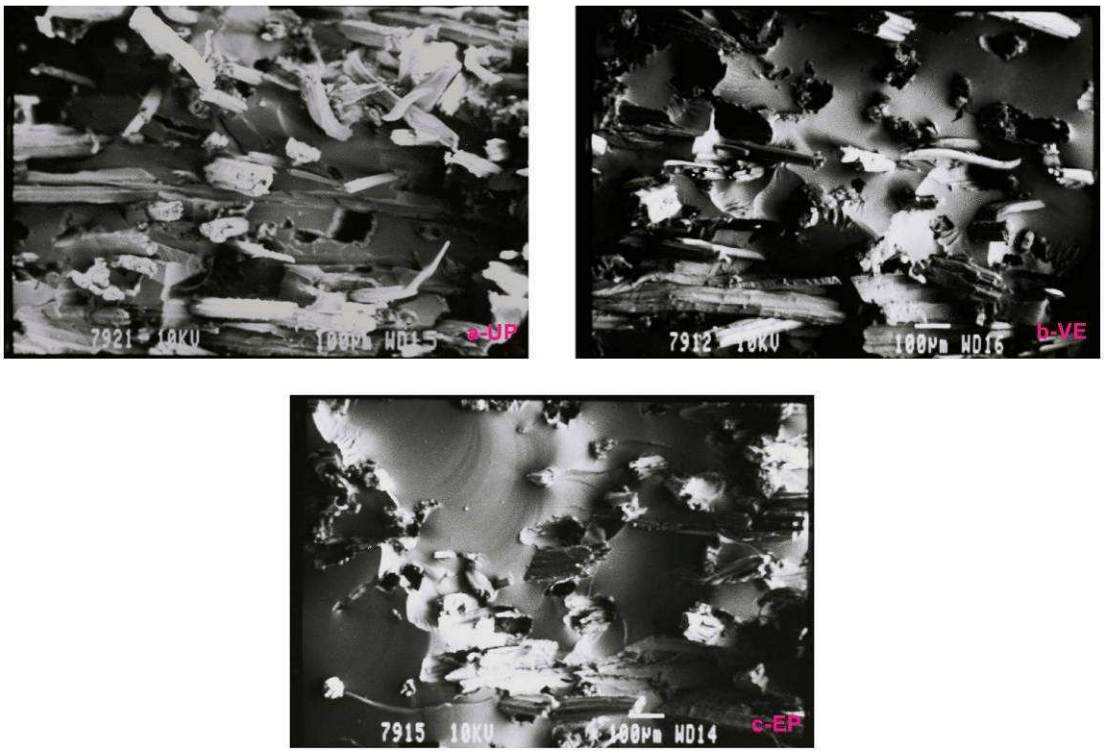

Figure 7.23 SEM micrographs of impact failure surfaces of composites made using various resin systems at 22.5 % fibre volume fraction

In Figure 7.23 the letters correspond to the following composites:

a: UP-AD-H b: VE-AD-H

c: EP-AD-H

7.5.5 Water absorption tests

Mass change

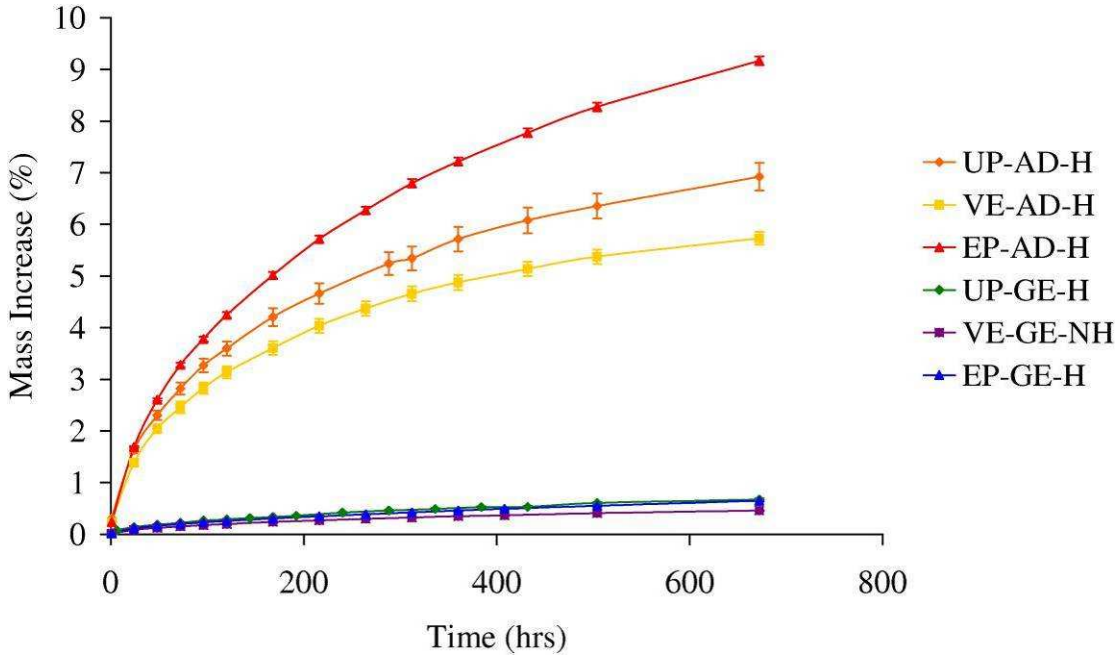

Figure 7.24 Effect of resin system on mass increase over four weeks of water absorption at 22.5 % fibre volume fraction

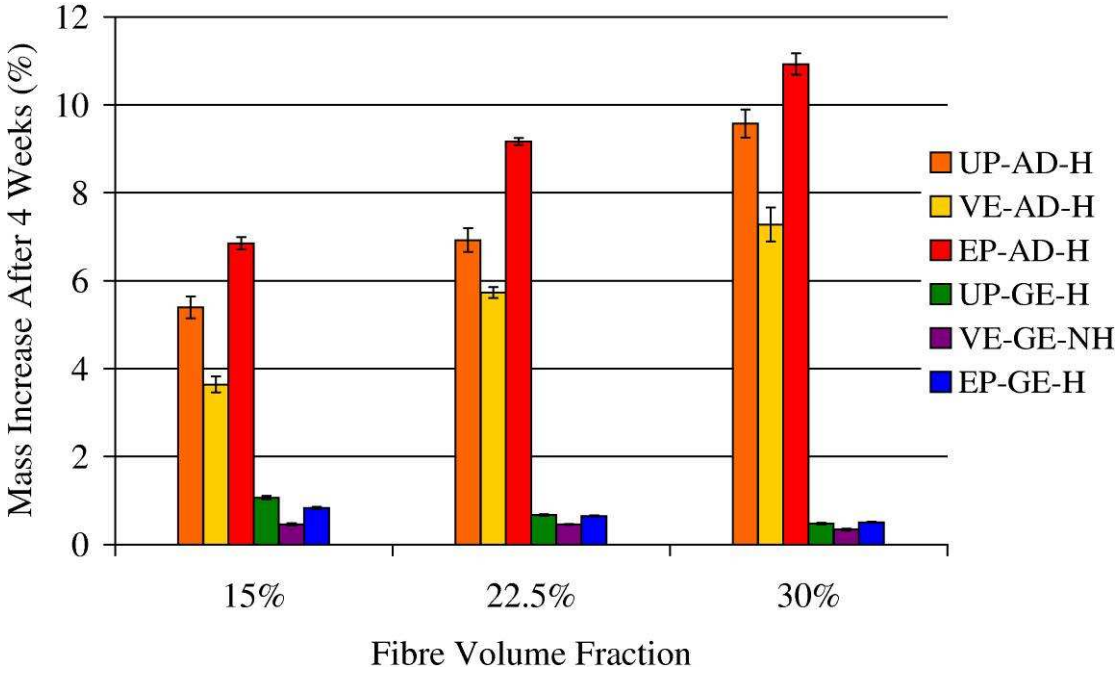

Figure 7.25 Effect of resin system on mass increase after four weeks of water absorption

Thickness change

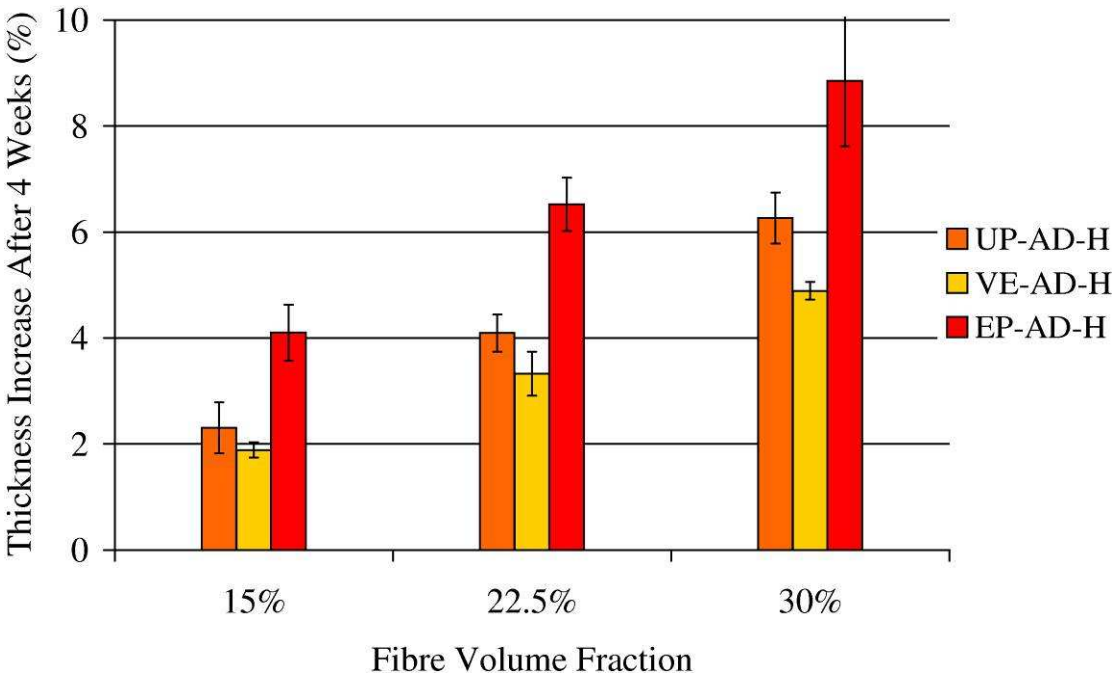

Figure 7.26 Effect of resin system on thickness increase after four weeks of water absorption

Length change

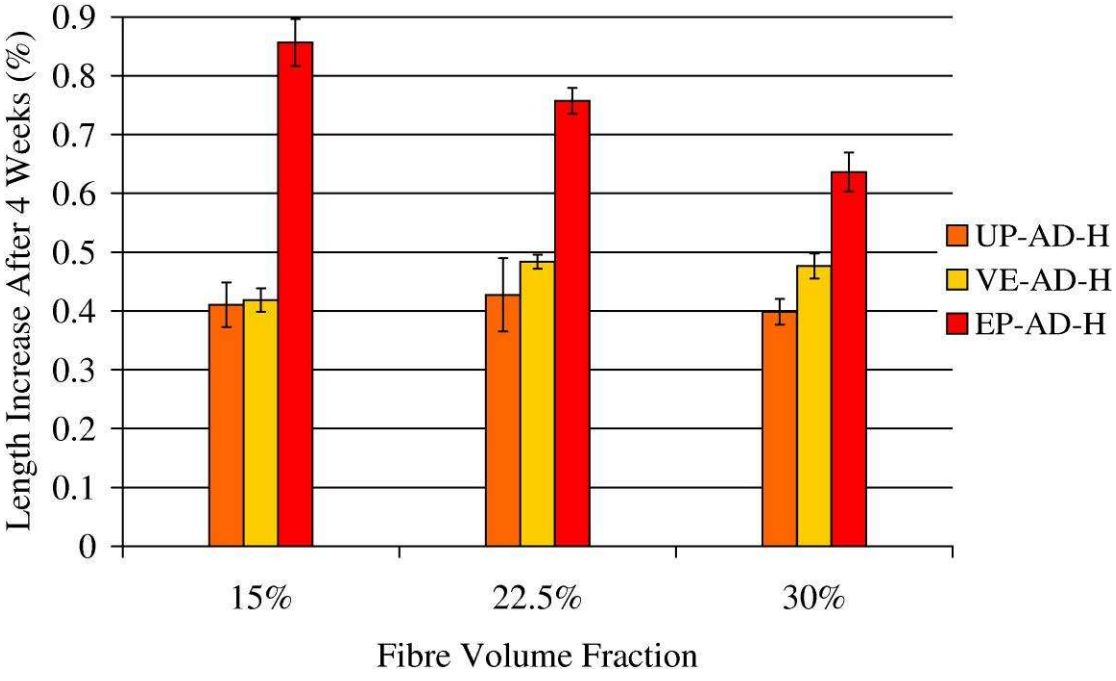

Figure 7.27 Effect of resin system on length increase after four weeks of water absorption

Width change

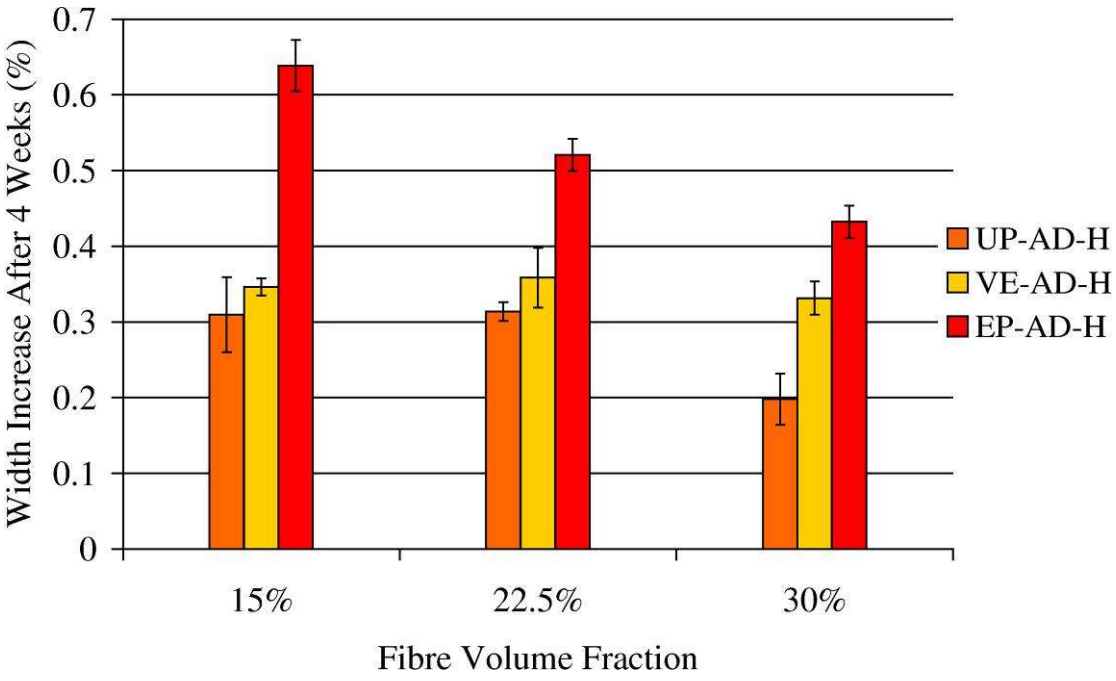

Figure 7.28 Effect of resin system on width increase after four weeks of water absorption

7.6 Results - specific properties

7.6.1 Specific tensile properties

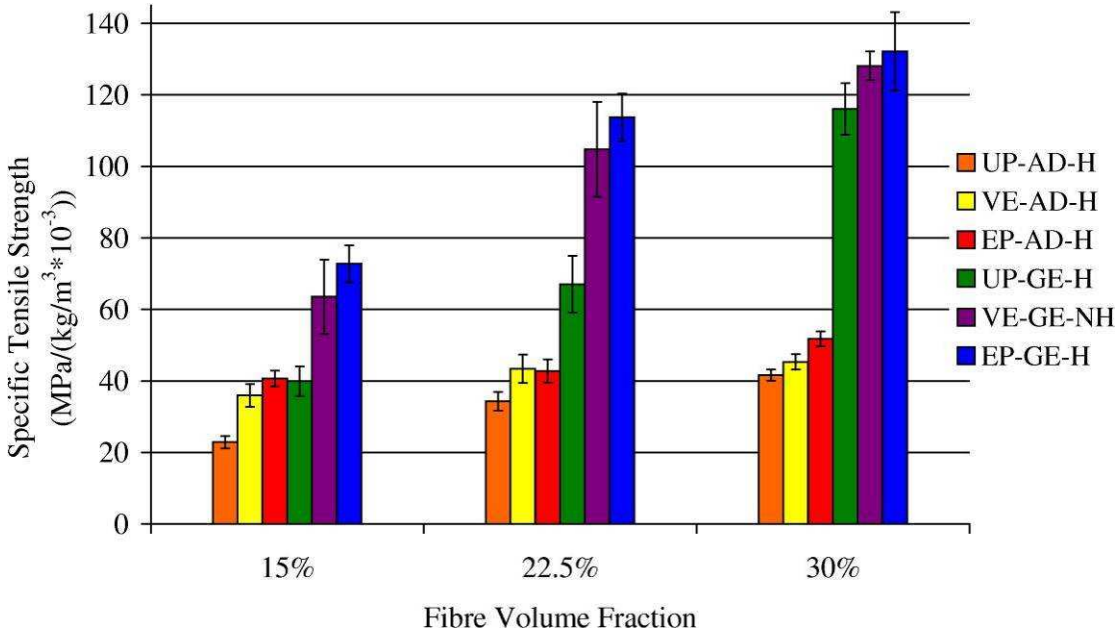

Figure 7.29 Comparison of specific tensile strength for kenaf fibre and glass fibre reinforced composites

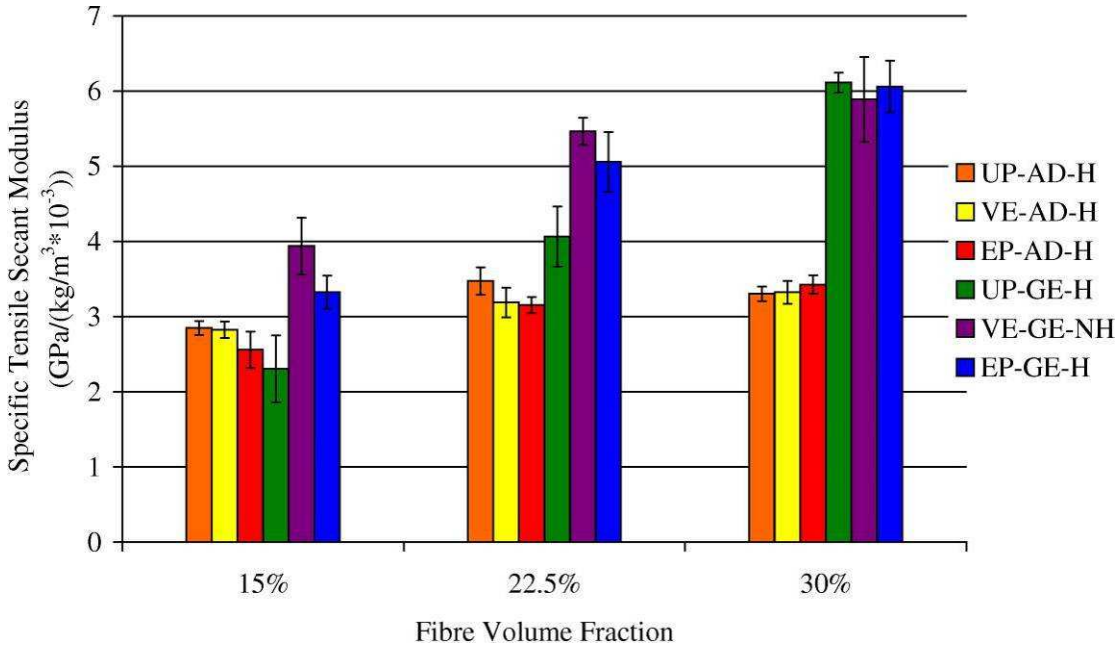

Figure 7.30 Comparison of specific tensile secant modulus for kenaf fibre and glass fibre reinforced composites

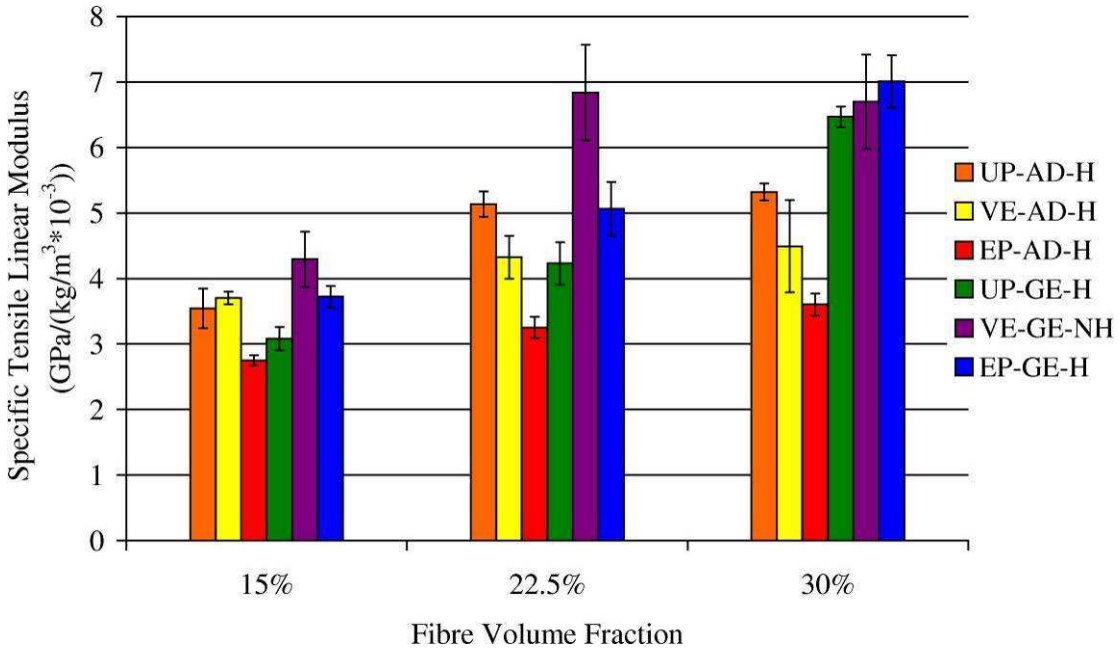

Figure 7.31 Comparison of specific tensile linear modulus for kenaf fibre and glass fibre reinforced composites

7.6.2 Specific flexural properties

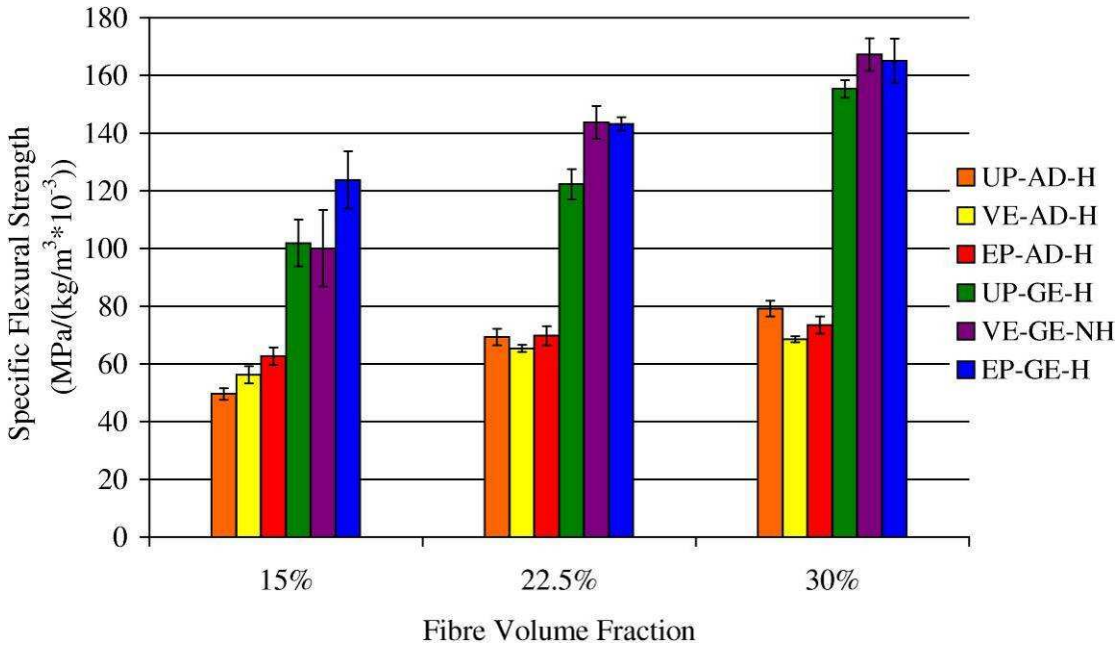

Figure 7.32 Comparison of specific flexural strength for kenaf fibre and glass fibre reinforced composites

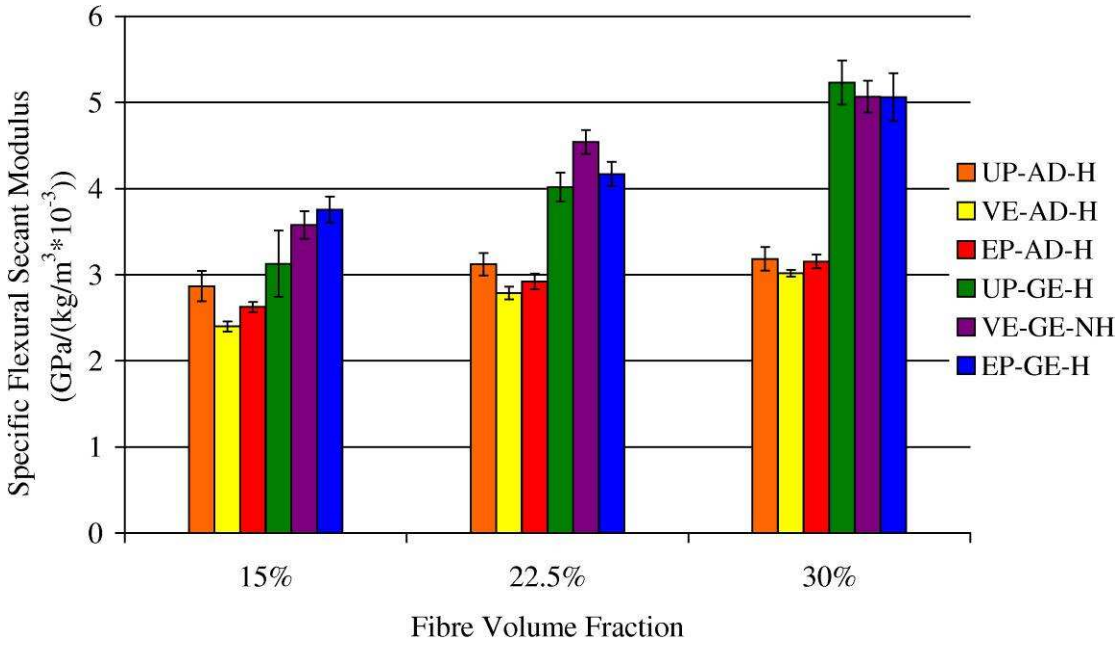

Figure 7.33 Comparison of specific flexural secant modulus for kenaf fibre and glass fibre reinforced composites

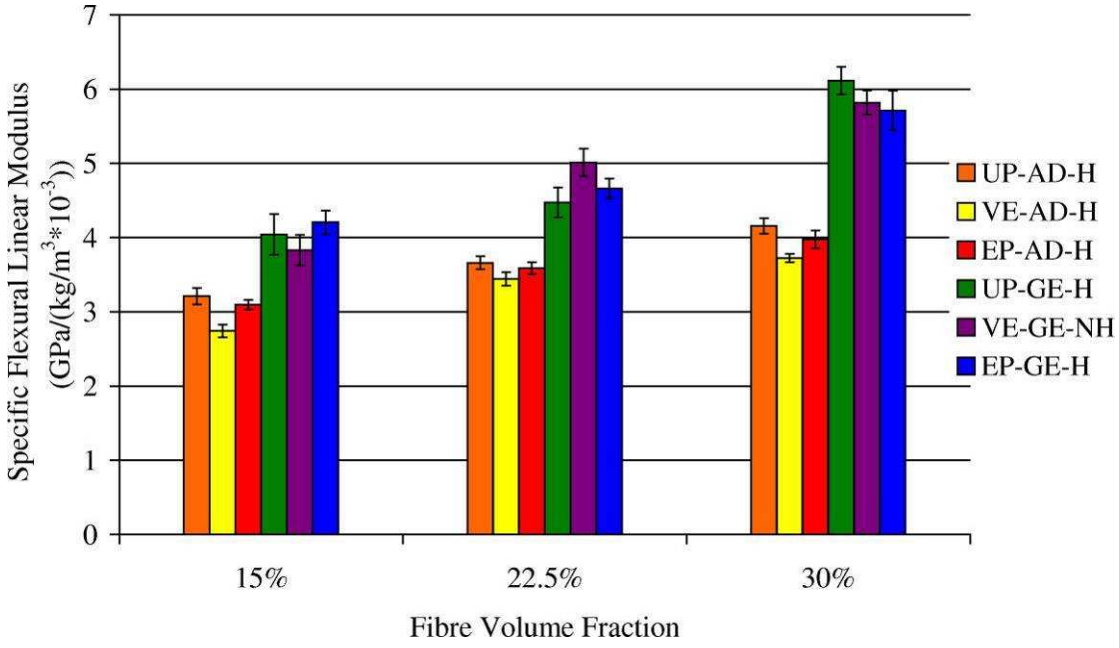

Figure 7.34 Comparison of specific flexural linear modulus for kenaf fibre and glass fibre reinforced composites

7.6.3 Specific impact properties

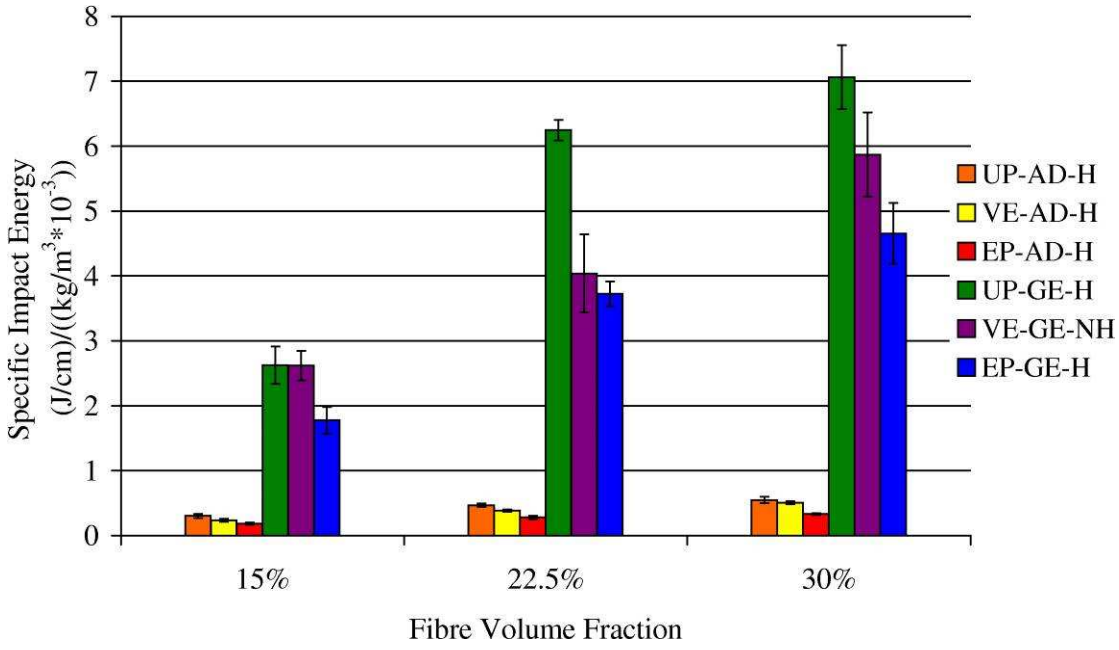

Figure 7.35 Comparison of specific impact energy for kenaf fibre and glass fibre reinforced composites

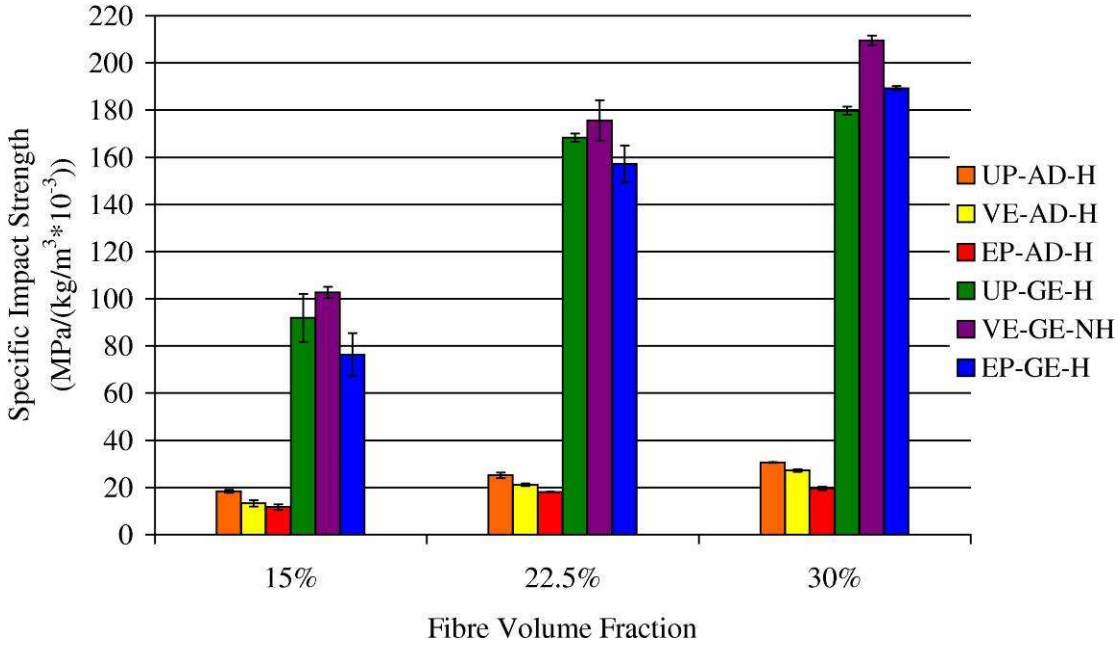

Figure 7.36 Comparison of specific impact strength for kenaf fibre and glass fibre reinforced composites

8 DISCUSSION

8.1 Processing conditions

8.1.1 Tensile tests

Results of the tensile tests show no significant difference in tensile strength (Figure 7.1), secant modulus (Figure 7.2) or linear modulus (Figure 7.3) for composites made with either dried or undried fibres for any fibre volume fraction. At 22.5 % and 30 % fibre volume fractions, for composites made using dried fibres (UP-AD-H, UP-AD-NH and UP-AD-H-P) it appears as though a cold mould might produce composites with slightly lower mechanical properties than those where the mould is heated. However, when taking into account the error bars and the results for each fibre volume fraction, the difference is not clear enough to be considered significant. Composites where the mould is pressurised after injection (UP-AD-H-P) produce the highest strength for all fibre volume fractions and in general produce slightly higher elastic moduli, but once again, the difference is not significant. Contrary to the findings of Bledzki and Gassan [(1)], composites made using dried fibres performed no better in tensile tests than those made using undried fibres.

It is interesting to note that the tensile strength of all the composites is lower than that of the unreinforced polyester resin which, according to the manufacturer, is equal to 63 MPa. This is contrary to normal expectation. The reduction in tensile strength is probably due to the inclusion of defects such as voids and poor interfaces during manufacture of specimens. The tensile strength, however, increases with fibre volume fraction as expected. Even though the introduction of fibres into the resin reduces the tensile strength, it improves the fracture toughness since the unreinforced resin is so brittle that it cannot be successfully machined into specimens. In addition, tensile secant moduli are slightly higher than the modulus of the unreinforced polyester resin (3.8 GPa) for all fibre volume fractions. Tensile linear moduli are also higher than the modulus of the unreinforced polyester resin for all fibre volume fractions and increase with fibre volume fraction. The measured tensile linear moduli must be viewed with caution however, since the linear region of the stress-strain curve is very small.

8.1.2 Flexural tests

Results of the flexural tests show no significant difference in flexural strength (Figure 7.4), secant modulus (Figure 7.5) or linear modulus (Figure 7.6) between the five composite types tested except for the case of the 15 % fibre volume fraction. In this case, the composites made using the pressurised mould (UP-AD-H-P) have the highest flexural strength which is around 15-20 % greater than that of the other composites. Secant and linear moduli are also higher but not by a significant amount. The reason for the increase could be attributed to the compression of voids during post-injection pressurisation. However, at higher fibre volume fractions, pressurisation of the mould has little effect on the flexural properties. This is especially true at 30 % fibre volume fraction where all five composites have almost identical values of flexural strength. Contrary to the findings of de Deus *et al.* [5] the flexural properties of composites made using dried fibres are no better than those made using undried fibres.

The flexural strength of the resin was not supplied by the manufacturer. It is likely that, as in the case of tensile strength, the addition of fibres decreases the flexural strength of the resin at low fibre volume fractions. Flexural strength increases with increasing fibre volume fraction after the initial reduction. Both flexural secant and linear moduli increase with increasing fibre volume fraction and there is a larger increase from 22.5 % to 30 % than from 15 % to 22.5 % fibre volume fraction.

Tensile, compressive and shear stresses exist in specimens loaded in flexure. The tensile and compressive stresses exist in the lower and upper halves of a specimen. Shear stresses through the thickness of the specimen are often critical at the interface between the fibres and the matrix. Failure of a specimen can result from any of these three types of stresses. I'Ons [33] found that flexural properties of polypropylene fibres and glass fibres in a polyester matrix were improved by treating fibres using the oxyflourination process. The improvement was attributed to better shear stress transfer between the constituents. In his work, specimens made using untreated fibres failed by debonding which indicates that shear stresses were responsible for the failure. In specimens made using treated fibres, however, tensile stresses were found to be the cause of failure. Flexural test specimens in the current research never failed

by delamination and always failed by cracking across the tensile surface. This indicates that, for these natural fibre reinforced composites, an improvement in bonding between fibres and matrix would not necessarily result in an increase in flexural properties.

8.1.3 Impact tests

Figure 7.7 shows the results obtained for impact energy. In this figure, the division in each bar indicates the division between initial and propagative impact energies and the sum of the two represents the total energy absorbed.

For all fibre volume fractions, composites made using undried fibres absorb slightly more total energy than composites made using dried fibres except at 30 % fibre volume fraction where the UP-ND-H composite absorbs the least energy. It is possible that the fibres dried partially during the time taken to close the mould with such a high fibre volume fraction. Composites where the fibres were dried absorb significantly more total energy however. The reduced impact energy of this composite can therefore probably be attributed to variability between specimens.

At 15 % fibre volume fraction, the UP-AD-NH composite absorbs the least total energy but at 22.5 % and 30 % fibre volume fractions, the energy absorbed is similar to that of the other composites in which fibres were dried. It is therefore unlikely that better fibre-matrix adhesion is the cause of the reduction in total impact energy and is probably due once more to variability between specimens. This is supported by the results of tensile and flexural tests where at 15 % fibre volume fraction, the UP-AD-H-P composite has better properties than the UP-AD-NH composite. Since the UP-AD-H-P composite is better in tensile and flexural tests than the UP-AD-NH composite, it could have better fibre-matrix adhesion which is expected to reduce its impact energy due to the reduction in fibre pull-out during failure [35].

At all fibre volume fractions, the initial impact energy is approximately equal indicating that the mode of failure is similar for all processing conditions because the initial impact energy shows how much energy is absorbed prior to the onset of failure.

Impact strength (Figure 7.8) at each fibre volume fraction was found to be similar for all composites. The UP-AD-NH composite has the lowest strength at 15 % fibre volume fraction. As discussed previously, it is believed that this is likely to be the result of variability between specimens and not of processing conditions.

The initial impact energy and strength are not significantly affected at any fibre volume fraction by the processing conditions. This leads to the conclusion that the processing conditions have little influence on fibre-matrix adhesion.

8.1.4 SEM examinations

Figure 7.9 shows SEM micrographs of the failure surfaces of the 22.5 % fibre volume fraction composites after impact testing. All composites failed by fibre pull-out, confirming why the results of the mechanical testing are so similar. It is evident that the variation of processing conditions does not alter failure mechanism. SEM examinations were also conducted for 15 % and 30 % fibre volume fractions. These images are not presented in the results because they are not significantly different from those of Figure 7.9 but can be found in Appendix E.

8.1.5 Water absorption tests

Figure 7.10 shows the water absorption of the 22.5 % fibre volume fraction composites over a four week period. Composites of 15 % and 30 % fibre volume fraction show similar trends. The rate of mass increase due to water absorption is at first high and then diminishes with time. Due to practical considerations, water absorption tests could not be carried out for longer than four weeks so equilibrium was not reached. The results however suggest that equilibrium would eventually be obtained.

Figure 7.11 shows that water absorption increases with fibre volume fraction as expected due to the increasing numbers of hydrophilic fibres. At 15 % and 22.5 % fibre volume fractions the UP-AD-H-P composite absorbs the least water. This trend suggests that pressurising the mould after injection helps reduce water absorption at lower fibre volume fractions, probably as a result of the reduction in void size. There is, however, no benefit from pressurisation at 30 % fibre volume fraction. At this fibre

volume fraction, the UP-AD-NH composite absorbs the least amount of water. The UP-AD-NH composites also absorb less water than most of the other composites at 15 % and 22.5 % fibre volume fractions. Thus, it is not possible to suggest a single combination of processing conditions that will reduce water absorption. Depending on fibre volume fraction, using dried fibres in a cold mould or pressurising the mould after resin injection can result in reduced water absorption.

Figure 7.12 presents the increase in thickness of the specimens after four weeks of water immersion. The effect of processing conditions on the thickness does not show any consistent trend. At 15 % fibre volume fraction, the increase in thickness is almost identical for all composites. At 22.5 % fibre volume fraction, all composites made using dried fibres show an almost identical increase in thickness. This is also true for the composites made using undried fibres. These, however absorb slightly less water than those made from dried fibres.

A comparison of Figure 7.11 and Figure 7.12 shows that both the amount of water absorbed and the thickness increase with fibre volume fraction. Further comparison of these figures at 15 % and 22.5 % fibre volume fractions shows no similarity between changes in thickness and in mass for the various processing conditions. For example, at 15 % fibre volume fraction, the UP-AD-H-P composite absorbs the least water but shows the largest increase in thickness. At 30 % fibre volume fraction, there is some similarity in the results for the various processing conditions. At this fibre volume fraction, the UP-AD-NH and UP-ND-H composites absorb the least water and show the lowest increases in thickness while the mass and thickness increases in the other composites are approximately equal.

Figure 7.13 and Figure 7.14 present the increase in length and width of the specimens after four weeks of water absorption. It can be seen that they exhibit different trends. At 15 % fibre volume fraction for example, the UP-AD-H-P composite shows the second lowest increase in length but the highest increase in width.

It is interesting to note that the increase in length of all the composites is larger than that of width. This indicates that the non-woven fibre mats are not isotropic in the plane and that more fibres are orientated along the width of the specimens i.e. in the

direction of the length of the non-woven roll. Thus, because the hygroscopic strain of the fibres is greater across their diameter than along their length [34, 36], the widths of the specimens increase less than their lengths. A representation of this can be seen in Figure 8.1.

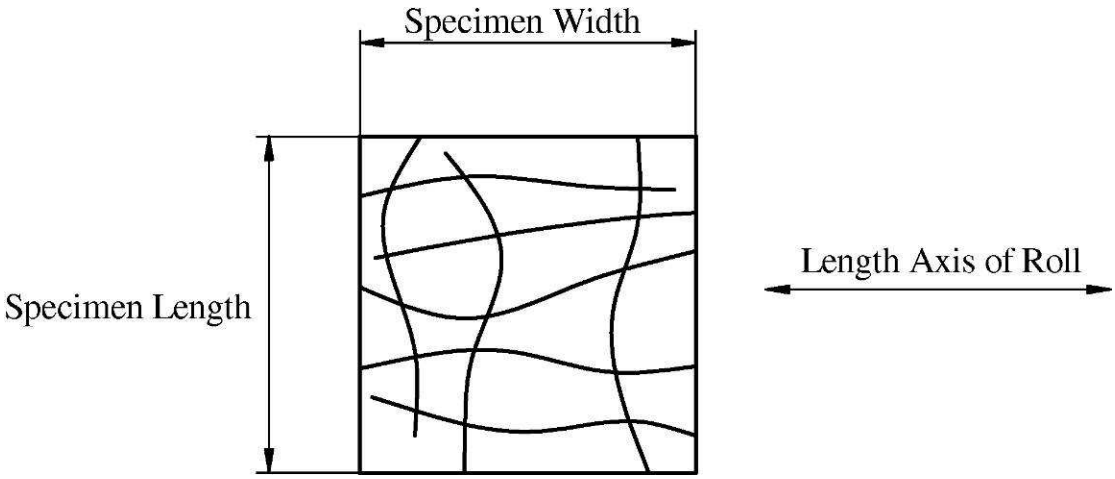

Figure 8.1 Representation of fibre orientation in water absorption specimen

When comparing thickness, length and width increases, in Figure 7.12, Figure 7.13 and Figure 7.14, it is evident that the increase in thickness is much larger than those of length and width. This indicates that the coefficient of hygroexpansion is greatest in the through-thickness direction of the specimens. This is believed to be due to the greater swelling of the fibres in their radial direction than along their length and the fact that the preferentially in-plane alignment of the fibres prevents strains in the through-thickness direction from being constrained.

8.2 Resin System

8.2.1 Tensile tests

Figure 7.15 shows the tensile strengths of the different composites. It is evident that both the vinyl ester and epoxy resin produce composites with higher tensile strength than those made using polyester. The tensile strengths of the unreinforced resin systems are reported by the manufacturers to be 69 MPa, 86 MPa and 73.3 MPa for the polyester, vinyl ester and epoxy resins, respectively. These values are greater than the tensile strengths measured for any fibre volume fraction. As in section 8.1.1, this is probably due to the inclusion of defects such as voids and poor interfaces during

manufacturing of the composites. Epoxy composites have the highest tensile strength when considering all fibre volume fractions. This is a good indication that the epoxy bonds better with the fibres than the other resins because it has a tensile strength that is similar to that of the polyester and lower than that of the vinyl ester resin. The higher tensile strength of the vinyl ester composites in comparison to the polyester composites is believed to be a result of the high strength of the resin but it could also be an indication of improved bonding between the fibres and the matrix.

Tensile secant moduli (Figure 7.16) are not significantly different for the various resin systems at all fibre volume fractions. For 22.5 % and 30 % fibre volume fractions, the values of modulus are higher than those of the unreinforced resins (3.8 GPa, 3.2 GPa and 3.5 GPa for the polyester, vinyl ester and epoxy respectively). The largest increase in tensile secant modulus occurs for the vinyl ester composite at 30 % fibre volume fraction which has a modulus just under 30 % greater than that of the unreinforced resin.

When considered across all fibre volume fractions, the tensile linear modulus (Figure 7.17) of the polyester composites is the highest and that of the epoxy composites the lowest. This result is unexpected considering that the results of tensile strength indicate that the epoxy bonds well to the fibres and that the unreinforced epoxy has the second highest elastic modulus of the resin systems. If the secant and linear moduli of the epoxy composites are compared however, it is seen that they are quite similar which indicates that the epoxy composites behave more linearly than those made using polyester or vinyl ester resins. Thus, although the epoxy composites have lower values of modulus than composites made using the other resins, their strain response is more predictable. Figure 8.2 shows examples of typical stress-strain curves for a polyester and an epoxy composite specimen.

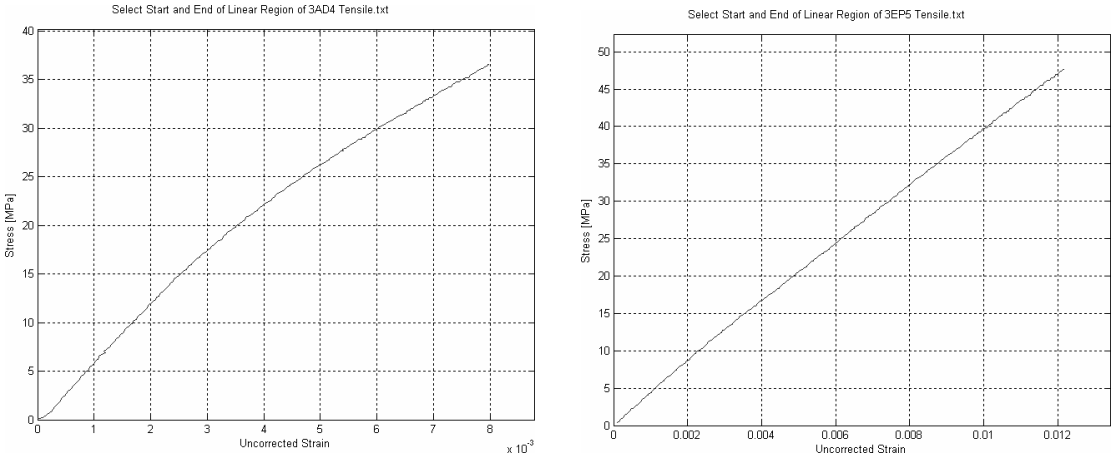

Figure 8.2 Typical stress-strain curve for a polyester (left) and an epoxy (right) composite specimen

Results of tensile tests show that epoxy composites perform best in terms of strength and polyester composites in terms of modulus. Vinyl ester composites strike a middle ground performing comparatively well in terms of both strength and modulus.

8.2.2 Flexural tests

Results for flexural strength are presented in Figure 7.18. It can be seen that at 15 % fibre volume fraction, the epoxy composite has the highest flexural strength followed by the vinyl ester and then the polyester. At 22.5 % fibre volume fraction, composites made using all three resin systems possess similar strength although epoxy and polyester composites are slightly stronger than the vinyl ester composite. At 30 % fibre volume fraction, the polyester composite has the highest strength followed by the epoxy and then the vinyl ester composite. The polyester composites therefore appear to improve in relative performance with fibre volume fraction. A possible explanation is the combination of fibre volume fraction and the presence of voids brought on by the need for vinyl ester and epoxy resins to be mixed by hand and degassed in a pressure pot instead of using the RTM machine. At lower fibre volume fractions, stress concentrations around voids are smaller than at higher fibre volume fractions and thus the presence of voids plays a larger role at higher fibre volume fractions than at lower fibre volume fractions. Figure 8.3 shows examples of SEM micrographs where voids can be seen in vinyl ester and epoxy composites. No voids were found when examining polyester composites.

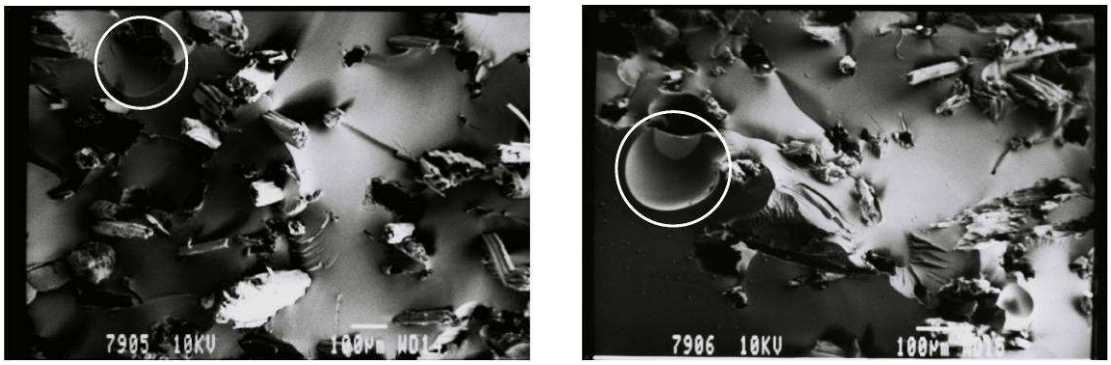

Figure 8.3 Voids in a vinyl ester composite (left) and an epoxy composite (right)

Flexural secant modulus (Figure 7.19) is highest for polyester and lowest for vinyl ester composites for all fibre volume fractions. Although data for flexural moduli were not available for all the resins, this trend is expected since the tensile moduli of the unreinforced resins are highest for polyester and lowest for vinyl ester. Flexural linear moduli (Figure 7.20) show similar trends to those of flexural secant moduli but the values are higher. Figure 7.19 and Figure 7.20 indicate that the resin system has little effect on the flexural moduli of the composites across all fibre volume fractions.

8.2.3 Correlation of experimental and theoretical results for tensile and flexural tests

Theoretical values obtained for tensile strength (Figure 7.15) show poor correlation with experimental results. The difference between theoretical values and experimental values increases with fibre volume fraction. Theoretical moduli show poor correlation with tensile secant modulus (Figure 7.16) except that the difference is approximately equally large for all fibre volume fractions. Comparison with tensile linear moduli (Figure 7.17) shows reasonably good correlation with experimental values for polyester composites and poor correlation for epoxy composites. Vinyl ester composites show the best correlation between theoretical moduli and experimental linear moduli with the largest difference for any fibre volume fraction within 5 %.

Theoretical flexural strength (Figure 7.18) shows reasonably good correlation with experimental results especially at 22.5 % fibre volume fraction. Polyester composites correlate best when considering all fibre volume fractions. At low fibre volume fractions the theoretical model under-predicts the values obtained for vinyl ester and

epoxy composites while at higher fibre volume fractions, values are over-predicted. The good correlation of theoretical with experimental flexural strength is thus probably coincidental especially when considering that the theoretical value is based on tensile failure criterion.

Flexural secant moduli (Figure 7.19) show poor correlation with theoretical moduli which are over-predicted. Flexural linear moduli (Figure 7.20) are also lower than predicted moduli. It is clear from these results that a simple rule of mixtures as applied in this work is not suitable for predicting flexural moduli. This is likely to be because of three reasons; the first being that theoretical moduli were calculated using the tensile moduli of resins and not the flexural moduli, second because the compressive behaviour of the fibres is not known and third because the value of the efficiency factor (η) does not take into account the out-of-plane orientation of the fibres caused by the needle-punching manufacturing process. For CSM, the value of η is typically set equal to 0.3 and this value was used for all calculations. However, in CSM the fibres are orientated in the plane. This means that in kenaf fibre reinforced composites there are fewer fibres orientated in the plane of the applied load. Thus, using a lower value of η may result in better correlation with experimental results.

8.2.4 Impact tests

Figure 7.21 presents the results for impact energy. It can be seen that the impact energy strongly depends on the resin system. Polyester composites absorb the most energy before failure while the epoxy composites absorb the least for all fibre volume fractions. A number of authors [9, 27, 28, 35 & 30] have observed a reduction in impact energy with increased fibre-matrix adhesion. These results therefore suggest that the epoxy resin bonds better with the fibres than the other two resin systems. This suggestion is reinforced when the propagative energy is considered. It is evident that the propagative energy is similar for the polyester and vinyl ester composites at any fibre volume fraction while epoxy composites have slightly lower propagative energy. The lower propagative energy of the epoxy composites indicates that there is less fibre pull-out and thus better adhesion between fibres and matrix than in the composites made using the other resin systems. van den Oever *et al.* [35], suggest that better fibre matrix adhesion results in shorter average fibre pull-out lengths which

reduces energy absorption. Examination of the SEM micrographs of Figure 7.23 shows that the epoxy composites have cleaner failure surfaces than polyester or vinyl ester composites. This indicates that the fibres in epoxy composites have a shorter average fibre pull-out length than those in other composites. Further examination of these SEM micrographs shows that the polyester composites fail by fibre pull-out, the epoxy composites fail by fibre fracture and the vinyl ester composites seem to fail by a combination of both fibre pull-out and fibre fracture.

Sèbe *et al.* [9] reported that the addition of hemp fibres lowered the impact energy of the polyester resin used in their research but following the initial reduction, impact energy was found to increase with increasing fibre fraction and eventually surpass that of the unreinforced resin. Rousion *et al.* [25] found that the addition of hemp / kenaf fibres to polyester increased the impact strength of the polyester resin they used. In this work, testing of unreinforced resins was attempted but polyester and vinyl ester specimens cracked easily during machining and full sets could not be obtained for testing. Five epoxy specimens were tested but the impact was not large enough to be registered by the equipment. Thus, it is unlikely that any of the three unreinforced resin systems have impact energies greater than the kenaf fibre reinforced composites even at low fibre volume fractions.

Impact strength (Figure 7.22) is also strongly affected by the resin system. Impact strength is highest for polyester composites and lowest for epoxy composites. According to van den Oever *et al.* [35], a consequence of shorter fibre pull-out length is that the matrix deformation zone is smaller. Concentration of the strain energy into a smaller region causes the apparent impact strength to be reduced.

8.2.5 Water absorption tests

Figure 7.24 shows the water absorption of the 22.5 % fibre volume fraction composites over a four week period. Composites of 15 % and 30 % fibre volume fraction show similar trends. The trends observed in these figures are similar to those observed for processing conditions. The rate of water absorption is significantly higher in the kenaf fibre reinforced composites than in the glass fibre reinforced

composites however. As in case of the effects of processing conditions, water absorption tests could not be carried out for longer than four weeks.

Figure 7.25 indicates that the kenaf fibre reinforced composites absorb significantly more water after four weeks than the glass fibre reinforced composites at all fibre volume fractions. The resin system has a significant effect on the water absorption of kenaf fibre composites but not on that of glass fibre composites. It can also be seen that among the kenaf fibre composites, the ones made with vinyl ester resin absorb the least amount of water.

While epoxy composites absorb the most water for kenaf fibre reinforcement, the polyester composites absorb the most water for those made with glass fibre reinforcement. It is suspected that this is due to better wetting of the glass fibres by the epoxy resin than the polyester resin. Examination of glass composites made using the two resins showed that epoxy composites appeared almost transparent, while in polyester composites, glass fibre bundles could be observed. As a result, many pathways existed around fibres in the polyester composites along which water could move and be absorbed. The trends observed for water absorption of kenaf composites made using the three resin systems are similar to those for the unreinforced resins for which epoxy absorbs the most water followed by the polyester and finally the vinyl ester. Results of water absorption tests conducted on unreinforced resins can be found in Appendix F. Water absorption is affected by the resin system because water can diffuse through it and into fibres. Thus, the greater the amount of water that is able to diffuse through the resin, the greater the amount of water and the rate at which it can enter the fibres. This in turn results in the entire specimen absorbing more water.

Comparing Figure 7.25 and Figure 7.26, the trend for mass and thickness increase is the same for the three resin systems i.e. the epoxy composites experience the largest increase in mass and thickness and vinyl ester composites the smallest increase in mass and thickness. This is however not true for the length (Figure 7.27) and width (Figure 7.28). Epoxy composites experience the largest increase in length and width while polyester composites experience the smallest increase in length and width. For all resin systems, test specimens experience a larger increase in thickness than in

length or width. As discussed in section 8.1.5, this is due to the greater swelling of the fibres in their radial direction than along their length.

The results for processing conditions showed that the length of polyester composite specimens increase more than the width. Examination of Figure 7.27 and Figure 7.28 reveals the same phenomenon occurs for vinyl ester and epoxy composites, once again confirming that the fibre mats are not isotropic in the plane. Further examination of these figures shows that as fibre volume fraction increases, there is a general trend of decreasing length and width increases for composites made using all three resin systems. A theoretical investigation of the hygroexpansion of the composites was conducted in order to explain this. Results of this investigation are discussed in section 8.2.6.

Vinyl ester composites generally perform best in water absorption tests showing the lowest mass and thickness increases. Polyester composites perform better than vinyl ester ones in terms of length and width increases but, this effect is not significant.

8.2.6 Hygroexpansion of kenaf fibre reinforced composites

Water absorption tests of kenaf fibre reinforced composites showed that the increases in length and width of the specimens decrease with increasing fibre volume fraction. This is especially true in the case of epoxy composites (see Figure 7.27 and Figure 7.28). It is likely that this is more pronounced in epoxy composites due to better fibre matrix adhesion. Composites made using all three resin systems increase more in length and width than the unreinforced resins. This indicates that the decreasing trend in length and width with increasing fibre volume fraction cannot be the result of restraint of swelling of the matrix by the fibres (see Appendix F for dimensional change of unreinforced resins).

A theoretical model was used to determine the expected trends in dimensional changes that occur as a result of water absorption. More information regarding the model can be found in Appendix G. The model predicts the coefficients of hygroexpansion of a unidirectional ply of fibres and matrix and then uses classical lamination theory to determine the coefficients of hygroexpansion for a composite

with randomly orientated fibres. Because a change in dimension during water absorption is equal to the corresponding coefficient of hygroexpansion multiplied by the change in water content (as shown by equation 8.1), trends observed for coefficients of hygroexpansion will therefore be the same as those observed for changes in thickness, length and width. Through-thickness and in-plane coefficients of hygroexpansion determined theoretically and experimentally for kenaf epoxy composites at various fibre volume fractions can be seen in Figure 8.4. In the figure, the experimental in-plane coefficient of hygroexpansion was determined using the average of the length and width dimensions because the model does not account for the lack of in-plane isotropy of the fibre mats. Epoxy composites were chosen due to the large hygroexpansion experienced by these composites.

$$\Delta\varepsilon = \beta\Delta m \tag{8.1}$$

In equation 8.1, $\Delta\varepsilon$ represents the change in dimension, β the coefficient of hygroexpansion and Δm the mass change in water content.

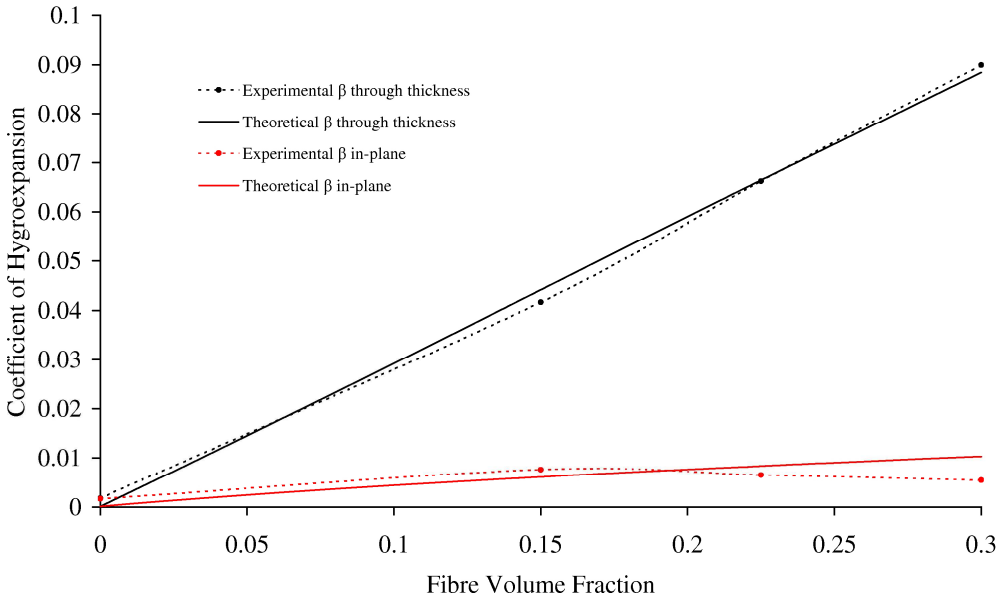

Figure 8.4 Theoretical and experimental coefficients of hygroexpansion for kenaf composites

The results of the theoretical model indicate that as fibre volume fraction is increased, length and width increase, but at a decreasing rate. This does not however explain why experimental measurements taken from specimens show smaller increases in

length and width at high fibre volume fractions than at low fibre volume fractions. It is possible that as the fibre volume fraction is increased, the three-dimensional arrangement of the non-woven fibre mats is flattened into a more two-dimensional arrangement. As previously stated, the fibres swell more through their thickness than they do along their length. Thus, at low fibre volume fractions, where the structure of the non-woven mat is three-dimensional, the radial swelling of the fibres during water absorption contributes more to the in-plane hygroscopic strain of the composite specimens than at high fibre volume fractions where the non-woven mat is more two-dimensional in structure. Figure 8.5 gives a visual representation of how increasing the fibre volume fraction makes the fibre arrangement more two-dimensional. This hypothesis is supported by the experimental through-thickness coefficient of hygroexpansion which at a fibre volume fraction of approximately 15 % begins to increase at an increased rate. From this point, the increasingly two-dimensional arrangement of the fibres causes a decrease in in-plane swelling and conversely results in an increase in through-thickness swelling.

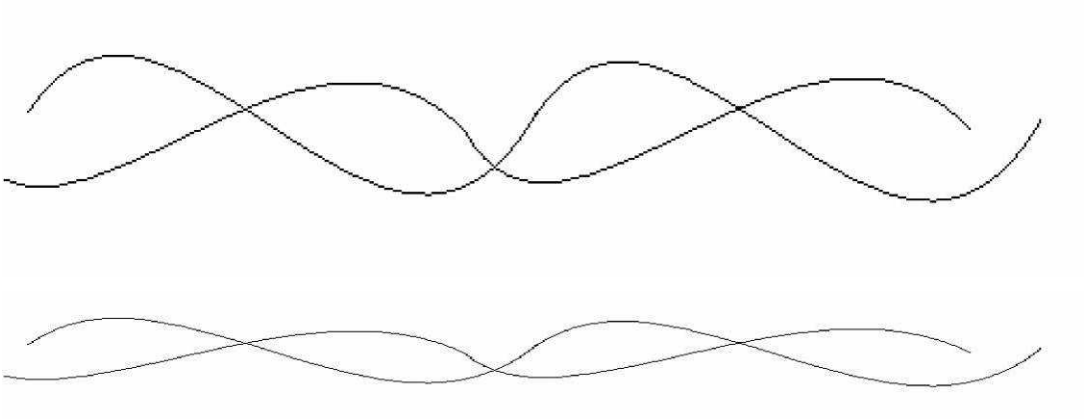

Figure 8.5 Representation of two fibres in an uncompressed and a compressed non-woven fibre mat

Thus, the combination of the effects shown by the theoretical model and the better alignment of the fibres in the plane as the fibre volume fraction increases could be the reason that the composite specimens experience smaller in-plane dimensional increases at high fibre volume fractions than at low fibre volume fractions.

8.3 Specific mechanical properties

8.3.1 Specific tensile properties

The specific tensile strengths (Figure 7.29) of the glass fibre composites in comparison to the kenaf fibre composites are superior for all fibre volume fractions. The specific strength of the kenaf fibre reinforced composites displays a small increase with fibre volume fraction whereas that of the glass fibre reinforced composites increases significantly.

Figure 7.30 shows that the specific tensile secant moduli of the glass fibre composites are superior to those of the kenaf fibre composites at 22.5 % and 30 % fibre volume fractions for all resin systems. The kenaf fibre polyester composite is slightly better than the glass fibre equivalent at 15 % fibre volume fraction. At 30 % fibre volume fraction, the resin system has little effect on the specific tensile secant moduli of both the kenaf fibre and glass fibre composites.

Figure 7.31 presents the results of specific tensile linear moduli. It is evident that kenaf fibre composites made using all three resin systems are comparable to the glass fibre composites at 15 % fibre volume fraction. At 22.5 % fibre volume fraction, the kenaf fibre polyester composite is still comparable to the glass equivalent and actually has a higher specific tensile linear modulus. At 30 % fibre volume fraction, all of the kenaf fibre composites have specific tensile linear moduli lower than those of the glass equivalents. It must be noted however that the kenaf fibre composites have a small linear region when compared to the glass fibre composites. These results must therefore be viewed with caution. A comparison of stress-strain curves for the kenaf and glass fibre composites can be seen in Figure 8.6.

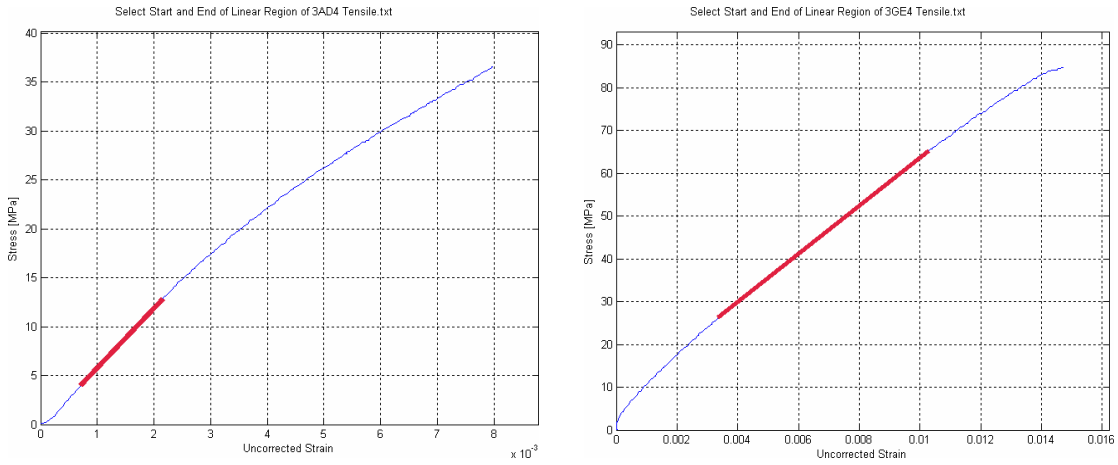

Figure 8.6 Comparison of linear regions for kenaf fibre (left) and glass fibre (right) composite specimens

At 15 % and 22.5 % fibre volume fractions, the resin system has a significant influence on the specific tensile linear moduli of both kenaf and glass fibre composites. At 30 % fibre volume fraction there is still a significant difference for the kenaf fibre composites but the different glass fibre equivalents all have similar values.

8.3.2 Specific flexural properties

The specific flexural properties displayed in Figure 7.32 to Figure 7.34 show that for all fibre volume fractions, the glass fibre composites are superior to the kenaf fibre composites. At 15 % and 22.5 % fibre volume fractions both the secant and linear moduli of the glass fibre composites are about 30 % greater than those of the kenaf fibre composites. At 30 % fibre volume fraction, however, this difference increases to about 50 %. For kenaf fibre and glass fibre composites, the resin system has some influence on both specific flexural secant and linear moduli at 15 % and 22.5 % fibre volume fraction. At 30 % fibre volume fraction, the influence is less significant.

8.3.3 Specific impact properties

Specific properties for the impact tests (Figure 7.35 and Figure 7.36) show that for specific impact energy and specific impact strength, the glass fibre composites are superior to the kenaf fibre composites by an order of magnitude. While polyester composites have the highest specific impact energy for both kenaf fibre and glass fibre reinforcement, epoxy composites have the lowest specific impact energy. For the

glass fibre composites however, the difference in the specific impact strengths of the different resin systems is not significant at any fibre volume fraction.

8.4 Practical implications for kenaf fibre reinforced composites

None of the kenaf fibre reinforced composites produced possess tensile or flexural strength in excess of that of the unreinforced resins. For this reason, the use of kenaf fibre reinforced composites in load bearing applications is not recommended. The addition of kenaf fibres in sufficient quantities can increase the tensile and flexural elastic moduli of the resins. Special consideration must however be made due to the largely non-linear behaviour of the composites. Although kenaf epoxy composites have a lower elastic modulus than polyester or vinyl ester ones, they act in a more linear manner and are therefore more predictable materials. Epoxy is much more expensive however and this would have to be considered in justifying the use of it.

Although the addition of kenaf fibres does improve the impact behaviour of the resins, the composites that result perform poorly in impact tests especially when compared to glass fibre composites. The use of kenaf fibre reinforced composites in applications where impact resistance is a requirement is not recommended.

When comparing thickness, length and width increases in water absorption tests, the increase in thickness is much larger than the increase in length and width. This is due to the greater swelling of the fibres through their thickness than along their length. There are also fewer fibres in the thickness direction to constrain this effect. If the large increase in thickness is not a problem, kenaf fibre reinforced composites do show reasonably good dimensional stability. Total increases for length and width are lower than 1 % after four weeks of immersion in water. The implications that exposure to water / moisture have on the mechanical properties of composites would however first need to be tested.

In comparison to glass fibre composites, kenaf fibre composites cannot compete on a specific property basis except at low fibre volume fractions. At these low fibre volume fractions however, it is questionable whether or not the production process can be justified and an alternative material could probably be used to meet the

requirements of the application. In addition to poor performance, as shown in section 6.2, the use of kenaf fibres in RTM results in a more time consuming process than when using traditional fibres.

Using kenaf fibres as reinforcement in composites results in materials with usable mechanical properties. The primary function of the kenaf fibres should however be considered to be one of reducing the quantity of matrix material required for a specific application to reduce costs and impact on the environment. Any cost reduction would, however be likely to be offset by the increased cost of production and given that these resins are thermosetting, cannot be recycled and do not biodegrade, impact on the environment is still significant.

8.5 Closing remarks

Comparing the results obtained in this work to those contained in the literature, it can be seen that the mechanical properties of these kenaf composites are similar to the hemp / kenaf composites of Rouison *et al.* [24, 25], the hemp composites of Sèbe *et al.* [9] and the sisal composites of Sreekumar *et al.* [10].

These kenaf fibres have been shown to be a poor reinforcement for the polyester, vinyl ester and epoxy resins tested. The epoxy resin bonds better to the fibres when compared to the other resins and still, there is no significant improvement in mechanical properties and in some cases, properties in fact decrease. Attempts to improve kenaf fibre composite performance by altering processing conditions and utilisation of compatible resin systems are limited by the properties of the fibres. Bearing this in mind, it seems that these kenaf fibres may not offer the physical or mechanical properties required from a composite reinforcement to be effective.

9 CONCLUSIONS AND RECOMMENDATIONS

9.1 Conclusions

1. Neither drying of fibres nor altering of mould temperature has any significant effect on mechanical properties of non-woven kenaf fibre polyester composites.

2. At low fibre volume fractions, pressurising the mould improves tensile and flexural strengths of kenaf fibre polyester composites.

3. SEM examinations show no change in failure mode from fibre pull-out for any processing conditions in kenaf fibre polyester composites.

4. Water absorption is not significantly altered by any processing condition except by pressurisation at low fibre volume fractions.

5. Kenaf fibre epoxy resin composites produce the highest tensile strength followed by vinyl ester and then polyester composites. The opposite trend is true for tensile moduli.

6. Addition of kenaf fibres to the three resin systems results in lower tensile strengths but higher tensile moduli than those of the unreinforced resins.

7. At low fibre volume fractions (15 %) kenaf fibre epoxy composites have the highest flexural strength followed by vinyl ester and then polyester. At medium fibre volume fractions (22.5 %) flexural strength is similar for all kenaf fibre composites and at high fibre volume fractions (30 %) polyester produces the strongest kenaf composites. Flexural moduli are approximately equal for all three resin systems at each fibre volume fraction.

8. Polyester composites have the highest impact energy and strength, followed by the vinyl ester and then the epoxy composites.

9. Mechanical properties increase with increasing fibre volume fraction for all three resin systems.

10. SEM examinations of impact test specimens show that epoxy composites failed by fibre fracture, polyester composites by fibre pull-out and vinyl ester ones by a combination of fibre pull-out and fibre fracture. This indicates that epoxy resin bonds better to the kenaf fibres than vinyl ester or polyester resins. These observations are further supported by the results of the impact tests.

11. Theoretical values for tensile strength and secant moduli show poor correlation with experimental results. Theoretical values for tensile linear moduli correlate reasonably well for polyester and vinyl ester composites but poorly for epoxy ones.

12. Theoretical values for flexural strength show good correlation with experimental results for all resin systems. Theoretical values for flexural secant moduli show poor correlation with experimental values and linear moduli show reasonable correlation. The model used for the prediction of flexural moduli should however be adjusted to account for the flexural moduli of the resin and the three-dimensional structure of the fibre mats.

13. All kenaf fibre composites absorb substantially more water than those made with glass fibres.

14. Among the kenaf fibre composites, those made with the vinyl ester resin absorb the least water while those made with the epoxy resin absorb the most. The average value of the coefficient of hygroexpansion of the kenaf composites in the thickness direction is substantially larger than those along the length or width.

15. The specific tensile and flexural properties for all kenaf fibre composites are inferior to glass equivalents. At low to moderate fibre volume fractions, some of the specific properties of kenaf fibre composites are comparable with those

of glass fibre composites. However, specific impact energy and strength of kenaf fibre composites are an order of magnitude lower than their glass equivalents for all fibre volume fractions.

16. The use of kenaf fibre reinforced composites requires careful evaluation right from the requirements of the material through to production and on to end of life disposal before they can be considered for practical applications.

9.2 Recommendations

1. If the mould is to be temperature controlled in future work, it is recommended that it is redesigned to incorporate heating and cooling to make production simpler. Furthermore, it would also be beneficial if a redesign incorporated an automated closing mechanism.

2. Thermal expansion of fibres should be investigated in order to determine conclusively if curing of composites at elevated temperatures is beneficial, destructive or has no effect on the resulting composite properties.

3. Pressurising the mould following injection should be experimented with further using a cold mould and a number of resins as this could be beneficial for increasing tensile and flexural properties and reducing water absorption at low fibre volume fractions.

4. A fibre treatment such as mercerisation or acetylation should be applied to fibres and the resulting composite properties determined. Kenaf fibres are not the strongest fibres available and this would show if there is any room for improvement in composite properties. Alternatively some of this research could be repeated using a stronger fibre such as flax and thus any improvements in properties would be more evident.

5. Mechanical properties of the composites should be evaluated following immersion in water to determine if the water absorption process is detrimental to composite performance.

6. The use of epoxy resin for further research should be avoided. The cost of the resin is not justifiable when considering that it only showed superior tensile strength and other properties were inferior when compared to polyester and vinyl ester resins. Vinyl ester seems the best candidate since it produces comparatively good mechanical properties and greatly reduces water absorption of composites.

7. Modelling of exposure of kenaf fibre reinforced composites to moisture should be further investigated as there is great scope for research on many levels in this area.

8. Hybrids should be investigated. For example in applications where good flexural properties are required, kenaf fibre mats could be sandwiched between outer glass layers and function as a structural filler. Glass flakes could be incorporated into the resin of kenaf composites to help control water absorption.

REFERENCES

1. A.K. Bledzki and J. Gassan. Composites reinforced with cellulose based fibres. Progress in Polymer Science, 24:221-274, 1999.

2. K. Oksman. High quality flax fibre composites manufactured by the resin transfer moulding process. Journal of Reinforced Plastics and Composites 20(7):621-627, 2001.

3. A.K. Mohanty, M. Misra and L.T. Drzal. Surface modifications of natural fibers and performance of the resulting biocomposites: an overview. Composite Interfaces 8(5):313-343, 2001.

4. N. Reddy and Y. Yang. Biofibers from agricultural byproducts for industrial applications. Trends in Biotechnology, 23(1):22-27, 2005.

5. J.F. de Deus, S.N. Monteiroa and J.R.M. d'Almeida. Effect of drying, molding pressure, and strain rate on the flexural mechanical behavior of piassava (Attalea funifera Mart) fiber–polyester composites. Polymer Testing, 24:750–755, 2005.

6. D.G. Hepworth, D.M. Bruce, J. F. V. Vincent and G. Jeronimidis. The penetration of epoxy resin into plant fibre cell walls increases the stiffness of plant fibre composites. Composites - Part A: Applied Science and Manufacturing, 31:599-601, 2000.

7. E.S. Rodriguez, P.M. Stefani and A. Vasquez. Effects of fibers' alkali treatment on resin transfer moulding processing and mechanical properties of jute- vinylester composites. Journal of Composite Materials, 41:1729-1741, 2007.

8. M.Z. Rong, M.Q. Zhang, Y. Liu, G.C. Yang and H.M. Zheng. The effect of fiber treatment on the mechanical properties of unidirectional sisal-reinforced epoxy composites. Composites Science and Technology, 61:1437–1447, 2001.

9. G. Sèbe, N.S. Cetin, C.A.S. Hill and M. Hughes. RTM hemp fibre-reinforced polyester composites. Applied Composite Materials, 7:341-349, 2000.

10. P.A. Sreekumar, K. Jospeh, G. Unnikrishnan and S. Thomas. A comparative study on mechanical properties of sisal-leaf fibre-reinforced polyester composites prepared by resin transfer and compression moulding techniques. Composites Science and Technology, 67:453-461, 2007.

11. B. Madsen. Properties of plant fibre yarn polymer composites. Doctoral thesis, Technical University of Denmark, Denmark, 2004.

12. T.L. Richardson and E. Lokensgard. Industrial plastics: theory and applications. Delmar, Albany, New York, 1997.

13. N.P. Cheremisinoff and P.N. Cheremisinoff. Fibreglass-reinforced plastics deskbook. Ann Arbor Science, Ann Arbor, 1979.

14. C.A. Harper. Handbook of plastics and elastomers. McGraw-Hill, New York, 1975.

15. Boost for Indigenous Fibre Industry http://www.csir.co.za/plsql/ptl0002/PTL0002_PGE038_ARTICLE?ARTICLE_NO=4420135 - 1 March 2007

16. Fibres and Textiles http://www.csir.co.za/plsql/ptl0002/PTL0002_PGE132_BUS_AREA?DIVISION_NO=1000025&BUSINESS_AREA_NO=7358944 - 23 February 2007

17. H.L. Bos. The potential of flax fibres as reinforcement for composite materials. Doctoral thesis, Technische Universiteit Eindhoven, Eindhoven, 2004.

18. K.G. Kavelin. Investigation of natural fibrer composites heterogeneity with respect to automotive structure. Doctoral thesis, Delft University of Technology, Netherlands, 2005.

19. K.E.F.I. Fibre Naturali http://www.kenaf-fiber.com/ - 12 November 2009

20. S. Thomas, J. George and S.S. Bhagawan. Effect of environment on the properties of low density polyethylene composites reinforced with pineapple-leaf fibre, Composites Science and Technology, 58:1471-1485, 1998.

21. J. Summerscales and T.J. Searle. Low-pressure (vacuum infusion) techniques for moulding large composites structures. Proceedings of the Institution of Mechanical Engineers Part L: Journal of Materials: Design and Applications, Professional Engineering Publishing, 219:45-58, 2005.

22. J.L. O'Dell. Natural fibers in resin transfer moulded composites. The Fourth International Conference on Woodfiber-Plastic Composites, Madison, 280-285, 1997.

23. R. Joffe, L. Wallstrőm and L.A. Berglund. Natural fiber composites based on flax – matrix effects. International Scientific Colloquium: Modelling for Saving Resources, Riga, 2001.

24. D. Rouison, M. Sain and M. Couturier. Resin transfer moulding of natural fiber reinforced composites: cure simulation. Composites Science and Technology, 64:629-644, 2004.

25. D. Rouison, M. Sain and M. Couturier. Resin transfer moulding of hemp fiber composites: optimisation of the process and mechanical properties of the materials. Composites Science and Technology, 66:895-906, 2006.

26. M.O.W. Richardson and Z.Y. Zhang. Experimental investigation and flow visualisation of the resin transfer mould filling process for non-woven, hemp

reinforced phenolic composites. Composites - Part A: Applied Science and Manufacturing, 31:1303-1310, 2000.

27. S.H. Aziz and M.P. Ansell. The Effect of alkalization and fibre alignment on the mechanical and thermal properties of kenaf and hemp bast fibre composites: Part 1 – polyester resin matrix. Composites Science and Technology, 64:1219-1230, 2004.

28. S.H. Aziz and M.P. Ansell. The Effect of alkalization and fibre alignment on the mechanical and thermal properties of kenaf and hemp bast fibre composites: Part 2 – cashew nut shell liquid matrix. Composites Science and Technology, 64:1231-1238, 2004.

29. J.A. Nairn. Thermoelastic analysis of residual stresses in unidirectional, high performance composites. Polymer Composites, 6(2):123-130, 1985.

30. S.H. Aziz, M.P. Ansell, S.J. Clark and S.R. Panteny. Modified polyester resins for natural fibre composites. Composites Science and Technology, 65:525-535, 2005.

31. W.A. Gray and R. Mueller. Engineering calculations in radiative heat transfer, Pergamon Press, Oxford, 1974.

32. T.R. Harrison. Radiation pyrometry and its underlying principles of radiant heat transfer. Jon Wiley and Sons, New York, 1960.

33. T.A. I'Ons. An investigation into the mechanical properties of glass fibre and oxyflourinated polypropylene fibre hybrid reinforced plastics. Master's dissertation, University of the Witwatersrand, Johannesburg, 2002.

34. K.M. Almgren, E.K. Gamstedt and J. Varna. Contribution of wood fiber hygroexpansion to moisture induced thickness swelling of composite plates. Polymer Composites, 00:000-000, 2009.

35. M.J.A. van den Oever, H.L. Bos and K. Molevnveld. Flax fibre physical structure and its effect on composite properties: Impact strength and thermo-mechanical properties. Macromolecular Materials and Engineering, 272:71-76, 1999.

36. E. Marklund and J. Varna. Modelling the hygroexpansion of aligned wood fiber composites. Composites Science and Technology, 69:1108-1114, 2009.

37. M. Jacob, S Joseph, L. A. Pothan and S. Thomas. A study of advances in characterization of interfaces and fiber surfaces in lignocellulosic fiber-reinforced composites. Composite Interfaces, 12(1-2):95-124, 2005.

38. M. L. Hassan, A. M. A. Nada. Utilization of Lignocellulosic Fibers in Molded Polyester Composites. Journal of Applied Polymer Science, 87:653-660, 2003.

39. M.S. Sreekala, S. Thomas. Effect of fibre surface modification on water-sorption characteristics of oil palm fibres. Composite Science and Technology, 63:861-869, 2003.

40. C.T. Herakovich. Mechanics of fibrous composites. John Wiley and Sons, New York, 1998.

41. Z. Hashin. Analysis of composite materials – A survey. Journal of Applied Mechanics, 50:481-505, 1983.

42. F.R. Cichocki Jr. and J.L. Thomason. Thermoelastic anisotropy of a natural fiber. Composites Science and Technology, 62:669-678, 2002.

43. L.N. McCartney and A. Kelly. Effective thermal and elastic properties of $[+\theta / -\theta]$ composites. Composites Science and Technology, 67:646-661, 2007.

Appendix A Overview of surface treatments

Surface treatments are a means by which the compatibility of natural fibres and various matrices can be increased. The incompatibility is caused by the difference in hydrophility between the fibres and the matrix. This is due largely to the hydroxyl groups present on the surface of plant fibres that react easily with moisture in the air thus reducing the number of sites for interphase bonding [(1)].

Natural fibres can be modified either by physical or chemical means. Physical treatments alter the structural and surface properties of the fibre thereby influencing the mechanical bonding to polymers [(1)]. Physical treatments include, stretching, calandering, thermotreatment, mercerisation, electric discharge and hybrid yarns.

Natural fibre composites simply consist of two materials, the fibres and the matrix. Chemical treatments of natural fibres involve introducing another material compatible with both [(1)]. This material can increase wettability of fibres, eliminate weak boundary layers or form bonds between the fibres and the matrix.

The following section has been divided into three parts. The first is dedicated to treatments which involve changing the fibre surface characteristics and changing surface tension, thus increasing wettability (fibre properties). The second is dedicated to treatments which result in bonding between fibre and matrix (chemical coupling) but these can also result in changes in fibre surface characteristics and surface tension. The third is dedicated to treatments which are not covered by the first two sections.

A1 Change in fibre properties

Mercerisation

The most common method of surface treatment is mercerisation. It involves the use of an alkali, usually sodium hydroxide (NaOH). The standard definition of mercerisation as put forward by the ASTM is: “the process of subjecting a vegetable fibre to an interaction with a fairly concentrated aqueous solution of a strong base to produce great swelling with resultant changes in the fine structure, dimension, morphology and mechanical properties” [(1)].

The process of mercerisation has two effects on the fibres that contribute to the resulting increase in strength of a composite when compared to those which have not undergone the treatment. The first of these involves the removal of some lignin, wax and oils covering the external surface of the fibre cell wall and it also depolymerises some of the cellulose exposing short crystallites on the inner fibrillar surface [(3)]. The second effect of the alkali is the removal of some hemicellulose [(1)].

Removal of lignin, wax and oils results in an increase in fibre roughness and frees up pores on the surfaces of fibres. The increase in fibre roughness and the subsequent increase in contact area, result in improved properties of composites due to the better mechanical interlocking that occurs between the fibres and the matrix [(3, 37)].

According to Bledzki and Gassan [(1)], it is likely that when the hemicellulose is removed, the interfibrillar region becomes less dense and less rigid. The result of this is that when the fibres experience tensile laods, the individual fibrils are more capable of realigning themselves along the direction of the applied load. The realignment allows for better load distribution among the fibrils and therefore higher stress development in the fibre [(1)]. There is however a certain limit to this. Excessive treatment with alkalis leads to softening of the hemicellulose, thus degrading the ability to transfer tensile loads between fibrils and therefore the tensile properties of the fibres are adversely affected. Excessive treatment with alkalis can also lead to excessive depolymerisation of the cellulose thus reducing fibre strength [(3)].

The effectiveness of mercerisation depends on the concentration and additives in the alkaline solution, the temperature and the treatment time [(1)].

Acetylation

Acetylation is a well known esterfication mode [(3)]. The principle of the method is to react hydroxyl groups on the surface of the fibres with acetyl groups. The result of this is that the fibre surface becomes more hydrophobic due to the lower number of hydroxyl groups that are free to react with water. Acetylation increases the surface

free energy of the fibres which increases wettability and interfacial adhesion [37]. Acetylation also removes non-crystalline constituents of fibres.

According to Mohanty *et al.* [3], acetylation has been extensively applied to wood to stabilise the cell walls of the fibres. This improves dimensional stability and environmental degradation. Both Bledzki and Gassan [1] and Mohanty *et al.* [3] have reported that when used in natural fibre reinforced composites, acetylation greatly reduces moisture uptake and prevents swelling or shrinking of the composite material if moisture is absorbed.

Acetylation is most commonly accomplished using acetic anhydride and acetic acid. Sometimes, co-solvents or catalysts are used with these chemicals in order to increase their effectiveness or decrease the treatment time. Bledzki and Gassan [1] state that the hydroxyl groups of cell walls are accessible in different ways but without a good catalyst or co-solvent, only easily accessible hydroxyl groups can be reached.

When co-solvents are used, the combinations for acetylation must be heated in solvents such as benzol or acetic acid [1]. Acetic acid can be used either as a co-solvent or as the source of the acetyls required for the reaction. According to Mohanty *et al.* [3], acetic acid does not react sufficiently with cellulose and acetic anhydride is preferred. Acetic anhydride however, is not a good swelling agent for cellulose (this is desired to ensure maximum penetration of treatment). Cellulose materials are therefore often soaked in acetic acid and then treated with acetic anhydride in order to ensure sufficient reaction and swelling of the cells.

As with mercerisation, the acetylation process has an optimum degree to which it should be carried out.

Sizing

Sizing is a method of modifying the surface of natural fibres using fatty acids. Through an esterfication reaction, carboxyl groups of the fatty acid react with the hydroxyl groups of the fibre surface. The result of the treatment is that there are fewer

hydroxyl groups that are free to react with water molecules and hence the fibres are hydrophobised [1].

One of the most common fatty acids used for sizing is stearic acid. Another advantage of the treatment when using stearic acid is that it is a long hydrocarbon chain which is hydrophobic thus resulting in improved water repellence. When fatty acids are oxidised however, they become water soluble and therefore lose their ability to repel water. One of the main causes of oxidation is high temperatures which are a problem in composite materials due to the temperatures experienced during production.

Sizing has been found to deteriorate the fibre-matrix interface in some cases. In tests done using stearic acid, this has been attributed to excess stearic acid acting more as a lubricant between the fibres and the matrix than an effective surface treatment [37]. This implies that there is an optimum degree of sizing i.e. treatment time, temperature and concentration.

Thermo treatment

Thermo treatment is one of the simplest methods for fibre modification. It involves heating natural fibres to the point where certain constituents begin to denature or undergo chemical change. According to Madsen [11] and Rouison *et al.* [25] temperatures of between 130-160°C are sufficient to begin this process. The principal behind thermo-treatment is in fact to alter the hydrophilic elements (hemicellulose) of the fibres using elevated temperatures. The method is reported to increase strength and decrease sensitivity to moisture in composites.

A2 Chemical coupling

Graft copolymerisation

This process involves treating the fibre with a suitable solution which is compatible with the matrix. The resulting copolymer possesses properties characteristic of both the cellulose of the fibre and the polymer of the matrix [1]. This method results in bonds being formed across the interface.

The actual way in which graft copolymerisation is accomplished is described briefly by Bledzki and Gassan [1]. Free radicals of the cellulose molecule initiate this reaction. First the fibre is treated in an aqueous solution containing selected ions following which it is exposed to high energy radiation. This causes the cellulose molecules to crack and free radicals are formed. Afterwards, the fibre is treated with the selected solution that is compatible with the matrix. This solution then reacts with the radical sites and the interface is formed.

The most common graft copolymerisation system is maleic anhydride and polypropylene. Maleic anhydride polypropylene copolymers result in covalent bonds across the interface between the matrix and the fibre. The surface energy of the fibres is also increased, the result of which is increased wettability and interfacial adhesion [1]. Water absorption is also decreased by the process due to the increase in hydrophility [37].

There is an optimum concentration of maleic anhydride that should be used but it has to be determined experimentally for a particular fibre. Maleic anhydride polypropylene is available commercially, with concentrations ranging from 0.1 % to 4 % by weight [3].

Treatment by graft copolymerisation is effective but complex [1]. Furthermore, the solutions and / or chemicals must be selected specifically for a particular chosen matrix. Some solutions can be used with a number of matrices in theory, however in practise, often do not work very well. Hassan and Nada [38] conducted tests using maleic anhydride treated natural fibres and polyester resin and observed no significant change in properties.

Silanation

Silanes are the main coupling agents used for glass fibre reinforced polymers [1]. In these compounds, different groups are appended to silicon in such a way that one end can interact with the fibres and the other end can react with the polymer matrix [37]. Most silane coupling agents can be represented as follows:

$R - (CH2)_n - Si(OR')_3$

OR' is the alkoxy group which reacts with the hydroxyl groups on the fibre surface and R is the functional organic group which reacts with the polymer. The reaction with the polymer could result in copolymerisation and / or the formation of an interpenetrating network [1].

Very often, silane compounds are inherently hydrophilic in nature. When this is the case, hydrophilic properties are contributed to the interface. This results in bonds with poor water resistance [1]. Some silanes can however decrease water absorption and increase mechanical properties of natural fibre reinforced composites.

According to Bledzki and Gassan [1], tests conducted using silanes produce varying results which shows that theories used for the treatment of natural fibres with silanes are contradictory and require further study. Some tests for example showed interfacial bonding to be quite poor when using silanes.

Isocyanates

Little information is available regarding isocyanates as they are a relatively new form of surface modification. The isocyanate group reacts readily with the hydroxyl groups on the fibre surface [1]. The bonds that result are strong covalent bonds [3]. The bonding with the hydroxyl groups of the fibres leaves fewer free hydroxyl groups to react with water. In tests conducted by Sreekala and Thomas [39], isocyanate treatment was found to be very effective in reducing water absorption.

Excess treatment with isocyanates can have a negative effect on properties such as moisture absorption. If too many isocyanates are present on the surface of the fibre, they can cause the fibre wall to split open resulting in new hydroxyl groups being exposed.

Surface modification using isocyanates, it would seem, is dependant on choosing a polymer to match the isocyanate and only polymers capable of forming covalent bonds can be used.

Triazine

Less information regarding triazine coupling agents is available than for silanes or isocyanates, the reason being that they are also relatively new surface treatments. Triazines form covalent bonds with cellulose fibres and polymer matrices. They bond to the hydroxyl groups on the fibre surface thus reducing hydrophility and therefore moisture absorption. Triazines not only reduce hydrophility but also restrain swelling of the fibres due to the cross-linked network created between the fibre and matrix [(1)].

Methanol compounds

Chemical compounds containing methanol groups (-CH_2OH) form covalent and / or hydrogen bonds with cellulose fibres. Treatments involving methanol groups are known to decrease water absorption and increase wet strength of composites [(1)].

A3 Other

Impregnation of fibres

Impregnation of fibres allows for the polymer matrix to form bonds across the fibre cell walls. This results in very good mechanical interlocking.

Impregnation involves using chemicals to first swell the cell walls. Once the cell walls have been swollen, matrix polymers can penetrate into the lumen and cross-link. Hepworth *et al.* [(6)], describes this process using urea to swell the walls which is slowly

replaced by a solution of ethanol and finally a slow-curing epoxy. Fibres having undergone impregnation should exhibit good dimensional stability and low water absorption due to the mechanical interlocking of the impregnated polymer.

Polymer solutions or dispersions must be of low viscosity in order to be used for this method. In order to obtain the required viscosities, solvents must be added to the polymers. However, for a number of polymers, the lack of solvents limits the use of the technique [(1)].

Appendix B Sample production log sheets

B1 Polyester production log sheet

Date	19/01/2009	**Date**	20/01/2009
Composite Code	GE2/UP/ND/250/45	**Composite Code**	2L/UP/ND/250/45-NH
Drying		**Drying**	
Temperature	-	Temperature	-
Pressure	-	Pressure	-
Fibres		**Fibres**	
No. Layers	5	No. Layers	2
Fibre Mass (RT)	110.63 g	Fibre Mass (RT)	71.1 g
Fibre Mass (Dry)	- g	Fibre Mass (Dry)	64.68 g
Sample Mass (RT)	- g	Sample Mass (RT)	23.48 g
Sample Mass (Dry)	- g	Sample Mass (Dry)	21.36 g
Humidity	- %	Humidity	55 %
Resin Injection		**Resin Injection**	
Injection Pressure	250 Kpa	Injection Pressure	250 Kpa
Vac. Assist Pressure	-40 Kpa	Vac. Assist Pressure	-40 Kpa
Time to Fill	00:35	Time to Fill	01:45
Composite		**Composite**	
Final Mass	390.5 g	Final Mass	350.1 g
Fibre Mass Fraction	28.3 %	Fibre Mass Fraction	18.5 %
Fibre Vol. Fraction	14.97 %	Fibre Vol. Fraction	14.69 %
Matrix Density	1140 kg/m^3	Matrix Density	1140 kg/m^3
Fibre Density	2560 kg/m^3	Fibre Density	1500 kg/m^3
Composite Density	1352.55 kg/m^3	Composite Density	1192.89 kg/m^3

B2 Vinyl ester production log sheet

Date	27/08/2009	**Date**	10/09/2009
Composite Code	3GE/VE/ND/NH//45	**Composite Code**	3VE/AD/250/45
Drying		**Drying**	
Temperature	-	Temperature	55
Pressure	-	Pressure	3 hrs Atm.
Fibres		**Fibres**	
No. Layers	5	No. Layers	3
Fibre Mass (RT)	158.3 g	Fibre Mass (RT)	103.2 g
Fibre Mass (Dry)	- g	Fibre Mass (Dry)	97.85343 g
Sample Mass (RT)	- g	Sample Mass (RT)	18.53 g
Sample Mass (Dry)	- g	Sample Mass (Dry)	17.57 g
Humidity	- %	Humidity	40 %
Resin Injection		**Resin Injection**	
Injection Pressure	100 Kpa	Injection Pressure	250 Kpa
Vac. Assist Pressure	-40 Kpa	Vac. Assist Pressure	-40 Kpa
Time to Fill	-	Time to Fill	-
Composite		**Composite**	
Final Mass	409.9 g	Final Mass	345.4 g
Fibre Mass Fraction	38.6 %	Fibre Mass Fraction	28.3 %
Fibre Vol. Fraction	21.89 %	Fibre Vol. Fraction	23.10 %
Matrix Density	1140 kg/m^3	Matrix Density	1140 kg/m^3
Fibre Density	2560 kg/m^3	Fibre Density	1500 kg/m^3
Composite Density	1450.78 kg/m^3	Composite Density	1223.17 kg/m^3

B3 Epoxy production log sheet

Date	29/08/2009	**Date**	15/09/2009
Composite Code	4GE/EP/ND/250/45	**Composite Code**	4EP/AD/350/45
Drying		**Drying**	
Temperature	-	Temperature	55
Pressure	-	Pressure	3 hrs Atm.
Fibres		**Fibres**	
No. Layers	7	No. Layers	4
Fibre Mass (RT)	220.6 g	Fibre Mass (RT)	137.77 g
Fibre Mass (Dry)	- g	Fibre Mass (Dry)	131.6919 g
Sample Mass (RT)	- g	Sample Mass (RT)	18.36 g
Sample Mass (Dry)	- g	Sample Mass (Dry)	17.55 g
Humidity	- %	Humidity	40 %
Resin Injection		**Resin Injection**	
Injection Pressure	250 Kpa	Injection Pressure	350 Kpa
Vac. Assist Pressure	-40 Kpa	Vac. Assist Pressure	-40 Kpa
Time to Fill	-	Time to Fill	-
Composite		**Composite**	
Final Mass	460.8 g	Final Mass	379.1 g
Fibre Mass Fraction	47.9 %	Fibre Mass Fraction	34.7 %
Fibre Vol. Fraction	29.01 %	Fibre Vol. Fraction	28.78 %
Matrix Density	1139 kg/m^3	Matrix Density	1139 kg/m^3
Fibre Density	2560 kg/m^3	Fibre Density	1500 kg/m^3
Composite Density	1551.21 kg/m^3	Composite Density	1242.91 kg/m^3

Appendix C Sample calculations

The following material properties were used for theoretical and experimental calculations (properties of the resins were supplied by the manufacturers):

Table C.1 Properties of kenaf fibres and resin systems

Property	Unit	Kenaf Fibre	Polyester	Vinyl Ester	Epoxy
Elastic Modulus	MPa	40000 [19]	3800	3200	3470
Elongation at Break	%	2.5-3.5 [19]	2.3	5-6	4.5
Density	kg/m^3	1500 [19]	1140	1140	1139

C1 Sample theoretical calculations

Elastic modulus

The elastic moduli of composites were calculated using the rule of mixtures by the following equation:

$$E = \eta E_f V_f + E_m V_m \qquad \text{(C.1.1)}$$

In this equation η = 0.3 for chopped strand mat.

Equation C.1.1 was used to evaluate both tensile and flexural elastic moduli of composites. No data were available for the flexural moduli of the polyester and epoxy resins and thus those values listed in Table C.1 were applied in both calculations for all three resin systems.

For the case of a kenaf fibre reinforced polyester composite with a fibre volume fraction of 22.5 %, theoretical elastic modulus is thus equal to:

$$E = 0.3 \times 40000 \times 0.225 + 3800 \times 0.775$$
$$E = 5645\ MPa = 5.645\ GPa$$

Tensile strength

Tensile strength of composites can be estimated using one of the two following equations:

$$\sigma = \eta E_f V_f \varepsilon_f \qquad \text{(C.1.2)}$$

or,

$$\sigma = E_m V_m \varepsilon_m \qquad \text{(C.1.3)}$$

Equation C.1.2 is applicable for composites where the fibre strain to failure is higher than the matrix strain to failure and equation C.1.3 is applicable for composites where the matrix strain to failure is higher than the fibre strain to failure. Looking at the data presented in Table C.1, it can be seen that equation C.1.2 is strictly speaking only valid for use with the polyester resin. It has however been applied to predict the tensile strength of all the composites for a number of reasons: it was found to produce the most conservative values of tensile strength (which best suited values obtained experimentally); equation C.1.3 results in tensile strength decreasing with increasing fibre content; non-woven fibre mats were used and not unidirectional fibres; fibre pull-out was assumed to be the mode of failure for all natural fibre reinforced composites and thus the matrix should fail first in all cases and finally, it was considered important that the same model be used to predict values for all composites.

In all calculations, fibre strain at failure was taken as the midway value presented in Table C.1 i.e. 3 %. Thus, for the case of a kenaf fibre reinforced composite with a fibre volume fraction of 22.5 %, the theoretical tensile strength is:

$$\sigma = 0.3 \times 40000 \times 0.225 \times 0.03$$
$$\sigma = 81\ MPa$$

Flexural strength

Flexural bending of a beam involves tensile, compressive and shear stresses and failure can result due to any of these. No data was available for the compressive strength of any of the resins or the fibres used in this research. It was assumed that failure due to shear stress was unlikely because the non-woven fibre mats contain some fibres that are aligned in the through-thickness direction and four layers were the maximum number of fibre mats used. Flexural failure was therefore assumed to be caused by tensile failure in the fibres on the lower test specimen surface. Thus, the theoretical values of flexural strength have been made equal to those for tensile strength.

C2 Sample experimental calculations

Composite density

The density of a composite can be determined using the following equation:

$$\rho_c = \frac{m_c}{v_c} \qquad \text{(C.2.1)}$$

The volume of a composite is difficult to determine without submerging it into some fluid (which might be absorbed) and measuring the resulting displacement. The approximate volume of a composite can be calculated using values of mass and density. Approximate composite density is equal to:

$$\rho_c = \frac{m_c}{\left(\frac{m_c - m_f}{\rho_m}\right) + \left(\frac{m_f}{\rho_f}\right)} \qquad \text{(C.2.2)}$$

This equation cannot take into account the existence of defects such as voids but it is still the best value obtainable in the context of this research. Even if the volume of the composite could be determined, there would still be other factors leading to inaccuracies. These inaccuracies arise primarily from the fibres which have variable

density and therefore volume depending on their moisture content and to a lesser extent on their chemical composition (specific to cultivation and geographical conditions). In addition, it is difficult to determine the actual fibre density because different fluids result in different values of density depending on the chemistry involved [(11)]. Apart from the fibres, there can also be density variation within the composites due to variation in fibre mats and / or to mould deflection depending on the quantity of fibres placed inside.

For the case of the polyester composite made from 3 layers of dried fibres in a heated mould, the composite density is:

$$\rho_c = \frac{360.2\times10^{.3}}{\left(\frac{(360.2-99.9)\times10^{-3}}{1140}\right)+\left(\frac{99.9\times10^{-3}}{1500}\right)}$$

$$\rho_c = 1221.3\ kg/m^3$$

Fibre volume fraction

The fibre volume fraction of a composite can be determined using the following equation:

$$V_f = \frac{v_f}{v_c} \qquad \text{(C.2.3)}$$

For the same reasons previously stated, it is difficult to determine the volume of the fibres and the composite and thus the following approximate equation was used to determine fibre volume fraction:

$$V_f = \frac{m_f \rho_c}{m_c \rho_f} \qquad \text{(C.2.4)}$$

For the case of the polyester composite made from 3 layers of dried fibres in a heated mould, the fibre volume fraction is:

$$V_f = \frac{99.9\times10^{-3}\times1221.3}{360.2\times10^{-3}\times1500} = 22.6\ \%$$

Tensile testing

The specimen used in this example is 3UP-AD-H-T4 (3 layers of fibres, polyester resin, fibres dried, heated mould, tensile specimen number 4).

Force at failure (F) = 1528 N
Strain at failure (ε) = 0.00787
Width (w) = 10.28 mm
Thickness (t) = 4.06 mm

Tensile strength

Using the values above, stress is obtained as follows:

$$\sigma = \frac{F}{wt} \qquad \text{(C.2.5)}$$

$$\sigma = \frac{1528}{10.28\times4.06} = 36.61\ MPa$$

Tensile modulus

According to ASTM D638, materials can exhibit linear or non-linear behaviour when examining stress-strain curves. Although the kenaf composites tested exhibited a region of linear behaviour, it was very small and it was decided that both the linear and non-linear values of modulus would be calculated. The linear modulus is determined by calculating the slope of the linear region on the stress-strain curve and the non-linear (or secant) modulus is determined by dividing the maximum stress by

the maximum strain. A Matlab programme was coded to process raw data and produce values of linear and secant modulus.

Tensile linear modulus

In order to calculate the linear modulus the Matlab programme prompts the user to select the start and end of the linear region. It then creates a “best-fit” line from the data points between the selected start and end points. The gradient of this line is the linear modulus. An example of the linear region can be seen in Figure C.1 and is highlighted in red. The tensile linear modulus for this specimen is 6.26 GPa.

Tensile secant modulus

In order to calculate the secant modulus, the Matlab programme extends a line (from the linear region) to determine a zero-stress point and the corresponding value of strain. This point of zero-stress is then used as a new origin for the curve, thus offsetting the “bedding-in” region. The secant modulus is then calculated by dividing the stress at failure by the corresponding strain.

The tensile secant modulus is calculated using the following:

$$E_{\sec ant} = \frac{\sigma}{\varepsilon} \qquad \text{(C.2.6)}$$

$$E_{\sec ant} = \frac{36.61}{0.00787} = 4.65\ GPa$$

An example of the secant modulus can be seen in Figure C.1 and is highlighted in green.

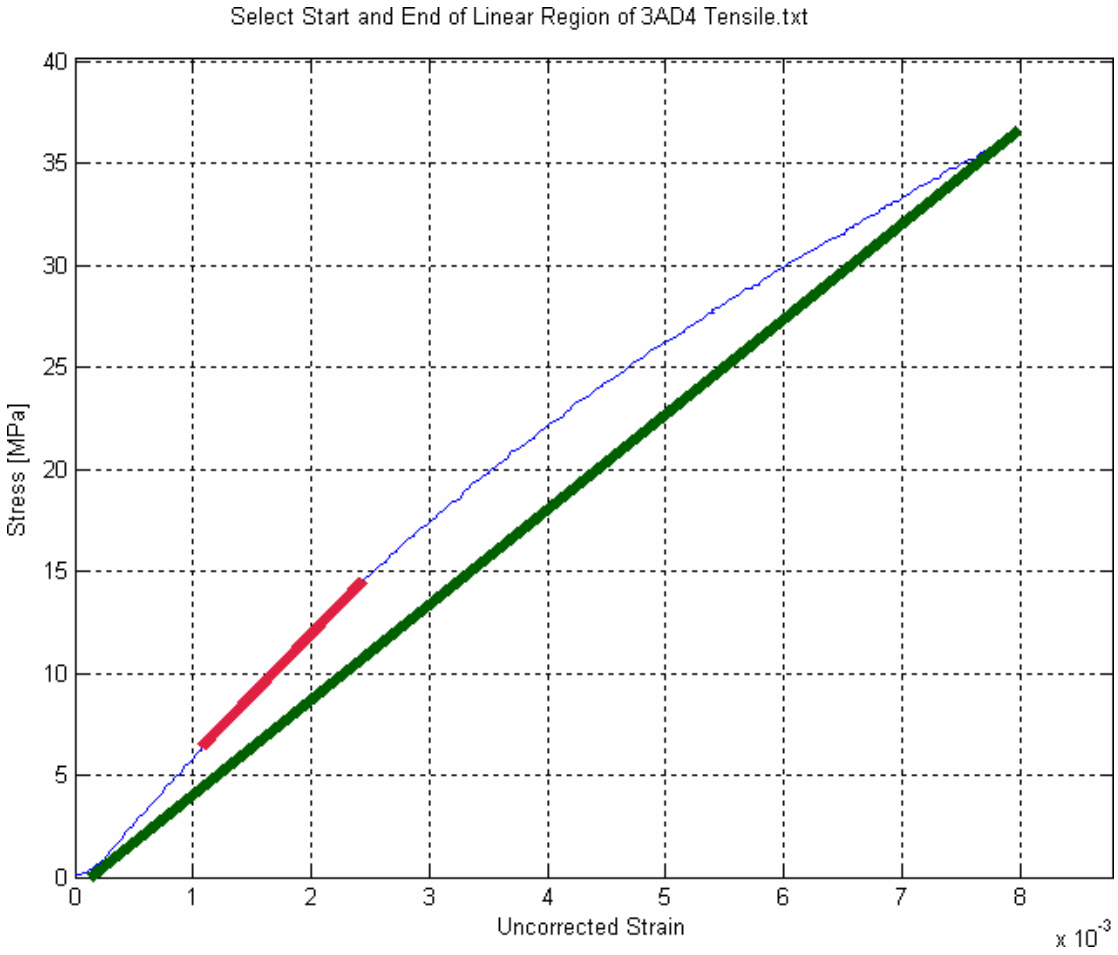

Figure C.1 Typical tensile stress-strain curve for a kenaf fibre composite specimen

Flexural testing

The specimen used in this example is 3UP-AD-H-F5 (3 layers of fibres, polyester resin, fibres dried, heated mould, flexural specimen number 5).

Force at failure (F) = 256.148 N
Deflection at failure (d) = 4.038 mm
Width (w) = 15.82 mm
Thickness (t) = 4.15 mm
Support Span (L) = 64 mm

Flexural strength

The stress at failure is calculated according to ASTM D790 by the following:

$$\sigma = \frac{3FL}{2wt^2} \qquad \text{(C.2.7)}$$

$$\sigma = \frac{3 \times 256.148 \times 64}{2 \times 15.82 \times 4.15^2} = 90.25\ MPa$$

Flexural modulus

As in the case of the tensile tests, it was observed that the kenaf composites exhibited linear and non-linear behaviour when examining stress-strain curves (this phenomenon is also detailed in ASTM D790). A Matlab programme was coded to process raw data and produce values of linear and secant modulus.

Flexural linear modulus

The programme performs the same operation to calculate the linear modulus as the programme for tensile testing (with the necessary changes made to stress and strain calculations). An example of the linear region can be seen in Figure C.2 and is highlighted in red.

The flexural linear modulus for this specimen is 4.48 GPa.

Flexural secant modulus

The strain at failure experienced by the specimen is calculated according to ASTM D790 using the following:

$$\varepsilon = \frac{6dt}{L^2} \qquad \text{(C.2.8)}$$

$$\varepsilon = \frac{6 \times 4.038 \times 4.15}{64^2} = 0.02455$$

Once the flexural strain is known, the flexural secant modulus can be calculated:

$$E_{secant} = \frac{\sigma}{\varepsilon} = \frac{90.25}{0.02455} = 3.68\ GPa$$

An example of the flexural secant modulus can be seen in Figure C.2 and is highlighted in green.

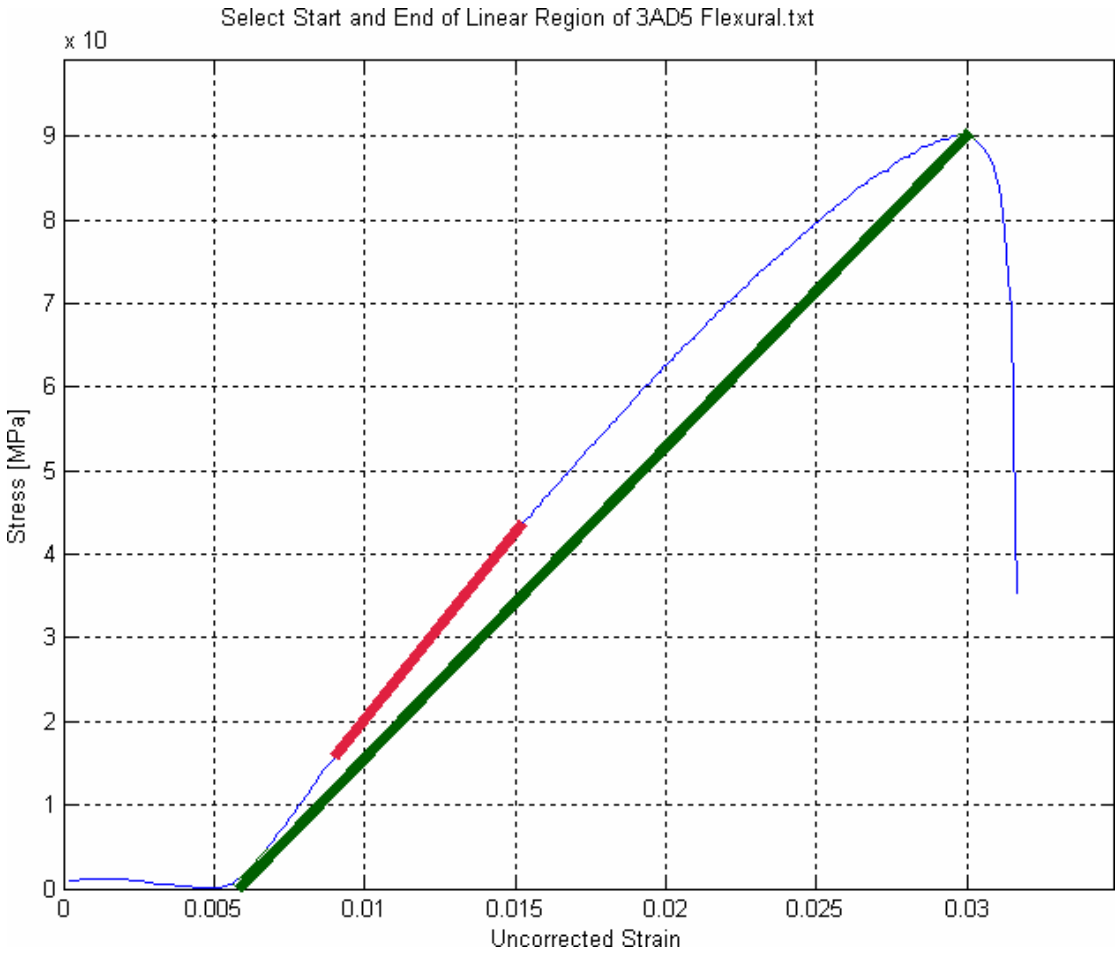

Figure C.2 Typical flexural stress-strain curve for a kenaf fibre composite specimen

Impact testing

The following flow diagram describes the method used to obtain the energy absorbed and the force experienced by a specimen during an impact test. A similar flow

diagram was used by I'Ons [33]. A Matlab program was written to analyse raw data and the code can be found in Appendix D.

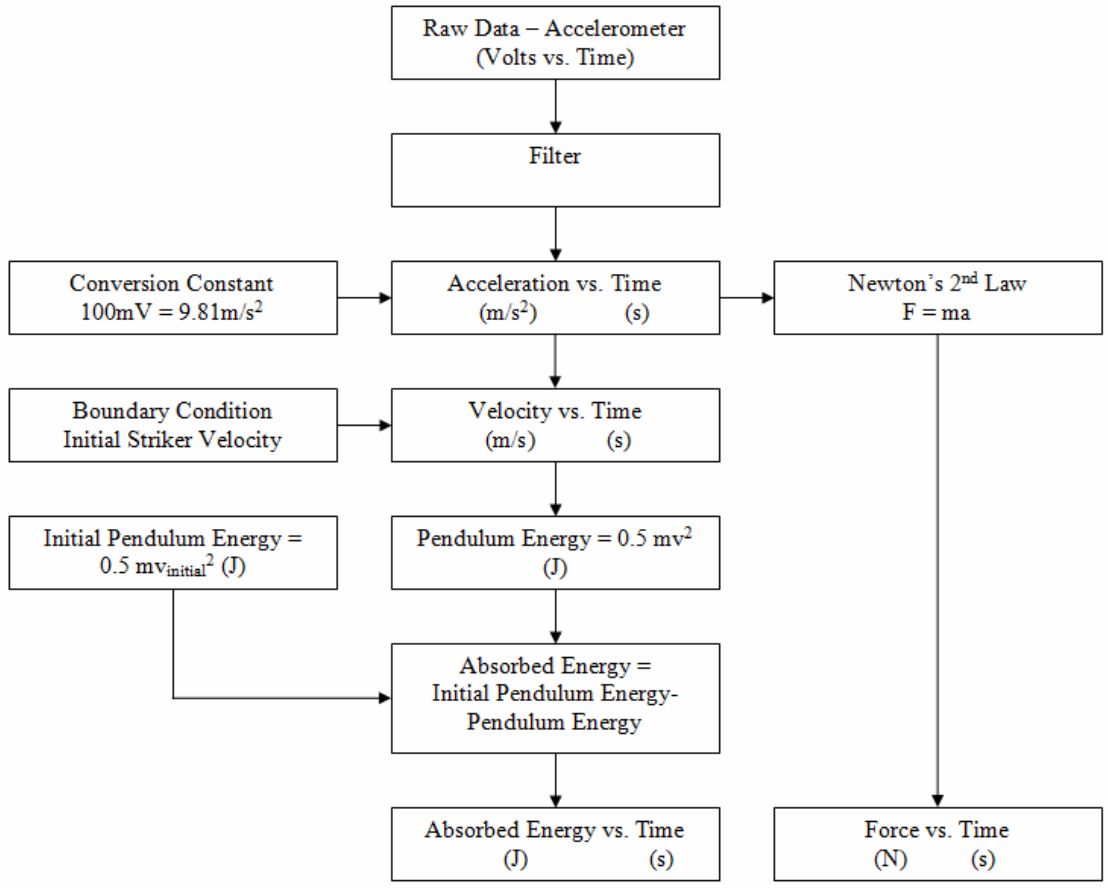

Figure C.3 Flow diagram describing matlab impact code

The specimen used in this example is 3UP-AD-H-I1 (3 layers of fibres, polyester resin, fibres dried, heated mould, impact specimen number 1).

Force at failure (F) = 104.22 N
Width (w) = 10.16 mm
Thickness (t) = 4.19 mm
Span (L) = 20 mm
Pendulum initial velocity ($vel_{t=0}$) = 2.1271 m/s
Pendulum velocity at end ($vel_{t=end}$) = 2.0711 m/s
Pendulum velocity at failure ($vel_{t=peak}$) = 2.1013 m/s

Impact resistance

The Matlab programme that was coded requests the user to select the start, end and peak force points of the impact event on a graph. Using the velocity of the pendulum at these points, the corresponding energies can be calculated. By subtracting the instantaneous pendulum energy from the initial pendulum energy, the energy absorbed by the specimen at the points of interest can be determined using the following:

Total Energy (E_{tot}): between t=0 and t=end

$$E_{tot} = \frac{1}{2} m\left(vel_{t=0}{}^{2} - vel_{t=end}{}^{2}\right) \quad \text{(C.2.9)}$$

$$E_{tot} = \frac{1}{2} \times 1.9955 \times \left(2.1271^{2} - 2.0711^{2}\right) = 0.2346\ J$$

Initial Energy (E_i): between t=0 and t=peak

$$E_{tot} = \frac{1}{2} m\left(vel_{t=0}{}^{2} - vel_{t=peak}{}^{2}\right) \quad \text{(C.2.10)}$$

$$E_{tot} = \frac{1}{2} \times 1.9955 \times \left(2.1271^{2} - 2.1013^{2}\right) = 0.1088\ J$$

Propagative Energy (E_p): between t=peak and t=end

$$E_p = E_{tot} - E_i \quad \text{(C.2.11)}$$

$$E_p = 0.2346 - 0.1088 = 0.1258\ J$$

ASTM D256 requires that these values of energy be converted to energy per unit thickness of the specimen. For this example:

$$\left(\frac{E}{t}\right)_{tot} = \frac{0.23464}{0.00419} = 56\ J/m$$

$$\left(\frac{E}{t}\right)_{i} = \frac{0.10894}{0.00419} = 26\ J/m$$

$$\left(\frac{E}{t}\right)_{p} = \frac{0.12570}{0.00419} = 20\ J/m$$

Impact strength

Stress in a beam is given by:

$$\sigma = \frac{My}{I} \qquad \text{(C.2.12)}$$

where, for a cantilever beam:

$$M = FL \qquad \text{(C.2.13)}$$

and for a rectangular section:

$$I = \frac{tw^3}{12} \qquad \text{(C.2.14)}$$

hence, substituting C.2.13 and C.2.14 into C.2.12,

$$\sigma = \frac{6FL}{tw^3} \qquad \text{(C.2.15)}$$

$$\sigma = \frac{6\times104.22\times20}{4.19\times10.16^3} = 28.91\ MPa$$

Water absorption

The specimen used in this example is 3UP-AD-H-W2 (3 layers of fibres, polyester resin, dried fibres, heated mould, water absorption specimen number 2). The values presented for this specimen are for water absorption after 168 hours.

Initial mass (m_i) = 12.7890 g
Initial length (l_i) = 50.57 mm
Initial width (w_i) = 50.55 mm
Initial thickness at centre (tc_i) = 4.12 mm
Initial thickness at edge (te_i) = 4.10 mm

Mass at 168 hours (m_{168}) = 13.3368 g
Length at 168 hours (l_{168}) = 50.66 mm
Width at 168 hours (w_{168}) = 50.64 mm
Thickness at centre at 168 hours (tc_{168}) = 4.21 mm
Thickness at edge at 168 hours (te_{168}) = 4.23 mm

The percentage change from the initial values is calculated using the following generalised equation:

$$\% X_{168} = \left(\frac{X_{168}}{X_i} - 1 \right) \times 100 \qquad \text{(C.2.16)}$$

hence,

$$\% m_{168} = \left(\frac{m_{168}}{m_i} - 1 \right) \times 100 = \left(\frac{13.3368}{12.7890} - 1 \right) \times 100 = 4.28\ \%$$

$$\% l_{168} = \left(\frac{l_{168}}{l_i} - 1 \right) \times 100 = \left(\frac{50.66}{50.57} - 1 \right) \times 100 = 0.18\ \%$$

$$\%\ w_{168} = \left(\frac{w_{168}}{w_i} - 1\right) \times 100 = \left(\frac{50.64}{50.55} - 1\right) \times 100 = 0.18\ \%$$

$$\%\ tc_{168} = \left(\frac{tc_{168}}{tc_i} - 1\right) \times 100 = \left(\frac{4.21}{4.12} - 1\right) \times 100 = 2.18\ \%$$

$$\%\ te_{168} = \left(\frac{te_{168}}{te_i} - 1\right) \times 100 = \left(\frac{4.23}{4.10} - 1\right) \times 100 = 3.17\ \%$$

Appendix D Matlab codes and accelerometer data sheet

D1 Tensile test matlab code

```
%CODE FOR ANALYSING TENSILE TEST DATA
% - Stefan Rassmann
%=======================================================

clear;
prompt = {'type the directory containing tensile test files'};
default =
{'C:\Tensile_Data\Polyester_Tensile\3_Layers_Tensile_Polyester\3AD
Tensile'};
title = 'directory';
lineNo = 1;
directory = inputdlg(prompt, title, lineNo, default);
directory = char(directory);
prompt = {'Enter the Number of Specimens'};
number_of_specimens = inputdlg(prompt);
M = str2num(number_of_specimens{1});

cd(directory);
[filename1, pathname1] = uigetfile('*.txt', ['Select File Containing
Dimensions ']);

for z=1:M

    specimen_number = num2str(z);

    % CONSTANTS

    strain_calibration_factor = 0.02903;
    guage_length = 50;

    %=======================================================
    %   1.  TENSILE DATA FILE GETS OPENED
    %   The data is sorted into FORCE and EXTENSION

    cd(directory);
    [filename2, pathname2] = uigetfile('*.txt', ['Select Specimen ',
specimen_number]);
    data = csvread(filename2, 39);

    %=======================================================
    %   2.  DIMENSIONS CAN BE OBTAINED EITHER FROM A *.txt FILE OR
ENTERED
    %   MANUALLY

    %   OPTION 1 - USE A *.txt FILE

    dimensions = dlmread(filename1);
    area = dimensions(z,1);

    %   OPTION 2 - ENTER DIMENSIONS MANUALLY

%     prompt = {'Enter specimen width (mm):', 'Enter specimen
thickness (mm):', 'or Enter specimen area (mm^2):'};
%     default={'0', '0', '0'};
%     title = 'Specimen Dimensions';
```

```
%     lineNo=1;
%     dimensions = inputdlg(prompt,title,lineNo,default);
%     width = str2num(dimensions{1});
%     thickness = str2num(dimensions{2});
%     area = str2num(dimensions{3});
%     if area <= 0
%         area = width*thickness
%     end

    %=====================================================
    %   3.  STRESS AND STRAIN ARE CALCULATED FROM THE INPUT DATA &
    %   DIMENSIONS

    stress = (1000/area)*data(:,1);
    strain = (strain_calibration_factor/guage_length)*data(:,2);

    %=====================================================
    %   4.  USER IS REQUESTED TO SELECT LINEAR REGION

    scrsz = get(0,'ScreenSize');
    figure('Position',[0.5*(scrsz(3)-scrsz(3)*0.75) 0.5*(scrsz(4)-
scrsz(4)*0.75) scrsz(3)*0.75 scrsz(4)*0.75]);
    figure(1)
    plot(strain, stress);
    xlim([0 1.1*max(strain)]);
    ylim([0 1.1*max(stress)]);
    xlabel('Uncorrected Strain');
    ylabel('Stress [MPa]');
    grid on
    %   Introduce crosshairs to select origin
    x = 0.15*max(xlim);
    y = 1.05*max(ylim);
    text(x,y, ['Select Start and End of Linear Region of ',
filename2]);
    [start_linear_strain, start_linear_stress]=ginput(1);
    [end_linear_strain, end_linear_stress]=ginput(1);

    %   Now we want to disregard anything before the start and end of
the
    %   linear region

    N=length(stress);
    a = 1;
    while a <= N
        if strain(a) <= start_linear_strain
            lowerlim = a;
        elseif strain(a) <= end_linear_strain
            upperlim = a;
        else
            break
        end
        a = a + 1;
    end

    lowerim = lowerlim + 1;
    linear_strain = strain(lowerlim:upperlim);
    linear_stress = stress(lowerlim:upperlim);
    p = polyfit(linear_strain, linear_stress, 1);
    f = polyval(p,linear_strain);

    %=====================================================
```

```
    %   5.  THE FITTED LINEAR CURVE IS USED TO DETERMINE THE POINT OF
ZERO
    %   STRAIN

    grad = p(1);
    y_int = p(2);
    zero_strain = (-y_int)/grad;
    for b=1:N
        strain(b)=strain(b)-zero_strain;
    end

    %=====================================================
    %   6.  THE MAXIMUM STRESS, MAXIMUM STRAIN AND ELASTIC MODULUS
ARE CALCULATED

    c = 1;
    max_stress = 0;
    while c <= N
        if stress(c) >= max_stress;
            max_stress = stress(c);
            failure_point = c;
        end
        c = c + 1;
    end

    maximum_stress(z)=stress(failure_point);
    maximum_strain(z) = strain(failure_point);
    secant_modulus(z) = (maximum_stress(z)/maximum_strain(z))/1000;
    linear_modulus(z) = grad/1000;

    maximum_stress_squared(z)=(stress(failure_point))^2;
    maximum_strain_squared(z)=(strain(failure_point))^2;

secant_modulus_squared(z)=(((stress(failure_point))^2)/((strain(failu
re_point))^2))/(1000^2);
    linear_modulus_squared(z) = (grad^2)/(1000^2);

    closereq;

end

average_maximum_stress = sum(maximum_stress)/M;
average_maximum_strain = sum(maximum_strain)/M;
average_secant_modulus = sum(secant_modulus)/M;
average_linear_modulus = sum(linear_modulus)/M;

stress_std_deviation=((sum(maximum_stress_squared)-
(average_maximum_stress^2)*M)/(M-1))^0.5;
strain_std_deviation=((sum(maximum_strain_squared)-
(average_maximum_strain^2)*M)/(M-1))^0.5;
secant_modulus_std_deviation=((sum(secant_modulus_squared)-
(average_secant_modulus^2)*M)/(M-1))^0.5;
linear_modulus_std_deviation=((sum(linear_modulus_squared)-
(average_linear_modulus^2)*M)/(M-1))^0.5;

%=====================================================
%   7.  THE RESULTING VALUES ARE WRITTEN INTO text FORMAT

results = [maximum_stress; maximum_strain; secant_modulus;
linear_modulus];
```

```
average_results = [average_maximum_stress; average_maximum_strain;
average_secant_modulus; average_linear_modulus];
std_deviation = [stress_std_deviation; strain_std_deviation;
secant_modulus_std_deviation; linear_modulus_std_deviation];

cd C:\Tensile_Results\Epoxy_Tensile_Results;
[filename3, pathname3] = uiputfile('*.txt', 'Save Results As:');
fid = fopen(filename3,'w');
fprintf(fid,'\t Stress \t Strain \t Secant_Modulus \t
Linear_Modulus\n');
fprintf(fid,'\t   MPa \t   mm/mm \t   GPa \t   GPa\n');

for y=1:M
    y_str=num2str(y);
    fprintf(fid,'Specimen %c', y_str);
    fprintf(fid,'\t %3.1f \t %7.5f \t %3.2f \t
%3.2f\n',results(:,y));
end

fprintf(fid,'\n');
fprintf(fid,'Average');
fprintf(fid,'\t %3.1f \t %7.5f \t %3.2f \t %3.2f\n',average_results);
fprintf(fid,'Std. Dev. %c');
fprintf(fid,'\t %3.1f \t %7.5f \t %3.2f \t %3.2f\n',std_deviation);
fclose(fid);
```

D2 Flexural test matlab code

```
%CODE FOR ANALYSING FLEXURAL TEST DATA
% - Stefan Rassmann
%=======================================================

clear;
prompt = {'type the directory containing flexural test files'};
default =
{'C:\Flexural_Data\Polyester_Flexural\3_Layers_Flexural_Polyester\3AD
Flexural'};
title = 'directory';
lineNo = 1;
directory = inputdlg(prompt, title, lineNo, default);
directory = char(directory);
prompt = {'Enter the Number of Specimens'};
number_of_specimens = inputdlg(prompt);
M = str2num(number_of_specimens{1});

cd(directory);
[filename1, pathname1] = uigetfile('*.txt', ['Select File Containing
Dimensions ']);

for z=1:M

    specimen_number = num2str(z);

    % CONSTANTS

    support_span = 64;

    %=======================================================
    %   1.  FLEXURAL DATA FILE GETS OPENED
    %   The data is sorted into FORCE and EXTENSION

    cd(directory);
    [filename2, pathname2] = uigetfile('*.txt', ['Select Specimen ',
specimen_number]);
    data = csvread(filename2, 39);

    %=======================================================
    %   2.  DIMENSIONS CAN BE OBTAINED EITHER FROM A *.txt FILE OR
ENTERED
    %   MANUALLY

    %   OPTION 1 - USE A *.txt FILE

    dimensions = dlmread(filename1);
    width = dimensions(z,1);
    thickness = dimensions(z,2);

    %   OPTION 2 - ENTER DIMENSIONS MANUALLY

%     prompt = {'Enter specimen width (mm):', 'Enter specimen
thickness (mm):'};
%     default={'16', '4'};
%     title = 'Specimen Dimensions';
%     lineNo=1;
%     dimensions = inputdlg(prompt,title,lineNo,default);
```

```
%     width = str2num(dimensions{1});
%     thickness = str2num(dimensions{2});

    %=====================================================
    %   3.  STRESS AND STRAIN ARE CALCULATED FROM THE INPUT DATA &
    %   DIMENSIONS

    stress = (3*support_span*1000*data(:,1))/(2*width*thickness^2);
    strain = 6*thickness*data(:,2)/support_span^2;

    %=====================================================
    %   4.  USER IS REQUESTED TO SELECT LINEAR REGION

    scrsz = get(0,'ScreenSize');
    figure('Position',[0.5*(scrsz(3)-scrsz(3)*0.75) 0.5*(scrsz(4)-
scrsz(4)*0.75) scrsz(3)*0.75 scrsz(4)*0.75]);

    figure(1)
    plot(strain, stress);
    xlim([0 1.1*max(strain)]);
    ylim([0 1.1*max(stress)]);
    xlabel('Uncorrected Strain');
    ylabel('Stress [MPa]');
    grid on

    %   Introduce crosshairs to select origin

    x = 0.15*max(xlim);
    y = 1.05*max(ylim);
    text(x,y, ['Select Start and End of Linear Region of ',
filename2]);
    [start_linear_strain, start_linear_stress]=ginput(1);
    [end_linear_strain, end_linear_stress]=ginput(1);

    %   Now we want to disregard anything before the start and end of
the
    %   linear region

    N=length(stress);
    a = 1;
    while a <= N
        if strain(a) <= start_linear_strain
            lowerlim = a;
        elseif strain(a) <= end_linear_strain
            upperlim = a;
        else
            break
        end
        a = a + 1;
    end

    lowerim = lowerlim + 1;
    linear_strain = strain(lowerlim:upperlim);
    linear_stress = stress(lowerlim:upperlim);
    p = polyfit(linear_strain, linear_stress, 1);
    f = polyval(p,linear_strain);

    %=====================================================
    %   5.  THE FITTED LINEAR CURVE IS USED TO DETERMINE THE POINT OF
ZERO
    %   STRAIN
```

```
    grad = p(1);
    y_int = p(2);
    zero_strain = (-y_int)/grad;
    for b=1:N
        strain(b)=strain(b)-zero_strain;
    end

    %=====================================================
    %   6.  THE MAXIMUM STRESS, MAXIMUM STRAIN AND ELASTIC MODULUS
ARE CALCULATED

    c = 1;
    max_stress = 0;
    while c <= N
        if stress(c) >= max_stress;
            max_stress = stress(c);
            failure_point = c;
        end
        c = c + 1;
    end

    maximum_stress(z) = stress(failure_point);
    maximum_strain(z) = strain(failure_point);
    secant_modulus(z) = (maximum_stress(z)/maximum_strain(z))/1000;
    linear_modulus(z) = grad/1000;

    maximum_stress_squared(z)=(stress(failure_point))^2;
    maximum_strain_squared(z)=(strain(failure_point))^2;

secant_modulus_squared(z)=(((stress(failure_point))^2)/((strain(failu
re_point))^2))/(1000^2);
    linear_modulus_squared(z) = (grad^2)/(1000^2);

    closereq;

end

average_maximum_stress = sum(maximum_stress)/M;
average_maximum_strain = sum(maximum_strain)/M;
average_secant_modulus = sum(secant_modulus)/M;
average_linear_modulus = sum(linear_modulus)/M;

stress_std_deviation=((sum(maximum_stress_squared)-
(average_maximum_stress^2)*M)/(M-1))^0.5;
strain_std_deviation=((sum(maximum_strain_squared)-
(average_maximum_strain^2)*M)/(M-1))^0.5;
secant_modulus_std_deviation=((sum(secant_modulus_squared)-
(average_secant_modulus^2)*M)/(M-1))^0.5;
linear_modulus_std_deviation=((sum(linear_modulus_squared)-
(average_linear_modulus^2)*M)/(M-1))^0.5;

%=====================================================
%   7.  THE RESULTING VALUES ARE WRITTEN INTO text FORMAT

results = [maximum_stress; maximum_strain; secant_modulus;
linear_modulus];
average_results = [average_maximum_stress; average_maximum_strain;
average_secant_modulus; average_linear_modulus];
std_deviation = [stress_std_deviation; strain_std_deviation;
secant_modulus_std_deviation; linear_modulus_std_deviation];
```

```
cd
C:\Flexural_Results\Polyester_Flexural_Results\4_Layers_Polyester_Fle
xural_Results;
[filename3, pathname3] = uiputfile('*.txt', 'Save Results As:');
fid = fopen(filename3,'w');
fprintf(fid,'\t Stress \t Strain \t Secant_Modulus \t
Linear_Modulus\n');
fprintf(fid,'\t   MPa \t   mm/mm \t   GPa \t   GPa\n');

for y=1:M
    y_str=num2str(y);
    fprintf(fid,'Specimen %c', y_str);
    fprintf(fid,'\t %3.1f \t %7.5f \t %3.2f \t
%3.2f\n',results(:,y));
end

fprintf(fid,'\n');
fprintf(fid,'Average');
fprintf(fid,'\t %3.1f \t %7.5f \t %3.2f \t %3.2f\n',average_results);
fprintf(fid,'Std. Dev. %c');
fprintf(fid,'\t %3.1f \t %7.5f \t %3.2f \t %3.2f\n',std_deviation);
fclose(fid);
```

D3 Impact test fast fourier transform code

This code was used “as is” from the work of I’Ons [33]

```
%=====================================================
%   1.  IMPACT DATA FILE GETS OPENED
cd C:\;                  %Set path to data files
[FileName,PathName] = uigetfile('*.txt','Select the File');
data=dlmread(FileName);
prompt={'Specify Sampling Interval in Seconds'};
sampling_interval=inputdlg(prompt);
sampling_interval=str2num(sampling_interval{1});
samplerate=1/sampling_interval;
time=sampling_interval*data(:,1);
volts=data(:,2);                         %Acquire signal
%=====================================================
%   2.  FAST FOURIER ANALYSIS IS PERFORMED ON THE VOLTS DATA
%
%   The FFT function works as follows: x=[data];
%   (Data to be analysed) samplerate;
%   (Used when creating frequency domain (Hz)) points=512;
%   (i.e. 2~9=512-Must be a power of 2 for computational efficiency)
%   Y=fft(x,points);
%   (FFT function gets used) Mag=Y.*conj (Y)/points;
%   (Magnitude data for y-axis from fft data)
%   Freq=samplerate*(0:points/2)/points;
%   (Frequency domain gets created from samplerate)
%   plot (Freq, Mag(1:257))
%   (Only half data is plotted due to the unwanted "wrap around
effect"
%   created by the FFT)
%   Data may be needed to be zoomed into!
%
%     Therefore:
points=4096;                             % 2~12=4096
fftvolts=fft(volts,points);
amp=fftvolts.*conj(fftvolts)/points;
freq=samplerate*(0:points/2)/points;
plot(freq, amp(1: (points/2+1)))
ylim([0 3])
xlim([0 25000])
%axis([0 samplerate/2 0 max(amp)])       %Half data!
grid on;
title=('Fast Fourier Transformation');
ylabel('Magnitude');
xlabel('Frequency [Hz]');
%     END
%=====================================================
```

D4 Impact test code

```
%=======================================================
% THIS PROGRAM IS INTENDED FOR THE INSTURMENTED IZOD
% IMPACT MACHINE IN THE COMPOSITE LABORATORY
% (ENERGY AND STRESS CALCULATIONS)
% - By Trevor I'Ons
% - Updated and Modified by Stefan Rassmann
%   - Changes include
%       - Adapting to work with new data capturing equipment
%       - Adapting to work with newer versions of Matlab
%       - Changing method of energy calculation to reduce inaccuracy
by
%       calculating energy from velocity instead of displacement
%       - Loop for multiple specimen analysis
%       - Coding to write results to a *.txt file
%=======================================================
clear;
clf;
% DECLARATION OF CONSTANTS
mass1=4.65;            %Mass of striker/pendulum         1.9955
acc_const=100*10^(-3); %100mV is '1g' (9.81m/s^2)
rs=0.481;              %Distance to STRIKER            0.350
rg=0.408;              %Distance to CENTRE OF GRAVITY   0.2411
ra=0.490;              %Distance to ACCELEROMETER       0.3875
v0=2.791;              %Initial velocity of CENTRE OF GRAVITY
2.1271
t0=0.000;              %Initial time
s0=0.000;              %Initial DISPLACEMENT of spec.
e0=0.000;              %Initial ENERGY of specimen
Lstrike=20;            %Length of specimen cantilver
%=======================================================
%   1.  THE USER IS PROMPTED TO ENTER THE PATH OF THE FOLDER
CONTAINING RAW
%   DATA, INPUT THE NUMBER OF SAMPLES, SELECT THE FILE CONTAINING THE
%   SAMPLE DIMENSIONS AND ENTER THE SAMPLING RATE AND FILTER
FREQUENCY

prompt = {'Type the Directory Containing Impact Test Files'};
default = {'C:\Impact_Data\Epoxy_Impact\4GE-EP_Impact'};
title = 'directory';
lineNo = 1;
directory = inputdlg(prompt, title, lineNo, default);
directory = char(directory);
prompt = {'Enter the Number of Specimens'};
number_of_specimens = inputdlg(prompt);
M = str2num(number_of_specimens{1});

cd(directory);
[filename1, pathname1] = uigetfile('*.txt', ['Select File Containing
Dimensions']);

prompt={'Specify Sampling Interval', 'Specify Filter Frequency'};
default={'0.000005', '1500'};
title='Sampling Interval & Filter Frequency';
lineNo=1;
sampling_filter=inputdlg(prompt,title,lineNo,default);
sampling_interval=str2num(sampling_filter{1});
samplerate=1/sampling_interval;
```

```
filterfreq=str2num(sampling_filter{2});
filterperiod=1/filterfreq;
bmatnum=filterperiod/(1/samplerate);

for z=1:M;

    specimen_number = num2str(z);

    %=======================================================
    %   2.  IMPACT DATA FILE GETS OPENED
    %   The data is sorted into TIME and VOLTS

    cd(directory);
    [filename2, pathname2]=uigetfile('*.txt*', ['Select Specimen ',
specimen_number]);
    data=dlmread(filename2);
    time=sampling_interval*data(:,1);
    volts=data(:,2);

    %=======================================================
    %   3.  DATA IS FILTERED ACCORDING TO USERS INPUT OF DESIRED LOW
PASS
    %   BAND !!!

    a=1;
    for b=1:bmatnum;
        c(b)=1/bmatnum;
    end
    voltsFiltered=filter(c,a,volts);

    %=======================================================
    %   4.  USER IS REQUESTED TO SELECT STRIKING POSITION (ORIGIN
POINT)

    figure(1);
    plot(time, voltsFiltered)
    xlabel('Time [s]');
    ylabel('Volts [V]');
    grid on
    %   Now introduce crosshairs to select origin
    x=0.15*max(xlim);
    y=1.05*max(ylim);
    text(x,y, 'Select Start and End of Impact Curve');
    [zero_time, zero_volts]=ginput(1);
    [finish_time, finish_volts]=ginput(1);
    %   From this, a new force vector is calculated, setting the true
    %   origin
    N=size(voltsFiltered);
    for d=1:N
        voltsFiltered(d)=voltsFiltered(d)-zero_volts;
        time(d)=time(d)-zero_time;
    end
    %   Now we want to disregard anything before t=0!
    for e=1:N
        if time(e)>=0
            if (finish_time-zero_time)>=time(e)
                VOLTS(e)=voltsFiltered(e);
                TIME(e)=time(e);
            end
        end
    end
```

```
    %=====================================================
    %   5.  DATA IS CONVERTED TO ACCELERATION (OF ACCELEROMETER)

    N=length(VOLTS);
    for f=1:N
        accel(f)=(-1)*(9.81/acc_const)*VOLTS(f);
    end
    accel=transpose(accel);

    %=====================================================
    %   6.1.    DATA IS USED TO COMPUTE VELOCITY OF ACCELEROMETER VIA
    %   NUMERICAL INTEGRATION

    for g=1:N-1
        vel(1)=v0*(ra/rg);
        vel(g+1)=vel(g)+((accel(g)+accel(g+1))/2*(TIME(g+1)-
TIME(g)));
    end
    vel=transpose(vel);

    %=====================================================
    %   6.2.    DATA IS USED TO COMPUTE DISPLACEMENT OF ACCELEROMTER
VIA
    %   NUMERICAL INTEGRATION

    for h=1:N-1
        disp(1)=s0;
        disp(h+1)=disp(h)+((vel(h)+vel(h+1))/2*(TIME(h+1)-TIME(h)));
    end
    disp=transpose(disp);

    %=====================================================
    %   7.  DATA IS USED TO COMPUTE FORCE FROM MOMENTS
    %   AND PENDULUM PROPERTIES.
    %   (F=MA)
    %   Fg*rg=Fs*rs
    %   Fs=(rg/rs)*Fg ------- (1)
    %   but
    %   Fg=Mg*ag ------- (2)
    %   ag=(rg/ra)*aa ------- (3)
    %
    %  where ag= acc. of centre of gravity
    %        as= acc. of striker
    %        aa= acc. Of accelerometer
    %  Fs=Mg*(rg/rs)*(rg/ra)*aa

    for i=1:N
        force(i)=(-1)*mass1*(rg/rs)*(rg/ra)*accel(i);
    end
    force=transpose(force);

    %=====================================================
    %   8.  DATA IS USED TO COMPUTE ENERGY VIA NUMERICAL INTEGRATION
OF
    %   MASS AND VELOCITY OF PENDULUM

    for j=1:N    %j=1:N-1
        %energy(1)=e0;
```

```
        energy(j)=0.5*mass1*((vel(1)*(rg/ra))^2-(vel(j)*(rg/ra))^2);
%energy(j+1)=energy(j)+(((force(j)+force(j+1))/2)*((disp(j+1)-
disp(j))*(rs/ra)));
    end
    energy=transpose(energy);

    %=====================================================
    %   9. DATA IS USED TO PLOT FORCE AND ENERGY VS.
    %   TIME OVERLAY
    %   Plot data

    clf;
    [AX,H1,H2]=plotyy(TIME, force, TIME, energy, 'plot');
    %   Labels all three axes
    set(get(AX(1), 'Ylabel'), 'String', 'Force [N]')
    set(get(AX(2), 'Ylabel'), 'String', 'Energy [J]')
    xlabel('Time [s]');
    %   Set axes limits and increments
    y1max=ceil(1.1*max(force));
    y2max=ceil(1.1*max(energy));
    ylim(AX(1), [0 y1max])
    ylim(AX(2), [0 y2max])
    set(AX(1), 'ytick', [0:y1max/5:y1max])
    set(AX(2), 'ytick', [0:y2max/5:y2max])
    grid on

    %=====================================================
    %   10.  USER IS PROMPTED FOR THE POINT OF PEAK FORCE

    x=0.12*max(xlim);
    y=1.05*max(ylim);
    text(x,y, 'Select Peak Force Along Force Curve');
    [TIMEPeak, FORCEPeak]=ginput(1);
    %   Now that the failure point is known, calculate the
corresponding
    %   energy!!!
        for k=1:N
        if TIMEPeak > TIME(k)
            energyPeak(k)=energy(k);
            forcePeak(k)=force(k);
        end
    end
    %   Now get the energies from the created arrays

    dimensions = dlmread(filename1);
    width = dimensions(z,1);
    thickness = dimensions(z,2);

    Peak_Energy_cm2 = max(energyPeak)/(width*thickness)*100;
    Total_Energy_cm2 = max(energy)/(width*thickness)*100;
    Impact_Strength_cm2 = Total_Energy_cm2;
    Peak_Energy_cm = max(energyPeak)/thickness*10;
    Total_Energy_cm = max(energy)/thickness*10;
    Impact_Strength_cm = Total_Energy_cm;
    Fmax = max(forcePeak);

    Ei_cm2(z) = Peak_Energy_cm2;
    Ep_cm2(z) = (Total_Energy_cm2-Peak_Energy_cm2);
    IS_cm2(z) = Impact_Strength_cm2;
    Ei_cm(z) = Peak_Energy_cm;
    Ep_cm(z) = (Total_Energy_cm-Peak_Energy_cm);
```

```
    IS_cm(z) = Impact_Strength_cm;
    Smax(z) = (6*Fmax*Lstrike)/(thickness*width^2);

    Ei_squared_cm2(z) = Peak_Energy_cm2^2;
    Ep_squared_cm2(z) = (Total_Energy_cm2-Peak_Energy_cm2)^2;
    IS_squared_cm2(z) = Impact_Strength_cm2^2;
    Ei_squared_cm(z) = Peak_Energy_cm^2;
    Ep_squared_cm(z) = (Total_Energy_cm-Peak_Energy_cm)^2;
    IS_squared_cm(z) = Impact_Strength_cm^2;
    Smax_squared(z) = ((6*Fmax*Lstrike)/(thickness*width^2))^2;

    closereq;
    clear volts voltsFiltered VOLTS time TIME accel vel disp force
energy;

end

average_Ei_cm2 = sum(Ei_cm2)/M;
average_Ep_cm2 = sum(Ep_cm2)/M;
average_IS_cm2 = sum(IS_cm2)/M;
average_Ei_cm = sum(Ei_cm)/M;
average_Ep_cm = sum(Ep_cm)/M;
average_IS_cm = sum(IS_cm)/M;
average_Smax = sum(Smax)/M;

Ei_cm2_std_deviation = ((sum(Ei_squared_cm2)-
(average_Ei_cm2^2)*M)/(M-1))^0.5;
Ep_cm2_std_deviation = ((sum(Ep_squared_cm2)-
(average_Ep_cm2^2)*M)/(M-1))^0.5;
IS_cm2_std_deviation = ((sum(IS_squared_cm2)-
(average_IS_cm2^2)*M)/(M-1))^0.5;
Ei_cm_std_deviation = ((sum(Ei_squared_cm)-(average_Ei_cm^2)*M)/(M-
1))^0.5;
Ep_cm_std_deviation = ((sum(Ep_squared_cm)-(average_Ep_cm^2)*M)/(M-
1))^0.5;
IS_cm_std_deviation = ((sum(IS_squared_cm)-(average_IS_cm^2)*M)/(M-
1))^0.5;
Smax_std_deviation = ((sum(Smax_squared)-(average_Smax^2)*M)/(M-
1))^0.5;

%=====================================================
%   11.  THE RESULTING VALUES ARE WRITTEN TO A *.txt FILE

results = [Ei_cm2; Ep_cm2; IS_cm2; Ei_cm; Ep_cm; IS_cm; Smax];
average_results = [average_Ei_cm2; average_Ep_cm2; average_IS_cm2;
average_Ei_cm; average_Ep_cm; average_IS_cm; average_Smax];
std_deviation = [Ei_cm2_std_deviation; Ep_cm2_std_deviation;
IS_cm2_std_deviation; Ei_cm_std_deviation; Ep_cm_std_deviation;
IS_cm_std_deviation; Smax_std_deviation];

cd C:\Impact_Results\Epoxy_Impact_Results;
[filename3, pathname3] = uiputfile('*.txt', 'Save Results As:');
fid = fopen(filename3,'w');
fprintf(fid,'\t Ei \t Ep \t IS \t Ei \t Ep \t IS \t S_max\n');
fprintf(fid,'\t J/cm^2 \t J/cm^2 \t J/cm^2 \t J/cm \t J/cm \t J/cm \t
MPa\n');

for y=1:M
    y_str=num2str(y);
    fprintf(fid,'Specimen %c', y_str);
```

```
    fprintf(fid,'\t %3.2f \t %3.2f \t %3.2f \t %3.2f \t %3.2f \t
%3.2f \t %3f\n',results(:,y));
end

fprintf(fid,'\n');
fprintf(fid,'Average');
fprintf(fid,'\t %3.2f \t %3.2f \t %3.2f \t %3.2f \t %3.2f \t %3.2f \t
%3f\n',average_results);
fprintf(fid,'Std. Dev. %c');
fprintf(fid,'\t %3.2f \t %3.2f \t %3.2f \t %3.2f \t %3.2f \t %3.2f \t
%3f\n',std_deviation);
fclose(fid);
```

D5 Accelerometer data sheet

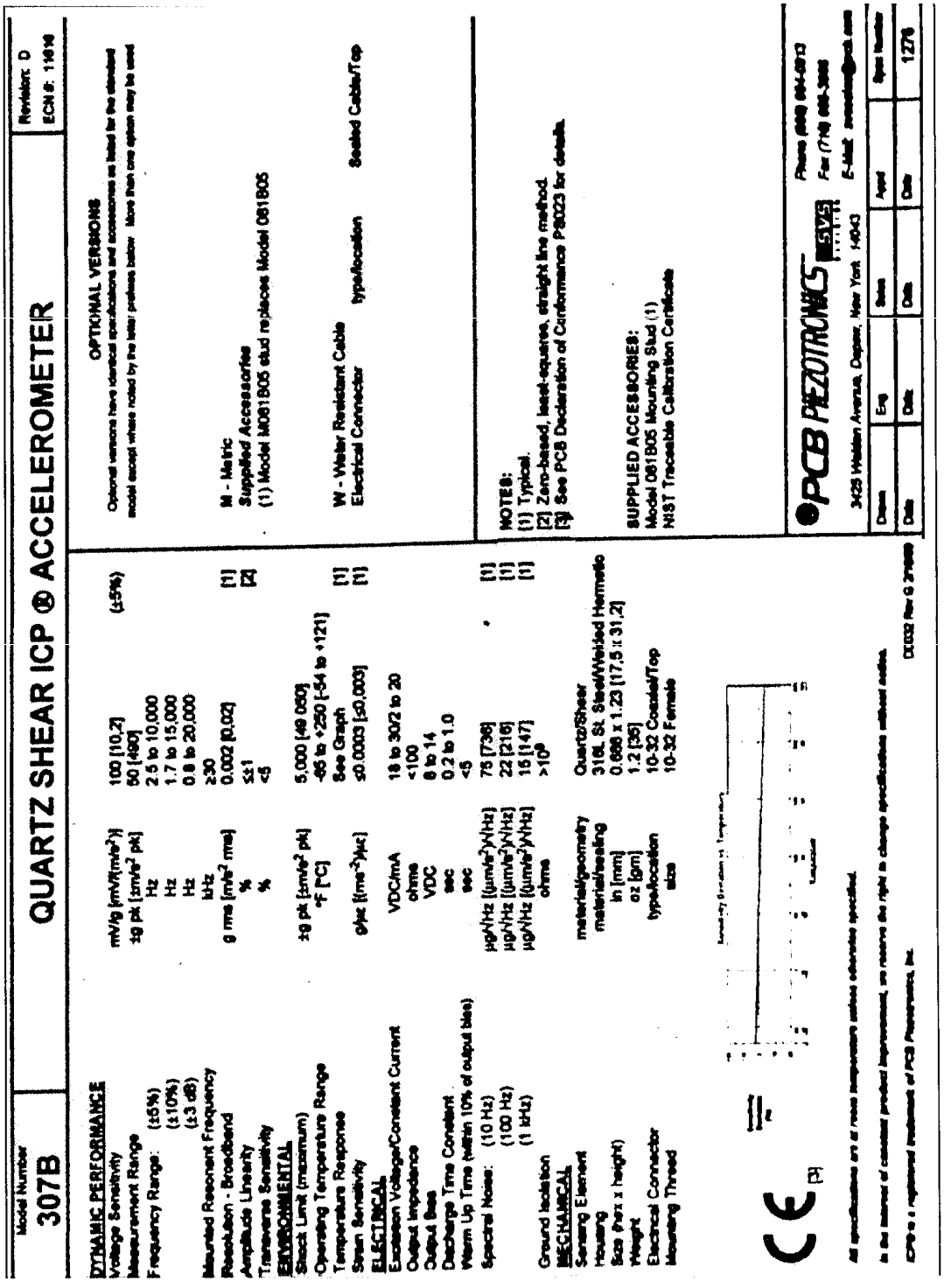

Model Number
307B

QUARTZ SHEAR ICP ® ACCELEROMETER

Revision: D
ECN #: 11618

DYNAMIC PERFORMANCE			
Voltage Sensitivity	mV/g [mV/(m/s²)]	100 [10.2]	(±5%)
Measurement Range	±g pk [±m/s² pk]	50 [490]	
Frequency Range: (±5%)	Hz	2.5 to 10,000	
(±10%)	Hz	1.7 to 15,000	
(±3 dB)	Hz	0.8 to 20,000	
Mounted Resonant Frequency	kHz	≥30	
Resolution - Broadband	g rms [m/s² rms]	0.002 [0.02]	[1]
Amplitude Linearity	%	≤±1	[2]
Transverse Sensitivity	%	<5	
ENVIRONMENTAL			
Shock Limit (maximum)	±g pk [±m/s² pk]	5,000 [49,050]	
Operating Temperature Range	°F [°C]	-65 to +250 [-54 to +121]	
Temperature Response		See Graph	[1]
Strain Sensitivity	g/με [(m/s²)/με]	≤0.0003 [≤0.003]	[1]
ELECTRICAL			
Excitation Voltage/Constant Current	VDC/mA	18 to 30/2 to 20	
Output Impedance	ohms	<100	
Output Bias	VDC	8 to 14	
Discharge Time Constant	sec	0.2 to 1.0	
Warm Up Time (within 10% of output bias)	sec	<5	
Spectral Noise: (10 Hz)	µg/√Hz [(µm/s²)/√Hz]	75 [736]	[1]
(100 Hz)	µg/√Hz [(µm/s²)/√Hz]	22 [216]	[1]
(1 kHz)	µg/√Hz [(µm/s²)/√Hz]	15 [147]	[1]
Ground Isolation	ohms	>10⁸	[1]
MECHANICAL			
Sensing Element	material/geometry	Quartz/Shear	
Housing	material/sealing	316L St. Steel/Welded Hermetic	
Size (hex x height)	in [mm]	0.686 x 1.23 [17.5 x 31.2]	
Weight	oz [gm]	1.2 [35]	
Electrical Connector	type/location	10-32 Coaxial/Top	
Mounting Thread	size	10-32 Female	

OPTIONAL VERSIONS

Optional versions have identical specifications and accessories as listed for the standard model except where noted by the letter prefixes below. More than one option may be used.

M - Metric
Supplied Accessories
(1) Model M081805 stud replaces Model 081805

W - Water Resistant Cable
Electrical Connector — type/location — Sealed Cable/Top

NOTES:
(1) Typical.
[2] Zero-based, least-squares, straight line method.
[3] See PCB Declaration of Conformance PS023 for details.

SUPPLIED ACCESSORIES:
Model 081805 Mounting Stud (1)
NIST Traceable Calibration Certificate

PCB PIEZOTRONICS ISO 9001 CERTIFIED
3425 Walden Avenue, Depew, New York 14043
Phone (716) 684-0001
Fax (716) 685-3886
E-Mail: sensinfo@pcb.com

Drawn	Eng	Sales	Appd	Spec Number
Date	Date	Date	Date	1276

All specifications are at room temperature unless otherwise specified.

In the interest of constant product improvement, we reserve the right to change specifications without notice.

ICP® is a registered trademark of PCB Piezotronics, Inc.

D0332 Rev G 2/1999

Appendix E SEM examinations

E1 Effects of processing conditions

In the following pictures the letters correspond to the following composites:

a: UP-AD-H

b: UP-AD-NH

c: UP-AD-H-P

d: UP-ND-H

e: UP-ND-NH

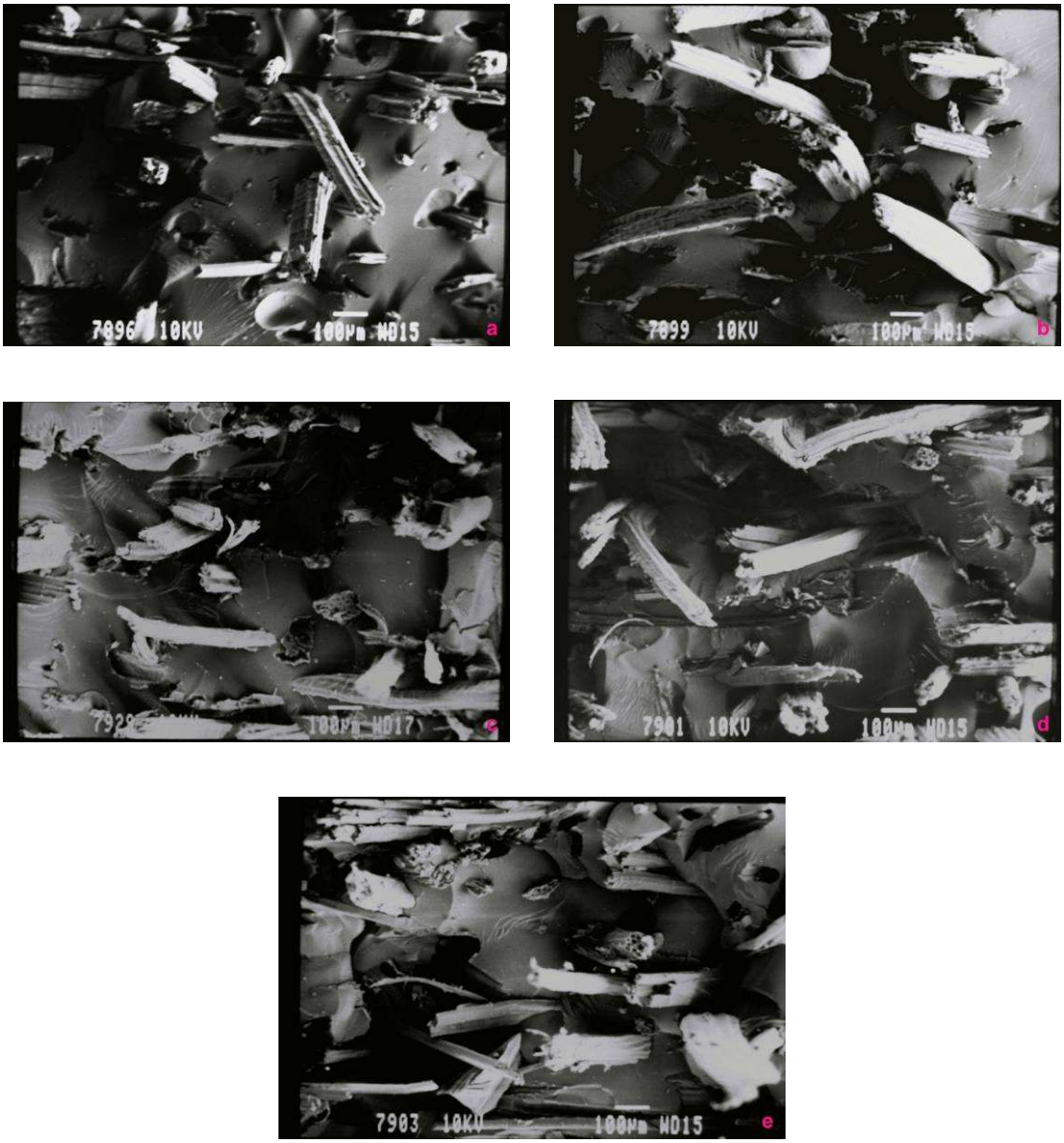

Figure E.1 SEM micrographs of impact failure surfaces of composites made using various processing conditions at 15 % fibre volume fraction

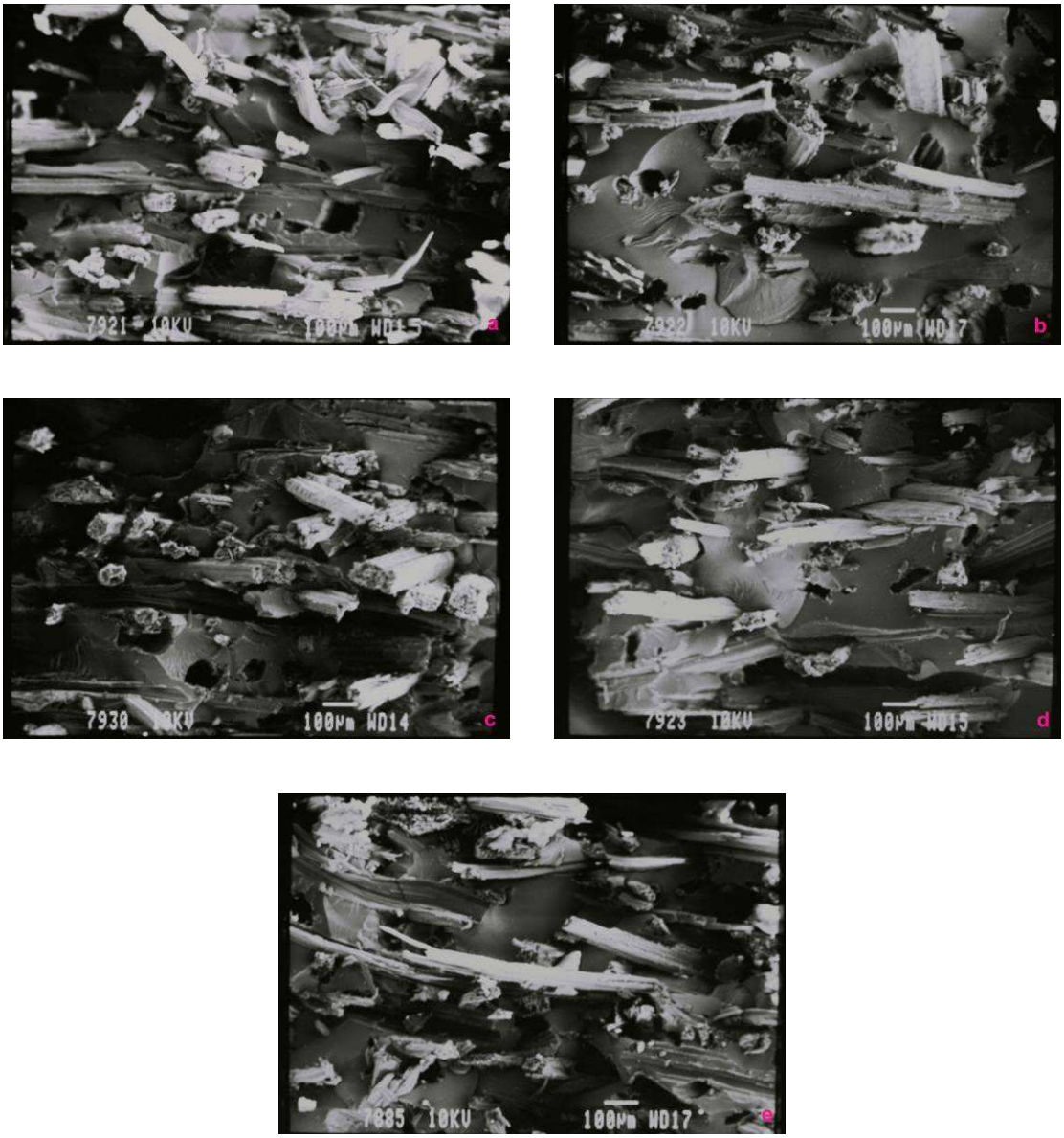

Figure E.2 SEM micrographs of impact failure surfaces of composites made using various processing conditions at 22.5 % fibre volume fraction

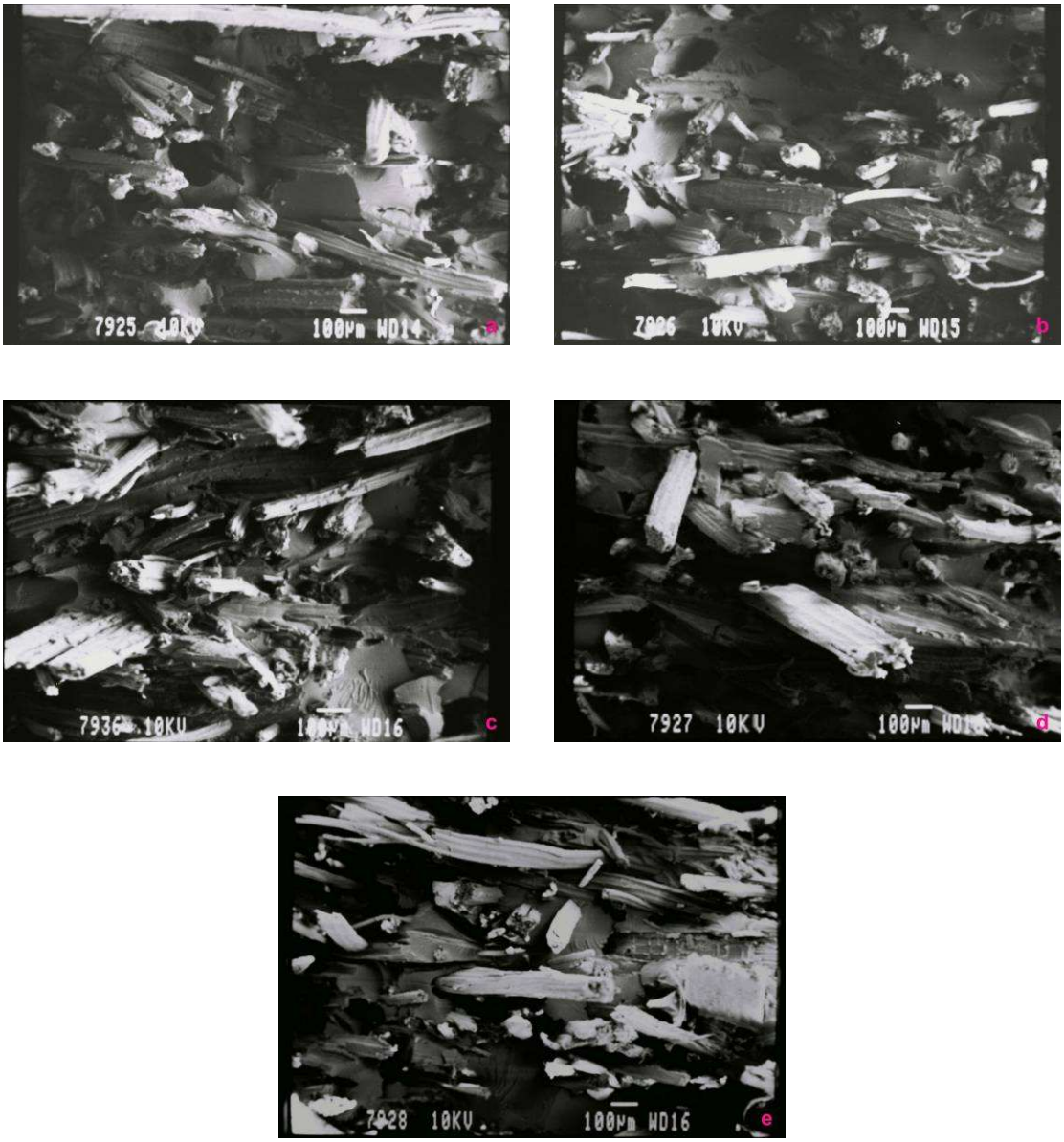

Figure E.3 SEM micrographs of impact failure surfaces of composites made using various processing conditions at 30 % fibre volume fraction

E2 Effects of resin system

In the following pictures the letters correspond to the following composites:

a: UP-AD-H b: VE-AD-H

c: EP-AD-H

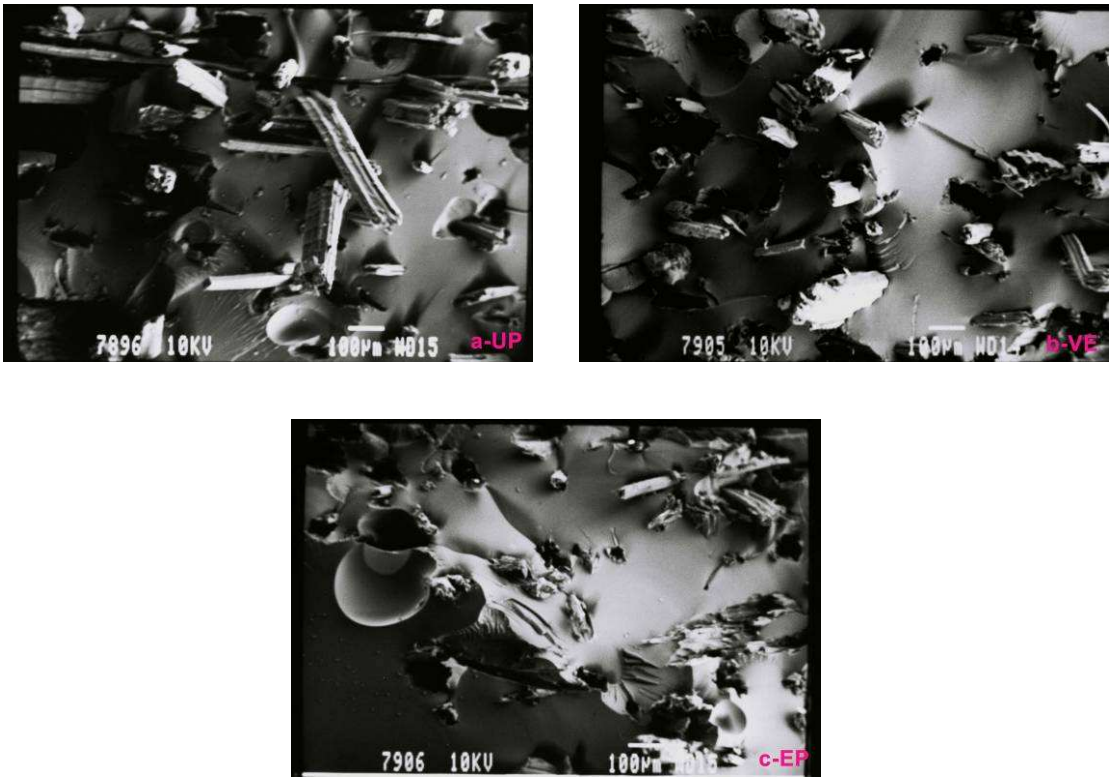

Figure E.4 SEM micrographs of impact failure surfaces of composites made using various resin systems at 15 % fibre volume fraction

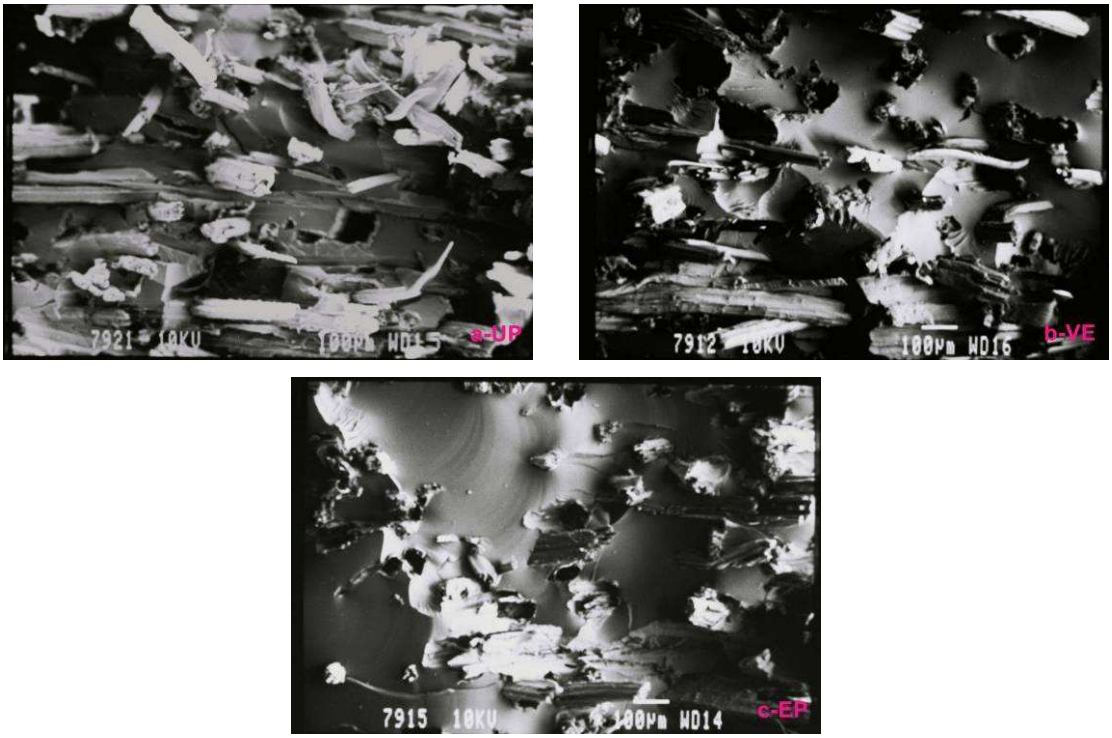

Figure E.5 SEM micrographs of impact failure surfaces of composites made using various resin systems at 22.5 % fibre volume fraction

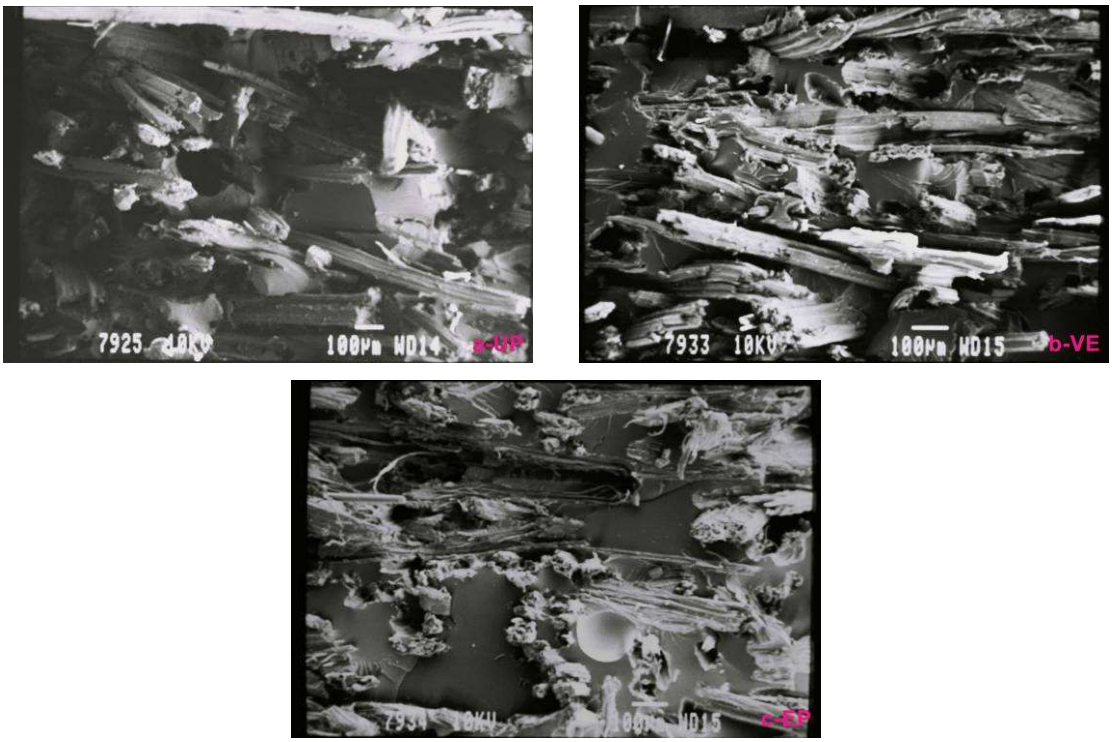

Figure E.6 SEM micrographs of impact failure surfaces of composites made using various resin systems at 30 % fibre volume fraction

E3 Other

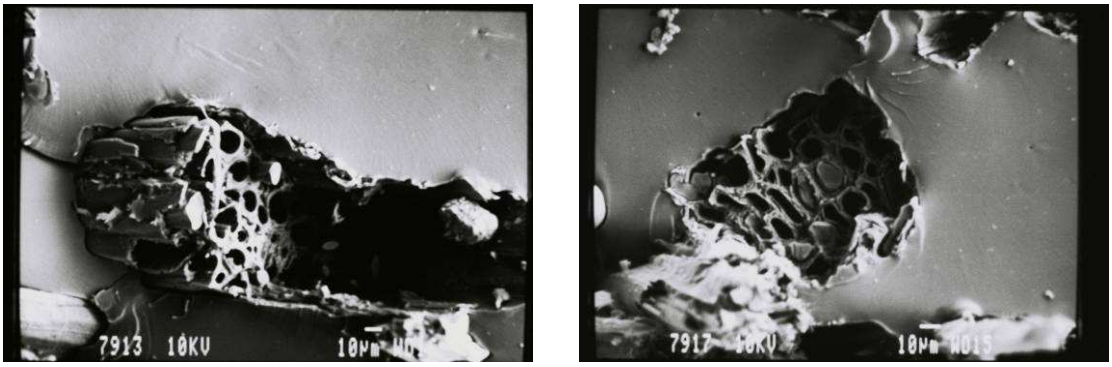

Figure E.7 Fibres fractured at surface of 22.5 % fibre volume fraction composites, vinyl ester (left) and epoxy (right)

Appendix F Water absorption tests

F1 Effects of processing conditions

Mass change

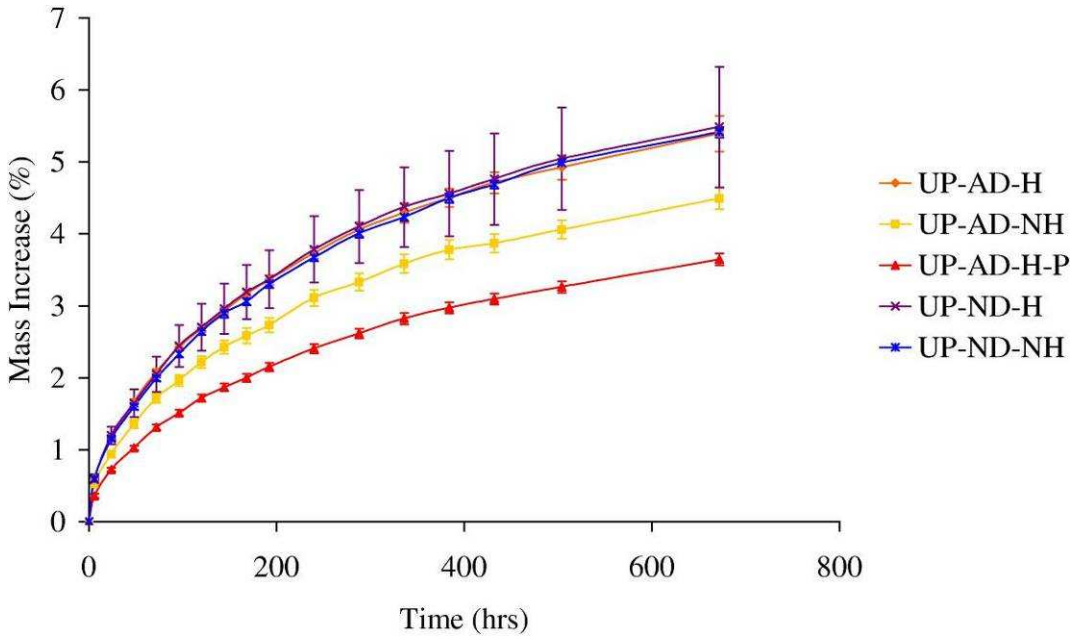

Figure F.1 Effect of processing conditions on mass increase over four weeks of water absorption at 15 % fibre volume fraction

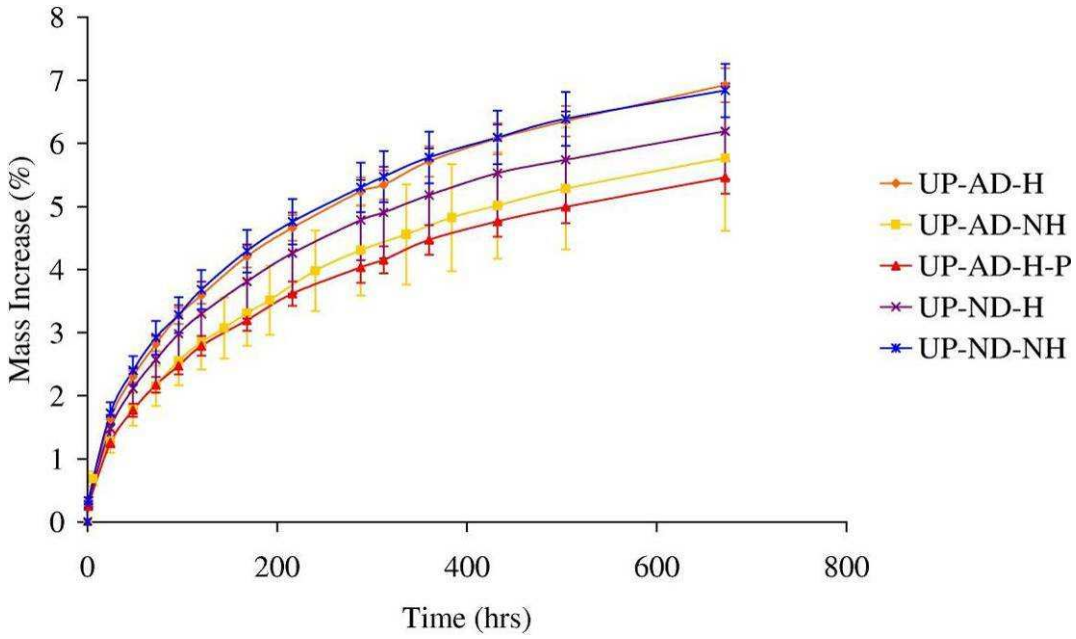

Figure F.2 Effect of processing conditions on mass increase over four weeks of water absorption at 22.5 % fibre volume fraction

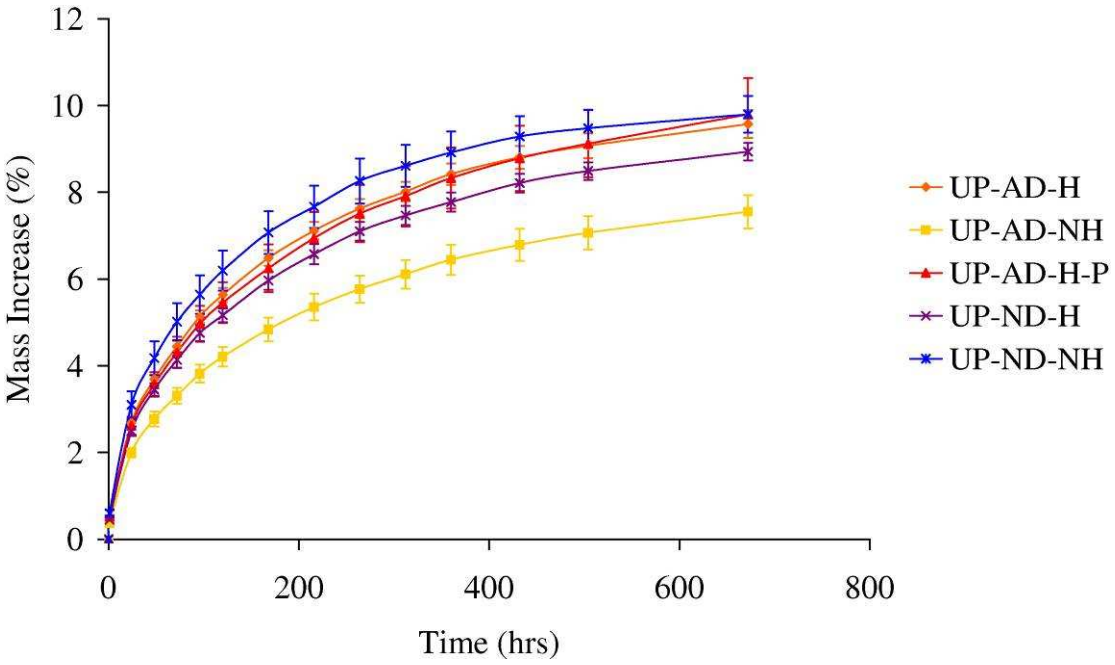

Figure F.3 Effect of processing conditions on mass increase over four weeks of water absorption at 30 % fibre volume fraction

Thickness change

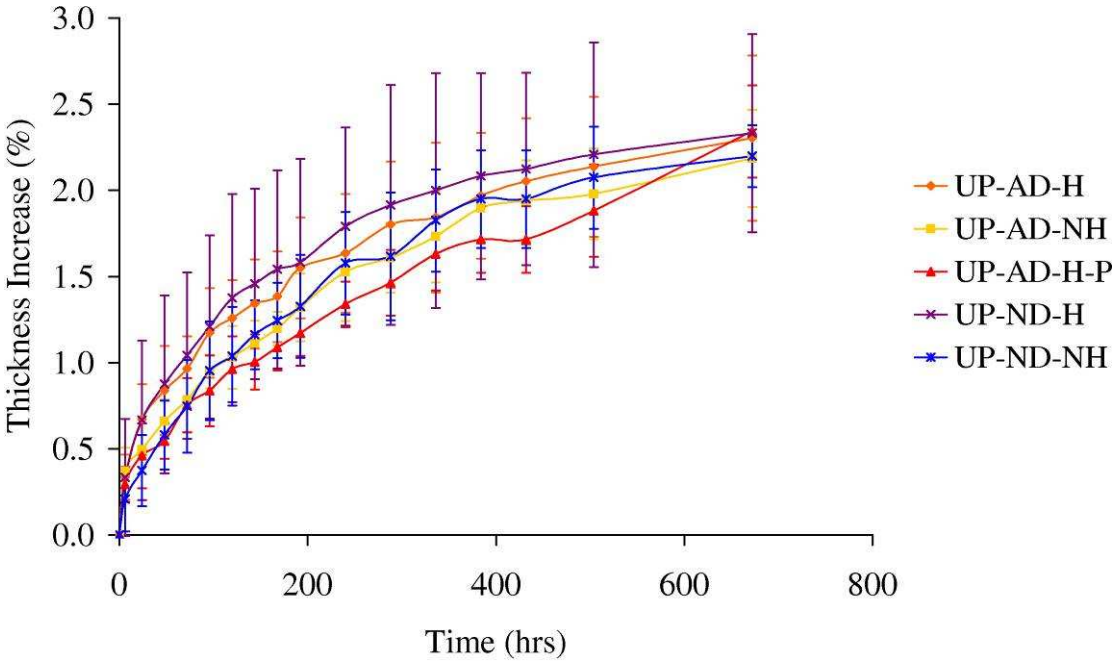

Figure F.4 Effect of processing conditions on thickness increase over four weeks of water absorption at 15 % fibre volume fraction

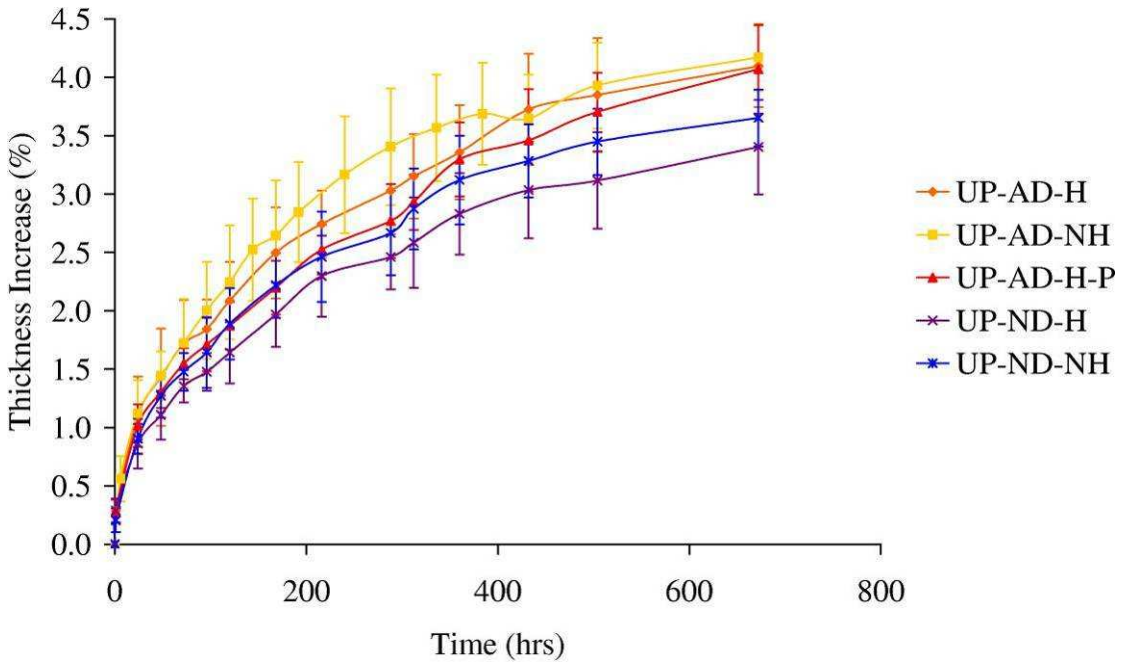

Figure F.5 Effect of processing conditions on thickness increase over four weeks of water absorption at 22.5 % fibre volume fraction

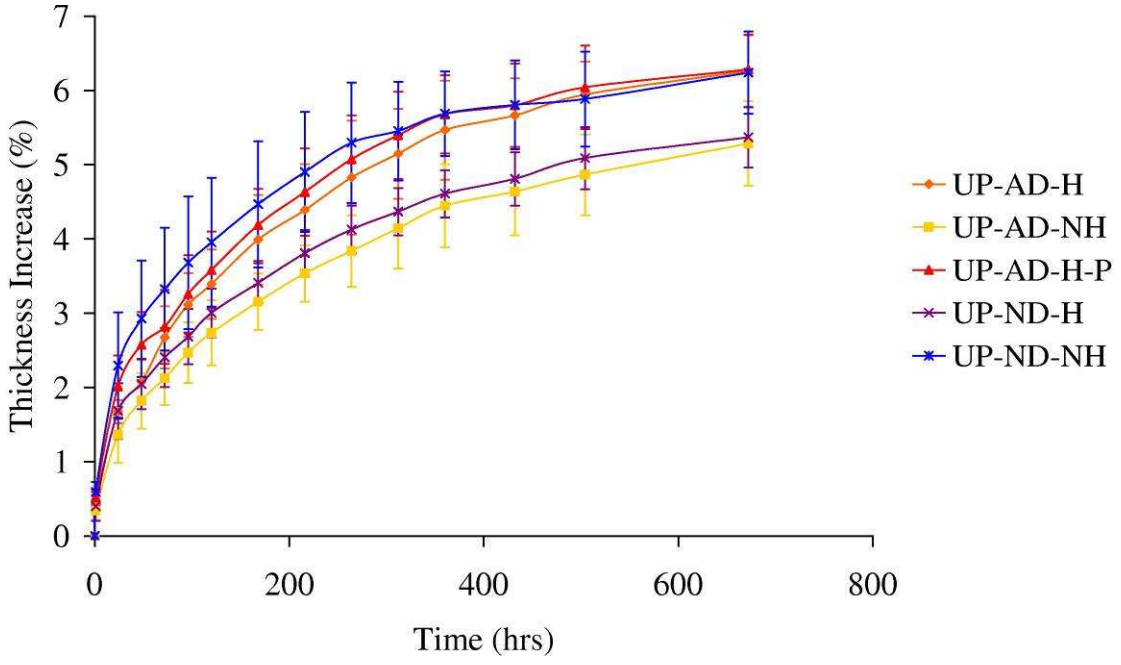

Figure F.6 Effect of processing conditions on thickness increase over four weeks of water absorption at 30 % fibre volume fraction

Length change

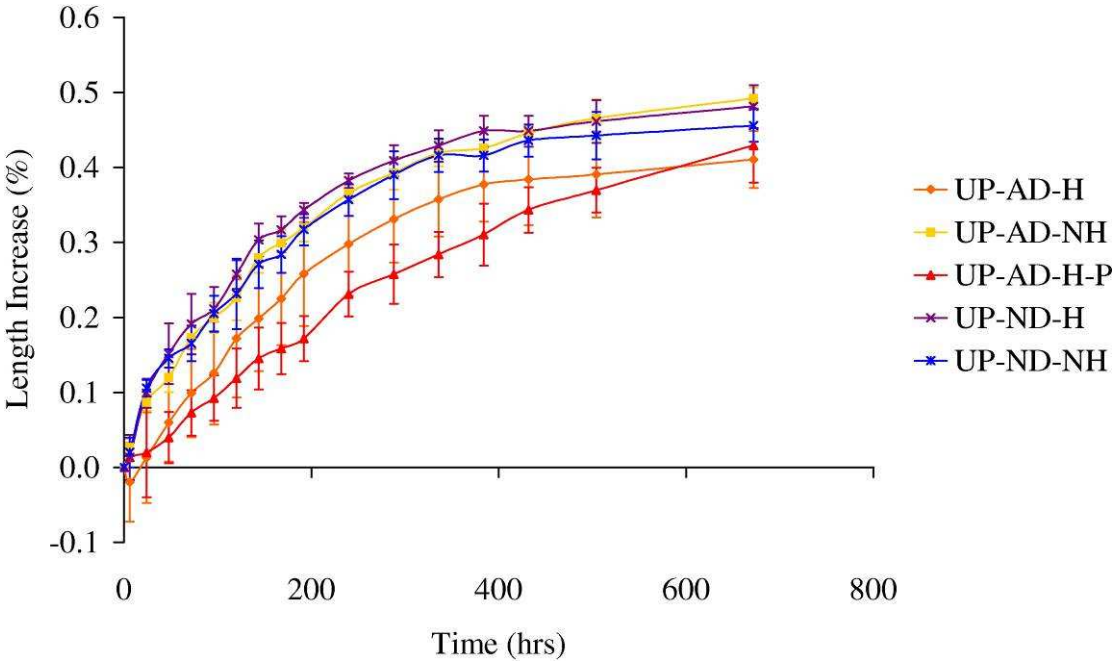

Figure F.7 Effect of processing conditions on length increase over four weeks of water absorption at 15 % fibre volume fraction

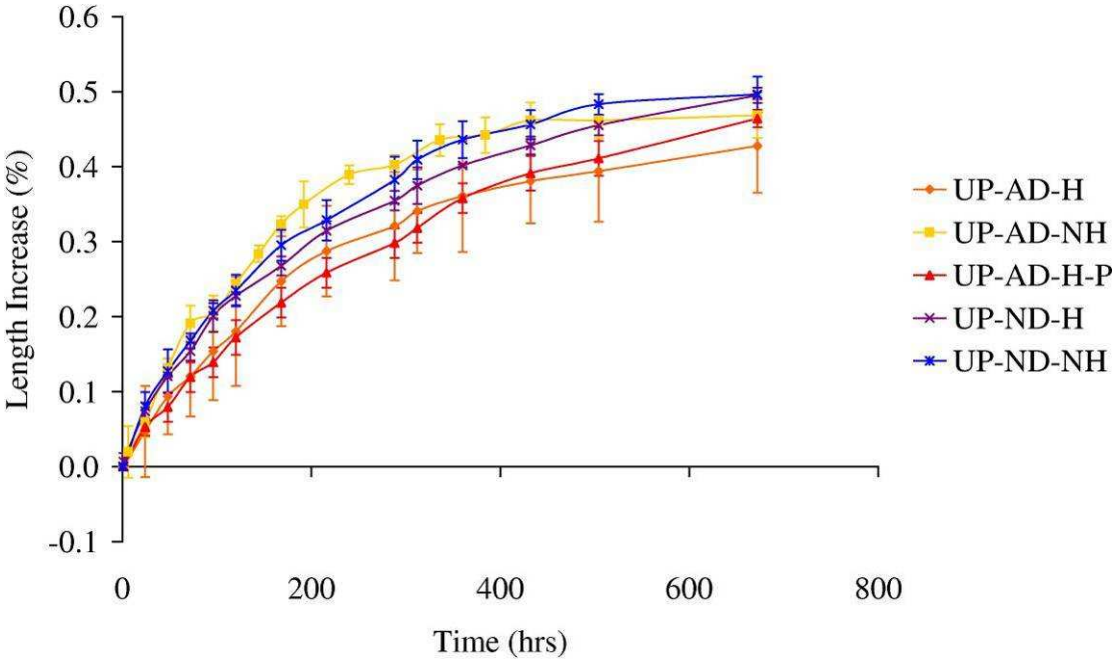

Figure F.8 Effect of processing conditions on length increase over four weeks of water absorption at 22.5 % fibre volume fraction

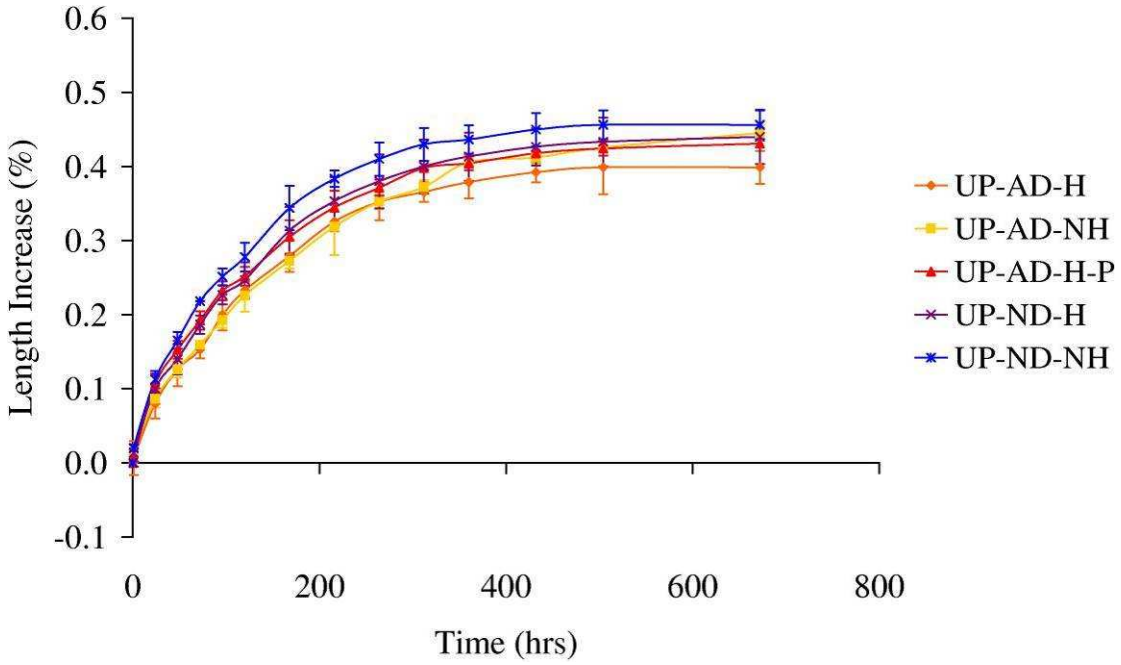

Figure F.9 Effect of processing conditions on length increase over four weeks of water absorption at 30 % fibre volume fraction

Width change

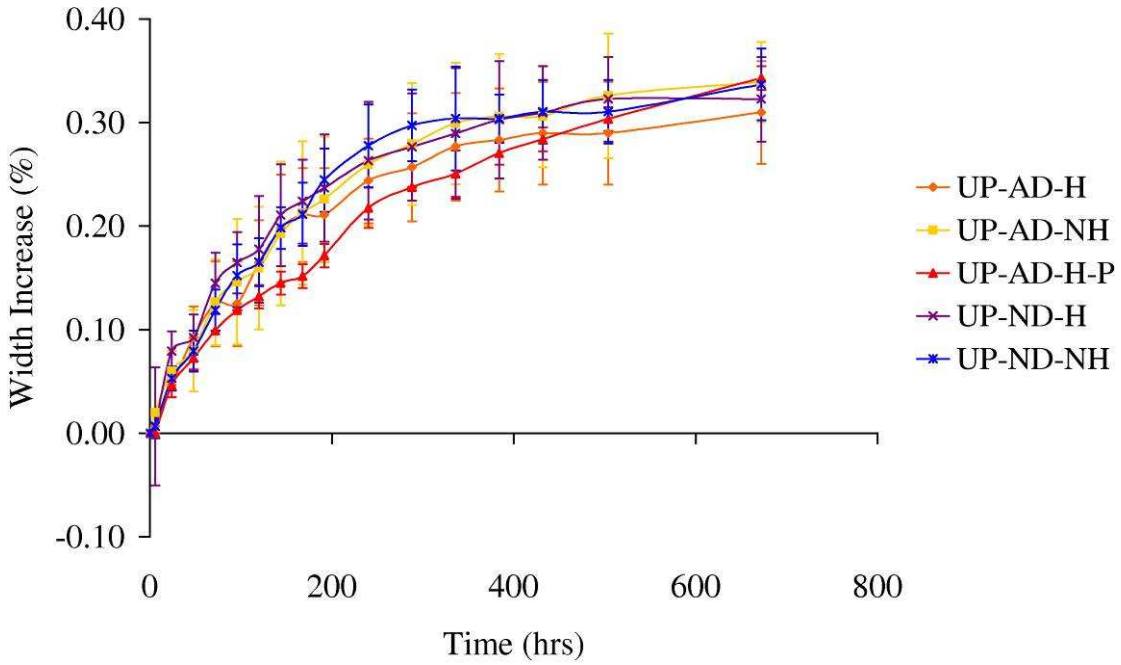

Figure F.10 Effect of processing conditions on width increase over four weeks of water absorption at 15 % fibre volume fraction

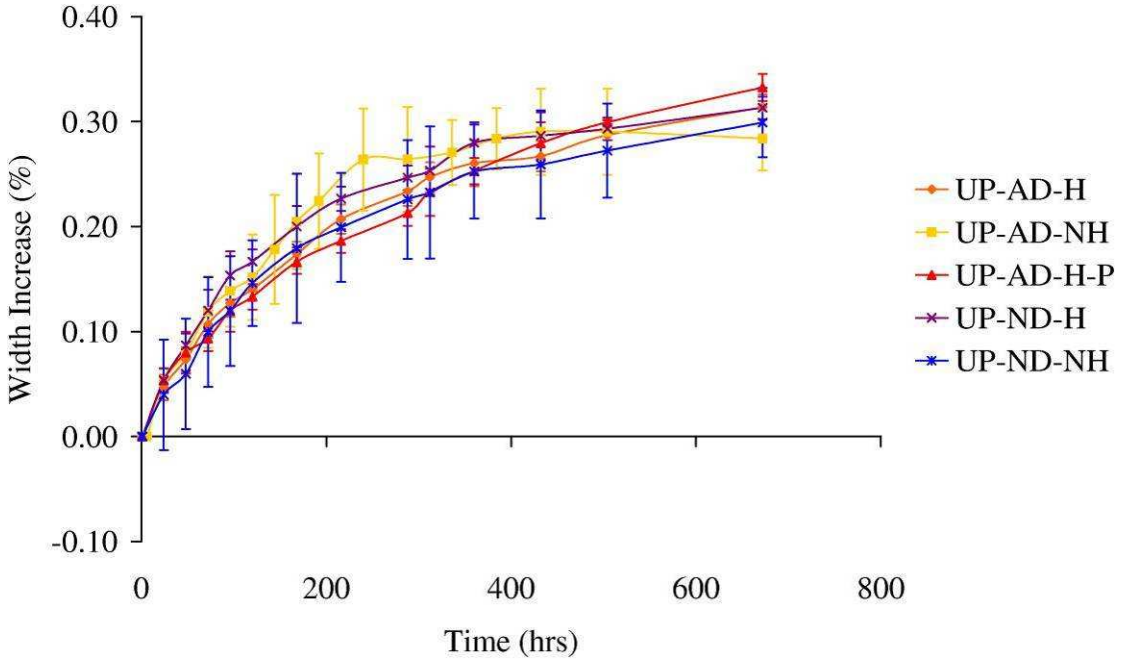

Figure F.11 Effect of processing conditions on width increase over four weeks of water absorption at 22.5 % fibre volume fraction

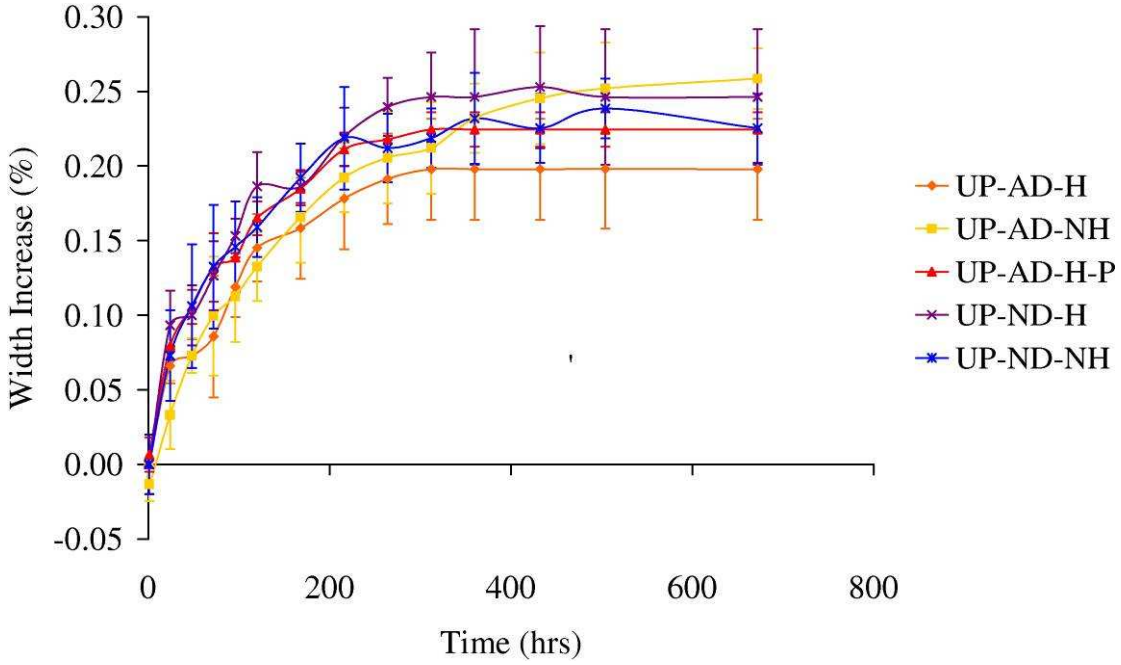

Figure F.12 Effect of processing conditions on width increase over four weeks of water absorption at 30 % fibre volume fraction

F2 Effects of resin system

Mass change

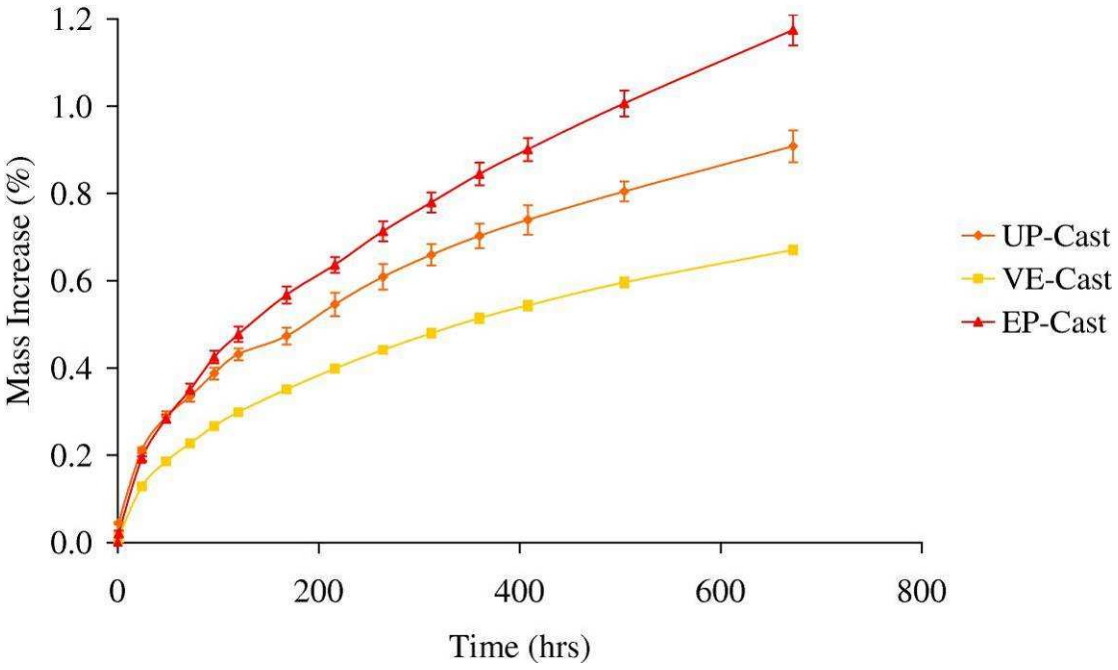

Figure F.13 Effect of resin system on mass increase over four weeks of water absorption at 0 % fibre volume fraction

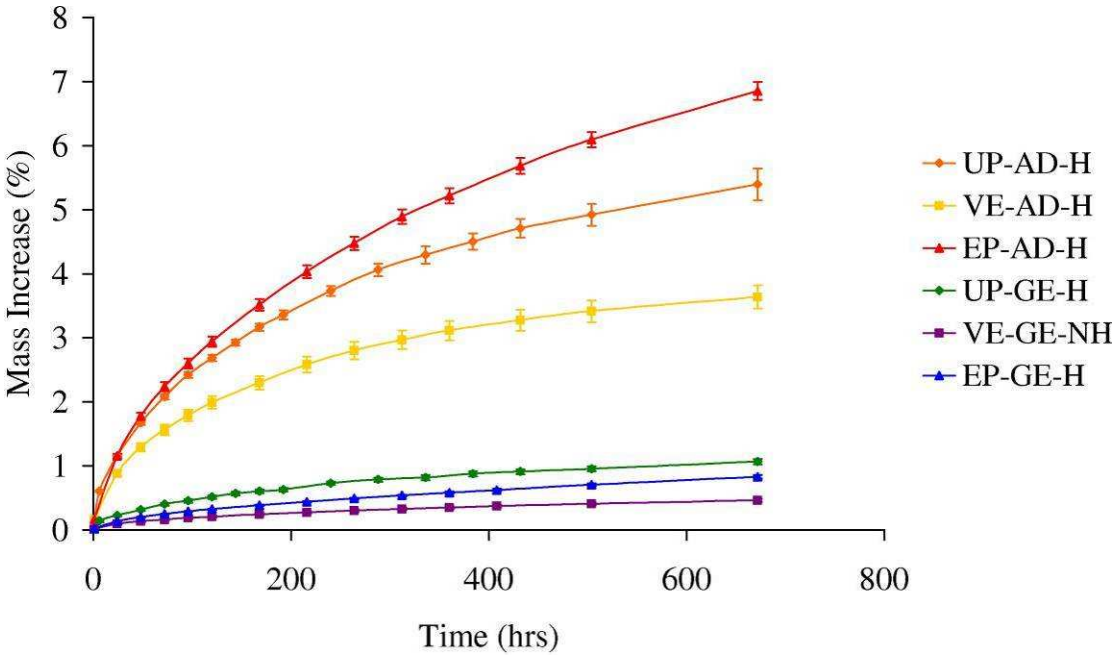

Figure F.14 Effect of resin system on mass increase over four weeks of water absorption at 15 % fibre volume fraction

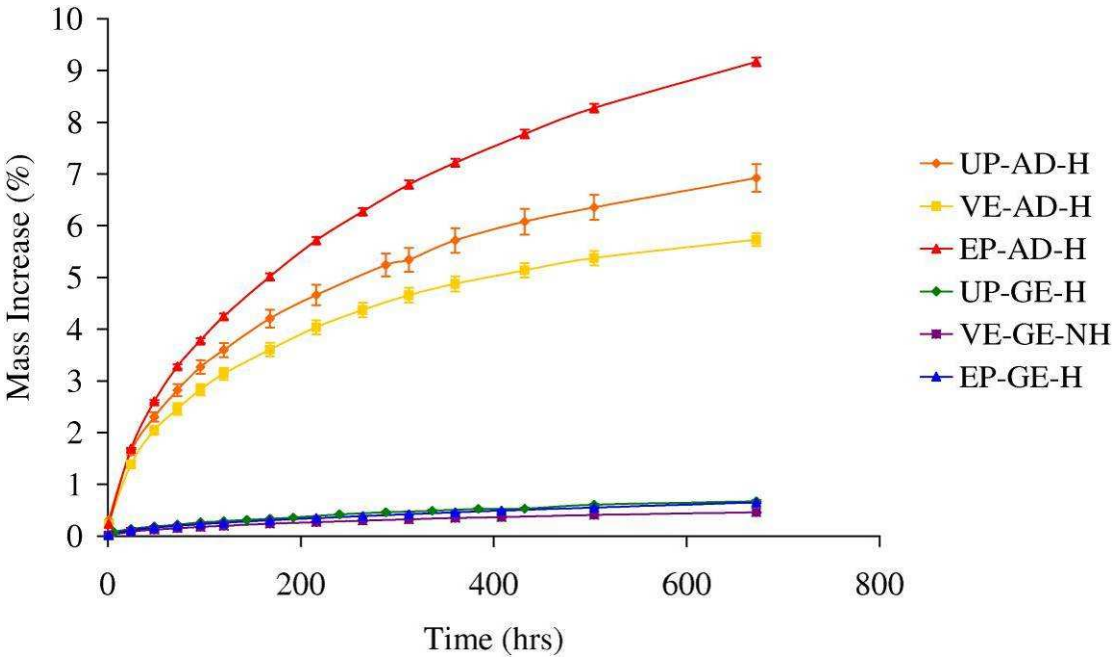

Figure F.15 Effect of resin system on mass increase over four weeks of water absorption at 22.5 % fibre volume fraction

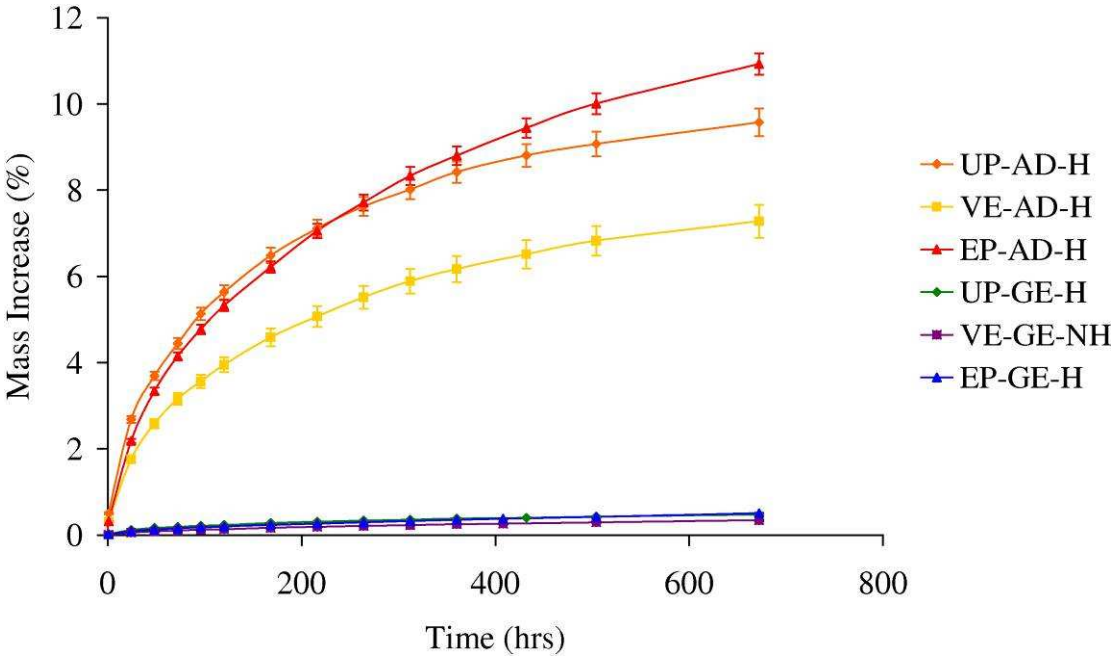

Figure F.16 Effect of resin system on mass increase over four weeks of water absorption at 30 % fibre volume fraction

Thickness change

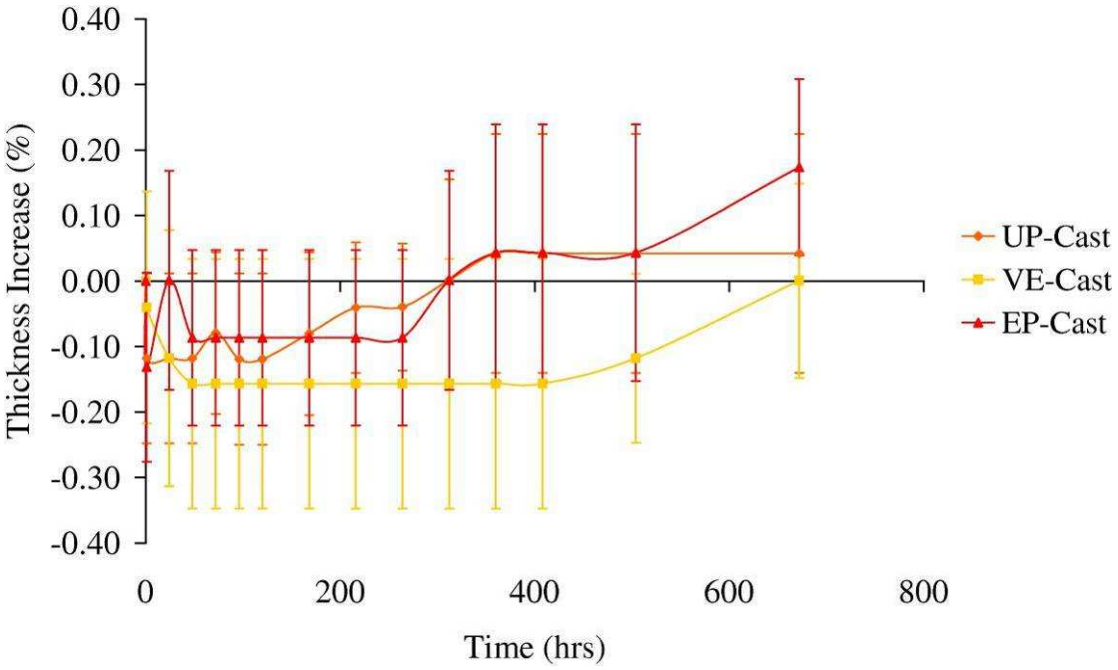

Figure F.17 Effect of resin system on thickness increase over four weeks of water absorption at 0 % fibre volume fraction

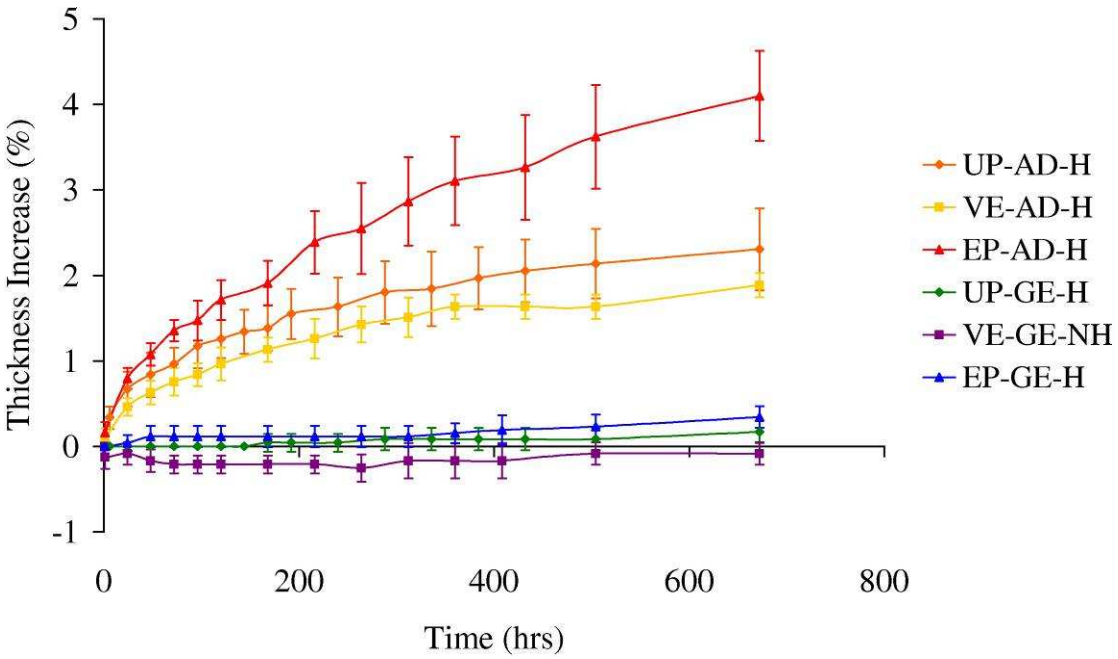

Figure F.18 Effect of resin system on thickness increase over four weeks of water absorption at 15 % fibre volume fraction

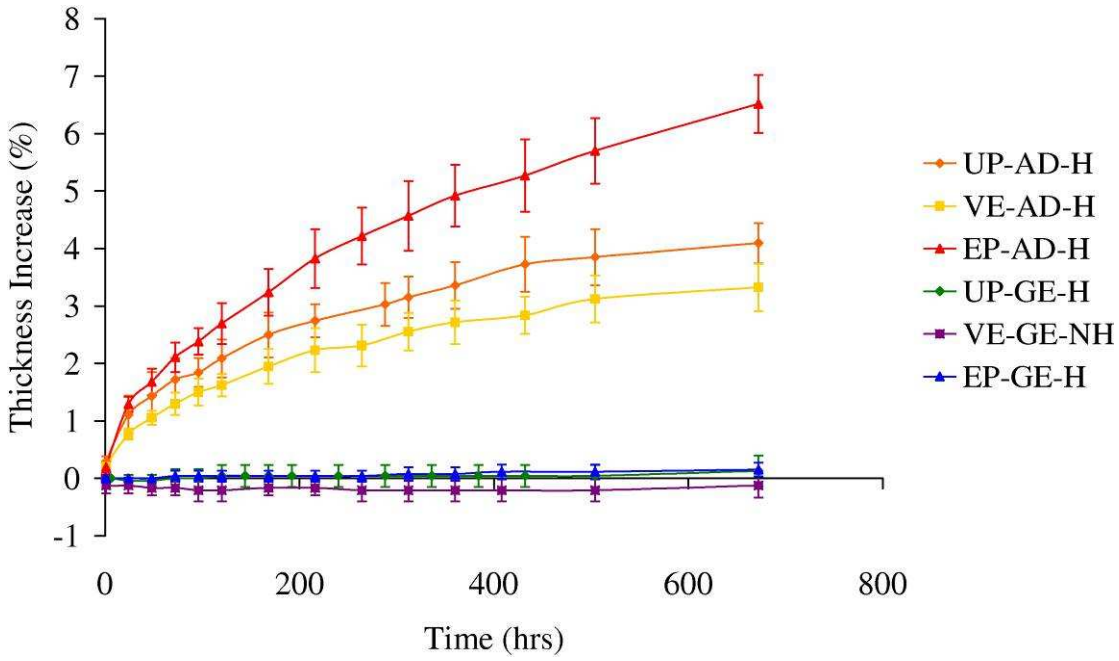

Figure F.19 Effect of resin system on thickness increase over four weeks of water absorption at 22.5 % fibre volume fraction

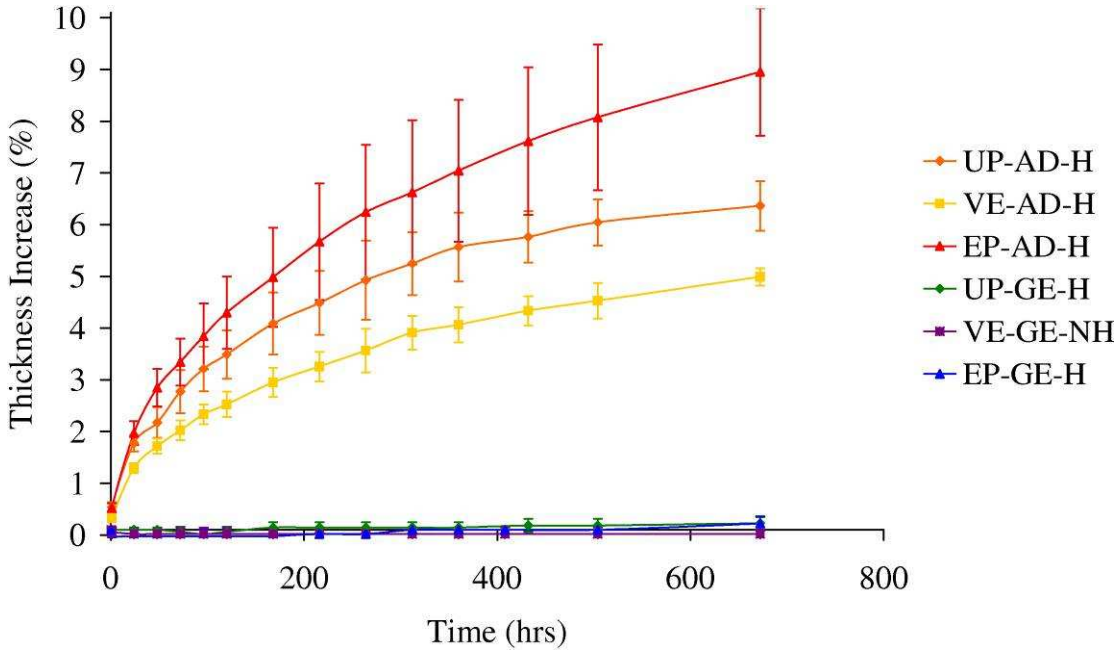

Figure F.20 Effect of resin system on thickness increase over four weeks of water absorption at 30 % fibre volume fraction

Length change

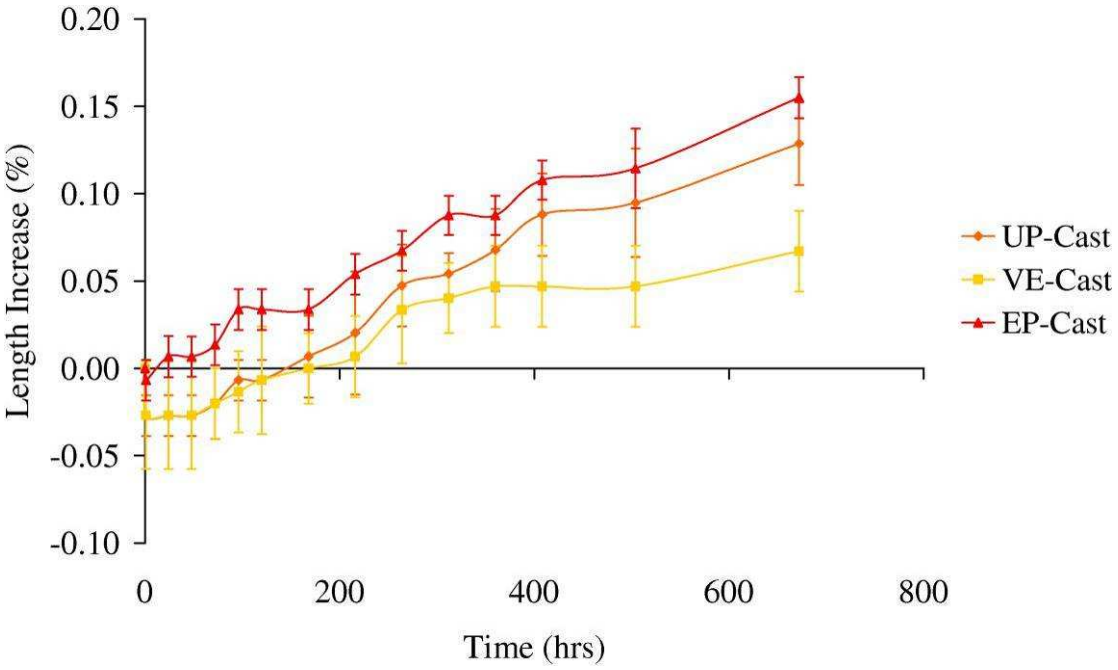

Figure F.21 Effect of resin system on length increase over four weeks of water absorption at 0 % fibre volume fraction

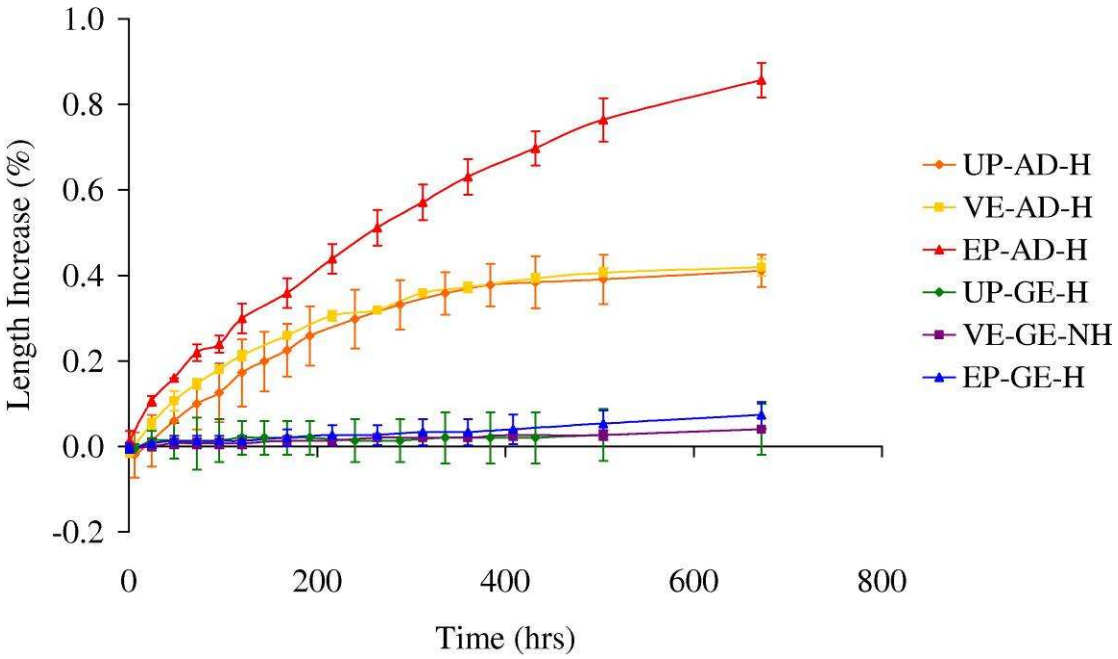

Figure F.22 Effect of resin system on length increase over four weeks of water absorption at 15 % fibre volume fraction

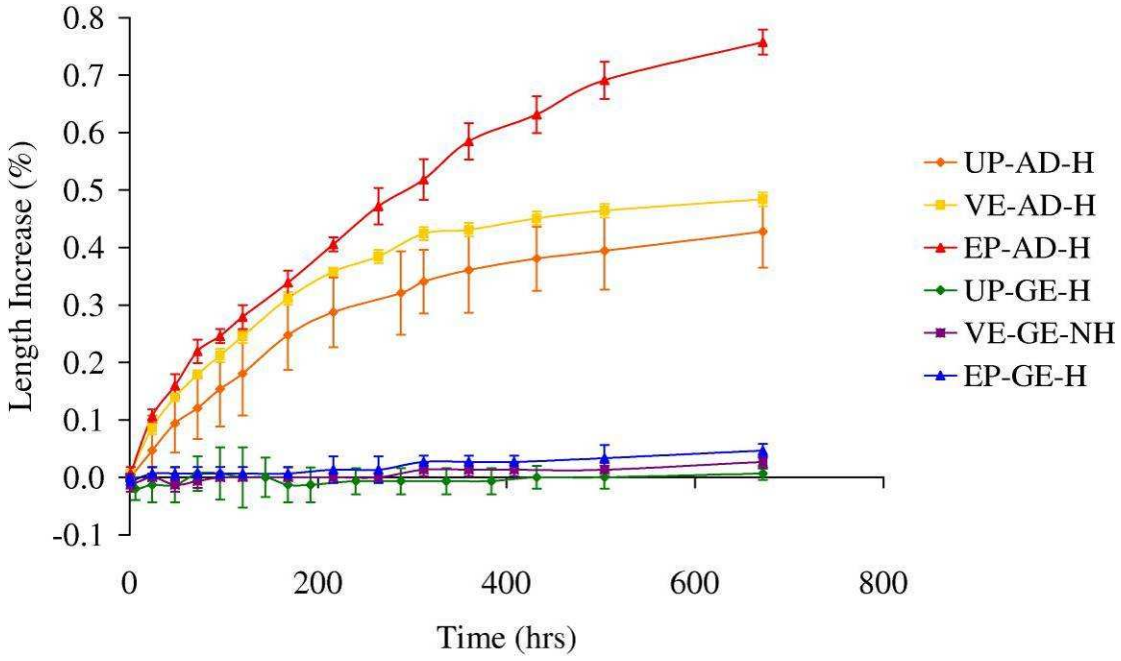

Figure F.23 Effect of resin system on length increase over four weeks of water absorption at 22.5 % fibre volume fraction

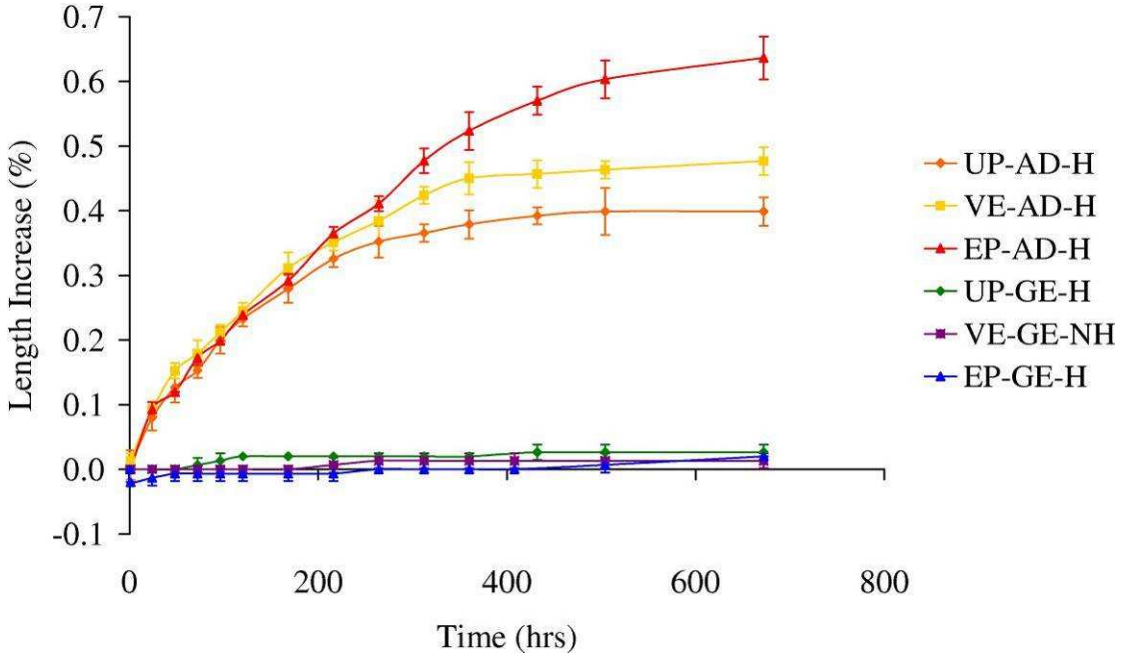

Figure F.24 Effect of resin system on length increase over four weeks of water absorption at 30 % fibre volume fraction

Width change

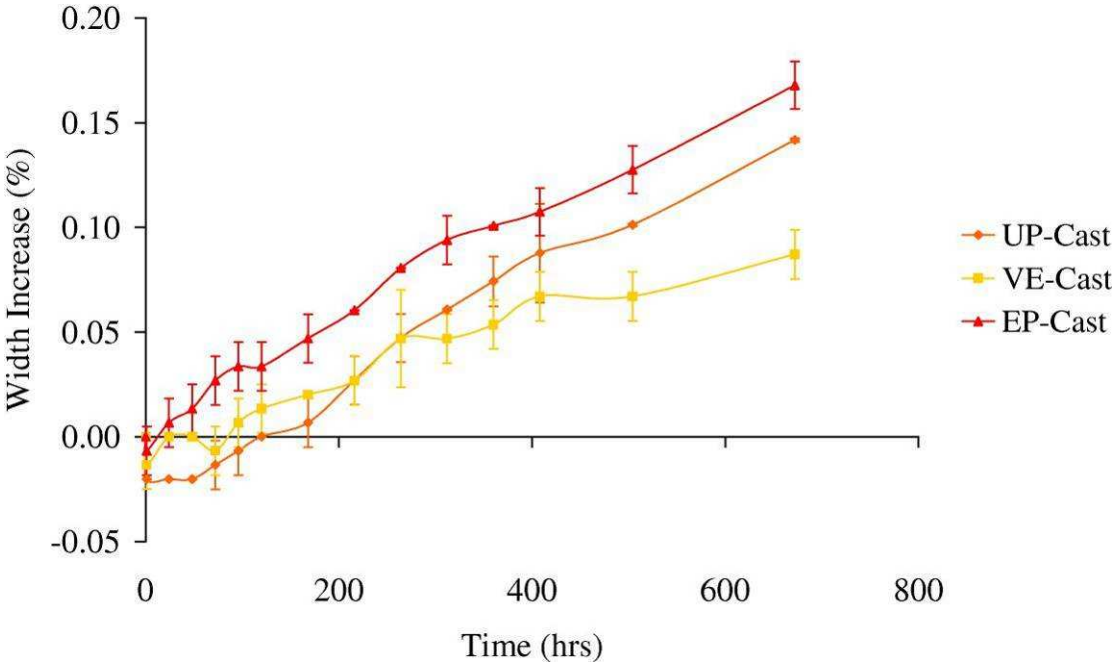

Figure F.25 Effect of resin system on width increase over four weeks of water absorption at 0 % fibre volume fraction

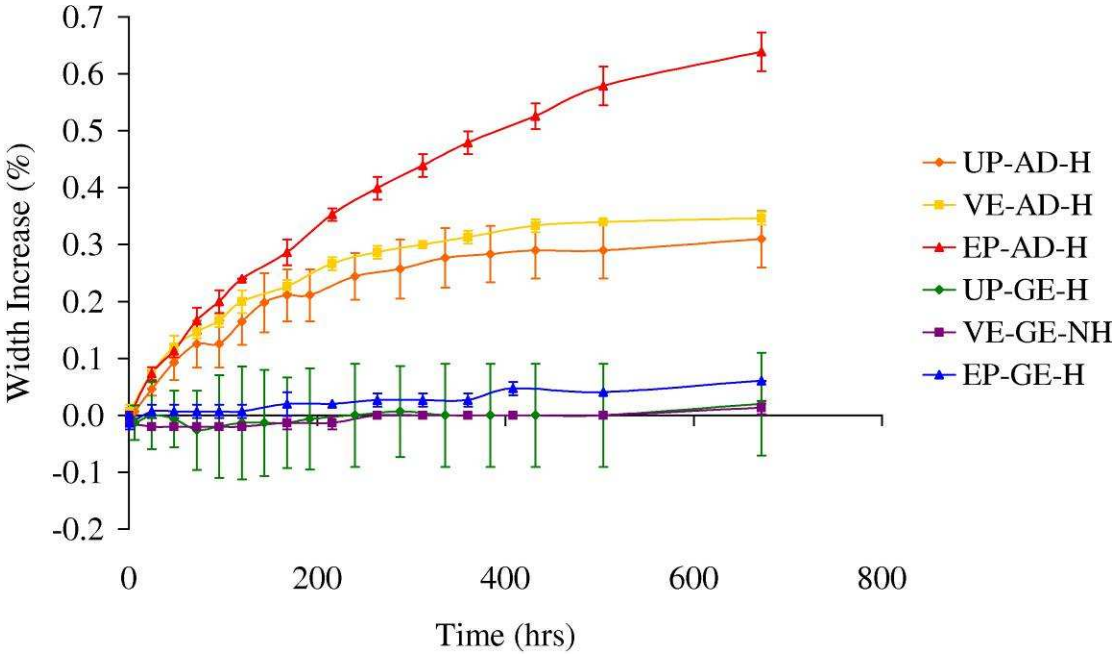

Figure F.26 Effect of resin system on width increase over four weeks of water absorption at 15 % fibre volume fraction

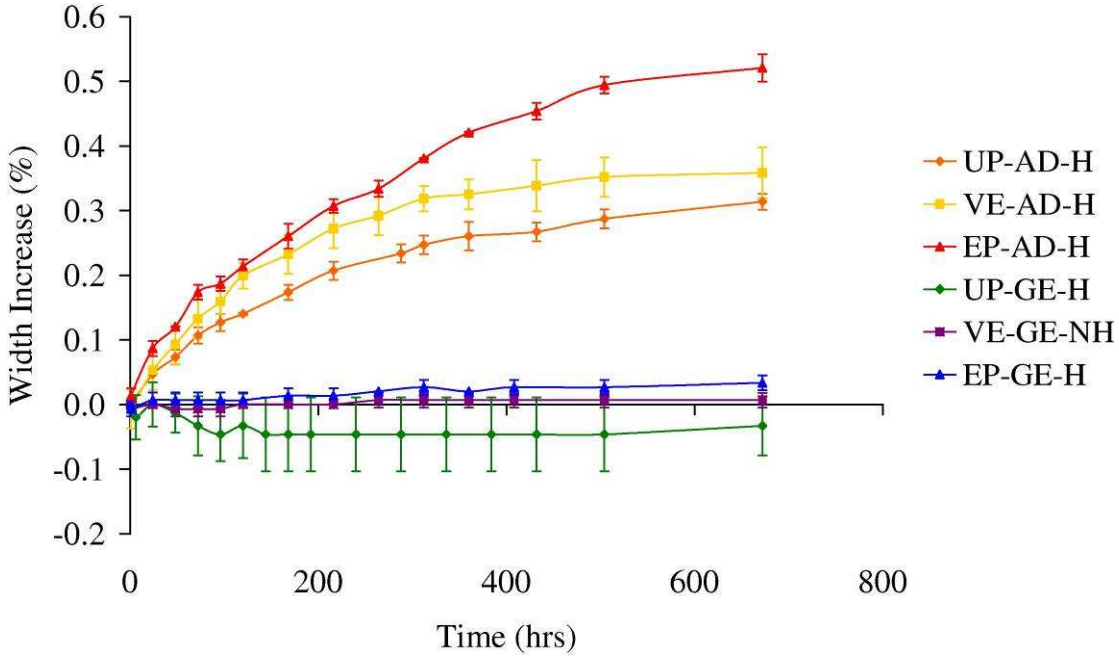

Figure F.27 Effect of resin system on width increase over four weeks of water absorption at 22.5 % fibre volume fraction

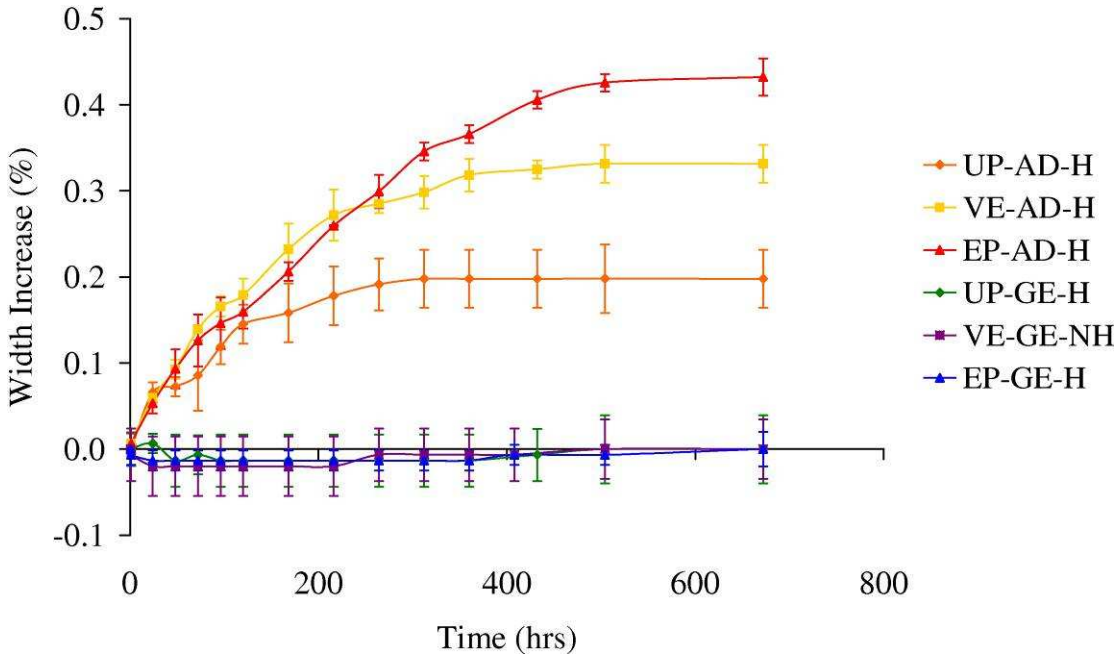

Figure F.28 Effect of resin system on width increase over four weeks of water absorption at 30 % fibre volume fraction

Appendix G Hygroexpansion of kenaf fibre reinforced composites

The following section details the theoretical modelling of hygroexpansion in kenaf fibre composites. The aim of this section is not to produce an absolute result but to determine approximate values of coefficients of hygroexpansion for the in-plane and through-thickness directions of composite specimens. This is done in order to explain the reduction in in-plane expansion with increasing fibre volume fraction experienced by the specimens during water absorption tests.

G1 Model

The model used to predict the behaviour of a composite with randomly orientated fibres exposed to moisture is that derived by Almgren *et al.* [34]. These authors used it to back calculate the coefficients of hygroexpansion for wood fibres by experimentally determining the coefficients of hygroexpansion of composite plates made from wood fibres and polylactic acid (PLA) matrix.

In order to predict the coefficients of hygroexpansion for a composite, a micromechanical model is first applied to a unidirectional ply of fibres and matrix to determine the longitudinal and transverse elastic moduli, Poisson's ratios and coefficients of hygroexpansion. Classical lamination theory [40] is then used to determine the coefficients for a composite with randomly orientated fibres. The micromechanical model used by Almgren *et al.* [34] is "Hashin's model" [41] for an assembly of concentric cylinders and it has also been applied in this analysis.

In the following, the subscripts *f* and *m* indicate fibre and matrix respectively and the subscripts *L* and *T* indicate the longitudinal and transverse directions respectively.

The axial Young's modulus of a unidirectional ply is given by:

$$E_L = V_f E_{fL} + V_m E_m + 2\lambda_1 \left(\nu_m - \nu_{fL}\right)^2 V_f V_m \tag{G.1}$$

where V_f and V_m are the volume fractions of fibres and matrix respectively, E_{fL} is the longitudinal Young's modulus of the fibres, E_m is the Young's modulus of the matrix, ν_{fL} is the major Poisson's ratio of the fibres and ν_m is the Poisson's ratio of the matrix. The coefficient λ_1 is given by:

$$\lambda_1 = \frac{2}{\left(\frac{1}{G_m} + \frac{V_f}{k_m} + \frac{V_m}{k_{fT}}\right)} \tag{G.2}$$

where G_m is the shear modulus of the matrix and k_m and k_{fT} are the bulk modulus of the matrix and transverse bulk modulus of the fibres respectively. These can be calculated using the following:

$$G_m = \frac{E_m}{2\left(1+\nu_m\right)} \tag{G.3}$$

$$k_m = \frac{E_m}{2\left(1-\nu_m - 2\nu_m^{\,2}\right)} \tag{G.4}$$

$$k_{fT} = \frac{E_{fL} E_{fT}}{2E_{fL}\left(1-\nu_{fT}\right) - 4\nu_{fL}^{\,2} E_{fT}} \tag{G.5}$$

where E_{fT} is the transverse Young's modulus of the fibres and ν_{fT} is the Poisson's ratio of the fibres in the transverse direction.

The major Poisson's ratio of a unidirectional ply is given by:

$$\nu_{LT} = V_f \nu_{fL} + V_m \nu_m + \frac{\lambda_1}{2}\left(\nu_m - \nu_{fL}\right)\left(\frac{1}{k_{fT}} - \frac{1}{k_{mT}}\right) V_f V_m \tag{G.6}$$

The transverse elastic modulus of a unidirectional ply is given by:

$$E_T = \frac{4G_T}{1+\frac{\lambda_2 G_T}{k_T}} \tag{G.7}$$

where,

$$\lambda_2 = 1+\frac{4k_T {v_{LT}}^2}{E_L} \tag{G.8}$$

and k_T is the transverse bulk modulus of a unidirectional ply, given by:

$$k_T = \frac{k_m\left(k_{fT}+G_m\right)V_m + k_{fT}\left(k_m+G_m\right)V_f}{\left(k_{fT}+G_m\right)V_m + \left(k_m+G_m\right)V_f} \tag{G.9}$$

The effective Poisson's ratio in the transverse plane of a unidirectional ply is given by:

$$v_{TT} = \frac{k_T-\lambda_2 G_T}{k_T+\lambda_2 G_T} \tag{G.10}$$

G_T is the lower bound of shear modulus in the transverse plane and is given by:

$$G_T = G_m + \frac{V_f}{\frac{1}{E_{fT}/2\left(1+v_{fT}\right)-G_m}+\frac{k_m+2G_m}{2G_m\left(k_m+G_m\right)}V_m} \tag{G.11}$$

Using the values obtained from equations G.1, G.6, G.7 and G.10, the coefficients of hygroexpansion for a unidirectional ply can be determined using the following:

$$\beta_L = \frac{V_f E_{fL} \beta_{fL} + V_m E_m \beta_m + 2\lambda_1 V_f V_m (\nu_m - \nu_{fL})((1+\nu_m)\beta_m - \beta_{fT} - \nu_{fL}\beta_{fL})}{E_L} \tag{G.12}$$

$$\beta_T = (\beta_{fT} + \nu_{fL})V_f + \beta_m(1+\nu_m)V_m + \frac{\lambda_1 V_f V_m((1+\nu_m)\beta_m - \beta_{fT} - \nu_{fT}\beta_{fL})}{2} \times \left(\frac{1}{k_{fT}} - \frac{1}{k_m}\right) - \nu_{LT}\beta_L \tag{G.13}$$

where, β_L and β_T are the longitudinal and transverse coefficients of hygroexpansion of the ply, β_{fL} and β_{fT} are the longitudinal and transverse coefficients of hygroexpansion of the fibres and β_m is the coefficient of hygroexpansion of the matrix. Nairn [29] gives approximate equations for determining β_L and β_T:

$$\beta_L = \frac{V_f E_{fL} \beta_{fL} + V_m E_m \beta_m}{V_f E_{fL} + V_m E_m} \tag{G.14}$$

$$\beta_T = \beta_m(1+\nu_m)V_m + \beta_{fL}(1+\nu_{fL})V_f - \beta_L(\nu_m V_m + \nu_f V_f) \tag{G.15}$$

Equations G.14 and G.15 were used as a check for G.12 and G.13.

Using classical lamination theory, it is possible to derive the hygroexpansion coefficients for a randomly oriented fibre reinforced composite. This derivation can be found in Almgren *et al.* [34]. The equations for calculating the hygroexpansion coefficients are:

$$\beta_{i-p} = \frac{E_L\beta_L + E_T\beta_T + \nu_{LT}E_T(\beta_L + \beta_T)}{E_L + E_T + 2\nu_{LT}E_T} \tag{G.16}$$

$$\beta_{tt} = \beta_T + \left(\frac{\nu_{TT}}{E_T} - \frac{\nu_{LT}}{E_L} \right) \frac{E_L E_T (\beta_T - \beta_L)}{E_L + E_T + 2\nu_{LT} E_T} \qquad \text{(G.17)}$$

where, $\beta_{i\text{-}p}$ and β_{tt} are the in-plane and through-thickness coefficients of hygroexpansion respectively.

G2 Data

Cichocki and Thomason [42] determined comprehensive mechanical properties of jute fibres and this is the only work found that contains this information for any natural fibre. They showed that the jute fibres have a longitudinal elastic modulus of 39.4 GPa which is similar to the 40 GPa [19] of kenaf fibres. The values determined by Cichocki and Thomason [42] for jute fibres were therefore applied to kenaf fibres with the assumption that their other mechanical properties would also be similar. The Young's modulus used is for epoxy and the value was supplied by the manufacturer. The Poisson's ratio of the epoxy was taken from McCartney and Kelly [43]. Epoxy was chosen because the epoxy composites show the most pronounced occurrence of decreasing in-plane extension with increasing fibre volume fraction. Furthermore, epoxy was found to bond best to fibres and the model assumes a perfect fibre matrix bond. The values of mechanical properties used for the fibres and epoxy can be found in Table G.1.

Apart from mechanical properties, values for the coefficients of hygroexpansion of the fibres and matrix had to be estimated. No information could be found for any natural fibre and there is little information available for polymer matrices. Values for the transverse coefficient of hygroexpansion for wood fibres and the coefficient of hygroexpansion for PLA have subsequently been taken from Almgren *et al.* [34] and applied to kenaf fibres and epoxy resin. According to Almgren *et al.* [34], it has been suggested that the transverse and longitudinal values of hygroexpansion and stiffness of fibres are inversely related as shown in equation G.18. This equation was used to determine the longitudinal coefficient of hygroexpansion of the fibres. The values used for the hygroexpansion coefficients of the fibres and the matrix can be found in Table G.1.

$$\frac{\beta_{fT}}{\beta_{fL}} = \frac{E_{fL}}{E_{fT}} \tag{G.18}$$

Note: Coefficients of hygroexpansion are usually defined in terms of strain per unit percentage mass increase of water as in Herakovich [40] and Marklund and Varna [36]. Moisture content will however differ from constituent to constituent in composite materials due to their particular hydrophility for a given moisture condition. Almgren *et al.* [34] suggests that coefficients of hygroexpansion should thus be expressed in terms of strain per unit increase in relative humidity. The purpose of this section is merely to illustrate the behaviour of specimens when exposed to moisture and thus it is assumed that specimens exposed to a particular change in atmospheric humidity level behave in the same manner as specimens immersed in water, as is the case in this work. Coefficients of hygroexpansion expressed in this manner were thus used.

Table G.1 Mechanical properties and coefficients of hygroexpansion of kenaf fibres and epoxy resin

Property	Unit	Value
E_{fL}	MPa	40000 [19]
E_{fT}	MPa	5500 [42]
E_m	MPa	3470 [manufacturer]
ν_{fL}	-	0.11 [42]
ν_{fT}	-	0.01 [42]
ν_m	-	0.35 [43]
β_{fL}	ε/ΔRH	0.034 [34]
β_{fT}	ε/ΔRH	0.25 [34]
β_m	ε/ΔRH	0.0001 [34]

It shall be shown in the following section that these values can be applied with reasonable confidence in determining the coefficients of hygroexpansion of kenaf fibre reinforced epoxy composites by varying these values and examining the effects on the resultant coefficients of hygroexpansion.

G3 Results

Figure G.1 shows the coefficients of hygroexpansion for a kenaf fibre reinforced epoxy composite with varying fibre volume fraction obtained using the values presented in Table G.1. Fibre volume fraction ranges from 0 % to 40 % in the figure.

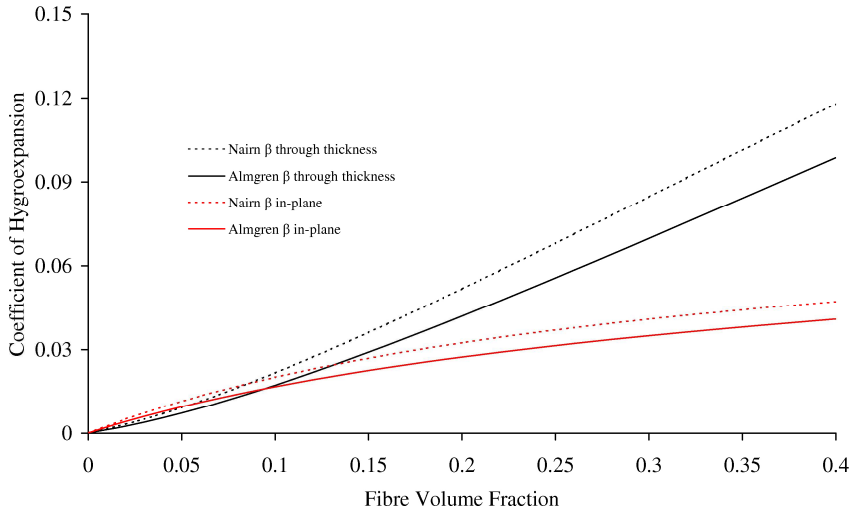

Figure G.1 Composite coefficients of hygroexpansion vs. fibre volume fraction

Because the values used in the model had to be estimated, the effects of varying the input parameters have been determined by plotting the curves of β_L and β_T against fibre volume fraction with an upper and lower bound of each estimated parameter. The central estimate used in each instance is equal to the values presented in Table G.1. E_{fT}, v_{fL}, v_{fT}, β_{fT} and β_m are varied. E_{fL}, E_m and v_m are not varied and β_{fL} has been changed in accordance with equation G.18 when β_{fT} is varied. The upper and lower bounds of E_{fT} were chosen to lie just over 25 % or 1500 GPa to each side of the central estimate. Almgren *et al.* [34] used values of v_{fL} and v_{fT} equal to 0.3 which have been set as the upper bounds for these two values and the lower bounds were then calculated by subtracting the difference between the upper bounds and central estimates from the central estimates. The upper and lower bounds for β_{fT} were taken from Almgren *et al.* [34]. The actual value of β_m is likely to be the value that differs most from that estimated and has therefore been varied by an order of magnitude for the lower and upper bound. The lower and upper bounds and central estimates for each variable parameter can be found in Table G.2.

Table G.2 Lower and upper bounds of variables

Property	Unit	Lower Bound	Central Estimate	Upper Bound
E_{fT}	MPa	4000	5500 [42]	7000
ν_{fL}	-	-0.08	0.11 [42]	0.3 [34]
ν_{fT}	-	-0.28	0.01 [42]	0.3 [34]
β_{fT}	ε/ΔRH	0.2 [34]	0.25 [34]	0.3 [34]
B_m	ε/ΔRH	0.001	0.0001 [34]	0.00001

Figure G.2 shows the resultant plots for each variable. Data was not plotted for the equations of Nairn [29] because equations G.14 and G.15 are only approximate and as described earlier were used as a check. The direction of the arrows in the figures indicates the direction of increasing value of the variable being altered.

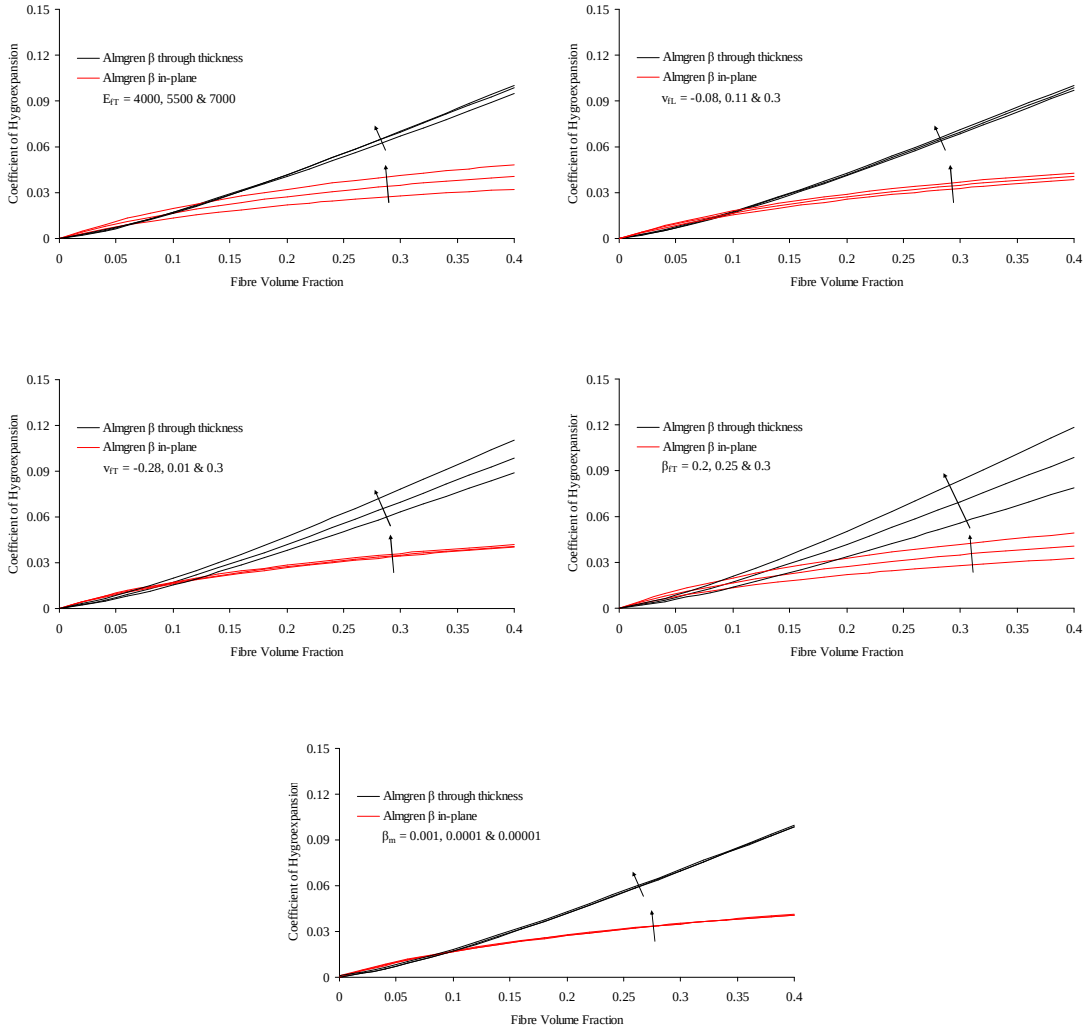

Figure G.2 Effect of varying input parameters on coefficients of hygroexpansion

G4 Correlation of theoretical and experimental results

Because the change in strain during hygroexpansion is equal to the coefficient of hygroexpansion multiplied by the unit change in relative humidity (equation G.19), the same trends observed for $\beta_{i\text{-}p}$ and β_{tt} will be observed for length and width and thickness respectively.

$$\Delta\varepsilon = \beta\Delta RH \qquad \text{(G.19)}$$

In order to compare the curves obtained in Figure G.1 to the length, width and thickness data collected experimentally, a spreadsheet was created to produce a least-squares fit of the experimental data to the theoretical data. Experimental data was divided by a variable and by using the solver function in Microsoft Excel, the variable was altered to achieve a least-squares fit. Dividing the data through by a variable is the equivalent of dividing equation G.19 by ΔRH to obtain a value of β except, the value of ΔRH is not known. As the aim of this investigation is to examine trends in hygroexpansion and not absolute values, the actual value of ΔRH is irrelevant. The results for kenaf composites made using epoxy resin can be seen in Figure G.3. In the figure, the experimental values of length and width have been combined as an average of the two.

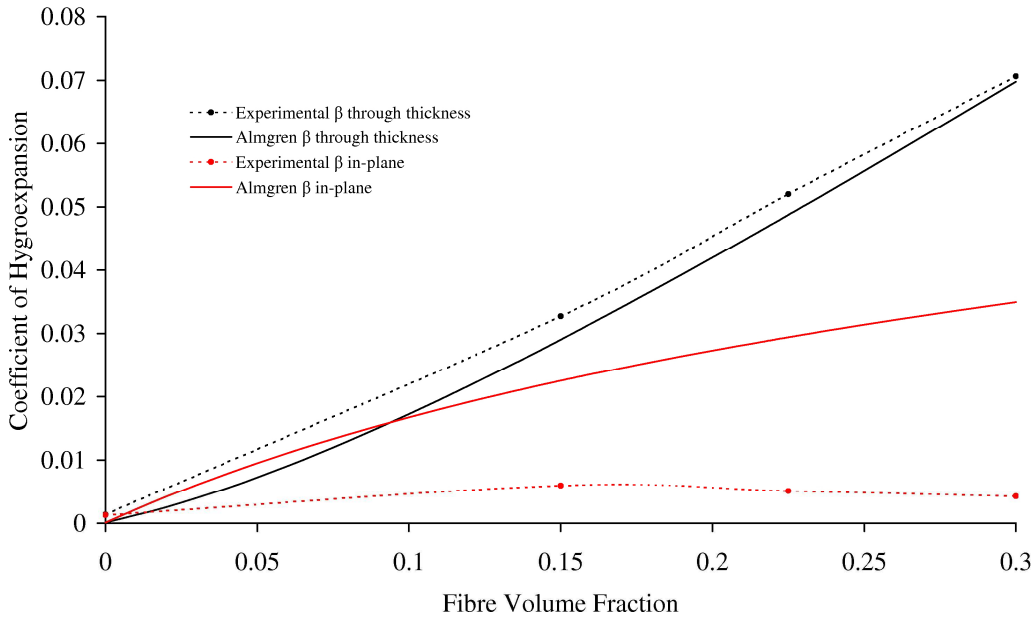

Figure G.3 Theoretical and experimental least-squares fit curves of hygroexpansion coefficients

It is clear from Figure G.3 that using the values presented in Table G.1 does not result in theoretical data that fits the experimental data very well. Values of β_{tt} need to be larger and values of $\beta_{i\text{-}p}$ need to be much smaller. Looking at Figure G.2, it is clear that varying E_{fT}, ν_{fL}, ν_{fT}, β_{fT} or β_m will not result in the required change. If however, the relationship given by equation G.18 is disregarded and the value of β_{fL} is reduced, the desired effect can be achieved. Marklund and Varna [36] found that the longitudinal coefficient of hygroexpansion in the S2 layer of a wood fibre can be negative. As was explained in section 1.3, the S2 layer of a natural fibre is primarily responsible for the mechanical properties of the fibre and this is also true for wood fibres [36]. Thus, it is plausible that the value of β_{fL} of a natural fibre can be negative. Figure G.4 shows the effect of varying β_{fL} on the resulting coefficients of hygroexpansion for a composite with randomly orientated fibres. In the figure, the upper bound is equal to the value presented in Table G.1 and the lower bound is equal to the negative of that value, the middle bound is equal to zero.

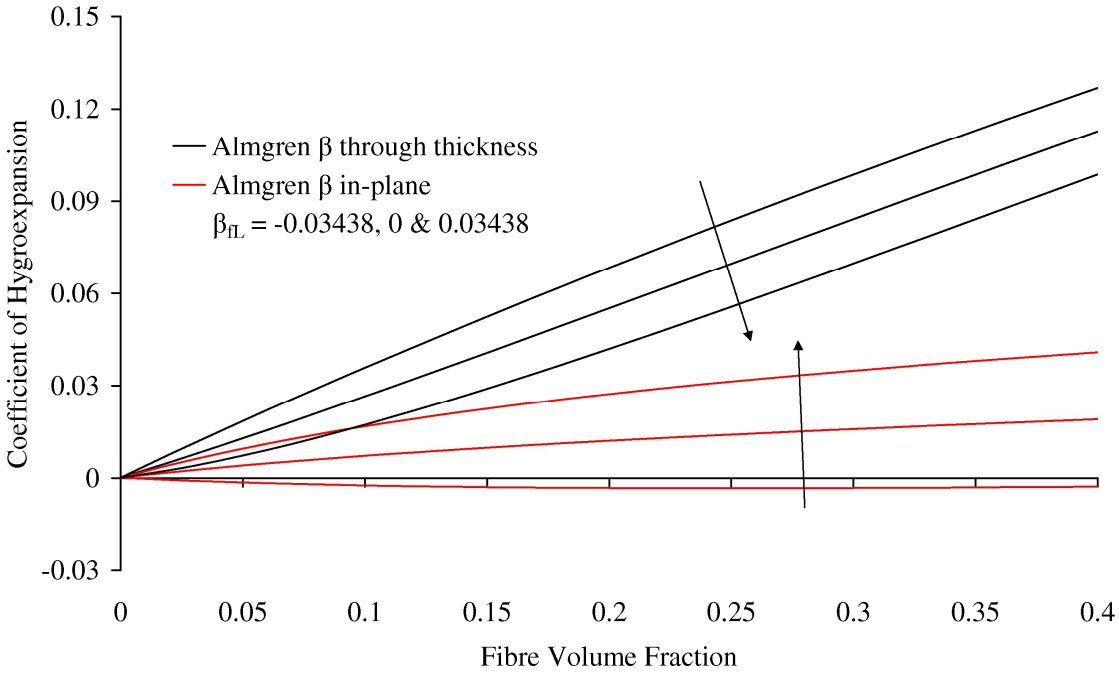

Figure G.4 Effect of varying β_{fL} on coefficients of hygroexpansion for a non-woven composite

Comparing Figure G.3 and Figure G.4, it can be seen that if β_{fL} is approximately equal to zero, the theoretical data would be a better match to the experimental data. It was found that making β_{fL} = -0.01 provides a good fit of the data. The result of making

β_{fL} = -0.01 and applying the same least-squares fit explained previously can be seen in Figure G.5.

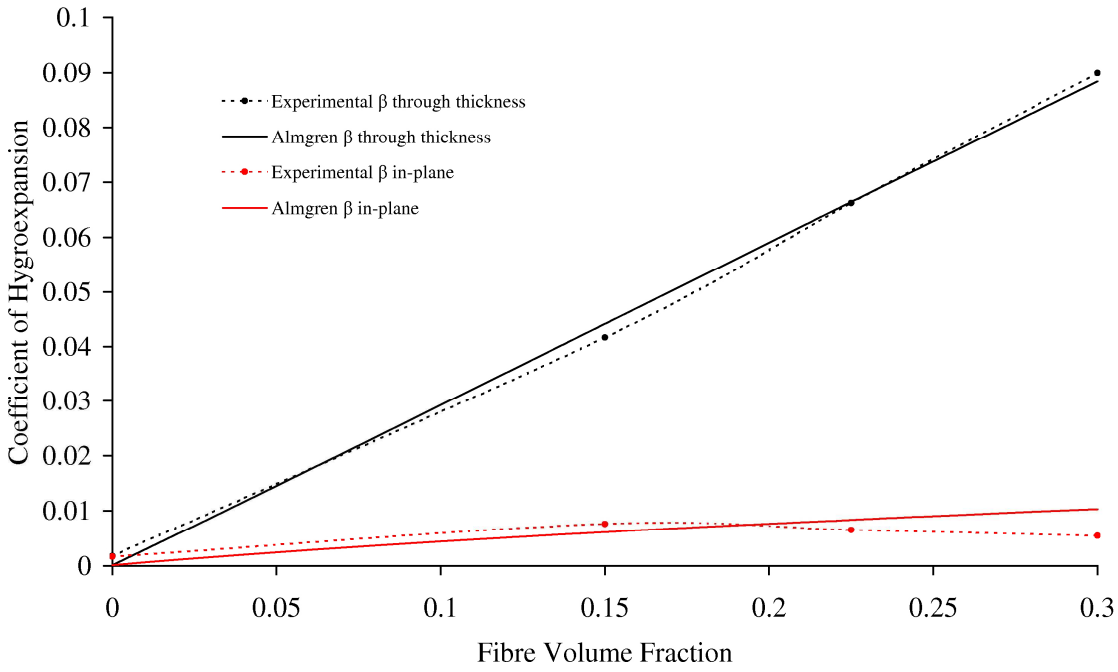

Figure G.5 Theoretical and experimental least-squares fit curves of hygroexpansion coefficients (β_{fL} = -0.01)

G5 Discussion of results

Looking at Figure G.5, it can be seen that the coefficient of through-thickness hygroexpansion predicted by the model increases approximately linearly with increasing fibre volume fraction. The predicted in-plane coefficient increases but at a decreasing rate with increasing fibre volume fraction. This suggests that the rate of in-plane dimensional increases could tend to zero or become negative at higher fibre volume fractions. It does not however explain why the experimental rate of in-plane swelling becomes negative at the fibre volume fractions investigated. Thus, there must be another mechanism causing this phenomenon. It is possible that as the fibre volume fraction is increased, the three-dimensional arrangement of the non-woven fibre mats is flattened into a more two-dimensional arrangement. Since the fibres swell more through their thickness than they do along their length, at low fibre volume fractions where the structure of the non-woven mat is three-dimensional, the radial swelling of the fibres during water absorption contributes more to the in-plane swelling of the composite specimens than at high fibre volume fractions where the

non-woven mat is more two-dimensional in structure. This hypothesis is supported by the experimental coefficient of hygroexpansion in the through-thickness plane which at a fibre volume fraction of around 15 % begins to increase at an increased rate. The flattening of the fibre arrangement causing a decrease in in-plane swelling conversely results in an increase in through-thickness swelling due to the increased in-plane alignment of the fibres.

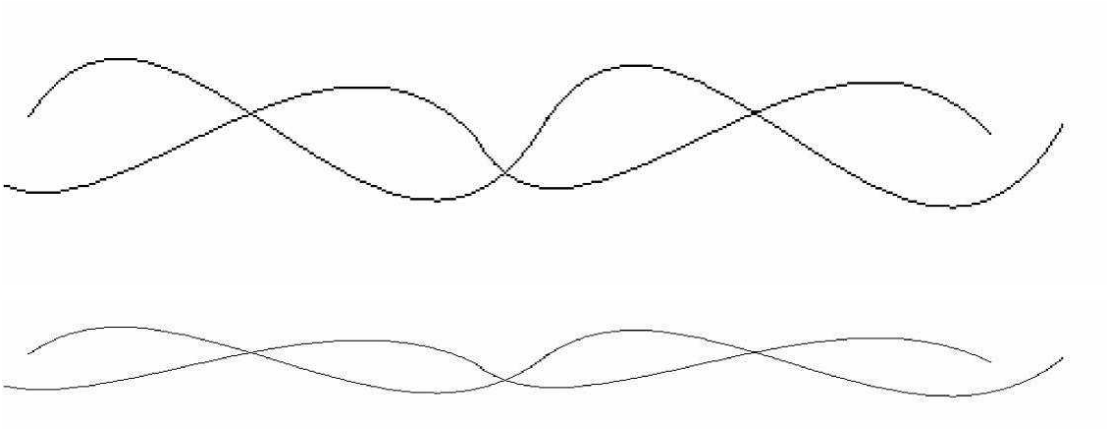

Figure G.6 Representation of two fibres in an uncompressed and a compressed non-woven fibre mat

A theoretical estimation of the swelling behaviour during water absorption of kenaf fibre reinforced epoxy composites has been implemented. It has been shown that reasonable estimates of fibre and matrix properties can be made. By altering the longitudinal coefficient of hygroexpansion of the kenaf fibres (Figure G.5), good agreement can be obtained between theoretical and experimental data for hygroexpansion coefficients of the composites in the through-thickness direction. In-plane coefficients of hygroexpansion of composites show reasonable agreement up to a fibre volume fraction of around 20 %. After 15 %, the experimental values begin to decrease while theoretical values continue to increase.

In conclusion, there is much scope for future work to be aimed at the determination of the exact mechanical and physical properties of kenaf fibres and the various matrices. Using this information, predictions of the behaviour of these composites when exposed to moisture could be made. There is also scope to extend the model to include the quasi three-dimensional arrangement of the fibres at low fibre volume fractions. One of the major drawbacks to natural fibre reinforced composites is their

poor dimensional stability. The use of a comprehensive model with accurate data would therefore be especially useful in the composite design phase when considering these types of materials.

Appendix H Results of mechanical testing

Table H.1 Tensile results for 15 % fibre volume fraction polyester composites

2UP-AD-H				
	Stress	Strain	Secant_Modulus	Linear_Modulus
	MPa	mm/mm	GPa	GPa
Specimen 1	28.4	0.00805	3.53	4.46
Specimen 2	25.2	0.00733	3.45	3.88
Specimen 3	26.7	0.00825	3.24	4.36
Specimen 4	25.3	0.00762	3.32	3.74
Specimen 5	27.2	0.00808	3.37	4.23
Specimen 6	30.9	0.00881	3.51	4.68
Average	27.3	0.00802	3.4	4.23
Std. Dev.	2.1	0.00051	0.11	0.36

2UP-AD-H-P				
	Stress	Strain	Secant_Modulus	Linear_Modulus
	MPa	mm/mm	GPa	GPa
Specimen 1	33.8	0.00895	3.78	4.86
Specimen 2	29.3	0.00766	3.82	4.54
Specimen 3	26.4	0.00669	3.95	4.73
Specimen 4	29.8	0.00757	3.94	4.47
Specimen 5	28.7	0.00765	3.75	4.43
Specimen 6	30.1	0.00835	3.6	4.76
Average	29.7	0.00781	3.81	4.63
Std. Dev.	2.4	0.00077	0.13	0.17

2UP-ND-NH				
	Stress	Strain	Secant_Modulus	Linear_Modulus
	MPa	mm/mm	GPa	GPa
Specimen 1	26.5	0.00789	3.36	4.27
Specimen 2	26.8	0.00812	3.29	4.13
Specimen 3	25	0.00648	3.86	4.79
Specimen 4	28.1	0.0081	3.47	4.46
Specimen 5	26.5	0.00952	2.79	4.51
Specimen 6	27.4	0.00783	3.5	4.55
Average	26.7	0.00799	3.38	4.45
Std. Dev.	1	0.00097	0.35	0.23

2UP-AD-NH				
	Stress	Strain	Secant_Modulus	Linear_Modulus
	MPa	mm/mm	GPa	GPa
Specimen 1	29.2	0.00757	3.85	4.99
Specimen 2	30.3	0.00843	3.59	4.6
Specimen 3	29.3	0.00788	3.72	4.72
Specimen 4	27.2	0.00699	3.88	4.99
Specimen 5	28.6	0.00797	3.59	4.56
Specimen 6	23.5	0.00615	3.82	4.82
Average	28	0.0075	3.74	4.78
Std. Dev.	2.4	0.00081	0.13	0.19

2UP-ND-H				
	Stress	Strain	Secant_Modulus	Linear_Modulus
	MPa	mm/mm	GPa	GPa
Specimen 1	28	0.00809	3.47	4.86
Specimen 2	26.5	0.00759	3.49	4.39
Specimen 3	26.3	0.00726	3.62	4.71
Specimen 4	28.7	0.00854	3.36	4.52
Specimen 5	28.8	0.00809	3.56	4.35
Specimen 6	27.5	0.00856	3.21	4.11
Average	27.6	0.00802	3.45	4.49
Std. Dev.	1.1	0.00052	0.15	0.27

2UP-GE-H				
	Stress	Strain	Secant_Modulus	Linear_Modulus
	MPa	mm/mm	GPa	GPa
Specimen 1	63.1	0.0202	3.12	4.37
Specimen 2	52	0.01822	2.86	3.91
Specimen 3	55.1	0.01988	2.77	4.03
Specimen 4	56.8	0.0206	2.76	4.02
Specimen 5	48.5	0.01124	4.32	4.55
Specimen 6	48.4	0.01666	2.91	4.16
Average	54	0.0178	3.12	4.17
Std. Dev.	5.6	0.00354	0.6	0.24

Table H.2 Tensile results for 22.5 % fibre volume fraction polyester composites

3UP-AD-H				
	Stress	Strain	Secant_Modulus	Linear_Modulus
	MPa	mm/mm	GPa	GPa
Specimen 1	42.6	0.01048	4.06	6.4
Specimen 2	44.8	0.01104	4.06	5.93
Specimen 3	41.9	0.01015	4.13	6.11
Specimen 4	36.6	0.00787	4.64	6.26
Specimen 5	45.3	0.0107	4.24	6.25
Specimen 6	40.4	0.00936	4.32	6.64
Average	41.9	0.00993	4.24	6.27
Std. Dev.	3.2	0.00116	0.22	0.24

3UP-AD-H-P				
	Stress	Strain	Secant_Modulus	Linear_Modulus
	MPa	mm/mm	GPa	GPa
Specimen 1	41.8	0.01101	3.79	5.75
Specimen 2	42.6	0.0105	4.06	6.51
Specimen 3	44.3	0.01014	4.37	6.95
Specimen 4	44.6	0.01073	4.16	6.96
Specimen 5	42.5	0.01017	4.18	6.06
Specimen 6	43.3	0.01073	4.03	6.11
Average	43.2	0.01054	4.1	6.39
Std. Dev.	1.1	0.00034	0.19	0.5

3UP-ND-NH				
	Stress	Strain	Secant_Modulus	Linear_Modulus
	MPa	mm/mm	GPa	GPa
Specimen 1	42.4	0.01197	3.54	6.73
Specimen 2	40	0.01141	3.51	5.68
Specimen 3	39.8	0.01127	3.53	5.54
Specimen 4	43.2	0.01184	3.65	6.99
Specimen 5	42.4	0.01233	3.44	6.2
Average	41.6	0.01176	3.53	6.23
Std. Dev.	1.6	0.00043	0.07	0.63

3UP-AD-NH				
	Stress	Strain	Secant_Modulus	Linear_Modulus
	MPa	mm/mm	GPa	GPa
Specimen 1	37.5	0.0102	3.67	4.87
Specimen 2	42.4	0.01189	3.57	5.45
Specimen 3	39.7	0.01074	3.69	4.99
Specimen 4	35.2	0.00996	3.53	4.61
Specimen 5	37.4	0.0104	3.6	4.69
Specimen 6	39.1	0.01237	3.16	5.33
Average	38.5	0.01093	3.54	4.99
Std. Dev.	2.5	0.00098	0.19	0.34

3UP-ND-H				
	Stress	Strain	Secant_Modulus	Linear_Modulus
	MPa	mm/mm	GPa	GPa
Specimen 1	44.4	0.01113	3.99	6.57
Specimen 2	38.9	0.00992	3.92	6.15
Specimen 3	39.8	0.00993	4.01	6.18
Specimen 4	42.2	0.01032	4.09	6.1
Specimen 5	42.8	0.01093	3.91	6.35
Specimen 6	41.9	0.01013	4.14	6.44
Average	41.7	0.01039	4.01	6.3
Std. Dev.	2	0.00052	0.09	0.19

3UP-GE-H				
	Stress	Strain	Secant_Modulus	Linear_Modulus
	MPa	mm/mm	GPa	GPa
Specimen 1	115.5	0.01703	6.78	6.9
Specimen 2	84.7	0.0138	6.13	6.33
Specimen 3	100.6	0.01711	5.88	5.99
Specimen 4	84.6	0.01606	5.27	5.64
Specimen 5	98.7	0.01888	5.23	5.68
Specimen 6	96.7	0.01637	5.91	6.14
Average	96.8	0.01654	5.87	6.11
Std. Dev.	11.5	0.00166	0.58	0.47

Table H.3 Tensile results for 30 % fibre volume fraction polyester composites

4UP-AD-H				
	Stress	Strain	Secant_Modulus	Linear_Modulus
	MPa	mm/mm	GPa	GPa
Specimen 1	48.7	0.01197	4.07	6.52
Specimen 2	52.8	0.01224	4.32	6.44
Specimen 3	52.3	0.01293	4.05	6.74
Specimen 4	54.1	0.01312	4.12	6.81
Specimen 5	51.2	0.01283	3.99	6.61
Average	51.8	0.01262	4.11	6.62
Std. Dev.	2	0.00049	0.12	0.16

4UP-AD-H-P				
	Stress	Strain	Secant_Modulus	Linear_Modulus
	MPa	mm/mm	GPa	GPa
Specimen 1	57.5	0.01307	4.4	6.9
Specimen 2	55.8	0.01364	4.09	6.81
Specimen 3	55.9	0.01671	3.34	6.97
Specimen 4	53.3	0.01299	4.1	6.53
Specimen 5	52.8	0.01351	3.91	6.36
Specimen 6	51.7	0.01276	4.05	6.93
Average	54.5	0.01378	3.98	6.75
Std. Dev.	2.2	0.00147	0.35	0.25

4UP-ND-NH				
	Stress	Strain	Secant_Modulus	Linear_Modulus
	MPa	mm/mm	GPa	GPa
Specimen 1	46.4	0.01214	3.82	6.62
Specimen 2	45	0.01075	4.19	6.25
Specimen 3	51	0.013	3.93	6.91
Specimen 4	44.6	0.01036	4.3	6.61
Specimen 5	46.8	0.01134	4.13	7.47
Specimen 6	46.4	0.01181	3.93	6.46
Average	46.7	0.01157	4.05	6.72
Std. Dev.	2.3	0.00096	0.19	0.43

4UP-AD-NH				
	Stress	Strain	Secant_Modulus	Linear_Modulus
	MPa	mm/mm	GPa	GPa
Specimen 1	46.6	0.01228	3.8	6.55
Specimen 2	49.5	0.01307	3.78	6.06
Specimen 3	50	0.01177	4.25	6.88
Specimen 4	46.7	0.012	3.89	6.03
Specimen 5	47.4	0.01126	4.2	6.32
Specimen 6	45.1	0.01133	3.98	6.07
Average	47.6	0.01195	3.99	6.32
Std. Dev.	1.9	0.00067	0.2	0.34

4UP-ND-H				
	Stress	Strain	Secant_Modulus	Linear_Modulus
	MPa	mm/mm	GPa	GPa
Specimen 1	52.2	0.01146	4.55	6.03
Specimen 2	51.4	0.01182	4.35	6.86
Specimen 3	50.7	0.0118	4.29	6.46
Specimen 4	50.5	0.0118	4.28	6.45
Specimen 5	43.3	0.00947	4.57	6.49
Average	49.6	0.01127	4.41	6.46
Std. Dev.	3.6	0.00102	0.14	0.29

4UP-GE-H				
	Stress	Strain	Secant_Modulus	Linear_Modulus
	MPa	mm/mm	GPa	GPa
Specimen 1	189.9	0.02024	9.38	9.98
Specimen 2	186.6	0.0197	9.47	9.97
Specimen 3	179.4	0.02012	8.92	9.43
Specimen 4	161.7	0.01732	9.34	10
Specimen 5	170.8	0.0182	9.39	9.9
Specimen 6	168.5	0.01835	9.18	9.61
Average	176.2	0.01899	9.28	9.82
Std. Dev.	11	0.0012	0.2	0.24

Table H.4 Tensile results for vinyl ester composites

2VE-AD-H				
	Stress	Strain	Secant_Modulus	Linear_Modulus
	MPa	mm/mm	GPa	GPa
Specimen 1	40.4	0.01203	3.36	4.29
Specimen 2	37.1	0.01034	3.59	4.36
Specimen 3	43.9	0.01348	3.25	4.62
Specimen 4	46.5	0.01427	3.26	4.43
Specimen 5	47.1	0.01356	3.47	4.54
Specimen 6	42.8	0.01277	3.35	4.37
Average	43	0.01274	3.38	4.43
Std. Dev.	3.8	0.0014	0.13	0.12

2VE-GE-NH				
	Stress	Strain	Secant_Modulus	Linear_Modulus
	MPa	mm/mm	GPa	GPa
Specimen 1	79	0.01608	4.91	5.32
Specimen 2	92.4	0.01923	4.8	5.18
Specimen 3	79.4	0.01468	5.41	5.83
Specimen 4	100	0.01778	5.62	6.22
Specimen 5	100.4	0.01631	6.15	6.69
Specimen 6	64.7	0.01279	5.05	5.61
Average	86	0.01615	5.33	5.81
Std. Dev.	14.1	0.00226	0.51	0.57

3VE-AD-H				
	Stress	Strain	Secant_Modulus	Linear_Modulus
	MPa	mm/mm	GPa	GPa
Specimen 1	53.5	0.01402	3.81	4.97
Specimen 2	53.2	0.01327	4.01	5.71
Specimen 3	57.6	0.0151	3.81	5.23
Specimen 4	43.8	0.01017	4.3	5.64
Specimen 5	56.6	0.01468	3.85	5.53
Specimen 6	54.1	0.01502	3.6	4.7
Average	53.1	0.01371	3.9	5.29
Std. Dev.	4.9	0.00187	0.24	0.4

3VE-GE-NH				
	Stress	Strain	Secant_Modulus	Linear_Modulus
	MPa	mm/mm	GPa	GPa
Specimen 1	148.8	0.01919	7.75	11.86
Specimen 2	176.3	0.02135	8.26	10.26
Specimen 3	151.3	0.01902	7.96	9.32
Specimen 4	139.9	0.01724	8.12	9.77
Specimen 5	171	0.02272	7.53	8.82
Specimen 6	124.7	0.01562	7.99	9.5
Average	152	0.01919	7.93	9.92
Std. Dev.	19.3	0.0026	0.26	1.06

4VE-AD-H				
	Stress	Strain	Secant_Modulus	Linear_Modulus
	MPa	mm/mm	GPa	GPa
Specimen 1	55.6	0.01304	4.26	5.77
Specimen 2	55.5	0.01404	3.95	6.41
Specimen 3	60.4	0.01508	4	5.38
Specimen 4	54.3	0.01297	4.18	4.91
Specimen 5	53.9	0.01217	4.42	6.71
Specimen 6	59.4	0.01489	3.99	4.41
Average	56.5	0.0137	4.14	5.6
Std. Dev.	2.7	0.00116	0.19	0.88

4VE-GE-NH				
	Stress	Strain	Secant_Modulus	Linear_Modulus
	MPa	mm/mm	GPa	GPa
Specimen 1	204	0.01948	10.47	11.83
Specimen 2	204.9	0.02263	9.06	10.75
Specimen 3	195.7	0.01922	10.18	11.14
Specimen 4	209.8	0.02491	8.42	11.03
Specimen 5	193	0.02147	8.99	9.42
Specimen 6	198.4	0.0238	8.34	8.87
Average	201	0.02192	9.24	10.51
Std. Dev.	6.3	0.0023	0.89	1.13

Table H.5 Tensile results for epoxy composites

2EP-AD-H				
	Stress	Strain	Secant_Modulus	Linear_Modulus
	MPa	mm/mm	GPa	GPa
Specimen 1	50.5	0.01719	2.94	3.25
Specimen 2	44.1	0.01342	3.29	3.42
Specimen 3	46.9	0.0139	3.38	3.31
Specimen 4	49	0.01537	3.19	3.32
Specimen 5	49.5	0.01912	2.59	3.19
Specimen 6	51.1	0.01747	2.93	3.18
Average	48.5	0.01608	3.05	3.28
Std. Dev.	2.6	0.00222	0.29	0.09

2EP-GE-NH				
	Stress	Strain	Secant_Modulus	Linear_Modulus
	MPa	mm/mm	GPa	GPa
Specimen 1	96.9	0.02417	4.01	4.93
Specimen 2	99.6	0.02176	4.58	4.97
Specimen 3	93	0.02015	4.62	5.05
Specimen 4	107.6	0.02263	4.75	5.16
Specimen 5	96.3	0.02331	4.13	4.54
Specimen 6	86.9	0.0197	4.41	5.05
Average	96.7	0.02195	4.42	4.95
Std. Dev.	6.9	0.00177	0.29	0.22

3EP-AD-H				
	Stress	Strain	Secant_Modulus	Linear_Modulus
	MPa	mm/mm	GPa	GPa
Specimen 1	49.8	0.01387	3.59	3.64
Specimen 2	52.6	0.01372	3.84	3.93
Specimen 3	49.2	0.01252	3.93	3.99
Specimen 4	55.3	0.01417	3.9	4.12
Specimen 5	47.6	0.0125	3.81	3.88
Specimen 6	58.2	0.01468	3.97	4.19
Average	52.1	0.01358	3.84	3.96
Std. Dev.	4	0.00089	0.13	0.2

3EP-GE-NH				
	Stress	Strain	Secant_Modulus	Linear_Modulus
	MPa	mm/mm	GPa	GPa
Specimen 1	178	0.0234	7.61	6.56
Specimen 2	162.2	0.0212	7.65	6.91
Specimen 3	162.3	0.0216	7.51	6.92
Specimen 4	150.8	0.02113	7.14	7.86
Specimen 5	153.8	0.02209	6.96	7.97
Specimen 6	160.4	0.026	6.17	6.88
Average	161.3	0.02257	7.17334991	7.183333333
Std. Dev.	9.4	0.001875	0.562691107	0.583323814

4EP-AD-H				
	Stress	Strain	Secant_Modulus	Linear_Modulus
	MPa	mm/mm	GPa	GPa
Specimen 1	62.7	0.01483	4.23	4.17
Specimen 2	61.8	0.01365	4.53	4.82
Specimen 3	65.5	0.01566	4.18	4.52
Specimen 4	67.9	0.01619	4.19	4.47
Specimen 5	61.8	0.01436	4.3	4.5
Specimen 6	66.4	0.01611	4.12	4.42
Average	64.3	0.01513	4.26	4.48
Std. Dev.	2.6	0.00102	0.15	0.21

4EP-GE-NH				
	Stress	Strain	Secant_Modulus	Linear_Modulus
	MPa	mm/mm	GPa	GPa
Specimen 1	218.8	0.02204	9.93	11.44
Specimen 2	181.8	0.01836	9.9	10.17
Specimen 3	211.9	0.0242	8.75	10.44
Specimen 4	190.5	0.02152	8.85	10.42
Specimen 5	201.3	0.02179	9.24	11.04
Specimen 6	226.1	0.02318	9.75	11.69
Average	205	0.02185	9.4	10.87
Std. Dev.	17	0.00198	0.53	0.62

Table H.6 Flexural results for 15 % fibre volume fraction polyester composites

2UP-AD-H				
	Stress	Strain	Secant_Modulus	Linear_Modulus
	MPa	mm/mm	GPa	GPa
Specimen 1	62.3	0.01679	3.71	4.06
Specimen 2	55.5	0.01647	3.37	3.81
Specimen 3	59.9	0.01905	3.14	3.82
Specimen 4	59.2	0.01648	3.59	3.87
Specimen 5	60.7	0.01869	3.25	3.73
Specimen 6	57.9	0.01673	3.46	3.7
Average	59.2	0.01737	3.42	3.83
Std. Dev.	2.4	0.00117	0.21	0.13

2UP-AD-H-P				
	Stress	Strain	Secant_Modulus	Linear_Modulus
	MPa	mm/mm	GPa	GPa
Specimen 1	79.5	0.0217	3.66	4.27
Specimen 2	81.1	0.02169	3.74	4.24
Specimen 3	73	0.01956	3.73	4.25
Specimen 4	73.6	0.01925	3.82	4.26
Specimen 5	71.4	0.0196	3.64	4.22
Specimen 6	72.8	0.01976	3.68	4.11
Average	75.2	0.02026	3.71	4.23
Std. Dev.	4	0.00113	0.07	0.06

2UP-ND-NH				
	Stress	Strain	Secant_Modulus	Linear_Modulus
	MPa	mm/mm	GPa	GPa
Specimen 1	61.1	0.0183	3.34	3.87
Specimen 2	63.2	0.01887	3.35	3.83
Specimen 3	65.5	0.01951	3.36	3.99
Specimen 4	61.1	0.01742	3.51	3.95
Specimen 5	58.9	0.01773	3.32	3.87
Specimen 6	59.5	0.01817	3.27	3.92
Average	61.5	0.01833	3.36	3.9
Std. Dev.	2.4	0.00076	0.08	0.06

2UP-AD-NH				
	Stress	Strain	Secant_Modulus	Linear_Modulus
	MPa	mm/mm	GPa	GPa
Specimen 1	68.5	0.01985	3.45	4.04
Specimen 2	60.8	0.01648	3.69	4.08
Specimen 3	68.7	0.02009	3.42	4
Specimen 4	66.4	0.01854	3.58	4.08
Specimen 5	61.9	0.01739	3.56	4.04
Specimen 6	65.5	0.01686	3.88	4.13
Average	65.3	0.0182	3.6	4.06
Std. Dev.	3.3	0.00154	0.17	0.05

2UP-ND-H				
	Stress	Strain	Secant_Modulus	Linear_Modulus
	MPa	mm/mm	GPa	GPa
Specimen 1	61.5	0.01714	3.59	4
Specimen 2	60	0.01702	3.52	4.07
Specimen 3	56.8	0.01568	3.63	4.01
Specimen 4	60.3	0.01686	3.58	4.04
Specimen 5	59	0.01649	3.58	4.07
Specimen 6	61.3	0.01927	3.18	3.75
Average	59.8	0.01707	3.51	3.99
Std. Dev.	1.7	0.0012	0.16	0.12

2UP-GE-H				
	Stress	Strain	Secant_Modulus	Linear_Modulus
	MPa	mm/mm	GPa	GPa
Specimen 1	135.7	0.03588	3.78	5.4
Specimen 2	142.9	0.03804	3.76	5.11
Specimen 3	118.8	0.03096	3.84	4.97
Specimen 4	145.3	0.02967	4.9	5.78
Specimen 5	149.6	0.03118	4.8	5.88
Specimen 6	135.3	0.03147	4.3	5.67
Average	137.9	0.03287	4.23	5.47
Std. Dev.	10.9	0.0033	0.52	0.37

Table H.7 Flexural results for 22.5 % fibre volume fraction polyester composites

3UP-AD-H				
	Stress	Strain	Secant_Modulus	Linear_Modulus
	MPa	mm/mm	GPa	GPa
Specimen 1	83.5	0.02275	3.67	4.29
Specimen 2	82.8	0.02163	3.83	4.45
Specimen 3	86.5	0.02135	4.05	4.63
Specimen 4	79.8	0.02167	3.68	4.43
Specimen 5	90.3	0.02455	3.68	4.48
Specimen 6	85	0.02169	3.92	4.53
Average	84.7	0.02228	3.81	4.47
Std. Dev.	3.5	0.00122	0.16	0.11

3UP-AD-H-P				
	Stress	Strain	Secant_Modulus	Linear_Modulus
	MPa	mm/mm	GPa	GPa
Specimen 1	83.7	0.02443	3.43	4.2
Specimen 2	80.9	0.02276	3.56	4.45
Specimen 3	93.1	0.02451	3.8	4.54
Specimen 4	80.8	0.02002	4.03	4.53
Specimen 5	86.5	0.02217	3.9	4.57
Specimen 6	80.5	0.02196	3.67	4.31
Average	84.2	0.02264	3.73	4.43
Std. Dev.	4.9	0.00169	0.23	0.14

3UP-ND-NH				
	Stress	Strain	Secant_Modulus	Linear_Modulus
	MPa	mm/mm	GPa	GPa
Specimen 1	77.5	0.02292	3.38	4.09
Specimen 2	79.4	0.02305	3.45	4.13
Specimen 3	75.8	0.02124	3.57	4.26
Specimen 4	78.3	0.0212	3.69	4.37
Specimen 5	76.7	0.02045	3.75	4.43
Specimen 6	75.8	0.02048	3.7	4.38
Average	77.3	0.02156	3.59	4.28
Std. Dev.	1.4	0.00116	0.15	0.14

3UP-AD-NH				
	Stress	Strain	Secant_Modulus	Linear_Modulus
	MPa	mm/mm	GPa	GPa
Specimen 1	80.8	0.02093	3.86	4.4
Specimen 2	80.7	0.02131	3.79	4.43
Specimen 3	78.3	0.02112	3.71	4.35
Specimen 4	78.1	0.02199	3.55	4.31
Specimen 5	78.2	0.02169	3.6	4.22
Specimen 6	79.6	0.02273	3.5	4.29
Average	79.3	0.02163	3.67	4.33
Std. Dev.	1.3	0.00066	0.14	0.08

3UP-ND-H				
	Stress	Strain	Secant_Modulus	Linear_Modulus
	MPa	mm/mm	GPa	GPa
Specimen 1	90	0.02452	3.67	4.53
Specimen 2	85.6	0.02281	3.75	4.55
Specimen 3	88.3	0.02276	3.88	4.57
Specimen 4	87.1	0.02277	3.82	4.51
Specimen 5	82	0.02192	3.74	4.42
Specimen 6	82.6	0.02202	3.75	4.36
Average	85.9	0.0228	3.77	4.49
Std. Dev.	3.2	0.00093	0.07	0.08

3UP-GE-H				
	Stress	Strain	Secant_Modulus	Linear_Modulus
	MPa	mm/mm	GPa	GPa
Specimen 1	178.7	0.02936	6.09	6.73
Specimen 2	178	0.03141	5.67	6.37
Specimen 3	181.5	0.02978	6.1	6.9
Specimen 4	179	0.03125	5.73	6.26
Specimen 5	161.3	0.02924	5.51	6.13
Specimen 6	181.1	0.0317	5.71	6.35
Average	176.6	0.03046	5.8	6.46
Std. Dev.	7.6	0.00112	0.24	0.29

Table H.8 Flexural results for 30 % fibre volume fraction polyester composites

4UP-AD-H				
	Stress	Strain	Secant_Modulus	Linear_Modulus
	MPa	mm/mm	GPa	GPa
Specimen 1	99	0.0269	3.68	5.04
Specimen 2	98.3	0.02475	3.97	5.17
Specimen 3	96.5	0.02484	3.89	5.15
Specimen 4	100	0.02388	4.19	5.31
Specimen 5	103.6	0.02581	4.01	5.35
Specimen 6	93.4	0.02327	4.01	5.03
Average	98.5	0.02491	3.96	5.17
Std. Dev.	3.4	0.00131	0.17	0.13

4UP-AD-H-P				
	Stress	Strain	Secant_Modulus	Linear_Modulus
	MPa	mm/mm	GPa	GPa
Specimen 1	106.6	0.02666	4	5.39
Specimen 2	98	0.02238	4.38	5.6
Specimen 3	94.7	0.02267	4.18	5.29
Specimen 4	102.7	0.02403	4.27	5.44
Specimen 5	98.6	0.02317	4.26	5.38
Specimen 6	96.8	0.02337	4.14	5.37
Average	99.6	0.02371	4.2	5.41
Std. Dev.	4.3	0.00155	0.13	0.1

4UP-ND-NH				
	Stress	Strain	Secant_Modulus	Linear_Modulus
	MPa	mm/mm	GPa	GPa
Specimen 1	99.4	0.02564	3.88	5.12
Specimen 2	102.1	0.02538	4.02	5.29
Specimen 3	98.6	0.02584	3.82	5.06
Specimen 4	95.1	0.02553	3.73	4.93
Specimen 5	96.6	0.02434	3.97	5.24
Specimen 6	98.6	0.02482	3.97	5.18
Average	98.4	0.02526	3.9	5.14
Std. Dev.	2.4	0.00057	0.11	0.13

4UP-AD-NH				
	Stress	Strain	Secant_Modulus	Linear_Modulus
	MPa	mm/mm	GPa	GPa
Specimen 1	96.6	0.02397	4.03	5.12
Specimen 2	96.5	0.02273	4.25	5.2
Specimen 3	105.9	0.02635	4.02	5.31
Specimen 4	98.8	0.02234	4.42	5.39
Specimen 5	98.1	0.02347	4.18	5.24
Specimen 6	93.8	0.02226	4.21	5.29
Average	98.3	0.02352	4.18	5.26
Std. Dev.	4.1	0.00154	0.15	0.09

4UP-ND-H				
	Stress	Strain	Secant_Modulus	Linear_Modulus
	MPa	mm/mm	GPa	GPa
Specimen 1	108.4	0.02478	4.37	5.51
Specimen 2	95.6	0.02178	4.39	5.49
Specimen 3	98.9	0.0221	4.48	5.55
Specimen 4	94.7	0.02149	4.41	5.4
Specimen 5	96	0.02161	4.44	5.37
Specimen 6	102.8	0.02453	4.19	5.27
Average	99.4	0.02271	4.38	5.43
Std. Dev.	5.3	0.00152	0.1	0.1

4UP-GE-H				
	Stress	Strain	Secant_Modulus	Linear_Modulus
	MPa	mm/mm	GPa	GPa
Specimen 1	236.2	0.02782	8.49	9.66
Specimen 2	238.3	0.02861	8.33	9.48
Specimen 3	226.7	0.02944	7.7	9.38
Specimen 4	238.2	0.03134	7.6	9.18
Specimen 5	236.6	0.02974	7.96	9.12
Specimen 6	238.6	0.0315	7.57	8.88
Average	235.8	0.02974	7.94	9.28
Std. Dev.	4.6	0.00146	0.39	0.28

Table H.9 Flexural results for vinyl ester composites

2VE-AD-H				
	Stress	Strain	Secant_Modulus	Linear_Modulus
	MPa	mm/mm	GPa	GPa
Specimen 1	68.9	0.02495	2.76	3.11
Specimen 2	66.3	0.02286	2.9	3.39
Specimen 3	63	0.02184	2.88	3.24
Specimen 4	73.6	0.02602	2.83	3.25
Specimen 5	66.6	0.02254	2.96	3.34
Specimen 6	65.6	0.02279	2.88	3.33
Average	67.3	0.0235	2.87	3.28
Std. Dev.	3.6	0.00162	0.07	0.1

2VE-GE-NH				
	Stress	Strain	Secant_Modulus	Linear_Modulus
	MPa	mm/mm	GPa	GPa
Specimen 1	125.2	0.02712	4.62	4.86
Specimen 2	121.3	0.02518	4.82	5.17
Specimen 3	138.9	0.02818	4.93	5.34
Specimen 4	161.5	0.03097	5.21	5.57
Specimen 5	115.2	0.02488	4.63	4.85
Specimen 6	150.5	0.03117	4.83	5.29
Average	135.4	0.02792	4.84	5.18
Std. Dev.	18	0.00273	0.22	0.28

3VE-AD-H				
	Stress	Strain	Secant_Modulus	Linear_Modulus
	MPa	mm/mm	GPa	GPa
Specimen 1	76.9	0.02277	3.38	4.22
Specimen 2	80.7	0.02474	3.26	4.08
Specimen 3	80.7	0.02409	3.35	4.06
Specimen 4	80.5	0.02324	3.47	4.31
Specimen 5	80.6	0.02304	3.5	4.29
Specimen 6	80.2	0.02301	3.49	4.3
Average	79.9	0.02348	3.41	4.21
Std. Dev.	1.5	0.00077	0.09	0.11

3VE-GE-NH				
	Stress	Strain	Secant_Modulus	Linear_Modulus
	MPa	mm/mm	GPa	GPa
Specimen 1	219.4	0.03261	6.73	7.64
Specimen 2	215.3	0.03241	6.64	7.44
Specimen 3	210.6	0.031	6.79	7.39
Specimen 4	198	0.03046	6.5	7.05
Specimen 5	200.4	0.03027	6.62	7.19
Specimen 6	207.5	0.03326	6.24	6.9
Average	208.5	0.03167	6.59	7.27
Std. Dev.	8.3	0.00125	0.2	0.27

4VE-AD-H				
	Stress	Strain	Secant_Modulus	Linear_Modulus
	MPa	mm/mm	GPa	GPa
Specimen 1	86.6	0.02316	3.74	4.7
Specimen 2	84.4	0.02238	3.77	4.64
Specimen 3	85.1	0.02291	3.71	4.52
Specimen 4	85.3	0.02254	3.78	4.64
Specimen 5	83.6	0.02255	3.71	4.61
Specimen 6	87.2	0.02266	3.85	4.73
Average	85.4	0.0227	3.76	4.64
Std. Dev.	1.3	0.00029	0.05	0.07

4VE-GE-NH				
	Stress	Strain	Secant_Modulus	Linear_Modulus
	MPa	mm/mm	GPa	GPa
Specimen 1	254.9	0.0341	7.48	8.76
Specimen 2	251.2	0.0311	8.08	9.13
Specimen 3	275.4	0.03349	8.23	9.47
Specimen 4	264.8	0.03422	7.74	8.96
Specimen 5	260.4	0.03259	7.99	9.13
Specimen 6	267.6	0.03265	8.19	9.34
Average	262.4	0.03303	7.95	9.13
Std. Dev.	8.8	0.00117	0.29	0.26

Table H.10 Flexural results for epoxy composites

2EP-AD-H				
	Stress	Strain	Secant_Modulus	Linear_Modulus
	MPa	mm/mm	GPa	GPa
Specimen 1	70.7	0.02206	3.2	3.68
Specimen 2	76.8	0.02477	3.1	3.67
Specimen 3	69.9	0.02165	3.23	3.81
Specimen 4	75.5	0.02471	3.06	3.64
Specimen 5	76.9	0.02519	3.05	3.59
Specimen 6	78.5	0.02509	3.13	3.75
Average	74.7	0.02391	3.13	3.69
Std. Dev.	3.6	0.00161	0.07	0.08

2EP-GE-NH				
	Stress	Strain	Secant_Modulus	Linear_Modulus
	MPa	mm/mm	GPa	GPa
Specimen 1	166.7	0.03426	4.87	5.52
Specimen 2	179.2	0.03409	5.26	5.98
Specimen 3	139.9	0.02723	5.14	5.42
Specimen 4	162.9	0.03191	5.11	5.62
Specimen 5	169	0.03538	4.78	5.46
Specimen 6	169	0.03512	4.81	5.51
Average	164.5	0.033	4.99	5.59
Std. Dev.	13.2	0.00308	0.2	0.21

3EP-AD-H				
	Stress	Strain	Secant_Modulus	Linear_Modulus
	MPa	mm/mm	GPa	GPa
Specimen 1	85.4	0.02459	3.47	4.4
Specimen 2	80.2	0.02218	3.62	4.33
Specimen 3	83.4	0.02288	3.65	4.35
Specimen 4	91.5	0.02637	3.47	4.4
Specimen 5	82.3	0.02387	3.45	4.22
Specimen 6	86.8	0.02336	3.71	4.54
Average	85	0.02387	3.56	4.37
Std. Dev.	4	0.00147	0.11	0.1

3EP-GE-NH				
	Stress	Strain	Secant_Modulus	Linear_Modulus
	MPa	mm/mm	GPa	GPa
Specimen 1	207.6	0.03541	5.86	6.68
Specimen 2	203.9	0.03276	6.22	6.93
Specimen 3	200.3	0.03494	5.73	6.46
Specimen 4	205.4	0.03505	5.86	6.55
Specimen 5	198.5	0.03488	5.69	6.39
Specimen 6	202.9	0.03344	6.07	6.66
Average	203.1	0.03441	5.91	6.61
Std. Dev.	3.3	0.00106	0.2	0.19

4EP-AD-H				
	Stress	Strain	Secant_Modulus	Linear_Modulus
	MPa	mm/mm	GPa	GPa
Specimen 1	93	0.02373	3.92	5.2
Specimen 2	92.1	0.02421	3.8	4.9
Specimen 3	93.6	0.02458	3.81	4.8
Specimen 4	90.8	0.02333	3.89	4.91
Specimen 5	94.7	0.02347	4.04	4.98
Specimen 6	84.4	0.02089	4.04	4.83
Average	91.4	0.02337	3.92	4.94
Std. Dev.	3.7	0.0013	0.1	0.15

4EP-GE-NH				
	Stress	Strain	Secant_Modulus	Linear_Modulus
	MPa	mm/mm	GPa	GPa
Specimen 1	268.1	0.03231	8.3	9.34
Specimen 2	269.6	0.03257	8.28	9.21
Specimen 3	247.8	0.03217	7.7	8.52
Specimen 4	248.7	0.03193	7.79	8.75
Specimen 5	241	0.03381	7.13	8.29
Specimen 6	261.4	0.03315	7.88	9.06
Average	256.1	0.03266	7.85	8.86
Std. Dev.	11.9	0.0007	0.43	0.41

Table H.11 Impact results for 15 % fibre volume fraction polyester composites

2UP-AD-H							
	Ei	Ep	IS	Ei	Ep	IS	S_max
	J/cm^2	J/cm^2	J/cm^2	J/cm	J/cm	J/cm	MPa
Specimen 1	0.18	0.2	0.38	0.18	0.2	0.39	21.4
Specimen 2	0.18	0.14	0.32	0.18	0.15	0.33	21.5
Specimen 3	0.18	0.2	0.39	0.19	0.2	0.39	21.4
Specimen 4	0.18	0.16	0.34	0.18	0.16	0.35	21.6
Specimen 5	0.19	0.22	0.41	0.19	0.22	0.42	22.8
Specimen 6	0.19	0.11	0.3	0.19	0.11	0.3	22.9
Average	0.18	0.17	0.36	0.19	0.18	0.36	21.9
Std. Dev.	0.01	0.04	0.04	0.01	0.04	0.04	0.7

2UP-AD-NH							
	Ei	Ep	IS	Ei	Ep	IS	S_max
	J/cm^2	J/cm^2	J/cm^2	J/cm	J/cm	J/cm	MPa
Specimen 1	0.13	0.1	0.24	0.14	0.1	0.24	13.8
Specimen 2	0.15	0.14	0.29	0.15	0.14	0.3	16.8
Specimen 3	0.15	0.11	0.26	0.15	0.11	0.26	16.8
Specimen 4	0.15	0.1	0.25	0.15	0.1	0.26	16.8
Specimen 5	0.15	0.1	0.25	0.15	0.1	0.25	16.8
Specimen 6	0.15	0.09	0.25	0.16	0.09	0.25	16.9
Average	0.15	0.11	0.26	0.15	0.11	0.26	16.3
Std. Dev.	0.01	0.02	0.02	0.01	0.02	0.02	1.2

2UP-AD-P-H							
	Ei	Ep	IS	Ei	Ep	IS	S_max
	J/cm^2	J/cm^2	J/cm^2	J/cm	J/cm	J/cm	MPa
Specimen 1	0.18	0.22	0.4	0.18	0.22	0.4	21.5
Specimen 2	0.18	0.12	0.29	0.18	0.12	0.3	21.4
Specimen 3	0.18	0.14	0.31	0.18	0.14	0.32	21.4
Specimen 4	0.18	0.14	0.32	0.18	0.15	0.33	20.7
Specimen 5	0.18	0.14	0.32	0.18	0.14	0.32	20.8
Specimen 6	0.18	0.13	0.31	0.18	0.14	0.32	20.8
Average	0.18	0.15	0.33	0.18	0.15	0.33	21.1
Std. Dev.	0	0.04	0.04	0	0.04	0.04	0.3

2UP-ND-H							
	Ei	Ep	IS	Ei	Ep	IS	S_max
	J/cm^2	J/cm^2	J/cm^2	J/cm	J/cm	J/cm	MPa
Specimen 1	0.16	0.2	0.36	0.16	0.21	0.37	19.0
Specimen 2	0.18	0.2	0.38	0.18	0.21	0.39	21.4
Specimen 3	0.2	0.21	0.4	0.2	0.21	0.41	21.3
Specimen 4	0.18	0.16	0.34	0.18	0.16	0.34	21.3
Specimen 5	0.18	0.19	0.37	0.18	0.19	0.37	21.5
Specimen 6	0.2	0.24	0.43	0.2	0.24	0.44	23.4
Average	0.18	0.2	0.38	0.18	0.2	0.39	21.3
Std. Dev.	0.01	0.02	0.03	0.01	0.03	0.03	1.4

2UP-ND-NH							
	Ei	Ep	IS	Ei	Ep	IS	S_max
	J/cm^2	J/cm^2	J/cm^2	J/cm	J/cm	J/cm	MPa
Specimen 1	0.2	0.23	0.43	0.2	0.23	0.44	23.2
Specimen 2	0.21	0.22	0.43	0.21	0.22	0.44	22.6
Specimen 3	0.21	0.19	0.4	0.21	0.19	0.41	21.6
Specimen 4	0.21	0.15	0.37	0.21	0.16	0.37	21.7
Specimen 5	0.21	0.17	0.38	0.21	0.17	0.39	21.6
Specimen 6	0.21	0.19	0.41	0.21	0.2	0.41	21.7
Average	0.21	0.19	0.4	0.21	0.2	0.41	22.1
Std. Dev.	0	0.03	0.03	0	0.03	0.03	0.7

2UP-GE-H							
	Ei	Ep	IS	Ei	Ep	IS	S_max
	J/cm^2	J/cm^2	J/cm^2	J/cm	J/cm	J/cm	MPa
Specimen 1	1.62	1.55	3.16	1.64	1.57	3.21	104.8
Specimen 2	2.04	1.53	3.57	2.07	1.56	3.62	116.0
Specimen 3	2.04	1.32	3.36	2.07	1.34	3.41	116.0
Specimen 4	2.42	1.79	4.21	2.46	1.81	4.27	136.3
Specimen 5	2.42	1.08	3.5	2.46	1.1	3.56	136.3
Specimen 6	2.43	0.73	3.16	2.47	0.74	3.21	136.6
Average	2.16	1.33	3.49	2.19	1.35	3.55	124.3
Std. Dev.	0.33	0.38	0.39	0.33	0.38	0.39	13.8

Table H.12 Impact results for 22.5 % fibre volume fraction polyester composites

3UP-AD-H							
	Ei	Ep	IS	Ei	Ep	IS	S_max
	J/cm^2	J/cm^2	J/cm^2	J/cm	J/cm	J/cm	MPa
Specimen 1	0.26	0.3	0.55	0.26	0.3	0.56	28.9
Specimen 2	0.26	0.27	0.52	0.26	0.27	0.53	28.8
Specimen 3	0.26	0.34	0.6	0.26	0.35	0.61	32.4
Specimen 4	0.23	0.36	0.59	0.23	0.37	0.6	31.1
Specimen 5	0.26	0.31	0.57	0.26	0.32	0.58	31.4
Specimen 6	0.25	0.29	0.55	0.26	0.3	0.56	31.4
Average	0.25	0.31	0.56	0.26	0.32	0.57	30.7
Std. Dev.	0.01	0.03	0.03	0.01	0.03	0.03	1.5

3UP-AD-NH							
	Ei	Ep	IS	Ei	Ep	IS	S_max
	J/cm^2	J/cm^2	J/cm^2	J/cm	J/cm	J/cm	MPa
Specimen 1	0.24	0.37	0.62	0.25	0.38	0.63	32.0
Specimen 2	0.25	0.29	0.54	0.25	0.3	0.55	32.2
Specimen 3	0.25	0.3	0.55	0.25	0.31	0.56	32.2
Specimen 4	0.27	0.38	0.65	0.27	0.39	0.66	32.2
Specimen 5	0.27	0.29	0.56	0.27	0.3	0.57	32.4
Specimen 6	0.27	0.28	0.55	0.27	0.28	0.56	32.4
Average	0.26	0.32	0.58	0.26	0.32	0.59	32.2
Std. Dev.	0.01	0.05	0.05	0.01	0.05	0.05	0.1

3UP-AD-P-H							
	Ei	Ep	IS	Ei	Ep	IS	S_max
	J/cm^2	J/cm^2	J/cm^2	J/cm	J/cm	J/cm	MPa
Specimen 1	0.24	0.36	0.59	0.24	0.36	0.6	31.3
Specimen 2	0.24	0.3	0.54	0.24	0.3	0.54	31.6
Specimen 3	0.24	0.35	0.59	0.25	0.36	0.6	32.1
Specimen 4	0.25	0.35	0.6	0.25	0.36	0.61	32.5
Specimen 5	0.26	0.36	0.62	0.26	0.37	0.63	31.5
Specimen 6	0.26	0.3	0.56	0.26	0.3	0.57	31.6
Average	0.25	0.34	0.58	0.25	0.34	0.59	31.8
Std. Dev.	0.01	0.03	0.03	0.01	0.03	0.03	0.5

3UP-ND-H							
	Ei	Ep	IS	Ei	Ep	IS	S_max
	J/cm^2	J/cm^2	J/cm^2	J/cm	J/cm	J/cm	MPa
Specimen 1	0.21	0.45	0.66	0.21	0.46	0.67	25.0
Specimen 2	0.2	0.44	0.64	0.21	0.44	0.65	24.9
Specimen 3	0.21	0.45	0.66	0.21	0.46	0.67	24.9
Specimen 4	0.23	0.58	0.81	0.23	0.59	0.83	28.1
Specimen 5	0.23	0.47	0.7	0.24	0.48	0.72	28.1
Specimen 6	0.26	0.3	0.55	0.26	0.3	0.56	29.0
Average	0.22	0.45	0.67	0.23	0.46	0.68	26.7
Std. Dev.	0.02	0.09	0.09	0.02	0.09	0.09	1.9

3UP-ND-NH							
	Ei	Ep	IS	Ei	Ep	IS	S_max
	J/cm^2	J/cm^2	J/cm^2	J/cm	J/cm	J/cm	MPa
Specimen 1	0.28	0.43	0.72	0.29	0.44	0.73	31.3
Specimen 2	0.28	0.39	0.67	0.29	0.39	0.68	31.5
Specimen 3	0.28	0.31	0.59	0.29	0.31	0.6	31.6
Specimen 4	0.37	0.47	0.84	0.37	0.48	0.85	39.4
Specimen 5	0.38	0.48	0.86	0.38	0.49	0.87	40.2
Specimen 6	0.38	0.35	0.73	0.38	0.36	0.75	40.4
Average	0.33	0.41	0.73	0.33	0.41	0.75	35.7
Std. Dev.	0.05	0.07	0.1	0.05	0.07	0.1	4.7

3UP-GE-H							
	Ei	Ep	IS	Ei	Ep	IS	S_max
	J/cm^2	J/cm^2	J/cm^2	J/cm	J/cm	J/cm	MPa
Specimen 1	3.08	6.07	9.15	3.13	6.16	9.29	239.4
Specimen 2	3.2	5.59	8.79	3.25	5.68	8.93	240.3
Specimen 3	3.54	5.45	8.99	3.6	5.54	9.14	244.7
Specimen 4	3.53	5.43	8.96	3.59	5.52	9.1	244.1
Specimen 5	3.53	4.96	8.49	3.59	5.04	8.63	244.1
Specimen 6	3.08	5.78	8.87	3.13	5.88	9.01	245.8
Average	3.33	5.55	8.87	3.38	5.64	9.02	243.0
Std. Dev.	0.23	0.37	0.22	0.23	0.38	0.23	2.6

Table H.13 Impact results for 30 % fibre volume fraction polyester composites

4UP-AD-H	Ei	Ep	IS	Ei	Ep	IS	S_max
	J/cm^2	J/cm^2	J/cm^2	J/cm	J/cm	J/cm	MPa
Specimen 1	0.32	0.4	0.72	0.33	0.41	0.73	37.8
Specimen 2	0.32	0.3	0.62	0.33	0.3	0.63	38.1
Specimen 3	0.32	0.34	0.66	0.33	0.35	0.67	37.9
Specimen 4	0.33	0.43	0.76	0.33	0.44	0.77	37.9
Specimen 5	0.33	0.3	0.63	0.33	0.31	0.64	38.1
Specimen 6	0.33	0.31	0.63	0.33	0.31	0.64	38.3
Average	0.32	0.35	0.67	0.33	0.35	0.68	38.0
Std. Dev.	0	0.06	0.06	0	0.06	0.06	0.2

4UP-AD-NH	Ei	Ep	IS	Ei	Ep	IS	S_max
	J/cm^2	J/cm^2	J/cm^2	J/cm	J/cm	J/cm	MPa
Specimen 1	0.26	0.44	0.7	0.26	0.45	0.71	35.2
Specimen 2	0.29	0.4	0.69	0.29	0.41	0.7	35.4
Specimen 3	0.29	0.41	0.7	0.3	0.42	0.71	37.2
Specimen 4	0.29	0.4	0.69	0.3	0.41	0.71	37.5
Specimen 5	0.4	0.42	0.82	0.41	0.43	0.83	42.4
Specimen 6	0.35	0.44	0.78	0.35	0.44	0.8	39.3
Average	0.31	0.42	0.73	0.32	0.42	0.74	37.8
Std. Dev.	0.05	0.02	0.06	0.05	0.02	0.06	2.7

4UP-AD-P-H	Ei	Ep	IS	Ei	Ep	IS	S_max
	J/cm^2	J/cm^2	J/cm^2	J/cm	J/cm	J/cm	MPa
Specimen 1	0.32	0.4	0.72	0.33	0.4	0.73	37.5
Specimen 2	0.32	0.35	0.67	0.33	0.35	0.68	37.4
Specimen 3	0.33	0.4	0.73	0.34	0.4	0.74	38.1
Specimen 4	0.33	0.35	0.68	0.34	0.35	0.69	38.1
Specimen 5	0.38	0.41	0.79	0.38	0.42	0.8	41.1
Specimen 6	0.36	0.42	0.77	0.36	0.43	0.79	39.2
Average	0.34	0.39	0.73	0.35	0.39	0.74	38.6
Std. Dev.	0.02	0.03	0.05	0.02	0.03	0.05	1.4

4UP-ND-H	Ei	Ep	IS	Ei	Ep	IS	S_max
	J/cm^2	J/cm^2	J/cm^2	J/cm	J/cm	J/cm	MPa
Specimen 1	0.36	0.38	0.74	0.36	0.39	0.75	37.1
Specimen 2	0.36	0.22	0.58	0.37	0.23	0.59	37.3
Specimen 3	0.36	0.2	0.56	0.37	0.21	0.57	37.4
Specimen 4	0.36	0.19	0.56	0.37	0.2	0.57	37.6
Specimen 5	0.37	0.11	0.48	0.37	0.11	0.49	38.0
Specimen 6	0.35	0.25	0.6	0.36	0.25	0.61	36.5
Average	0.36	0.23	0.59	0.37	0.23	0.6	37.3
Std. Dev.	0	0.09	0.09	0	0.09	0.09	0.5

4UP-ND-NH							
	Ei	Ep	IS	Ei	Ep	IS	S_max
	J/cm^2	J/cm^2	J/cm^2	J/cm	J/cm	J/cm	MPa
Specimen 1	0.33	0.39	0.73	0.34	0.4	0.74	38.1
Specimen 2	0.35	0.41	0.75	0.35	0.41	0.77	37.7
Specimen 3	0.35	0.4	0.75	0.35	0.41	0.76	37.8
Specimen 4	0.38	0.5	0.88	0.39	0.51	0.9	43.3
Specimen 5	0.38	0.49	0.87	0.39	0.49	0.88	41.4
Specimen 6	0.38	0.45	0.84	0.39	0.46	0.85	42.4
Average	0.36	0.44	0.8	0.37	0.45	0.82	40.1
Std. Dev.	0.02	0.05	0.07	0.02	0.05	0.07	2.5

4UP-GE-H							
	Ei	Ep	IS	Ei	Ep	IS	S_max
	J/cm^2	J/cm^2	J/cm^2	J/cm	J/cm	J/cm	MPa
Specimen 1	3.73	7.43	11.16	3.79	7.55	11.34	271.1
Specimen 2	3.72	5.85	9.57	3.78	5.95	9.72	270.4
Specimen 3	3.71	7.04	10.75	3.77	7.15	10.92	269.8
Specimen 4	3.46	7.33	10.79	3.51	7.45	10.96	275.5
Specimen 5	3.49	7.85	11.34	3.54	7.97	11.52	275.5
Specimen 6	3.48	6.23	9.71	3.53	6.33	9.86	274.8
Average	3.6	6.96	10.55	3.65	7.07	10.72	272.8
Std. Dev.	0.13	0.76	0.74	0.14	0.78	0.75	2.7

Table H.14 Impact results for vinyl ester composites

2VE-AD-H							
	Ei	Ep	IS	Ei	Ep	IS	S_max
	J/cm^2	J/cm^2	J/cm^2	J/cm	J/cm	J/cm	MPa
Specimen 1	0.12	0.12	0.24	0.12	0.12	0.24	13.9
Specimen 2	0.12	0.13	0.25	0.12	0.13	0.25	14.0
Specimen 3	0.13	0.16	0.29	0.14	0.16	0.3	16.7
Specimen 4	0.13	0.14	0.27	0.14	0.14	0.28	16.7
Specimen 5	0.13	0.14	0.27	0.13	0.15	0.27	15.8
Specimen 6	0.14	0.18	0.32	0.14	0.18	0.33	17.9
Average	0.13	0.14	0.27	0.13	0.15	0.28	15.8
Std. Dev.	0.01	0.02	0.03	0.01	0.02	0.03	1.6

2VE-GE-NH							
	Ei	Ep	IS	Ei	Ep	IS	S_max
	J/cm^2	J/cm^2	J/cm^2	J/cm	J/cm	J/cm	MPa
Specimen 1	2	1.59	3.58	2.03	1.61	3.64	132.6
Specimen 2	2.19	1.77	3.95	2.22	1.8	4.02	139.9
Specimen 3	2.19	1.14	3.33	2.22	1.16	3.38	139.9
Specimen 4	2.18	1.19	3.37	2.22	1.21	3.42	139.5
Specimen 5	2.19	0.88	3.07	2.23	0.89	3.12	140.2
Specimen 6	2.21	1.42	3.63	2.24	1.44	3.69	141.8
Average	2.16	1.33	3.49	2.19	1.35	3.54	139.0
Std. Dev.	0.08	0.33	0.3	0.08	0.33	0.31	3.2

3VE-AD-H							
	Ei	Ep	IS	Ei	Ep	IS	S_max
	J/cm^2	J/cm^2	J/cm^2	J/cm	J/cm	J/cm	MPa
Specimen 1	0.21	0.27	0.48	0.21	0.27	0.48	26.5
Specimen 2	0.23	0.24	0.47	0.24	0.24	0.48	25.6
Specimen 3	0.23	0.19	0.43	0.24	0.2	0.43	25.7
Specimen 4	0.23	0.24	0.47	0.24	0.24	0.48	26.1
Specimen 5	0.23	0.21	0.44	0.24	0.21	0.45	24.8
Specimen 6	0.23	0.23	0.47	0.24	0.24	0.47	26.4
Average	0.23	0.23	0.46	0.23	0.23	0.47	25.8
Std. Dev.	0.01	0.02	0.02	0.01	0.03	0.02	0.6

3VE-GE-NH							
	Ei	Ep	IS	Ei	Ep	IS	S_max
	J/cm^2	J/cm^2	J/cm^2	J/cm	J/cm	J/cm	MPa
Specimen 1	3.04	3.08	6.12	3.09	3.13	6.22	229.5
Specimen 2	4.26	3.11	7.37	4.33	3.16	7.49	259.6
Specimen 3	4.29	1.16	5.46	4.36	1.18	5.54	261.6
Specimen 4	4.27	0.95	5.22	4.34	0.97	5.31	257.2
Specimen 5	4.32	0.98	5.29	4.38	0.99	5.38	259.8
Specimen 6	4.34	0.81	5.15	4.41	0.82	5.23	261.1
Average	4.09	1.68	5.77	4.15	1.71	5.86	254.8
Std. Dev.	0.51	1.1	0.86	0.52	1.12	0.87	12.5

4VE-AD-H							
	Ei	Ep	IS	Ei	Ep	IS	S_max
	J/cm^2	J/cm^2	J/cm^2	J/cm	J/cm	J/cm	MPa
Specimen 1	0.25	0.33	0.58	0.25	0.34	0.59	33.0
Specimen 2	0.27	0.36	0.64	0.28	0.37	0.65	34.0
Specimen 3	0.26	0.35	0.61	0.26	0.36	0.62	33.0
Specimen 4	0.28	0.34	0.62	0.28	0.34	0.63	34.1
Specimen 5	0.3	0.36	0.66	0.3	0.37	0.67	34.8
Specimen 6	0.27	0.36	0.62	0.27	0.36	0.63	34.4
Average	0.27	0.35	0.62	0.28	0.36	0.63	33.9
Std. Dev.	0.02	0.01	0.03	0.02	0.01	0.03	0.8

4VE-GE-NH							
	Ei	Ep	IS	Ei	Ep	IS	S_max
	J/cm^2	J/cm^2	J/cm^2	J/cm	J/cm	J/cm	MPa
Specimen 1	5.5	4.51	10	5.58	4.58	10.16	327.2
Specimen 2	5.48	3.33	8.81	5.57	3.38	8.95	326.3
Specimen 3	5.58	4.27	9.85	5.67	4.34	10	332.1
Specimen 4	5.45	2.55	8	5.54	2.59	8.13	324.7
Specimen 5	5.58	2.23	7.81	5.67	2.27	7.94	332.1
Specimen 6	5.55	4.38	9.93	5.64	4.45	10.09	330.5
Average	5.52	3.54	9.07	5.61	3.6	9.21	328.8
Std. Dev.	0.05	0.99	1	0.05	1.01	1.02	3.2

Table H.15 Impact results for epoxy composites

2EP-AD-H							
	Ei	Ep	IS	Ei	Ep	IS	S_max
	J/cm^2	J/cm^2	J/cm^2	J/cm	J/cm	J/cm	MPa
Specimen 1	0.08	0.11	0.19	0.08	0.11	0.19	11.3
Specimen 2	0.09	0.14	0.23	0.09	0.15	0.24	13.7
Specimen 3	0.09	0.12	0.21	0.09	0.12	0.22	13.7
Specimen 4	0.1	0.15	0.25	0.1	0.15	0.25	15.0
Specimen 5	0.1	0.1	0.2	0.1	0.11	0.21	15.0
Specimen 6	0.1	0.11	0.21	0.1	0.11	0.21	15.0
Average	0.09	0.12	0.22	0.09	0.13	0.22	13.9
Std. Dev.	0.01	0.02	0.02	0.01	0.02	0.02	1.5
2EP-GE-H							
	Ei	Ep	IS	Ei	Ep	IS	S_max
	J/cm^2	J/cm^2	J/cm^2	J/cm	J/cm	J/cm	MPa
Specimen 1	0.91	1.07	1.97	0.92	1.08	2	86.3
Specimen 2	0.97	1.15	2.12	0.99	1.17	2.15	88.8
Specimen 3	1.28	1.06	2.34	1.3	1.08	2.38	103.8
Specimen 4	1.25	1.06	2.31	1.27	1.08	2.34	100.5
Specimen 5	1.55	1.18	2.73	1.58	1.2	2.78	114.2
Specimen 6	1.55	0.93	2.49	1.58	0.95	2.53	114.5
Average	1.25	1.08	2.33	1.27	1.09	2.36	101.3
Std. Dev.	0.28	0.09	0.27	0.28	0.09	0.27	12.1
3EP-AD-H							
	Ei	Ep	IS	Ei	Ep	IS	S_max
	J/cm^2	J/cm^2	J/cm^2	J/cm	J/cm	J/cm	MPa
Specimen 1	0.15	0.23	0.38	0.16	0.23	0.39	22.1
Specimen 2	0.15	0.18	0.33	0.16	0.18	0.34	22.0
Specimen 3	0.15	0.19	0.34	0.16	0.19	0.35	22.0
Specimen 4	0.15	0.19	0.34	0.16	0.19	0.35	22.0
Specimen 5	0.15	0.17	0.32	0.16	0.17	0.33	22.1
Specimen 6	0.15	0.15	0.3	0.16	0.15	0.31	22.1
Average	0.15	0.18	0.34	0.16	0.19	0.34	22.0
Std. Dev.	0	0.03	0.03	0	0.03	0.03	0.1
3EP-GE-H							
	Ei	Ep	IS	Ei	Ep	IS	S_max
	J/cm^2	J/cm^2	J/cm^2	J/cm	J/cm	J/cm	MPa
Specimen 1	2.8	2.23	5.02	2.84	2.26	5.1	209.4
Specimen 2	2.86	2.55	5.41	2.91	2.59	5.49	232.8
Specimen 3	2.86	1.9	4.76	2.91	1.93	4.83	232.8
Specimen 4	2.88	2.52	5.4	2.93	2.56	5.49	232.8
Specimen 5	2.65	2.52	5.17	2.7	2.56	5.26	213.4
Specimen 6	2.91	2.5	5.41	2.95	2.55	5.5	216.9
Average	2.83	2.37	5.2	2.87	2.41	5.28	223.0
Std. Dev.	0.09	0.26	0.27	0.09	0.27	0.27	11.0

4EP-AD-H							
	Ei	Ep	IS	Ei	Ep	IS	S_max
	J/cm^2	J/cm^2	J/cm^2	J/cm	J/cm	J/cm	MPa
Specimen 1	0.19	0.23	0.42	0.19	0.23	0.42	24.5
Specimen 2	0.19	0.19	0.38	0.19	0.19	0.39	24.5
Specimen 3	0.19	0.2	0.39	0.19	0.2	0.4	24.7
Specimen 4	0.19	0.23	0.42	0.19	0.23	0.43	24.9
Specimen 5	0.14	0.23	0.38	0.15	0.24	0.38	22.4
Specimen 6	0.15	0.27	0.42	0.15	0.27	0.43	25.1
Average	0.18	0.22	0.4	0.18	0.23	0.41	24.3
Std. Dev.	0.02	0.03	0.02	0.02	0.03	0.02	1.0

4EP-GE-H							
	Ei	Ep	IS	Ei	Ep	IS	S_max
	J/cm^2	J/cm^2	J/cm^2	J/cm	J/cm	J/cm	MPa
Specimen 1	3.97	3.39	7.37	4.04	3.45	7.48	294.0
Specimen 2	3.98	3.31	7.3	4.05	3.37	7.41	294.7
Specimen 3	4.83	3.09	7.91	4.9	3.14	8.04	291.3
Specimen 4	4.85	1.2	6.05	4.93	1.22	6.15	292.7
Specimen 5	4.87	1.57	6.44	4.95	1.59	6.54	294.1
Specimen 6	4.88	2.71	7.59	4.96	2.75	7.72	294.8
Average	4.56	2.55	7.11	4.64	2.59	7.22	293.6
Std. Dev.	0.45	0.94	0.71	0.46	0.95	0.73	1.4

Appendix I Summary of material properties

Composite Code & Fibre Volume Fraction		Tensile Strength	Tensile Secant Modulus	Tensile Linear Modulus	Flexural Strength	Flexural Secant Modulus	Flexural Linear Modulus	Initiitial Impact Energy	Propogative Impact Energy	Total Impact Energy	Impact Stress	Water Absorption at 24 hrs	Water Absorption at 4 weeks
		ASTM D638	ASTM D638	ASTM D638	ASTM D790	ASTM D790	ASTM D790	ASTM D256	ASTM D256	ASTM D256	ASTM D256	ISO R62	ISO R62
		MPa	GPa	GPa	MPa	GPa	GPa	J/cm	J/cm	J/cm	MPa	%	%
15%	UP-AD-H	27.3	3.4	4.23	59.2	3.42	3.83	0.19	0.18	0.36	21.9	1.1502	5.3921
	UP-AD-NH	28	3.74	4.78	65.3	3.6	4.06	0.15	0.11	0.26	16.3	0.9368	4.4908
	UP-AD-H-F	29.7	3.81	4.63	75.2	3.71	4.23	0.18	0.15	0.33	21.1	0.7260	3.6444
	UP-ND-H	27.6	3.45	4.49	59.8	3.51	3.99	0.18	0.2	0.39	21.3	1.1977	5.4850
	UP-ND-NH	26.7	3.38	4.45	61.5	3.36	3.9	0.21	0.2	0.41	22.1	1.1516	5.4127
	UP-GE-H	54	3.12	4.17	137.9	4.23	5.47	2.19	1.35	3.55	124.3	0.2261	1.0663
	VE-AD-H	43.0	3.38	4.43	67.3	2.87	3.28	0.13	0.15	0.28	15.8	0.8842	3.6375
	VE-GE-NH	86.0	5.33	5.81	135.4	4.84	5.18	2.19	1.35	3.54	139.0	0.0920	0.4625
	EP-AD-H	48.5	3.05	3.28	74.7	3.13	3.69	0.09	0.13	0.22	13.9	1.1522	6.8540
	EP-GE-H	96.7	4.42	4.95	164.5	4.99	5.59	1.27	1.09	2.36	101.3	0.1390	0.8306
22.5%	UP-AD-H	41.9	4.24	6.27	84.7	3.81	4.47	0.26	0.32	0.57	30.7	1.6267	6.9224
	UP-AD-NH	38.5	3.54	4.99	79.3	3.67	4.33	0.26	0.32	0.59	32.2	1.2766	5.7667
	UP-AD-H-F	43.2	4.1	6.39	84.2	3.73	4.43	0.25	0.34	0.59	31.8	1.2538	5.4590
	UP-ND-H	41.7	4.01	6.3	85.9	3.77	4.49	0.23	0.46	0.68	26.7	1.4773	6.1913
	UP-ND-NH	41.6	3.53	6.23	77.3	3.59	4.28	0.33	0.41	0.75	35.7	1.7204	6.8387
	UP-GE-H	96.8	5.87	6.11	176.6	5.8	6.46	3.38	5.64	9.02	243.0	0.1388	0.6714
	VE-AD-H	53.1	3.90	5.29	79.9	3.41	4.21	0.23	0.23	0.47	25.8	1.3859	5.7310
	VE-GE-NH	152.0	7.93	9.92	208.5	6.59	7.27	4.15	1.71	5.86	254.8	0.0836	0.4581
	EP-AD-H	52.1	3.84	3.96	85	3.56	4.37	0.16	0.19	0.34	22.0	1.6869	9.1656
	EP-GE-H	161.3	7.17	7.18	203.1	5.91	6.61	2.87	2.41	5.28	223.0	0.1133	0.6494
30%	UP-AD-H	51.8	4.11	6.62	98.5	3.96	5.17	0.33	0.35	0.68	38.0	2.6840	9.5740
	UP-AD-NH	47.6	3.99	6.32	98.3	4.18	5.26	0.32	0.42	0.74	37.8	1.9990	7.5517
	UP-AD-H-F	54.5	3.98	6.75	99.6	4.2	5.41	0.35	0.39	0.74	38.6	2.6153	9.7978
	UP-ND-H	49.6	4.41	6.46	99.4	4.38	5.43	0.37	0.23	0.6	37.3	2.4934	8.9354
	UP-ND-NH	46.7	4.05	6.72	98.4	3.9	5.14	0.37	0.45	0.82	40.1	3.0959	9.7978
	UP-GE-H	176.2	9.28	9.82	235.8	7.94	9.28	3.65	7.07	10.72	272.8	0.1128	0.4757
	VE-AD-H	56.5	4.14	5.60	85.4	3.76	4.64	0.28	0.36	0.63	33.9	1.7577	7.2793
	VE-GE-NH	201.0	9.24	10.51	262.4	7.95	9.13	5.61	3.6	9.21	328.8	0.0562	0.3415
	EP-AD-H	64.3	4.26	4.48	91.4	3.92	4.94	0.18	0.23	0.41	24.3	2.1867	10.9278
	EP-GE-H	205.0	9.40	10.87	256.1	7.85	8.86	4.64	2.59	7.22	293.6	0.0874	0.5046